The Influence of Process Factors on the Production of Semi Solid Feedstock

FREDRIK COOPER

Thesis submitted in partial fulfilment of the academic requirements for the degree of MSc Eng in the School of Mechanical Engineering, University of Natal, Durban.

December 2000

Declaration

I declare that this thesis is my own unaided work except where due acknowledgement is made to others. It is being submitted for the Master of Science in Engineering to the University of Natal, Durban. It has not been submitted before for any other degree or examination to any other university.

Fredrik Cooper

December 2000

Abstract

Semi-solid manufacturing is a near net shape forming process that takes advantage of an alloy's thixotropic behaviour. However, in order to obtain the desired thixotropic properties from an alloy in the semi-solid state, the microstructure of the as-cast feedstock metal needs to display a fine grained, equiaxed primary phase prior to reheating for the forming operation. Various methods are currently in use to obtain the required microstructure of which the MagnetoHydroDynamic (MHD) process is predominant. Two fundamental factors, namely shear rate and cooling rate, influence the formation of the fine grained, equiaxed primary phase during the MHD process. The aim of this research was to produce semi solid billets and in so doing, determine how the influence of the combination of the two fundamental factors contribute towards the final formation of the primary phase and to determine an optimal level of these factors' settings to deliver the desired microstructure.

An MHD apparatus was constructed and the Taguchi method was used to design an experiment to investigate the influence of the fundamental factors involved in casting semi solid feedstock of aluminium A356.2. The issues of the formation of a fine eutectic phase and solidification shrinkage were also investigated. An experimental method was designed to investigate the significance of the fundamental factors' influence towards the appearance of the primary phase; the latter was evaluated using an image analysis system. The shear rate was controlled by varying the line frequency and the base frequency supplied to the electromagnetic stirrer and the cooling rate was controlled by initiation of a fixed, fast cooling rate at a certain melt temperature (T_i).

Results showed that a fine grained, equiaxed primary phase, with an average grain size of 55 μm, was achieved after casting, prior to reheating for forming. The contribution of the base frequency and the line frequency were 8 % and 3.5 % respectively and the contribution of T_i was 86.5 % towards the outcome of the result. The cooling rate changed from approximately 0.3 ^{0}C/sec to 4.5 ^{0}C/sec at T_i. A fine textured eutectic phase was achieved with the fast cooling rate. The solidification shrinkage was accounted for by incorporating a riser on the mould. The feedstock produced in this research was compared, on a microstructural basis, to commercially available Semi Solid Metal (SSM) feedstock from Pechiney and SAG. The research feedstock had a larger, average primary grain size, however, it was more discrete and round grained than the commercial alloys which were finer and more rosette grained. Upon reheating to the semi solid state, ready for forming, the final, evolved grain sizes and shapes were almost identical between the research and commercial feedstock, despite the initial differences in grain sizes and shapes. However, the commercial alloys showed primary grains with trapped eutectic whereas in the research alloy, the primary grains were largely free of trapped eutectic.

Acknowledgements

To the CSIR and the industry sponsors in the Semi Solid Research collaboration for granting the opportunity to perform this research.

To Dr Jeff Ferreira for his motivation, support and guidance.

To Dr Gonasagren Govender for his supervision and guidance.

To my colleagues Clive Goodman, Vaneil Ramdhani, Subash Sharma, Alex Banach, and Belinda Burton for their assistance and support.

To the academic and workshop staff of the School of Mechanical Engineering, University of Natal, Durban for their valued assistance.

To my parents for their patience, support and motivation, without whom, this would not have been a reality.

Table of Contents

Chapter 3

List of Figures

Chapter 3

Appendix

List of Tables

CHAPTER 1

1 Introduction

Semi Solid Metal (SSM) Forming is a hybrid manufacturing method which utilizes mainly the pressure die casting and forging processes[1]. It was based on a discovery made at the Massachusetts Institute of Technology (MIT) in the early 1970's. The research at this time, conducted by Spencer in 1971[2], involved the investigation into the magnitude of forces involved in deforming and fragmenting dendritic growth structures using a high temperature rheometer[3]. Molten tin - lead alloys were poured into an annular space between two concentric cylinders and allowed to partially solidify. When the outer cylinder was rotated, shear forces were transmitted through the freezing alloy and measured at the stationary inner cylinder[3].

Spencer then conducted a different experiment. Instead of partially solidifying the alloy before beginning shear, he began to shear above the liquidus temperature of the alloy and then slowly cool the alloy into the solidification range while it was being sheared. Surprising results followed. The shear stress only increased very slowly as temperature was decreased below the liquidus temperature. The stress measured at a given temperature was orders of magnitude less than when the samples were cooled to the given temperature before shear[2].

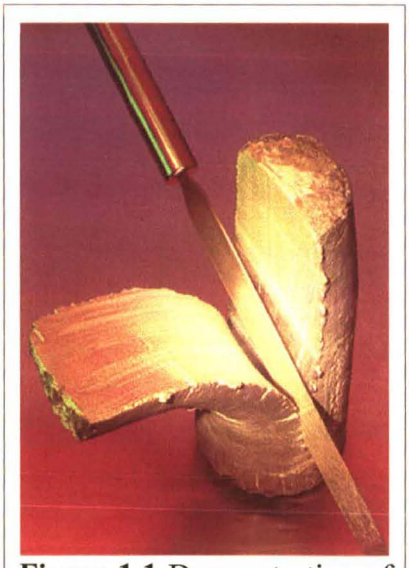

Figure 1.1 Demonstration of the thixotropic property of semi solid metal.

Further research showed that the material produced in this manner possessed thixotropic characteristics in the semi solid state. The semi solid alloys displayed viscosities that depended on shear rate. The viscosity rose very high to the consistency of butter when the material was at rest and yet decreased to the consistency of machine oils under the influence of intense shear forces. The thixotropic nature of the material can be demonstrated by cutting a free standing slug of semisolid material with a spatula (figure 1.1).

Several potential benefits were identified for the forming processes using semi solid metal compared to conventional casting.

- SSM forming operated at lower metal temperatures and reduced metal heat content.
- The viscous flow behaviour could provide more laminar cavity fill than could generally be achieved with liquid alloys. This could lead to reduced gas entrapment.
- Solidification shrinkage would be reduced in direct proportion to the fraction solidified within the SSM alloy, which should reduce shrinkage porosity and the tendency toward hot tearing.

Continuous cast bars could be cast into semi solid material. This represented a raw material that could be heated at a later time or different location to the semi solid temperature range to reclaim the thixotropic properties. Industry began to adopt this principle as a source feedstock material and SSM forming was used as a means to produce metal components used in military, aerospace, automotive or other high integrity, safety critical applications. The demand for SSM feedstock of high quality increased. There was a need for the exclusion of gases, oxides, nonmetallic inclusions and other discontinuities from the SSM feedstock supply. Amongst other processes, the Magnetohydrodynamic (MHD) stirrer continuous caster was developed to meet these requirements. This showed there was an important relationship between the stirring shear rate and the solidification rate of the metal being cast and this relationship determined the type of SSM forming microstructure that was generated[3].

A lengthy investigation into feedstock production using the MHD method found it was difficult to monitor the shear rate parameter without expensive equipment. Owing to the medium confinement and to the high degree of both the stirring intensity and temperature, methodical velocity measurements were particularly difficult. Furthermore, the working time of the sensors was limited to 30 minutes when they had been immersed into molten aluminium alloys which are very aggressive from the physical chemistry standpoint[4]. However, an indication of the shear rate can be realised by monitoring the process factors

governing the characteristics of the shear rate without having to directly measure the shear rate.

The aim of the study was to produce a billet of SSM feedstock using the MHD method, controlling the process indirectly by monitoring outside process parameters. In so doing, also determine the influence of the MHD process factors on the production of the SSM forming microstructure.

CHAPTER 2

2 Literature Survey

2.1 Metallurgy of Aluminium Alloys

Pure aluminum is a relatively poor casting material so aluminum castings are actually produced from alloys. The casting alloys used are those having properties particularly suited to casting purposes. Since a large number of aluminum base casting alloys are available it is evident that widely different properties may be obtained from the various alloys. For all these alloys two types of properties should be considered: the casting properties, characteristics of the alloy which determine the ease or difficulty of producing acceptable castings, and the engineering properties, those properties which are of interest to the designer or user of the castings. These two sets of properties can be used as a basis for studying the similarities and differences of the large number of aluminum casting alloys.

2.1.1. Aluminium Alloying Principles

The aluminum-base alloys may in general be characterized as eutectic systems, containing intermetallic compounds or elements as the excess phases. Because of the relatively low solubilities of most of the alloying elements in aluminum and the complexity of the alloys that are produced, any one aluminum-base alloy may contain several metallic phases, which sometimes are quite complex in composition. These phases usually are appreciably more soluble near the eutectic temperatures than at room temperature, making it possible to heat-treat some of the alloys by solution and aging heat-treatments[5].

All the properties of interest are influenced by the effects of the various elements with which aluminum is alloyed. Aluminium casting alloys must contain, in addition to strengthening elements, sufficient amounts of eutectic forming elements (usually silicon) in order to have adequate fluidity to feed the shrinkage that occurs in all but the simplest of castings [6]. The principle alloying elements in aluminum-base casting alloys are copper, silicon, magnesium, zinc, chromium, manganese, tin, and titanium. Iron is an element normally present and usually considered as an impurity.

Classification of aluminium alloys follows the Aluminium Association designation system that recognises alloy families by the following scheme[6]:

1xx.x: Controlled unalloyed compositions.

2xx.x: Aluminium alloys containing copper as the major alloying element.

3xx.x: Aluminium-Silicon alloys also containing magnesium and/or copper.

4xx.x: Binary Aluminium-Silicon alloys.

5xx.x: Aluminium alloys containing magnesium as the major alloying element.

6xx.x: Currently unused.

7xx.x: Aluminium alloys containing zinc as the major alloying element, usually also containing additions of either copper, magnesium, chromium, manganese, or combinations of these elements.

8xx.x: Aluminium alloys containing tin as the major alloying element.

9xx.x: Currently unused.

Designations in the form xxx.1 and xxx.2 include the composition of specific alloys in remelt ingot form suitable for foundry use. Designations in the form xxx.0 in all cases define composition limits applicable to castings. Further variations in specified compositions are denoted by prefix letters used primarily to define differences in impurity limits. Accordingly, one of the most common gravity cast alloys, 356, has variations A356, B356, C356; each of these alloys has identical major alloy contents but has decreasing specification limits applicable to impurities, especially iron content[6].

In 2xx.x through 8xx.x designations, the second and third digits have no numerical significance but only identify the various alloys in the group. The digit to the right of the decimal point indicates product form: 0 denotes castings, 1 denotes standard ingot and 2 denotes ingot having composition ranges narrower than but within those of standard ingot[6].

2.1.1.1 Silicon

The effect of silicon on the properties of Al-Si alloys is largely one of alloying since no significant benefits are obtained by attempts at solution heat-treating and aging. The

percentage of silicon in the alloy is first in importance, closely followed by the microstructural effects of modification by permanent mould or die casting or special melting practices. These factors are summarized in figure 2.1. The general effect of increasing silicon contents (figure 2.1) to be that of increasing the strength until the eutectic silicon percentage is reached. Ductility, however, is lowered. The beneficial effects of modification with elements such as sodium and by chill casting are also evident in figure 2.1. From these observations it follows that aluminum-silicon alloys will be at their best when modified by suitable additions, or better, when cast in metal moulds. Furthermore, since additional improvement cannot be obtained by heat treatment, these alloys are usually used in the as-cast condition[5].

Silicon is present in all commercial aluminum casting alloys. As an alloying element it is used in amounts up to about 14 per cent Si. The binary Al-Si system is shown in figure 2.2. The solubility of Si in aluminum, the α phase, is limited to 1.65 per cent at 577 °C and less than 0.05 per cent at room temperature. Undissolved silicon is present as β, silicon particles containing an extremely small percentage of aluminum.

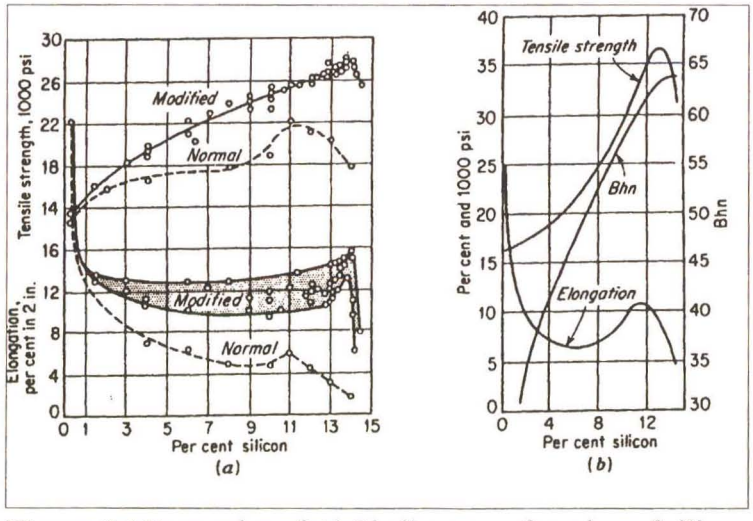

Figure 2.1 Properties of Al-Si alloys as a function of silicon in the alloy. (a) Applies to sand castings (normal and sodium treated modified alloys) and (b) to chill castings. [5]

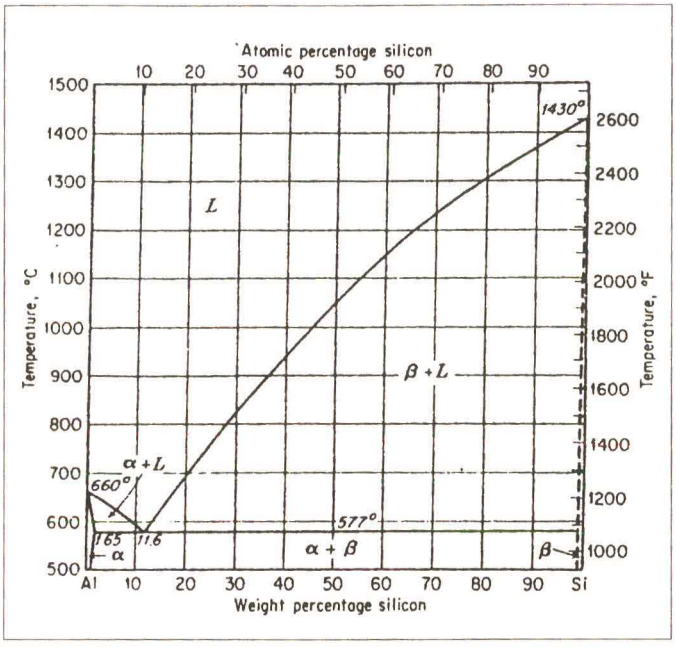

Figure 2.2 The Al-Si phase diagram. [5]

The hypoeutectic alloys are a two phase system constituting primary phase α grains and a surrounding matrix of the eutectic phase. The eutectic is formed of an aluminium solid solution containing just over 1% silicon and virtually pure silicon as a second phase[7]. The combined eutectic composition is close to Al-12.7 %Si[7].

Slow solidification of a pure Al-Si alloy produces a very coarse microstructure in which the eutectic comprises large plates or needles of silicon particles (which appear to be interconnected, individual cells[7]) in a continuous aluminium matrix. Alloys having this coarse eutectic exhibit low ductility because of the brittle nature of the large silicon plates. Rapid cooling greatly refines the microstructure and the silicon phase assumes a fibrous form[7] with the result that both ductility and tensile strength are much improved (figure2.1). The eutectic may also be refined by the process known as modification.

2.1.1.2 Modification of Hypoeutectic Aluminium-Silicon Alloys

Modification induces structural refinement of the normally occurring eutectic phase and is achieved by the addition of certain elements such as calcium, sodium, strontium and antimony[6], the most common being sodium and strontium.

The mechanism by which the eutectic and, more particularly, the size and form of the silicon phase is modified is not clearly defined. Most theories involve the possible effects of sodium on the nucleation and/or growth of eutectic silicon during solidification. These theories include the following:

- Sodium may depress the eutectic temperature by as much as 12 ^{0}C and a finer microstructure is therefore expected because the rate of nucleation will be greater in an undercooled condition[7].
- From the observation that the silicon particles appear to be interconnected within each cell, it has been suggested that there is no need for repeated nucleation to occur after each cell has formed. The theory is that sodium may segregate at the periphery of growing silicon plates and prevents or restricts further growth[7].

The use of sodium has presented problems such as reduced fluidity, but its major disadvantage arises through the rapid loss of the element through evaporation or oxidation during melting and remelting. To overcome this, excess amounts were added to compensate, but this practice sometimes lead to over modification of the final casting

Considerable commercial success has been achieved by replacing sodium and modifying with strontium. The addition of 0.03 to 0.05 % of this element also produces a refined eutectic and the tensile properties of castings are comparable with those obtained when sodium was used. Loss of strontium during melting is much less and the modified structure is retained after remelting[7].

2.1.1.3 Magnesium

The alloying behaviour of magnesium in aluminum results in an increase in the hardness and strength and a decrease in ductility of the alloy with an increase in magnesium content. The equilibrium diagram for the binary system is shown in figure 2.3. The alloy system shows a solid-solubility change of the α phase with temperature, 14.9 per cent Mg being soluble at 451 °C and less than 2.90 per cent at room temperature. A second, harder β phase exists when the solid-solubility limit is exceeded. The opportunity for solution and ageing heat-treatments is present, and the mechanical-property relationships with magnesium

percentage are similar to those in the Al-Cu alloys. Several alloys are based on this binary system, and normally contain 4, 8, and 10 per cent Mg[8].

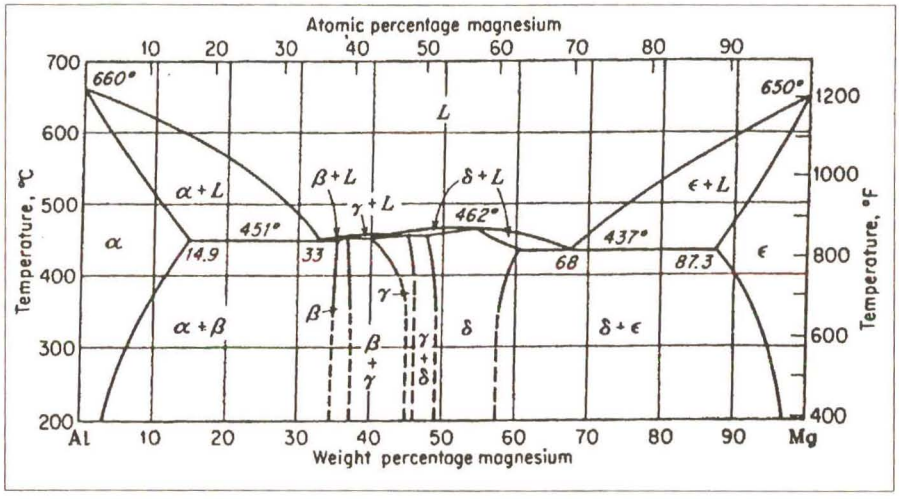

Figure 2.3 The Al-Mg phase diagram. [5]

2.1.1.4 Magnesium and Silicon

Certain combinations of magnesium and silicon have been found to exhibit important alloying effects in aluminium. The two elements are able to combine and form the metallic compound Mg_2Si. They then behave as a quasi-binary alloy system (figure 2.4). The Al-Mg_2Si system is also of the type permitting solution and ageing treatments and their accompanying property changes. Ternary alloys taking advantage of this quasi-binary system and the beneficial effects of silicon contain small percentages of Mg, up to about 0.30 per cent, and larger percentages of Si, 6 to 8.0 per cent. The excess of silicon is present to improve casting properties of these alloys since it is not needed to form Mg_2Si[8].

In some alloys, the combined effects of Si and Mg are undesirable, and they may then be limited as impurities. Since all aluminum alloys contain silicon, the addition of magnesium is all that is necessary to obtain the hardening effect of Mg_2Si. The alloys may then become brittle. For this reason impurity limits for magnesium in many alloys (the Cu-Al, Si-Al, and their complex alloys, for example) are set at 0.03 to 0.10 per cent maximum. Thus the combined effects of the Mg and Si in Al alloys provide another case study of elements which are beneficial in some alloys when used as alloying elements or harmful when unintentionally present as impurities in other alloy types.[8]

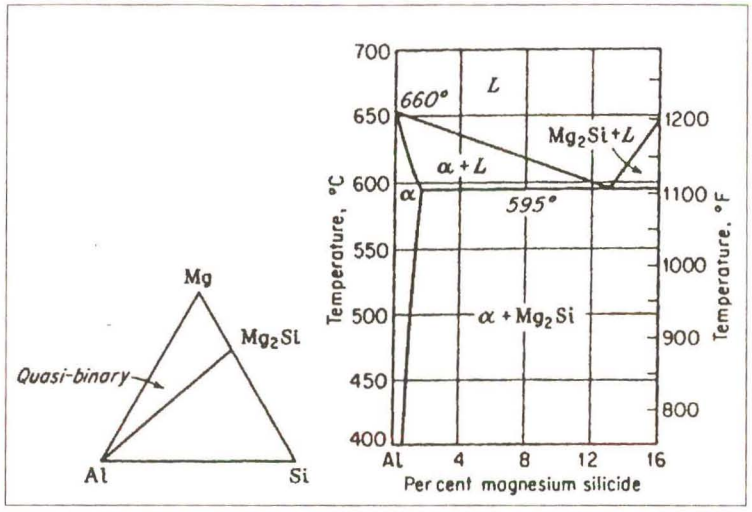

Figure 2.4 The Al-Mg-Si phase diagram and quasi-binary system. [5]

2.2 Casting Technology

The technology associated with castings has been developed through an understanding of the mechanics of solidification of a molten metal. Solidification shrinkage, microstructural evolution, melt flow, etc have to be considered for sound casting practices. These can be further understood by investigating the process of solidification of metals.

2.2.1 Solidification of Metals

Solidification occurs by the nucleation of stable nuclei which then grow under the influence of the crystallographic and thermal conditions that prevail. The size and character of these grains are controlled by the composition of the alloy and by the cooling rate. Growth ceases when all the available liquid metal has solidified. It is apparent that solidification proceeds in any of the following categories[9]:

1. At a constant temperature (pure metals and eutectic alloys, figure 2.5)
2. Over a temperature range (solid solutions, figure 2.6)
3. By a combination of solidification over a temperature range followed by constant temperature freezing. (Proeutectic plus eutectic type freezing).

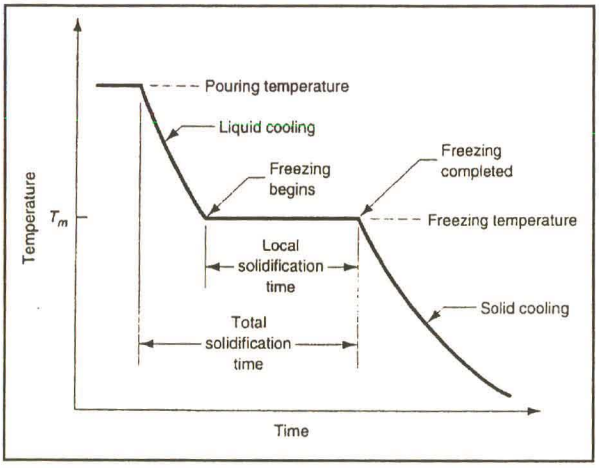

Figure 2.5 Cooling curve for a pure metal during casting. [10]

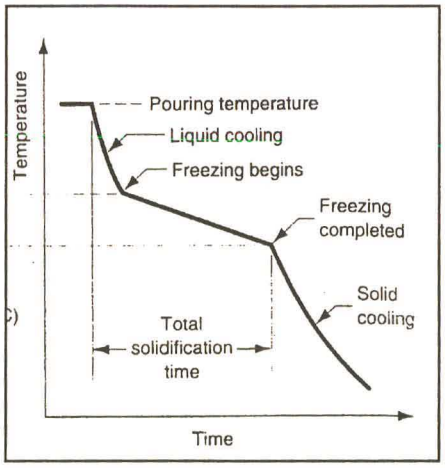

Figure 2.6 Cooling curve for a solid solution alloy during casting (e.g. 50% Ni - 50% Cu composition). [10]

During the freezing process, heat is extracted from the molten metal as soon as the metal enters the mould. This heat is referred to as superheat since it represents that which must be removed before solidification can begin. Then there is the latent heat of fusion which evolves from the actual freezing of the metal as it changes from a liquid to a solid. This must be transferred to the mould before complete solidification can be achieved. Finally, the solid metal transfers heat to the mould and then to the atmosphere as it cools to room temperature[9].

During the three stages of cooling (i.e. liquid, liquid-solid, and solid), shrinkage is occurring. Thus the metal contracts as it loses superheat, as it transforms to a solid, and as the solid cools to room temperature. There are therefore three points to consider when a casting solidifies[9]:

1. Growth of the solid grains.
2. Heat evolution and transfer.
3. Dimensional changes.

2.2.1.1 Nucleation and Growth

That part of the casting which is near the mould wall is supercooled and solidifies first as fine equiaxed grains. Nucleation of the supercooled grain is governed by two factors. The first factor is the free energy available from the solidification process which is dependant on the volume of the particle formed. The second factor is the energy required to form a liquid-solid interface which is dependant upon the surface area of the particle[9]. The net effect of these two factors is that the total energy of the particle reaches a maximum at a given particle size for a given supercooling temperature (figure 2.7). This is the critical particle size which must be created before the nucleus is stable for that particular supercooled temperature. As the degree of supercooling increases the free energy available from the liquid-solid transformation also increases. Consequently, the critical particle size required for stability decreases, but simultaneously the thermal fluctuations which tend to create stable nuclei also decrease. As a consequence, the rate of nucleation builds up to a maximum with increasing supercooling and then drops off [9].

The preceding explanation represents homogenous nucleation. Usually foreign particles are present which alter the liquid-solid interface energy enough to assist in nucleation, thereby reducing the amount of supercooling required to effect nucleation. This is heterogeneous nucleation and usually prevails in castings.

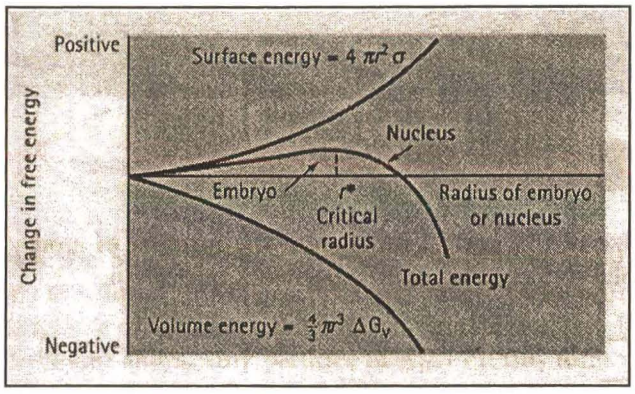

Figure 2.7 The net effect of the surface energy and volume energy of a nucleus, with respect to its radius, results in the total energy of the nucleus reaching a maximum at a critical radius. [11]

Once a stable nucleus is formed, it grows by acquiring atoms from the liquid. The rate of growth is governed by the amount of supercooling below the melting point, with the growth rate increasing with the degree of supercooling until it reaches a maximum and then drops off. Therefore the rate of nucleation and the rate of growth follow the same general trend with increasing amount of supercooling. The relative rates differ to the extent that nucleation is predominant in the early stages of freezing and the first layer of solid metal at the metal mould interface consists of fine equiaxed grains mentioned previously.

When the first skin of solid metal is produced, the latent heat of fusion is released and the remaining liquid loses most of its supercooling. This change stops further nucleation. Growth continues, however, on the grains already formed. This growth is controlled by the rate of heat transfer from the casting and since this establishes a temperature gradient toward the casting surface, the growth occurs in a direction opposite to the heat flow. In addition, because growth is also dependant on crystallographic direction as well as the direction of heat flow, only those grains which happen to be favourably oriented will grow toward the centre of the castings and other less favourably oriented grains will be blocked

off. The net effect creates a zone of columnar grains next to the outer layer of fine grains. In pure metals these columnar grains extend to the centre of the casting, but in alloys the columnar grain growth may be interrupted by an equiaxed grain growth (figure 2.8.).

The columnar growth can occur dendritically, where the grains grow in a fir-tree like fashion. This type of growth represents about 10% of the total freezing process of pure metals, whereas it is commonplace for the freezing of alloys[9].

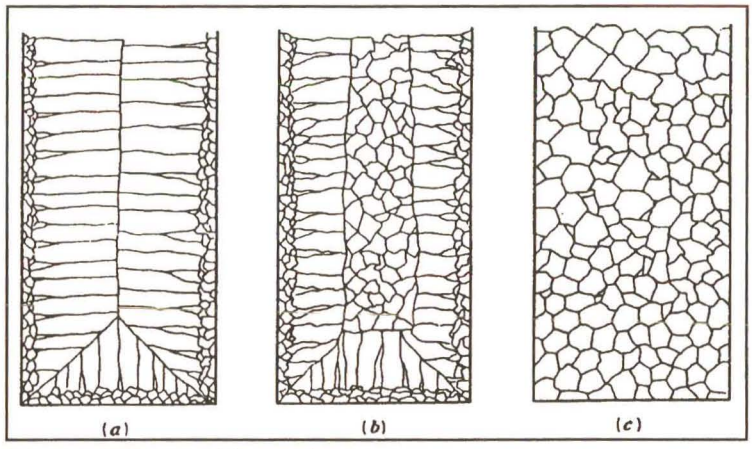

Figure 2.8 Possible casting structures.

a. Wholly columnar except for chill zone of equiaxed grains at mould wall, typical of pure metals.

b. partially columnar and partially equiaxed grains, typical of solid solution alloys.

c. wholly equiaxed grains, a result of heterogeneous nucleation from an absence of thermal gradients or the use of a nucleation catalyst. [9]

2.2.1.2 Freezing of Alloys

Alloys can be divided into those which:

1. Start and complete their freezing by precipitating an essentially pure component, but over a temperature range.
2. Start and complete their freezing as solutions.

3. Freeze at constant temperature by precipitating simultaneously two or three phases. These alloys are known as eutectics.
4. Start their freezing by precipitating an essentially pure component and complete it with eutectic type freezing.
5. Start their freezing as solutions and complete it as eutectic type.

The aluminium alloy A356.2 solidifies according to case 4 above. Referring to the phase diagram in figure 2.2, an aluminium alloy with 7 % silicon, such as A356.2, solidifies through an α+L region between 620 ^{0}C and 577 ^{0}C before the eutectic freezing occurs at 577 ^{0}C. The α phase is the essentially pure component with 98.5 % Al. This type of solidification occurs in two stages: the dendritic growth of the primary α phase, followed by the final solidification of the remaining liquid as a eutectic phase.

The first stage of freezing, dendritic growth, starts and moves inward, followed by an "end" wave after the "start" wave has completed its travel, thus creating a semi solid condition throughout the casting. Near the surface of the casting the eutectic freezing seems to start coincidentally with the completion of the dendritic "end" wave. The rate at which the eutectic structure extends into the interior appears to slow down drastically as soon as the eutectic begins to develop, because the beginning of the eutectic freezing near the centre of the casting is delayed until well after the dendrites have completed their growth. This results from the combined effect of the heat of fusion and the poor heat transfer out of the casting. The difference in time between the "start" and "end" of eutectic freezing at any point in the casting would not be expected to be very great since the eutectic solidification range is not large. Figure 2.9 shows a schematic explanation of the eutectic alloy solidification.

The morphology of the eutectic structure in Al-Si alloys is dependant upon the temperature at which the silicon phase nucleates. The order, in terms of decreasing nucleation temperature, being polyhedral shaped silicon grains, coarse silicon plates, fine silicon plates and globular silicon particles. The globular structure is produced most readily by an addition of a modifying agent such as strontium, the resultant alloy being referred to as a modified alloy. A type of globular eutectic can also be produced by chill casting[9].

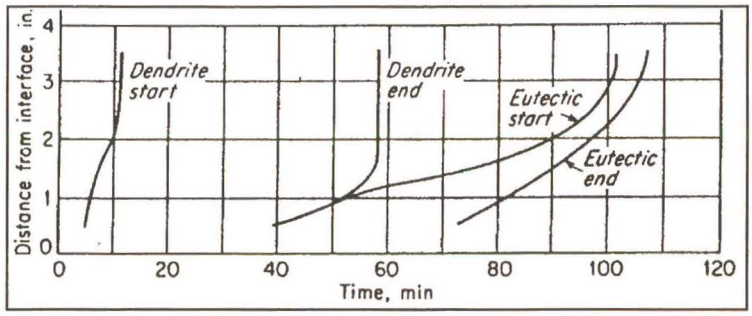

Figure 2.9 Chart of dendritic and eutectic solidification start and end times of an arbitrary eutectic alloy, showing the mode of solidification of such alloys. [9]

The eutectic alloys are known to freeze either exogenously (i.e. from the surface to the centre of the casting) or endogenously (i.e. random nucleation of eutectic cells consisting of individual clusters of the two phases growing in the liquid as spherical masses). The result of exogenous freezing is to provide a wall like solidification from the surface to the centre of the casting while endogenous freezing leads to a mushy condition due to liquid surrounding each eutectic cell. Modified Al-Si alloys are found to freeze exogenously whereas the normal Al-Si alloys freeze endogenously (figure 2.10).

Normal eutectic alloys will freeze in the endogenous cellular like fashion which tends to produce the mushy condition. Nevertheless, the greater nucleation of cells near the surface of the casting does cause the solidification to progress in a wavelike fashion, with the start of eutectic freezing progressing toward the interior some distance in advance of the completion of freezing[9].

2.2.2 Pouring and Feeding Castings

The soundness of a casting depends upon how the metal enters a mould and solidifies. A sound knowledge of the behaviour of the various alloys in the molten state, of the flow of liquids and of the solidification characteristics is necessary. The main factors to be considered when designing for castings are the fact that liquid metals absorb gases and also exhibit shrinkage on cooling.

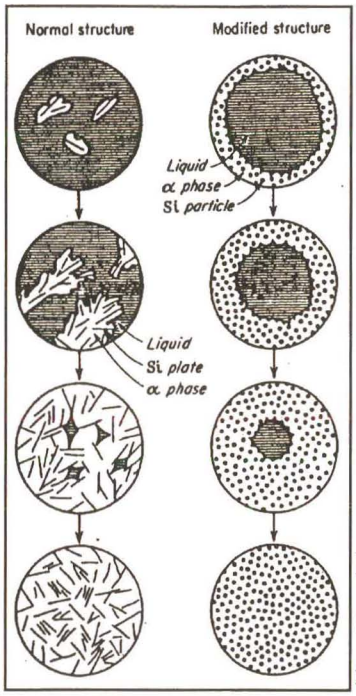

Figure 2.10 Mode of solidification in normal and modified Al-Si alloys. [9]

2.2.2.1 Gas Solubility

The presence of gases in the liquid metal may cause defects in the resulting casting known as gas holes, pin holes, or porosity. This comes about because of the decrease in the solubility of the gases in the metals with a temperature decrease. (figure 2.11).

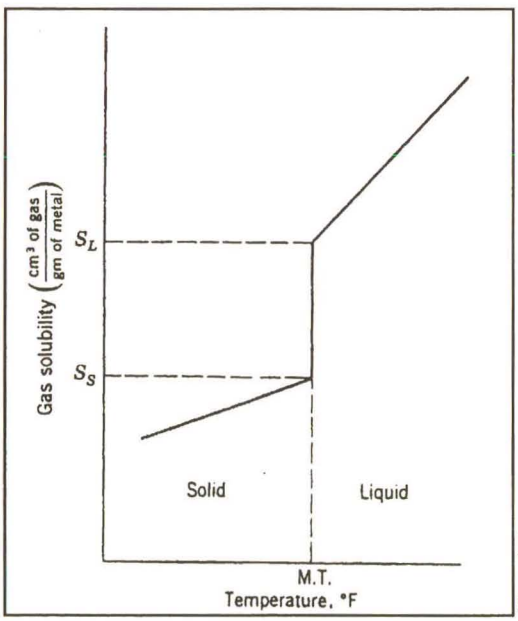

Figure 2.11 Solubility of a gas in a metal as a function of the temperature. [12]

The solubility of the common gases such as hydrogen, nitrogen, moisture and carbon monoxide in liquid metal increases with temperature. The desirability of keeping the amount of superheat to a minimum when melting a metal is readily apparent. Although the gas liberated, as the liquid metal cools to the liquidus temperature, can escape from an open top casting, it requires considerable permeability in a mould that completely surrounds the casting. Also, when a casting is made in a completely enclosed mould, a thin shell of solid forms around the hot liquid metal. As this encased liquid metal cools to the freezing temperature, the liberated gas collects into large bubbles that result in large gas holes within the casting.

Much of the gas that is liberated during solidification becomes trapped within the growing dendrites. In this case the gas is well dispersed in microscopic bubbles throughout the solid, and referred to as micro porosity.

Several techniques are used in foundries to reduce or completely eliminate gas from liquid metal. Melting and casting of the metal can be done in vacuum chambers where there would be no air to dissolve into the melt. The most common technique is to bubble a gas that has a low solubility and no harmful effects, such as chlorine, nitrogen or argon, that removes the hydrogen from the liquid metal. This process is very simple since a porous ceramic tube through which the gas flows is moved around throughout the melt. As the bubbles flow upward, the dissolved hydrogen within the liquid diffuses to these hydrogen depleted regions and mixes with the scavenging gas to form a uniform hydrogen content throughout. As the bubbles float to the surface, the hydrogen and the scavenge gas diffuse out into the atmosphere. If this bubbling is continued for a few minutes, most of the dissolved hydrogen is removed[12].

2.2.2.2 The Freezing Process

The usual freezing process in a mould grows from the outside to the interior. This condition of having a solid-liquid zone growing from the outside inward is referred to as progressive solidification. Gating design in the mould must control this progressive solidification in such a way that no part of the casting is isolated from active feed channels during the entire freezing cycle. This is referred to as directional solidification. Directional solidification is

a product of casting design, location of gates and risers, and the use of chills and other means for controlling the freezing process.

In principle, it means that if a casting is so proportioned and disposed with respect to the feeding system that the sections most distant from the available liquid metal will solidify first, there will be a successive feeding of the contracting metal by still liquid metal until the heaviest last to freeze section is reached. This, in turn, can be fed by extra reservoirs of metal provided for that purpose and referred to as risers. These risers continually supply hot liquid metal to the shrinking casting until it is completely solidified[8].

2.2.2.3 Risers

The primary function of these risers is to feed metal to the casting as it solidifies. Many of the non-ferrous alloys which have an extended solidification range, require excessive and sometimes elaborate feeding systems to obtain sound castings.

Shrinkage is an important factor in determining riser size since a variation in molten metal required for the casting can be expected in the volumetric shrinkage of metals. The riser must supply this variation in molten metal, referred to as feed metal. The riser and the casting it feeds should be considered an integral system because a casting cannot be made sound without adequate feed metal. A relatively small amount of feed metal is necessary to compensate for shrinkage but the metal in risers is subject to the same laws of solidification as the metal in castings. To be effective, a riser must remain fluid at least as long as the casting and be able to feed the casting during this time. The process of providing feed metal during the entire solidification period of the casting involves quite a few variables, some of which will be discussed in the following paragraphs[8].

Riser shape

A casting loses its thermal energy by transferring it to its surroundings by radiation, conduction and convection. The shape requirements can best be described by the following explanation[12].

The rate of heat loss of a casting is given by equation 2.1.

$$q = \rho C_p V \frac{dT}{dt} \quad \ldots (2.1)$$

where:

C_p = heat capacity

ρ = density

V = volume

T = temperature

t = time

This assumes a material with a high thermal conductivity so that no thermal gradients exist within the casting.

The rate of heat flow across an interface or a surface is given by equation 2.2.

$$q = hA\Delta T \quad \ldots (2.2)$$

where:

h = heat transfer coefficient

A = surface area or interface area

ΔT = temperature difference across interface

For a casting completely surrounded by a mould, all of the heat will flow through the casting surface into the mould. By equating the two above equations, the rate of cooling of the casting is given by equation 2.3.

$$\frac{dT}{dt} = \frac{h\Delta T}{\rho C_p} \frac{A}{V} \quad \ldots (2.3)$$

Although these relationships do not include the heat of fusion that is evolved as the metal solidifies, nor does the interface temperature remain constant, they do serve to illustrate the importance of the area to volume ratio. Thus if a casting has a high area to volume ratio, it will have a high cooling rate. Similarly, since it is desired to have the riser freeze more slowly than the casting it is feeding, the riser should have a low surface area to volume ratio.

Probably the first study that yielded quantitative values for the design of risers is the one by Chvorinov[9] in which he showed that the solidification time for a simple casting is related to its shape (equation 2.4).

$$t_f = K\left(\frac{V}{A}\right)^2 \quad \ldots (2.4)$$

where:

t_f = time required for casting to freeze

K = constant that includes the thermal properties of both mould and melt

V = volume of casting

A = area of casting

Since the guiding rule of riser design is that the riser be the last to solidify, the riser itself can be considered as another casting. Then, if $(t_f)_R > (t_f)_C$, it follows that the ratio $\left(\frac{V_R}{A_R}\right)$ must be greater than $\left(\frac{V_C}{A_C}\right)$.

{The subscripts "**R**" and "**C**" refer to riser and casting respectively}.

The relationship is only an approximation since some of the original volume of the riser metal flows into the casting during the early stages of solidification. However, it is accurate enough for a good engineering first approximation in designing riser sizes[12].

Riser size as a function of casting shape

If a cylindrical casting poured on end is to be fed by a riser, it is obvious that this riser must have a diameter at least as large as that of the cylinder. On the other hand, if the same volume of the metal used in the cylindrical casting is distributed over a greater area in the form of a plate, the riser needed to feed this plate will not be as large as the one for the cylinder, since it will not have to remain molten as long as the riser on the cylinder. Therefore, the surface area-volume ratio of the riser can be related to the surface area-volume ratio of the casting[8].

Riser connections to the casting

Riser attachments to the casting determines how well the riser can feed the casting and how readily the riser can be removed from the casting. It may also control to some extent the depth of shrinkage cavity by solidifying just before the riser freezes, thereby preventing the cavity from extending into the casting. Riser neck dimensions for a top riser are given in figure 2.12. These dimensions are for cases where the material surrounding the neck has the same thermal properties as the moulding material used elsewhere. If insulating necks are used, the dimensions may be smaller[8].

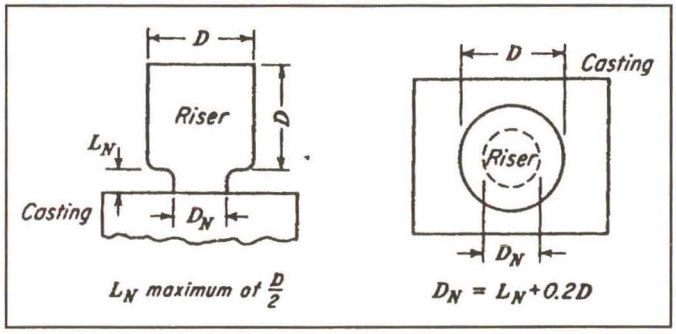

Figure 2.12 Guidelines for a top riser design. [8]

Use of insulators and exothermic compounds

A riser can be made more efficient by employing some artificial means to keep the top of the riser from freezing over so that the molten metal beneath can be exposed to atmospheric pressure. This can be done by use of certain additions made to the surface of the molten metal in the riser, preferably as soon as possible after the metal enters the riser. Insulating effects are obtained by such additions as powdered graphite or charcoal, rice or oat hulls, and refractory powders.Besides supplying insulation on the top of the riser, it is possible to use insulating sleeves to form the sides of the riser, thereby making it possible to secure a lower solidification rate in the riser and hence better feeding of the casting. For non-ferrous work such sleeves can be made from plaster of paris[8].

2.3 Semi Solid Manufacturing Background & Behaviour

Semi solid manufacturing is a process where a casting or forging is performed when the feedstock metal is in the partially remelted state. It displays thixotropic properties where it remains as a soft solid until a shear force is applied to it. The metal then flows like a liquid whose viscosity depends on the magnitude of the shear force. This thixotropic state is achieved when the feedstock is heated to the region between the metal's solidus and liquidus temperature, otherwise known as the semi solid region. The reason for the feedstock metal's thixotropic properties lies in the type of microstructure the feedstock metal contains (figure 2.13).

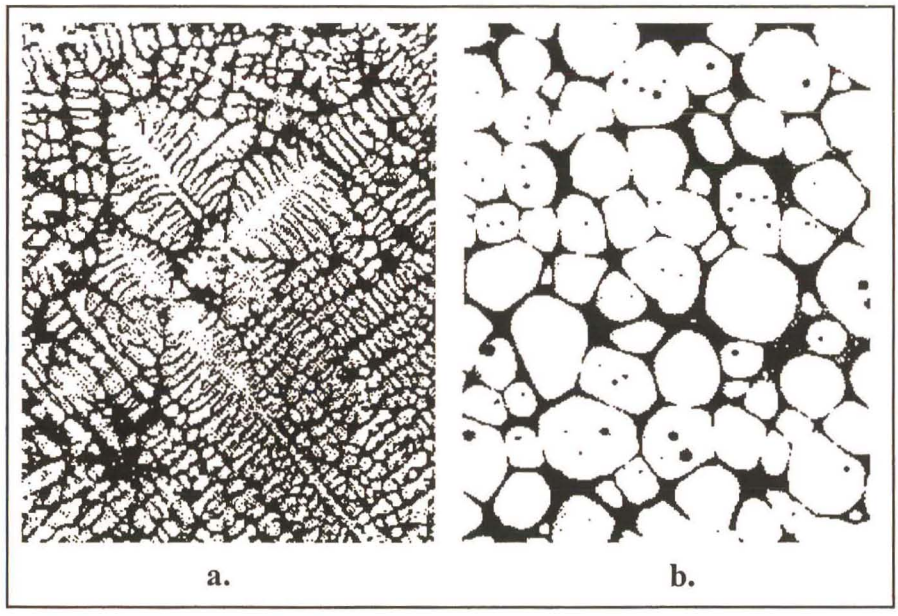

Figure 2.13 **a.** The dendritic microstructure.
b. The microstructure of thixotropic material.

The microstructure present in the normal or raw metal (i.e. as cast metal) is known as the dendritic microstructure. The metal containing this structure does not display thixotropic properties when heated to the semi solid region. The metal's microstructure must contain fine round or spherical grains. When the feedstock is heated to the semi solid region, the solid spherical grains are suspended in a liquid phase. This condition gives the metal its thixotropic properties. The reasons for this phenomenon can be explained with reference to the figure 2.13 as follows.

When the material is heated to the semisolid region the lower melting point phase (known as the eutectic phase) is in the liquid state and is shown as the dark areas in figure 2.13. The light regions of figure 2.13 are the primary phase and are in a solid state when the material is in the semi solid region. Therefore, the material in the semi solid state consists of solid particles suspended in a liquid matrix. The morphology of the solid particles determines the thixotropic properties of the semi solid metal used in semi solid forming processes.

Referring to figure 2.13 a., the solid regions consist of branched, tree-like, solid grains (dendrites) suspended in the liquid phase. When the semi solid material is deformed by a particular forming process, the dendritic branches latch on to each other as they move relative to one another thus resisting easy forming of the semi solid material.

Referring figure 2.13 b., the spheroidal solid grains are suspended in the liquid phase. When the semi solid material is deformed, the solid particles are able to move relative to one another with very little resistance. This results in a material that is readily formed whilst in the semi solid state.

2.4 Methods of Producing Semi Solid Feedstock

Presently, spheroidal structured feedstock for thixoforming can be produced using a number of techniques (figure 2.14). Almost all techniques use shear forces at the solid/liquid interface in order to shear off the dendrites and to reshape them to a spheroidal structure. Exceptions are the SIMA method (Strain-Induced-Melt-Activated) and the use of chemical grain refining treatments.

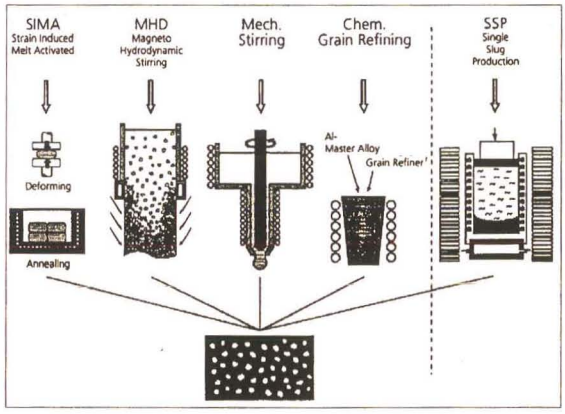

Figure 2.14 Various methods of producing feedstock material with the SSM microstructure. [13]

2.4.1 Strain Induced Melt Activated (SIMA) and Recrystallization and Partial Melting (RAP)

The SIMA and RAP methods use conventional continuous cast round bars. By extruding or cold forming these bars, a high dislocation density is induced in the feedstock. The dislocation density is responsible for the recrystallization of the primary α-phase to a globular structure during the reheating process to the semi-solid-state. The fundamental difference between the SIMA and RAP process is the temperature at which the cast bars have been cold worked. The SIMA process extrudes feedstock above the recrystallization temperature and the RAP process extrudes feedstock below the recrystallization temperature. The SIMA material shows a fine texture. It has some possible advantages when compared with the MHD method, especially for use with difficult to cast materials.

The disadvantages of this method are the high production cost associated with the additional forming step and the restriction to small billets[13].

2.4.2 Chemical Grain Refining

At the beginning of the nineties a new method of chemical grain refining was developed as an innovative technique to produce feedstock. The grain refining offers a simple alternative using special grain refiners (e.g. Al Ti_5Bi). Addition of grain refiners results in heterogeneous nucleation which results in the the globular structure required for the subsequent shaping. The combination of the MHD and grain refining methods shows an increased refinement of the resulting structure[13].

The most common case of grain refinement involves a prealloyed wire which is proportioned into the hot metal flow in a launder which feeds continuous castings lines. The prealloyed wire releases a number of heterogenous (mostly titanium and boron based) crystallizing agents[14].

2.4.3 Mechanical Stirring

The mechanical stirring method (figure 2.15) was one of the first methods used to produce semi solid feedstock. It was a relatively cheap apparatus to develop and was used in the early research into the behaviour of semi solid materials.[2]

The mechanical stirring method shears the molten metal by forcing it into a narrow annular space between two concentric cylinders, one of which is rotating while the other is stationary. The shear rate is developed by the velocity profile between the two cylinder walls. The molten metal is then extracted from this stirring chamber and chilled thereby forming a continuous strand.

The advantages and disadvantages of this method are:

Advantages:

* High shear rates are possible.
* Low power consumption.

Disadvantages:

* Low machine life due to wear in moving cylinder parts.
* Slow production time due to restricted volume flow.

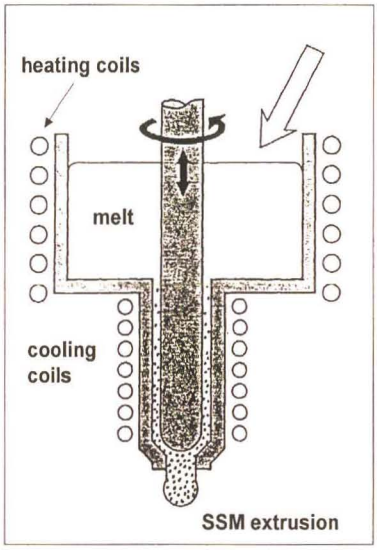

Figure 2.15 The mechanically stirred process. [2]

The mechanical stirring method has not gained popularity in industry because of problems with erosion of the stirring device, problems with synchronization of the stirring with the continuous casting process, and the requirement of a high stirring rate to obtain fine particles[13].

2.4.4 Magneto Hydrodynamic (MHD) Stirring

The most common technique to produce feedstock that is used in industry is the Magneto Hydrodynamic (MHD) stirring technique. Because this method is similar to the conventional continuous casting process, only small modifications of this process are needed[13].

The MHD stirring method shears the molten metal by placing a volume thereof into the path of a moving magnetic field. The shear rate is developed by the velocity profile at the mould wall. The volume of molten metal solidifies by being chilled with water while being stirred thereby forming a billet of semi solid feedstock (figure 2.16).

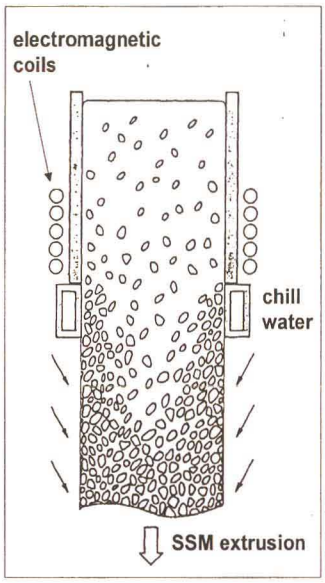

Figure 2.16 The MHD stirred process. [2]

The advantages and disadvantages for the MHD method are:

Advantages:

* No moving parts.
* Little wear.
* Quicker production time due to higher volume flow.

Disadvantages:

* Higher power consumption.

2.4.4.1 The Theory behind the MHD Process

The two critical parameters in this process are the shear rate and the solidification rate. The shear rate has to be large enough to cause the remelting and fragmentation of dendrite arms and also to circulate the molten matrix sufficiently. The solidification rate must allow for

all dendrite arms to be fragmented before the matrix solidifies and also limit the grain growth time so that the primary, fragmented grains do not grow too large. These two parameters have previously been determined on an essentially empirical basis, based on the shear rates and solidification rates which generate as near perfect fine, round grained microstructures as possible. On the other hand, the most efficient process would be one which produced the finest grain size at the highest solidification rates and the lowest shear rates.

For this to occur, there exists a unique relationship between the shear rate and the solidification rate which is universally applicable to all thixotropic metal alloy systems, and it has been shown that a single range of values can be used to specify acceptable operating limits for the ratio of shear rate to solidification rate. The slurry structured metal compositions produced in accordance with the above ratio have a microstructure which combines the best forming or shaping characteristics and the most economical forming costs[15].

2.4.4.2 The Theory behind Producing a SSM Structure

If metal alloy systems were allowed to freeze under equilibrium conditions, the result would be a solid with perfect crystallographic orientation and a uniform composition as determined by the equilibrium phase diagram. In practice such equilibrium conditions are seldom achieved. Dendrites grow as metals freeze because the metals are freezing under various degrees of non equilibrium in which growth rate and temperature gradient considerations are important. The dendrites grow in the crystallographic direction which permits the most rapid transfer of the heat released at the liquid/solid interface and the branching of the dendrites represents an efficient means to distribute the solute[15].

The vigorous agitation of a metal or alloy as it freezes to convert the dendrites to a degenerate dendritic form is a dendrite fragmentation and coarsening process. A dendrite with its multiple branches has a very high surface to volume ratio and therefore a very high total surface energy. As in any other system, the tendency is to minimise the total energy

content and therefore to minimise surface area to volume ratio. This is the driving force which tends to give rise to dendrite coarsening (i.e. the tendency to transform to a morphology which provides the minimum surface energy to volume ratio)[15].

The coarsening process is in direct competition with the freezing or solidification process which is causing the dendrite to form. Thus alloys tend to have large dendrite arm spacings as the cooling rate decreases. (A metallurgical tool for the examination of cast structures is to measure the secondary dendrite arm spacing to determine an approximate cooling rate). Alloys which are cooled very rapidly have very small dendrite arm spacing and therefore very high surface to volume ratios. Alloys which are cooled slowly have coarser particles and thus a lower surface to volume ratio. The vigorous agitation of a metal as it freezes to produce a slurry cast structure is believed to accentuate the degree of liquid motion within the liquid-solid mixture. This enhances the liquid phase transport, which is a key to the coarsening process, thus accelerating the coarsening process[15].

The degree of coarsening can be approximately equated with the degree of agitation, an accurate measure of the latter is shear rate. The coarsening process must remove material from the extremities of the dendrite at about the rate that the freezing process is causing it to form. The range of ratios necessary to achieve the desired balance between the process has been determined experimentally by first determining the microstructure that produces the best forming characteristics (i.e. that which is most economically forged or otherwise formed into a final product). The critical range of ratios of shear rate to solidification rate was then determined to produce that microstructure[15].

The relationship of shear rate to solidification rate is expressed in the ratio (2.5).[15]

$$\frac{\dot{\gamma}}{\left(\frac{\partial fs}{\partial t}\right)} \qquad \ldots (2.5)$$

where

$\dot{\gamma}$ = shear rate (sec^{-1})

∂fs = change in fraction solids (by volume)

∂t = change in time

$\partial fs/\partial t$ = solidification rate (sec^{-1}) (equation 2.6).

$$\frac{\partial fs}{\partial t} = \frac{solid \cdot volume \cdot fraction \cdot of \cdot quench \cdot sample(\partial fs)}{time \cdot of \cdot passage \cdot through \cdot mixing \cdot zone(\partial t)} \quad \ldots (2.6)$$

where

$$\partial t = \frac{volume \cdot capacity \cdot of \cdot mixing \cdot zone}{discharge \cdot flow \cdot rate \cdot of \cdot alloy} \quad \ldots (2.7)$$

The average bulk cooling rate can be calculated (equation 2.8).

$$T_{pour} = \frac{T_{exit}}{\partial t} \quad \ldots (2.8)$$

and since

$$f_L = \phi^{\frac{-1}{1-K}} \quad \ldots (2.9)$$

where

$$\phi = \frac{T_M - T^*}{T_M - T_L} \quad \ldots (2.10)$$

and

f_L = fraction liquid

K = equilibrium partition coefficient

T_L = the alloy liquidus temperature

T^* = exit temperature

T_M = melting point of the pure solvent.

The solidification rate is the rate at which new solid is formed with respect to time and should be equally applicable to all alloys. If this ratio ($\partial fs/\partial t$) is kept between the range $2x10^3$ and $8x10^3$ (preferably from $4x10^3$ to $8x10^3$) good quality shaped components will be produced. If this ratio is allowed to fall below the minimum values then unacceptably

dendritic structures result leading to inconsistent and inhomogeneous flow and properties in the final shaping stage. Ratios in excess of maximum require uneconomical power inputs to provide the required $\dot{\gamma}$ or uneconomically low freezing rates. Also, beyond a certain high $\dot{\gamma}$, turbulence and fluid cavitation is a processing problem, while low freezing rates result in very large grain sizes and poor resultant flow[15].

An acceptable microstructure has been defined as one capable of producing good quality shaped parts (i.e. a part which does not contain chemical segregation to the extent that major variations in mechanical properties will occur from region to region). The finer and rounder the solid particles (degenerate dendrites), the more homogeneous the semi solid flow. Variations in fraction solid which occurs in the shaped parts because of poor microstructure and consequent inhomogeneous flow is also indicative of a chemical difference which will affect such factors as corrosion, plate ability and mechanical performance.

However, it is unnecessary to generate as near perfect spheres as possible to obtain good quality shaped components. The microstructure of successful compositions contains discrete degenerate dendritic particles which typically are substantially free of dendritic branches and approach a spherical shape; the particles are less than perfect spheres[15].

In practice, a predetermination is made of the microstructure of a shaped metal part having acceptable forming properties and good quality. After this, the metal is heated until it is entirely molten and then added to a heated mould equipped with agitation means (mechanical or magnetic). The solidification rate is then measured and either the solidification rate, the shear rate or both are adjusted to fall within the foregoing range for the ratio of shear rate to solidification rate.

The shear rate may range as low as 50 sec^{-1}, but will normally fall from 500 sec^{-1} to 800 sec^{-1}. Any solidification rate may be used which, in the absence of agitation, would produce a dendritic structure. The specific value of the ratio of shear rate to solidification rate is selected by comparison of the microstructure of various ratios with that of the predetermined microstructure[15].

2.4.4.3 Microstructure Evolution of SSM Materials

When the temperature reaches below the liquidus of an alloy, nucleated primary crystals begin to grow in a dendritic pattern within the molten alloy. However such dendritic primary crystals tend to transform into a rosette and/or spheroidal shaped crystals if the molten alloy is stirred vigorously.

Some experimental observations such as fragmentation of the primary dendrite crystals, spheroidisation of the primary crystals, and coalescence of the primary crystals are considered to be responsible for such a morphological change[16]. Five steps, which are time and temperature dependant, may be identified in a partly solidified casting , starting with the separation of dendritic side arms in the mushy columnar region and ending with the blocking of the columnar front by a network of equiaxed grains[17] (figure 2.17). The five steps in the cycle are:

1. Columnar growth / dendrite fragmentation.
2. Fragment transport from mushy region.
3. Melting vs. survival
4. Growth and sedimentation.
5. Columnar / equiaxed transition.

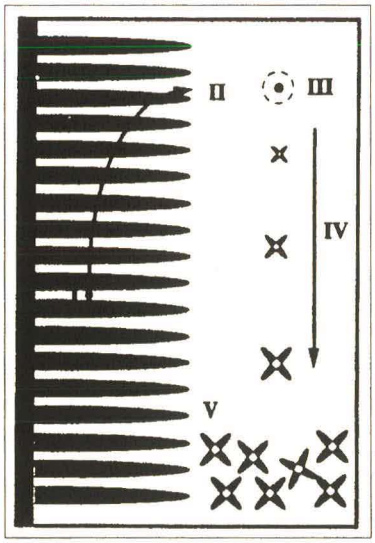

Figure 2.17 The grain evolutionary cycle. [17]

Step 1: In the initial stages of stirring, the dendrites formed are remelted and fragmented into smaller particles. The metallic dendrites do not break mechanically in the course of a casting operation. They may be plastically bent, but some simple estimates based on bending moments and fluid flow calculations indicate that this will be a rare event[17]. The dendritic crystals exist as a permeable array attached to the mould walls or as relatively isolated dendritic crystals floating about in open liquid, being swept along with the liquid in natural or induced flow patterns. To cause detachment of the columnar dendritic grains at the mould wall, the local temperature and/or the local solute concentration must rise so that the arms melt off at the necked roots[17].

Step 2: The fragmented dendrites are transported to the open liquid regions by fluid flow caused by natural convection and/or induced stirring. Natural convection (or thermalsolutal convection) occurs because there are density variations caused by temperature and composition gradients. Usually, the composition dependance density exceeds that of temperature dependance density. This causes the solute enriched interdendritc liquid to become more or less dense than the open liquid, therefore the liquid tends to rise or sink within the mushy region. This fluid flow spews many dendrite fragments into the open melt. With electromagnetically induced liquid stirring, the fluid flow may not significantly penetrate the permeable dendritic array of the mushy zone. However, the fragments that escape by thermosolutal convection, are rapidly swept away into the open liquid to provide nucleation sites for further grain growth[17].

Step 3: Without stirring, these fragments are unlikely to survive long in the warmer liquid before they remelt and dissolve into the liquid. However, the ambient liquid temperature falls continuously ahead of the columnar front due to a small solute accumulation at the dendritic front and the liquid in this region becomes slightly supercooled. With imposed stirring, the fragments can be transported into these cooler regions and have a much higher chance of survival than in a quiescent liquid. This may be one reason why liquid stirring favours a refined equiaxed structure[17].

Steps 4 and 5: When a fragment reaches liquid at a temperature below the liquidus, it begins to grow dendritically. Due to the induced stirring, there is a cloud of growing

dendritic crystals. When the number and size of these grains reach a certain level, continued growth of the initial front is blocked and the columnar to equiaxed transition has occured[17].

The essential point is that fragmentation or crystal multiplication takes place by local remelting. Fluid flow due to induced stirring does not break up the structure in a mechanical sense but rather it disperses the remelted fragments which subsequently form equiaxed grains due to the liquid circulation[17].

In addition, the reduction of the interfacial energy between particles and liquid provides the driving force for spheroidisation of the particles. Oswald ripening would also take place, wherein solutes diffuse from small particles to larger particles resulting in the coarsening phenomenon. Stirring would enhance the ripening by accelerating solute diffusion. At this stage a rosette type of structure would form. A further mechanism also prevails, which is structure agglomeration due to bond formation among particles caused by impingement and reaction. As the stirring time increases, the structure evolution is governed by the balance among dendritic fragmentation, Oswald ripening, and structure agglomeration. As particles become further spheroidized, the dendrite fragmentation mechanism becomes less and less prevalent. A second rosette type of structure due to particle coalescence may develop when the agglomeration mechanism dominates. In the subsequent stage a steady state may be reached with the structure agglomeration, after which the Oswald ripening might become the prevalent mechanism[18].

In the initial stage of stirring, the dendrite fragmentation dominates, for which a high shear rate would lead to a smaller particle size. In the subsequent stage, when the Oswald ripening dominates, a higher shear rate would enhance the solute diffusion, thus accelerating the coarsening resulting in a larger particle size. The average grain size decreases as the shear rate increases, which should happen in the initial stage of stirring when dendrite fragmentation is dominant. The sphericity increases as the shear rate increases because the spheroidizing mechanisms, the reduction of the interfacial area, is enhanced by the higher shear rate[18].

When the controlling mechanism for Oswald ripening is volume diffusion during coarsening, the average particle radius increases with time (equation 2.11).[18]

$$r^n - r_0^n = k \cdot t \quad \ldots (2.11)$$

where:

k = coarsening rate constant

n = coarsening exponent (n = 3 for volume diffusion)

t = time

r_o = radius of particle at t = 0

r = radius of particle at time t

The coarsening exponent n would be 4 for grain boundary diffusion, 3 for volume diffusion and 2 for interfacial reaction controlled coarsening. Results from experimentation with constant shear rate and stirring time with varying rest times after stirring showed that the grains became coarsened as the rest time increased (figure 2.18). The plot of average grain size vs. the rest time after stirring shows a slope, the reciprocal of the coarsening exponent, which was calculated to be 3.2. This indicates that the coarsening of particles during the rest time following stirring is controlled by the particle volume diffusion. Sphericity increases as the rest time increases because the spheroidising mechanisms were in operation for a longer time[18].

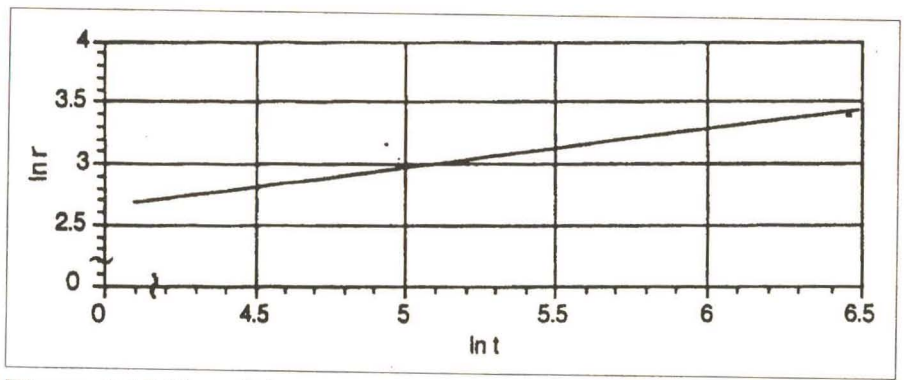

Figure 2.18 Plot of the average grain size vs the rest time. [18]

In the presence of stirring where liquid convection and grain rotation must be considered, the grain size has been shown to increase with stirring time. However, results from

experimentation with constant shear rates and rest time after stirring with increasing stirring times have shown that the grain size decreases with stirring time. It has been determined, however, that a stirring time of less than 600 sec. is still in the initial stage of stirring where the dendrite fragmentation mechanism is dominant, resulting in a smaller grain size as stirring time is increased. There is a critical stirring time, below which the grain size decreases with stirring time, while above which the grain size increases with stirring time[18].

Summary[18]

1. The grain size decreases and the sphericity increases as the shear rate increases for short stirring times at 600 ^{0}C.
2. Both the grain size and sphericity increase as rest time following stirring increases, for constant shear rate and stirring time. The coarsening exponent is 3.2 suggesting that the coarsening is controlled by volume diffusion of the grains.
3. For a stirring time less than 600 sec., the grain size decreases and sphericity increases with the stirring time for a constant shear rate and rest time after stirring. This suggests that dendrite fragmentation is dominant. It is proposed that there is a critical stirring time, below which the grain size decreases with stirring time, while above which the grain size increases with stirring time.

2.4.4.4 Electromagnetic Stirring Equipment

Two electromagnetic stirring techniques are suggested to provide the MHD stirring effect. AC or pulsed DC magnetic fields are used to produce indirect stirring of the solidifying melt. While the indirect nature of the of the electromagnetic stirring is an improvement over the mechanical process, there are still limitations imposed by the nature of the stirring technique.[19, 20, 21]

With AC inductive stirring, the maximum electromagnetic forces and associated shear are limited to the penetration depth of the induced currents. Accordingly, the section size that can be effectively stirred is limited due to the decay of the induced forces from the periphery to the interior of the melt. This is particularly aggravated when a solidifying shell is present.

The inductive electromagnetic process also requires high power consumption and the resistance heating, due to induced currents in the melt, in turn increases the required amount of heat extraction for solidification.[19, 20, 21]

The pulsed DC magnetic field technique is also effective, however, it is not as effective as desired because the force field rapidly diverges as the distance from the DC electrode increases. Accordingly, a complex geometry is required to produce the required shear rates and fluid flow patterns to insure production of slurry with a proper microstructure. Large magnetic fields are required for this process therefore the equipment is very costly and bulky.[19, 20, 21]

In order to overcome the disadvantages of inductive electromagnetic stirring, it has been found that electromagnetic stirring can be made more effective if a magnetic field is rotating transversely of the mould or casting axis. One or more multi poled, AC stators are arranged about the mould in order to stir the molten metal to provide a sufficiently high shear rate. In this application, a rotating magnetic field generated by a two pole, AC multi phase motor stator is used to achieve the required high shear rates.[19, 20, 21]

The electromagnetic stirring inductors

Electromagnetic stirring induces fluid flow in the liquid metal without any physical contact with a stirrer. The inductor coils carry an alternating current within close proximity of the molten metal thereby inducing eddy currents into the melt. This creates the stirring motion required to produce the desired shear rate.

Depending on the pattern of the inductor coils, two fundamental motions may be produced, namely axial stirring and tangential stirring (figure 2.19 a. an b. respectively). Axial stirring forces the melt into diametrically opposite circulations parallel to the longitudinal axis of a cylinder (i.e. up the longitudinal axis and down the mould wall or *vice versa*). The inductor coil pattern is shaped like a spiral or coil spring around the mould and produces a magnetic field travelling parallel to the longitudinal axis, over the spiral coil. The depth of penetration of the field into the melt is dependant on the current and frequency of the electrical power

applied to the coil. Current and frequency capacities to the order of 10^3 (A, Hz) are typical for this application.

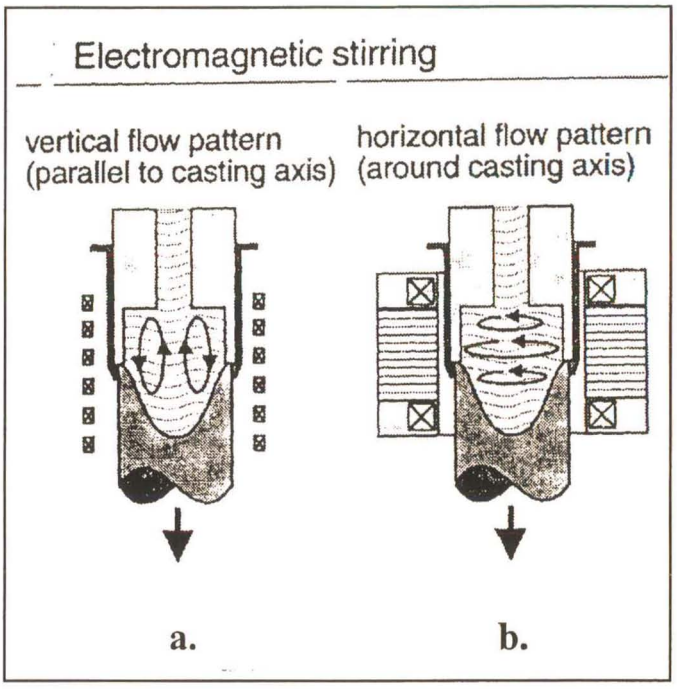

Figure 2.19 **a.** Axial stirring pattern.
b. Tangential stirring pattern. [14]

Single phase, AC power supplies are usually used to generate a changing magnetic field that induces eddy currents into the molten metal. However, the eddy currents tend to vibrate rather than stir the metal since the field changes from one direction to the opposite at one spot. To overcome this problem, a three phase power supply is used to produce a travelling magnetic field to generate eddy currents that travel within the molten metal and thus stir it.

Tangential stirring forces the melt to rotate about the longitudinal axis of a cylinder (e.g. stirring tea in a teacup). The inductor coil pattern is a series of longitudinal bars equally spaced around the circumference. This pattern is typically found in induction motor stator cases. The magnetic field produced with this layout cuts normal to the longitudinal axis and the depth of penetration not only depends on the current and frequency but also the number of poles of the stator since this affects the field pattern. The field forms a loop around a pole, normal to the longitudinal axis. Hence, if there were four poles, there would be four loops

of field, dividing the cross section into quarters (figure 2.20 a.). Similarly, for two poles, there would be two loops of field, dividing the cross section into halves (figure 2.20 b.).

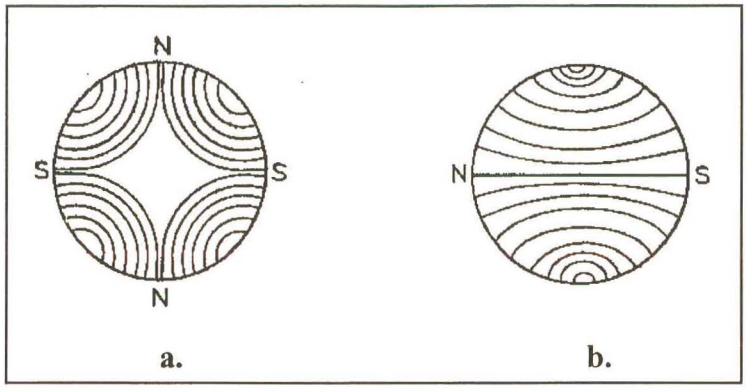

Figure 2.20 **a.** The four pole field pattern.
b. The two pole field pattern. [20]

The two pole layout indicates that it would be more suitable for semi solid production because the field lines travel right through the centre of the billet generating a non zero field across the entire cross section of the mould [19, 20, 21, 22]. This overcomes the problem of the limited depth of penetration of the previous coil layout, thereby requiring much less electrical power to operate. Typical current ratings are in the order of 10^1 A and frequency ratings in the order from 10^1 to 10^2 Hz.

Three phase power supplies are also used in this regard to generate a rotating magnetic field that causes the induced eddy currents to rotate about the longitudinal axis, thus stirring the molten metal. In fact, this system is a direct representation of a three phase induction motor. Due to the alternating nature of the fields, an oscillating magnetic field **B** and an electrical current density field **j** are induced in the liquid metal[23]. An electromagnetic force[24] or Lorentz force field $\mathbf{F} = \mathbf{j} \times \mathbf{B}$[23, 24, 25] appears (figure 2.21) which, due to its non-zero time average, has a rotational component which is responsible for fluid motion[23].

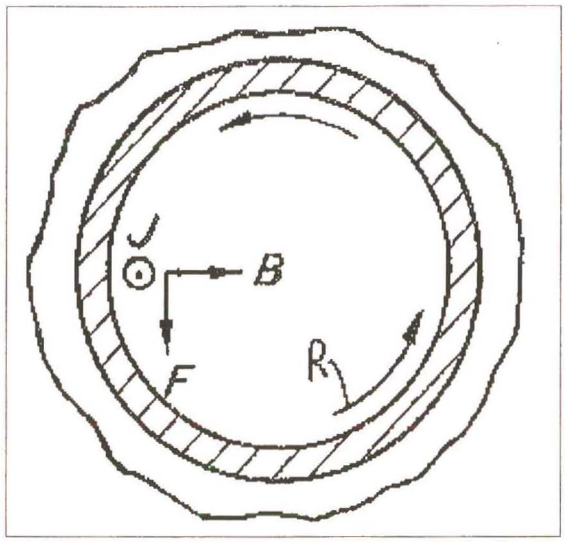

Figure 2.21 Instantaneous fields and forces which cause the molten metal to rotate. 19, 20, 21]

In both of these systems (i.e. the axial and tangential stirrers) the shear rate depends on the velocity of the travelling field. The adjustment of the velocity of the travelling field, hence the adjustment of the shear rate, can be achieved by:

a. changing the number of poles of the inductor.
b. changing the line frequency of the electrical power supply.

Method a. requires the modification of the coil windings and offers a very limited control over the adjustment of the velocity. Method b. requires the use of a variable frequency power source and offers infinite control over the adjustment range of the velocity.

Horizontal stirring turns out to be more efficient than vertical stirring for the following reasons:

- In vertical stirring, the rotational component of the Lorentz force is small compared to its gradient component, which has no effect on fluid motion (it only contributes to static pressure). This effect leads to fluid velocities of about 5 times smaller than the case of horizontal stirring for a same value of the electrical power applied to the

inducting elements. In horizontal stirring (figure 2.22), the Lorentz force is almost purely rotational[23].

- In vertical stirring, fluid motion does not follow isotherms and velocities are extremely small near the mushy zone at the ingot centre (figure 2.23). This gives a heterogenous grain structure[23].

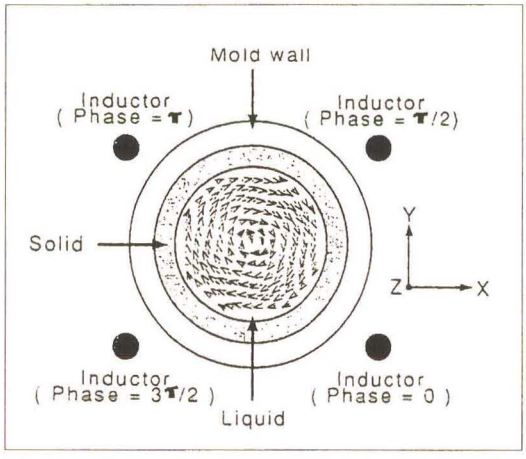

Figure 2.22 Liquid metal velocity field in the case of horizontal stirring. [23]

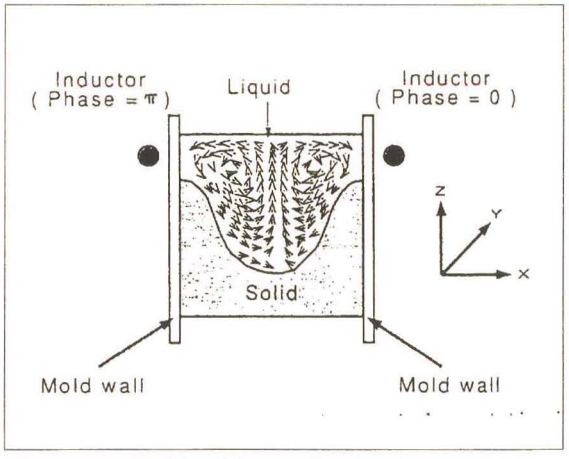

Figure 2.23 Liquid metal velocity field in the case of vertical stirring. [23]

2.4.4.5 MHD Stirred Feedstock Production Processes

The semi solid feedstock which is produced with the MHD method can be done using one of two processes. It may be produced as a single slug (figure 2.24 a.), or it may be continuously extracted through the magnetic field and then chilled to form a continuous strand, (figure 2.24 b.).

The Single Slug Process (SSP)

This method is an alternative to the established MHD continuous casting technology that allows the production of near net shape billets. The SSP method provides the flexibility to change alloys rapidly and the capability to process alloys that are usually difficult to cast, both of which are technological advantages. Of economical significance is the reduction in energy consumption due to the fact that the hot billet can be used immediately after production[13].

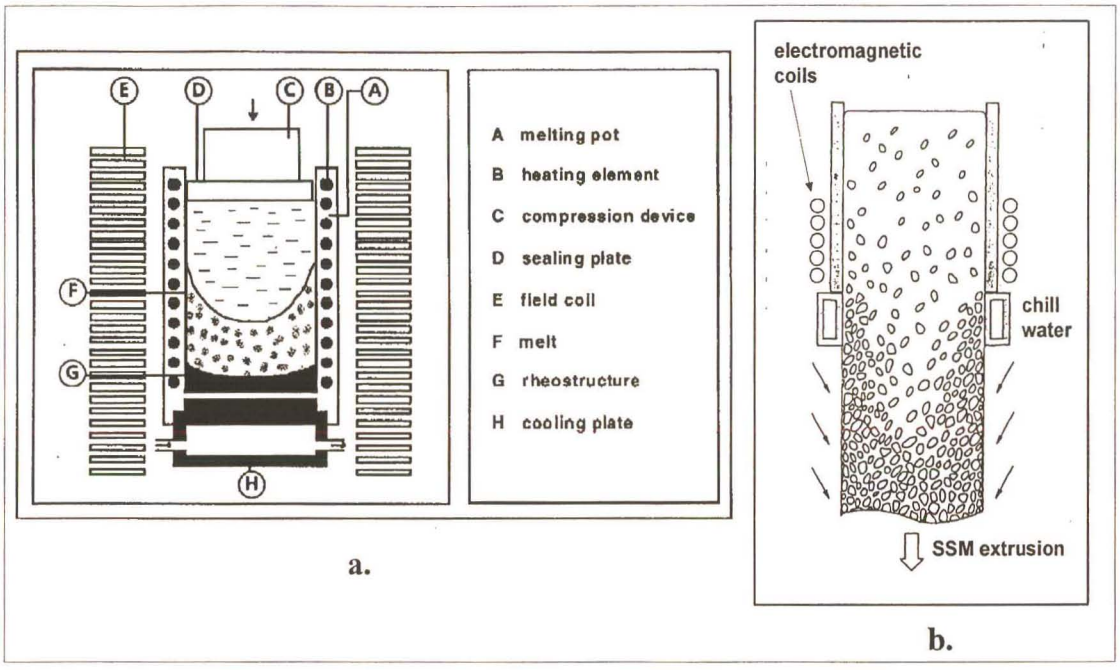

Figure 2.24 **a.** The MHD Single Slug Process (SSP) apparatus. [13]
b. The MHD continuous casting process. [2]

The SSP-process is a possible alternative to other known technologies, especially to the MHD technique. It exhibits the following technological and economical advantages[13]:

* High flexibility for rapidly changing between alloys.
* Handling of difficult to cast alloys and alloys with hot crack susceptibility (wrought alloys or high tensile alloys).
* Billets have 'near-net shape" quality (lower production costs due to fewer production steps).
* Energy savings because the billet that is still warm after the production process can be directly processed in the heating device.

Concept and construction of the SSP device

The spheroidal structure is generated in the same way as in the MHD method. A magnetic field causes a stirring of the molten mass. The growing dendrite structure is destroyed by the shear forces generated by the flow. With the SSP process, billets can be produced in near-net shape quality. That means the billet can be processed directly in the heating device without any modifications. An economical production of billets with regard to an industrial series

production can be achieved with the use of several, parallel producing SSP devices, a high energy utilisation and a fast feeding of the reheating device.

A schematic illustration of the SSP pilot plant is shown in figure 2.24 a. The melting pot consists of two cylindrical high grade steel tubes. The inner tube has four resistance coil heaters at the outside which are used to preheat the mould. Each heating coil is controlled separately Therefore, it is possible to adjust them in a way that generates a temperature gradient leading to directional solidification of the billet. A graphite mould was put inside the steel tube and a graphite disc was put at the bottom of the mould. Graphite is an appropriate material for this task because it is resistant to molten aluminium and it has a good resistance against thermal shocks. The outer steel tube serves the dual purpose of preventing heat loss and providing a fixture for mounting of the copper chill plate. The combination of parts yields a complete unit consisting of a heated graphite mould with a water cooled copper plate. The cooling water flows inside the copper plate and is controlled by a flow regulator. To prevent macro-shrinkage at the top of the billet, which originates from the solidification contraction of the metal, a special compression device is used. A graphite disc that is preheated to 400 - 500 ^{0}C is used to seal the mould and the molten material. A continuous contact between molten material and graphite disc is achieved by continuous cycling of the pressurization of the compression device[13].

The MHD Continuous Casting Process

The continuous casting production process consists of a chilled mould and a moving end plug at one end of the mould while the other end is open to a tundish of molten metal. Electromagnetic inductor coils are placed over the solidification zone of the mould which stirs the molten metal as it solidifies (figure 2.25). Initially, the end plug is inserted into the mould exit and the molten metal solidifies onto it thereby locking the end of the continuous strand thereon. The end plug is then slowly extracted, pulling the strand as it solidifies while exiting the mould. The electromagnetic stirrers are operating continuously during the extraction. Once the end plug has reached the end of its run, the molten metal supply is stopped, the stirrer coils switched off and the strand removed to be cut into segments.

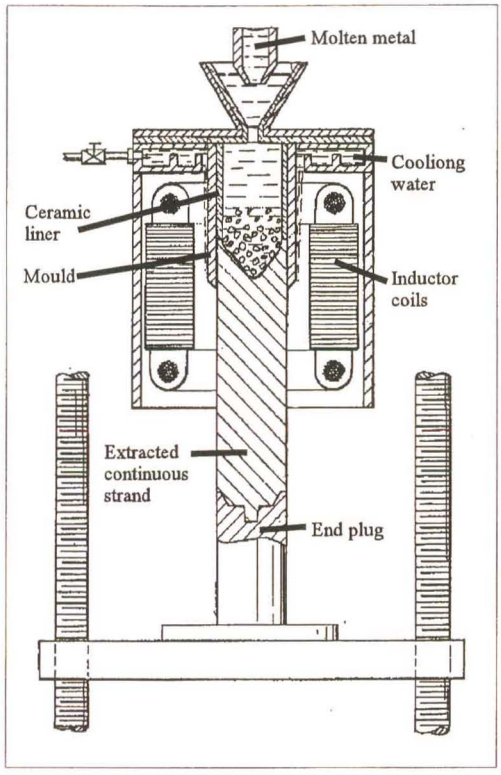

Figure 2.25 The continuous casting production apparatus. [20]

The mould for this process is specifically designed to control the solidification rate (i.e. the cooling rate) of the molten metal as it passes from entrance to exit of the mould. The molten metal must be in the semi solid region as it passes through the stirring magnetic field. This is achieved by controlling the heat transfer along the length of the mould by placing ceramic liners to retard the heat flow and extra cooling fins on the outer mould wall to promote heat flow. Direct chill methods are used to solidify the exiting strand.

2.4.5 Summary of the Process of Producing SSM Feedstock

The apparatus (figure 2.25) will continuously or semi-continuously cast thixotropic semi solid metal from a cylindrical mould. The mould may be formed of any desired non-magnetic material such as austenitic stainless steel, copper, copper alloy, aluminium or aluminium alloy. The apparatus and process are particularly adapted for making cylindrical ingots utilizing a conventional two pole polyphase induction motor stator for stirring. The magnetic field moves around the mould in a direction normal to the longitudinal axis of the casting[19].

The bottom block, a standard direct chill casting type block, of the mould is arranged for the movement from within the confines of the mould cavity to a position away from the mould as the casting forms a solidifying shell. Lead screws or hydraulic means are used to raise or lower the bottom block at a desired casting rate.

A cooling manifold is arranged around the mould wall. A coolant jacket, formed from a non magnetic material, is attached to the mould and a discharge slot is defined by the gap between the coolant jacket and the outer surface of the mould. The coolant serves to carry heat away from the molten metal via the mould wall and discharges directly against the solidifying ingot. A suitable valving arrangement is provided to control the flow rate of the coolant discharged in order to control the solidification rate of the melt. The molten metal which is poured into the mould is cooled under controlled conditions by means of the water sprayed upon the outer surface of the mould. By controlling the rate of water flow against the mould surface, the rate of heat extraction from the molten metal within the mould is partly controlled.

A two poled, multi phase induction motor stator is arranged surrounding the mould to provide a means for stirring the molten metal within the mould. Although any suitable means for providing power and current at different frequencies and magnitudes may be used, the power and current are preferably supplied to the stator by a variable frequency generator. A two poled three phase induction motor stator is used because there is a non zero field across the entire cross section of the mould. It is therefore possible to solidify a strand having the desired semi solid structure over its full cross section[19].

As the thixotropic slurry rotates within the mould , centrifugal forces in the cavity cause the metal to try advance up the mould wall. A partially enclosing cover is used to prevent the spill out of the molten metal due to the stirring action induced by the magnetic field of the motor stator. The cover comprises a metal plate, lined with a suitable insulating lining, arranged above the manifold and includes a funnel opening through which molten metal flows into the mould cavity. The funnel portion of the cover also serves as a reservoir of molten metal to keep the the mould filled in order to avoid the formation of a U-shaped cavity in the end of the casting due to centrifugal forces[19].

A further advantage of the rotary magnetic field stirring approach is associated with the Flemings right hand rule (figure 2.22). The force vector **F** is tangential to the to the heat extraction direction and is therefore normal to the direction of dendrite growth. By obtaining a desired average shear rate over the solidification range, i.e. from the centre to the inside of the mould wall, improved fragmenting of the dendrites as they grow may be obtained. This improves the quality of the slurry cast structure. The stirring force field generated by the stator must extend over the full solidification zone of molten metal and thixotropic slurry, otherwise the structure of the casting will comprise regions within the field of the stator having a semi solid structure and regions outside the stator field tending to have a non semi solid structure[19].

Under normal solidification conditions, the periphery of the ingot will exhibit a columnar dendritic grain structure. In order to eliminate this outer dendritic layer the thermal conductivity of the upper region of the mould is reduced by means of a partial mould liner formed from an insulator such as ceramic. The ceramic mould liner extends from the insulating liner of the mould cover down into the mould cavity for a distance sufficient for the magnetic stirring force field, of the two pole motor stator, to be intercepted in part by the ceramic mould liner. The liner postpones solidification, due to the low heat extraction rate, until the molten metal is in the region of the strong magnetic stirring force and thereby helps the resultant slurry to have a degenerate dendritic structure throughout its cross section.

Below the region of controlled thermal conductivity, the normal type of water cooled metal casting mould is present. The high heat transfer rates associated with this portion of the mould promotes ingot shell formation. Even the peripheral shell of the casting may consist of degenerate dendrites because of the zone of low heat extraction rate.

In order to form the semi solid microstructure at the surface of the casting, any initial solidified growth must be fragmented from the mould liner. This can be accomplished by ensuring that the field associated with the motor stator extends over at least that portion at which solidification is first initiated[19].

The dendrites which initially form normal to the periphery of the casting mould are readily fragmented due to the metal flow resulting from the rotating magnetic field of the induction motor stator . The dendrites which are fragmented continue to be stirred to form degenerate dendrites until they are trapped by the solidifying interface. Degenerate dendrites can also form directly within the slurry because the rotating stirring action of the melt does not permit preferential growth of dendrites. To ensure this, the stator length should preferably extend over the full length of the solidification zone. In particular, the stirring force field associated with the stator should extend over the full length and cross section of the solidification zone with a sufficient magnitude to generate the desired shear rates[19].

To form a semi solid microstructure casting using the apparatus, molten metal is poured into the cavity while the motor stator is energised by a suitable three phase AC current of a desired magnitude and frequency. After the molten metal is poured into the mould cavity, it is stirred continuously by the rotating magnetic field produced by the motor stator. Solidification begins from the mould wall, where the highest shear rates are generated, and at the advancing solidification front. By properly controlling the solidification rate the desired thixotropic slurry is formed in the mould cavity. As a solidifying shell is formed on the casting, the bottom block is withdrawn at a desired casting rate[19].

The two competing processes, shearing and solidification, are the controlled variables in the system. The magnetic induction field rotation frequency and the physical properties of the molten metal combine to determine these resulting motions. The contribution of the above properties of both the process and the melt can be summarized by the formation of two dimensional groups, namely β (equation 2.12) and **N** (equation 2.13).

$$\beta = \sqrt{j2\pi f \sigma u_0 R^2} \quad \ldots \textbf{(2.12)}$$

$$N = \frac{\sigma R^2 \langle B_r \rangle_0^{\,2}}{\eta_0} \quad \ldots \textbf{(2.13)}$$

where:

$$j = \sqrt{-1}$$

f = line frequency

σ = melt electrical conductivity

μ_0 = magnetic permeability

R = melt radius

$\langle B_r \rangle$ = radial magnetic induction at wall

η_0 = melt viscosity

The first group ,β , is a measure of the field geometry effects while the second group, **N**, appears as a coupling coefficient between the magnetomotive body forces and the associated velocity field. The computed velocity and shearing fields for a single value of β as a function of the parameter **N** can be determined[19].

From these parameters it has been found that the shear rate is a maximum toward the outside of the mould. This maximum shear rate increases with increasing **N**. It has been recognized that the shearing is produced in the melt because the mould wall is rigid. Therefore, when a solidifying shell is present, shear stresses in the melt should be maximised at the liquid-solid interface. Furthermore, because there are always shear stresses at the advancing interface, it is possible to make a full section ingot with the appropriate degenerate dendritic semi solid microstructure.

It has also been found that operating within a defined range of line frequencies can produce a desired shear rate for attaining a desired cast structure at reduced levels of power consumption and current and that efficiency is improved due to reduced heating losses in the stator[19].

The ability to define a range of operating line frequencies enables the quality of the structures being produced to be markedly improved in that the degenerate dendrites become more spheroidal in shape as a result of the increased stirring effect at reduced levels of power consumption and current. It is an important guide in the selection of a frequency to

minimize stator heating while generating a desired average shear rate for any specific casting size. Stator heating is the result of the magnetising current. By using a variable frequency generator to control the line frequency in accordance with the above equations, the improved efficiency, reduced power consumption and minimization of wasteful stator heat can be achieved[19].

Figure 2.26 shows examples of desired frequencies for producing reduced power consumption vs. the effective cross section diameter of an aluminium alloy slurry being cast in a ¼" thick aluminium mould, copper mould, and austenitic stainless steel mould.

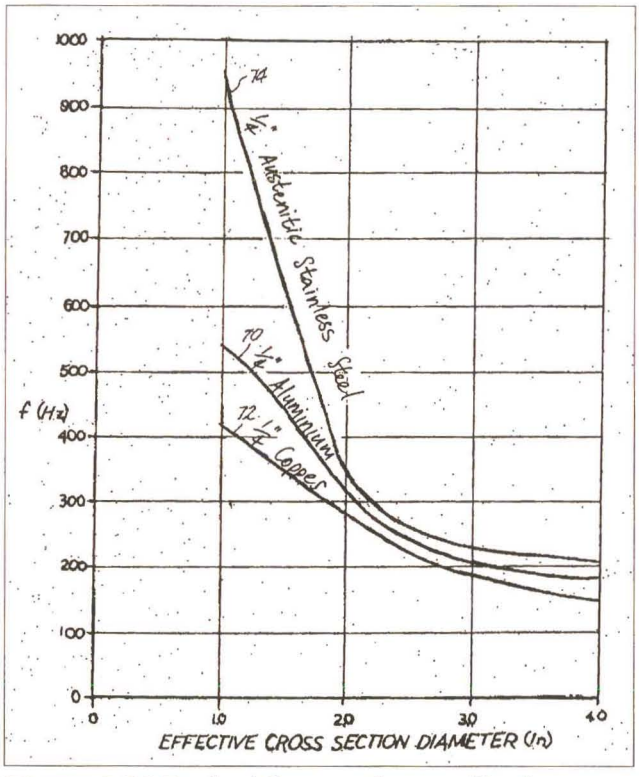

Figure 2.26 Desired frequencies vs effective cross section diameter of a mould. [19]

Suitable shear rates for carrying out the process comprise from at least 400 s^{-1} to 1500 s^{-1}. For aluminium and its alloys a shear rate from about 700 s^{-1} to about 1100 s^{-1} has been found desirable[19].

The average cooling rates through the solidification temperature range of the molten metal in the mould should be from about 0.1 °C per minute to about 1000 °C per minute. For

aluminium and its alloys, an average cooling rate from about 40 °C per minute to about 500 °C per minute has been found to be suitable. The efficiency of the magnetohydrodynamic stirring allows the use of higher cooling rates than with other stirring processes. Higher cooling rates yield highly desirable finer grain structures in the resulting casting[19].

The parameter β^2 (equation 2.12), should range from about 1 to 10 and preferably from about 3 to 7[19].

The parameter **N** (equation 2.13), should range from 1 to 1000 and preferably from about 5 to 200[19].

The line frequency *f* for casting of an aluminium alloy having a radius from about 1 to about 10 inches should be from 3 to 3000 Hz and preferably from about 9 to 200 Hz[19].

The magnetic field strength which is a function of the line frequency and the melt radius should comprise for aluminium alloy casting from about 50 to 1500 gauss and preferably from about 100 to 600 gauss[19].

2.4.6 Comparisons of Microstructures Produced by SSP and MHD Continuous Casting

Although no exact statement about the ideal feedstock structure can be made, conclusions from the investigated SSP-structure can be made regarding the peculiarities and the advantages of this material. A representative cutting of the SSP and MHD microstructures is shown in figure 2.27. The α phase in the MHD-structure exists in the form of dendrite fragments that are often combined into small "groups". This phenomenon leads to a formation of agglomerates of the α particles. The SSP material has a completely different microstructure. The rounded and isolated particles of the α phase are uniformly distributed in the eutectic phase. Consequently, the SSP material requires a shorter reheating time since it already has the necessary globular structure. Because of this special microstructure some advantages in the reheating and the forming process can be expected[13].

2.4.7 Characterisation of the Reheated SSP and MHD Continuous Cast Materials

In the reheated state the MHD-materials also have a globular α phase (figure 2.28 b.). It can be seen that the particles of the α phase have many inclusions of eutectic phase. A possible reason for the formation of the eutectic "islands" might be the structure of the MHD feedstock (figure 2.17 b.). As cast, the MHD microstructure appears like a network of α particles. Because of the coarsening process that take place during the reheating cycle, the fragments of the α phase can grow together. The consequence is that the eutectic lying between the particles is included in them. Therefore, a part of the liquid phase is not available for the forming process. This leads to a decreasing flowability of the MHD material. This phenomenon did not occur in the SSP material (figure 2.28 a.) because the α particles are already isolated as cast and therefore the inclusion of eutectic is prevented.

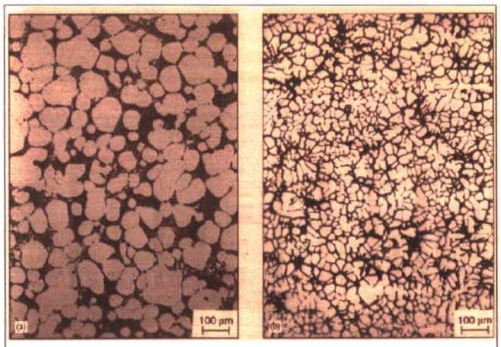

Figure 2.27 a. The spheroidal α structure of the SSP process prior to reheating.

b. The fragmented α structure of the MHD process prior to reheating. [13]

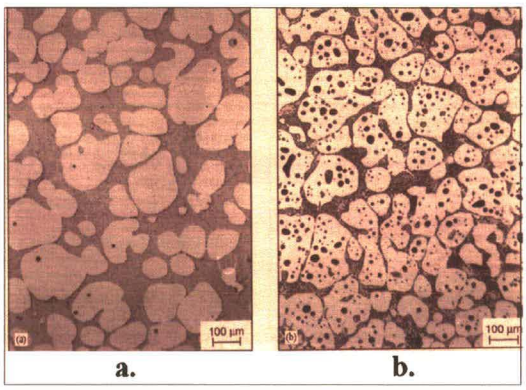

Figure 2.28 a. The reheated SSP material is nearly free of eutectic inclusions.
b. A large number of eutectic islands are present in the primary particles of the reheated MHD material. [13]

With an interactive image analysis system, it was possible to determine the fineness of the SSP structure that has an important influence on the flowability of the material in the casting process. The particle diameter of the primary phase in the reheated state was the measured variable. Comparison of the primary phase grain diameter (figure 2.29 b.) and shape factor (figure 2.29 a.) Showed that the SSP material had comparable grain diameters and an improved shape factor. The shape factor of the SSP material is about 3% better when compared with the MHD material (figure 2.29 a.).

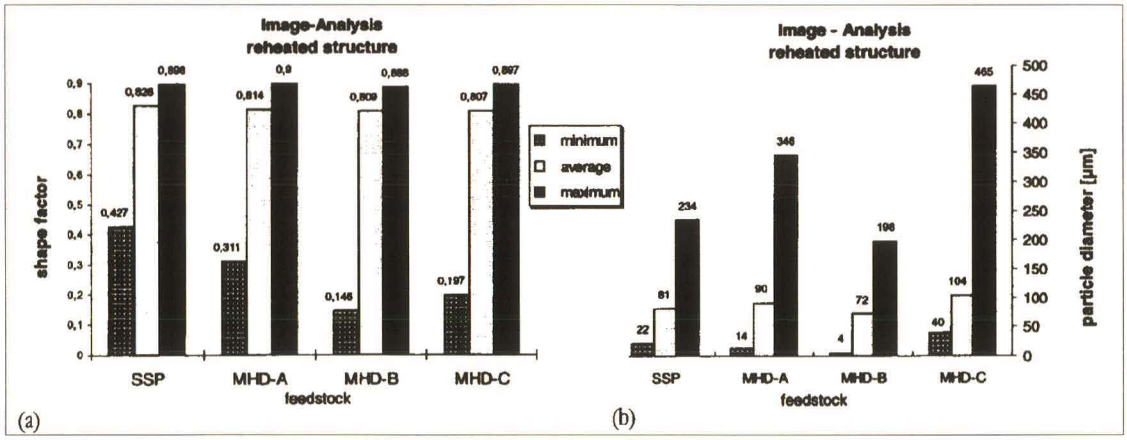

Figure 2.29 A comparison of (b.) the particle diameter of the primary phase and (a.) the shape factor of the primary phase between the SSP and MHD materials.[13]

The investigation during reheating shows that the SSP material has a good form stability, i.e. it holds its shape well when in the semi solid state. This is important for a safe handling of the billet. The "cutting" technique, where the billet is cut by hand using a knife, is a helpful but not a consistent method to test the softness of the billet.. The required force and the appearance of the cut off surface are important for evaluation the consistency of the material. The cutting force was relatively low and the cut off surface showed a "creamy" structure. This leads to the conclusion that the flowability in the casting process would be good. The MHD-material showed similar results after an ideal heating process[13].

2.5 Multiple Variable Analysis Techniques

The technique of defining and investigating all possible conditions in an experiment involving multiple factors is known as the design of experiments, also referred to as factorial design. In the case of design of experiments, a number of factors (or variables) at two or more different levels (e.g. high and low) are selected that will affect the result or outcome of the experiment. These factors would be tabulated according to factorial design rules to produce treatments for running an experiment[26].

For a full factorial design the number of possible designs is N (equation 2.14).

$$N = L^m \quad \ldots (2.14)$$

where:

L = number of levels of each factor.

m = number of factors.

Thus, if the qualities of a product depends on three factors A, B and C and each factor is to be tested at two levels then, using equation 2.14, 2^3 (8) possible design configurations are required. This three factor, two level experiment is represented by figure 2.30.

	A_1		A_2		
	B_1	B_2	B_1	B_2	AVERAGE
C_1					
C_2		Cell			
Average					

Figure 2.30 Test matrix with three factors at two levels. [26]

The size of the test matrix is still easily managed and every combination can be investigated. Each box in the table is called a cell. In order to improve accuracy, several observations are made per cell and the significance of the results are determined by a form of statistical analysis called Analysis of Variance (ANOVA)[26].

Now consider the case where the experiment under consideration has 15 factors, at two levels each. In this case, 2^{15} (32 786) possible varieties of experiments need to be investigated before the most desirable treatment can be established. A research program of this magnitude would be exorbitant in cost and time. Techniques such as fractional factorial experiments are used to simplify the experiment. Fractional factorial experiments investigate a fraction of all the possible combinations and this saves considerable time and money. However, a rigorous mathematical treatment is required, both in the design of the experiment and in the analysis of the results. Furthermore, each experimenter may design a different set of fractional factorial experiments, making comparisons between like experiments unreliable[26].

Dr Genichi Taguchi simplified and standardised the fractional factorial designs in such a manner that two experimenters will always use similar designs and tend to obtain similar results. Factorial and fractional factorial designs of experiments are widely and effectively used however they suffer the following limitations[26]:

1. The experiments become expensive in terms of cost and time when the number of variables is large.
2. Two designs for the same experiment may yield different results.
3. The designs normally do not permit determination of the contribution of each factor.
4. The interpretation of experiments with a large number of factors may be quite difficult.

Taguchi overcame the limitations of factorial and fractional factorial experiments by contributing discipline and structure to the design of experiments. The result is a standardised design methodology that can be easily applied by different experimenters. Different designs for the same type of experiments by different experimenters will yield similar data and lead to similar conclusions[26].

2.5.1 Taguchi Experiment Design Strategy

Taguchi constructed a special set of orthogonal arrays (OAs) to lay out his experiments. He combined orthogonal Latin squares in a unique manner and prepared a new set of standard OAs to be used for a number of experimental situations[26].

A common OA for 2 level factors is shown in figure 2.31. This array, designated by the symbol L_8, is used to design experiments involving up to seven 2 level factors. The array has 8 rows and 7 columns. Each row represents a trial condition with factor levels indicated by the numbers in the row. The vertical columns correspond to the factors specified in the study.

	FACTORS						
TRIAL NUMBER	*A*	*B*	*C*	*D*	*E*	*F*	*G*
1	1	1	1	1	1	1	1
2	1	1	1	2	2	2	2
3	1	2	2	1	1	2	2
4	1	2	2	2	2	1	1
5	2	1	2	1	2	1	2
6	2	1	2	2	1	2	1
7	2	2	1	1	2	2	1
8	2	2	1	2	1	1	2

Figure 2.31 Orthoganal array L_8 (2^7). [26]

Each column contains four level 1 and four level 2 conditions for the factor assigned to the column. Two 2 level factors combine in four possible ways, such as (1,1), (1,2), (2,1), and (2,2). When two columns of an array form these combinations the same number of time, the columns are said to be balanced or orthogonal. Note that any two columns of an L_8 (2^7) have the same number of combinations of (1,1),(1,2),(2,1), and (2,2). Thus, all seven columns of an L are orthogonal to each other[26].

The OA facilitates the experiment design process. To design an experiment is to select the most suitable orthogonal array, assign the factors to the appropriate columns, and finally,

describe the combinations of the individual experiments called the trial conditions. Assume that there are at most seven 2 level factors in the study. Call these factors A, B, C, D, F, F and G, and assign them to columns 1, 2, 3, 4.5, 6, and 7 respectively of L_8. The table identifies the eight trials needed to complete the experiment and the level of each factor for each trial run. The experiment descriptions are determined by reading numerals 1 and 2 appearing in the rows of the trial runs. A factorial experiment would require 2^7 or 128 runs, but would not provide appreciably more information[26].

The array forces all experimenters to design almost identical experiments. Experimenters may select different designations for the columns but the eight trial runs will include all combinations independent of column definition. Thus the OA assures consistency of design by different experimenters[26].

2.5.2 Analysis of Results

In the Taguchi method the results of the experiments are analyzed to achieve one or more of the following three objectives:

1. To establish the best or the optimum condition for a product or a process
2. To estimate the contribution of individual factors
3. To estimate the response under the optimum conditions

The optimum condition is identified by studying the main effects of each of the factors. The process involves minor arithmetic manipulation of the numerical results and usually can be done with the help of a simple calculator. The main effects indicate the general trend of the influence of the factors. The levels of the factors which produce the best results can be predicted from the main effects.[26]

The knowledge of the contribution of individual factors is a key to deciding the nature of the control to be established on a production process. The analysis of variance (ANOVA) is the statistical treatment most commonly applied to the results of the experiment to

determine the percent contribution of each factor. Study of the ANOVA table for a given analysis helps to determine which of the factors need control and which do not[26].

Once the optimum condition is determined, it is usually a good practice to run a confirmation experiment. It is, however, possible to estimate performance at the optimum condition from the results of experiments conducted at a non-optimum condition. It should be noted that the optimum condition may not necessarily be among the many experiments already carried out, as the OA represents only a small fraction of all the possibilities[26].

2.5.3 Limitations of the Taguchi Method

The most severe limitation of the method is the need for timing with respect to product/process development. The technique can only be effective when applied early in the design of the product/process system. After the design variables are determined and their nominal values are specified, experimental design may not be cost effective. Also, there are situations in which classic techniques are better suited; in simulation studies involving factors that vary in a continuous manner, such as the torsional strength of a shaft as a function of its diameter, the Taguchi method may not be a proper choice[26].

CHAPTER 3

3 Experimental Procedure

There were two possible options for producing semi solid feedstock using the MHD method. These options included the SSP process and the continuous casting method, both horizontal and vertical. The continuous casting approach was considered however it required a lot of floor space and supporting items such as a holding furnace, withdrawal mechanism and a flying saw. Furthermore, casting practice of this scale and nature should be performed in proper, established cast houses as it posed a serious safety hazard. There was a large amount of molten metal used at one time to produce a single batch of billets. The premises available for the equipment was in a multistoried building, where it was not advisable to operate a casting apparatus of this nature.

The SSP process required only a small mount of molten metal at one time, being only enough to produce a single billet. This lent itself for to the testing of different types of materials since only a small quantity of metal was needed at a time.

Furthermore, the experimental system had to achieve the following objectives:

1. Produce a feedstock material which displayed thixotropic properties, when heated to the semi solid state, and allowed the fastest heating times possible, from solid state to semi solid state, for the feedstock material. The primary phase had to display a fine grained and discrete microstructure surrounded by a eutectic phase which displayed a fine, speckled texture.

2. Produce a slug or billet of the proportions 50 mm in diameter and approximately 100 mm in length to suit the high pressure die casting machine used by the Semi Solid Metal Research and Technology Group (SSMRTG) at the University of Natal.

3. To be of compact proportions to allow its use in limited space in the laboratory.

4. To have as much flexibility as possible over the control variables (shear rate and cooling rate).

5. To have the ability to use different types of metals for later investigations.

The SSP process was decided as the base for the experiment apparatus design since it satisfied all the above requirements.

The design of the experimental apparatus emulated the fundamental process of producing semi solid feedstock. This required the introduction of a liquid metal into a mould and to be placed in the path of a rotating magnetic field. As the melt was vigorously stirred by the rotating magnetic fields, it was cooled to complete solidification.

The MHD Single Billet Caster (SBC) experimental system was designed and built to evaluate the process factors, which influenced the shear rate and the cooling rate in the melt, during the production of the semi solid feedstock.

There were six areas of the SBC production under investigation to satisfy the aims of this research. These were:

1. A356.2 material characterisation.
2. Primary phase formation.
3. Fine eutectic phase formation.
4. Single Billet Caster billet quality.
5. Mould cooling curve measurements.
6. Feedstock reheating trials.

3.1 Material Characterisation of A356.2

The aim of this investigation was to established the fundamental metallurgical properties of the alloy A356.2. The information determined from this experiment included the chemical composition, the liquidus and solidus temperature and microstructural analysis of the raw material as supplied by Alusaf Bayside Smelter, Richards Bay.

The chemical composition was determined by spectral analysis from Alusaf, PDC (Pty Ltd), Pietermaritzburg and chemical anlysis by Scrooby's Laboratory Service (SLS), Johannesburg. The results were compared with the nominal specifications of A356.0[6].

A sample from the as cast bar of A356.2 alloy was mounted, polished and etched with a 5% HF solution. The microstructure was obtained by using a 35mm film camera, attached to a Nikon Epiphot inverted light microscope, to capture the image of a prepared sample of raw material.

The liquidus and solidus temperatures were determined using the Differential Thermal Analysis (DTA) technique [27, 28, 29] applied to the heating and cooling profiles of the aluminium alloy.

3.1.1 The Temperature Profile Experiment Apparatus Description

The DTA technique obtained the temperature profile of the A356.2 alloy undergoing phase changes in controlled temperature conditions. This profile was compared to a temperature profile of a control sample which remained a single phase under the same controlled temperature conditions. The temperature gradient of the A356.2 alloy would deviate from the temperature of the control block when a change of state of the alloy occurred due to the latent heat of formation transfer at the time. The DTA profile showed the difference in the temperature gradient of the A356.2 sample and the control block. This profile showed peaks and troughs which indicated the positions of the solidus and liquidus temperatures on the corresponding temperature profiles.

The A356.2 sample was a cube, with approximate dimensions 1 cm x 1 cm x 1cm (mass = 2.6 g), with a 1.6 mm diameter hole drilled from one side to the centre of the cube to

house a thermocouple tip. A K-type, 1.5 mm diameter thermocouple was inserted into the cube.

The control block was made of copper since it did not melt under the temperature conditions present when profiling the aluminium. An identical thermocouple to the one used for the aluminium sample was inserted into the block. Furthermore, the copper block was dimensioned in a manner to minimise the difference of effects the furnace temperature conditions would have had, on the sample and control block, due to the different types of materials used. The copper block was sized with respect to the mass of the aluminium sample according to the equation: $mass_{(copper)} \times C_{P(copper)} = mass_{(aluminium)} \times C_{P(aluminium)}$[28]. The size of the copper block was determined to be 0.9 cm x 0.9 cm x 0.9 cm (mass = 6.2g).

When the profile for the A356.2 alloy was determined, the control block temperature was used as both the comparator to for the aluminium sample temperature as well as the temperature feedback source for the furnace control.

The equipment consisted of two small (5 cm^3) ceramic crucibles one each for the aluminium sample and copper control block placed inside the muffle furnace (figure 3.1). The muffle furnace was controlled with a REX P90 furnace controller (figure 3.2) which controlled the furnace temperature via the control block thermocouple. Each thermocouple was connected to a FEMA electrónica s.a., ESASGARD CCT - 23 series, thermocouple transmitter module (figure 3.3 b.). This unit converted the thermocouple temperature range into a 0 -10 V DC signal, for use as an analogue input signal to a PC input/output (I/O) card..

The temperature profiles were recorded with the use of a PC running a LABVIEW sampling program and an EAGLE PC 30 GA data (I/O) card which read the thermocouples via the thermocouple transmitter modules (figure 3.3 a.).

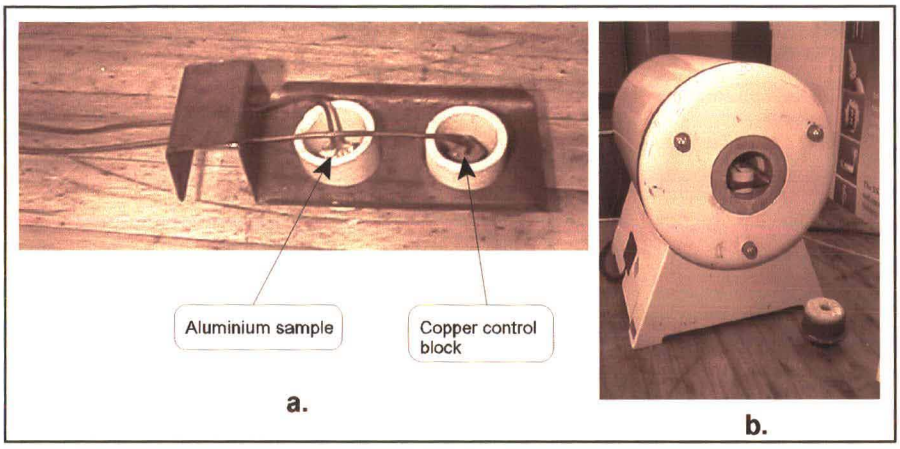

Figure 3.1 **a.** The ceramic crucibles containing the aluminium sample and the copper control block.

b. The positioning of the samples inside the muffle furnace. The samples were located at mid-length of the muffle tube during the experiment.

Figure 3.2 The REX P90 furnace controller and muffle furnace used for the heating and cooling profile experiment.

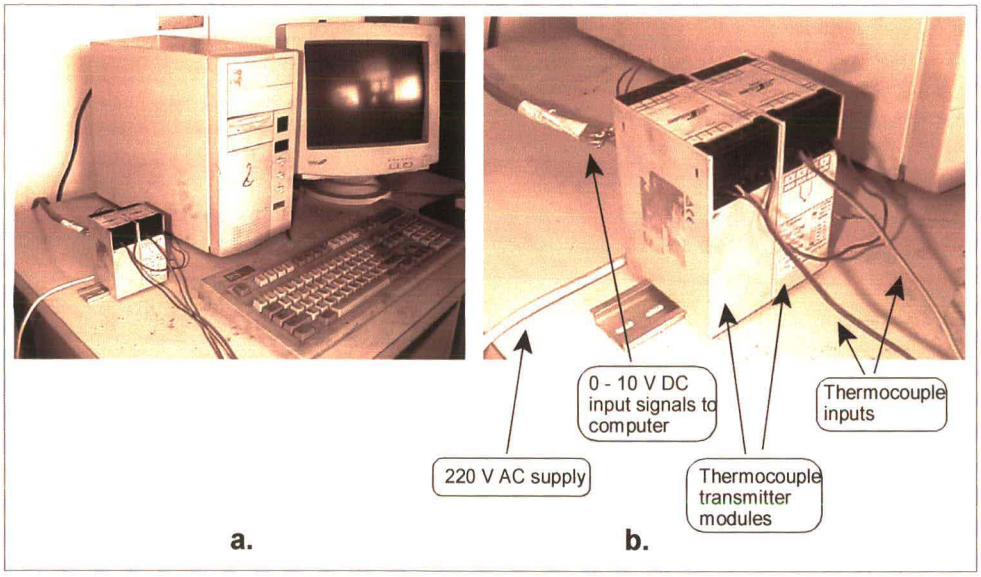

Figure 3.3 **a.** Equipment setup of the temperature profile measurement experiment.

b. Thermocouples were connected to the transmitter modules which relayed a 0 -10 V DC signal to the PC I/O card, proportional to the temperature measured by the thermocouples.

3.1.2 Parameters Selected for the Temperature Profile Measurements

The furnace was set to follow the profile shown in figure 3.4. The profile followed the following steps:

1. From room temperature, ramp up to and soak at 525 ^{0}C for 90 minutes to stabilize the temperature conditions prior to the heating profile measurements.
2. Ramp up at approximately 5 ^{0}C/minute to 670 ^{0}C and then soak for 60 minutes to stabilize the furnace temperature conditions prior to the cooling profile measurements.
3. Ramp down at approximately 5 ^{0}C/minute to and then soak for 60 minutes to stabilize furnace temperature conditions after the temperature profile measurements were complete.
4. Cool to room temperature.

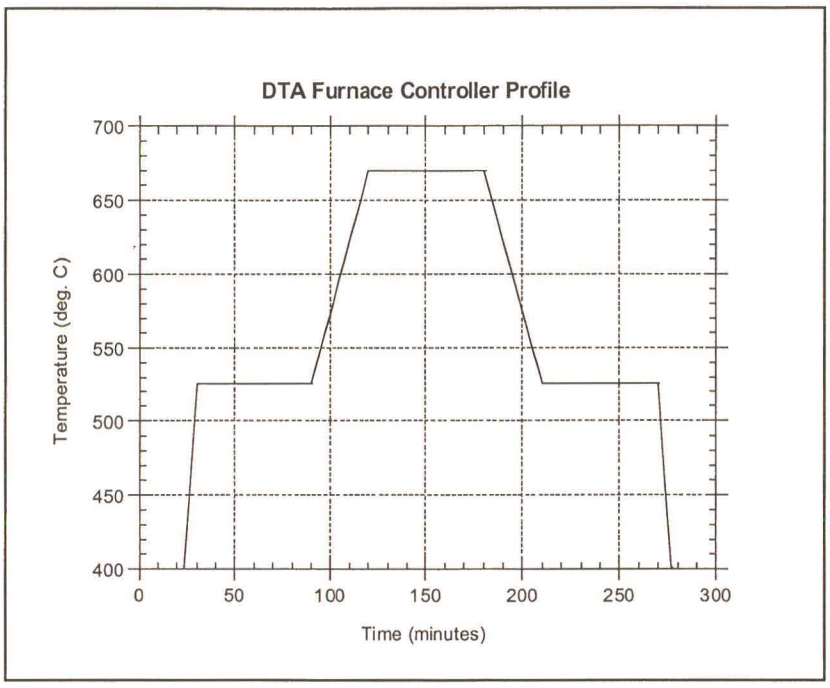

Figure 3.4 The temperature profile programmed into the furnace controller which set the heating and cooling conditions for the DTA experiment.

The temperature profile measurements were started approximately 1 minute before the ramp up to 670 ^{0}C. The measurements were ended when the temperature difference between the aluminium sample and control block had stabilized while soaking at 525 ^{0}C after the ramp down from 670 ^{0}C. During the profile measurement period, the temperatures were sampled at 1 second intervals by the temperature logging system on the PC.

3.2 Experimental Procedure to Establish a Fine Grained, Equiaxed Primary Phase Formation

This experiment was concerned with the investigation of the process factors influencing the shear rate and cooling rate of the melt. These parameters were not easily monitored directly with instruments during the actual production process. Instead, the indirect process factors were monitored and controlled to establish the optimum condition for the formation of the fine grained, equiaxed primary phase.

3.2.1 Experimental Apparatus Description

3.2.1.1 The Single Billet Caster System

The SBC system (figure 3.5) was suitable for the experimental lab application since it was compact, of simple design and allowed for a degree of flexibility in the adjustment of process factors. A single billet was produced which allowed its properties to be checked and the process factors adjusted, if necessary, after a minimal amount of molten aluminium was used. The two fundamental parameters, shear rate and solidification rate, were set by the combination of the frequency controller (a three phase induction motor speed controller) and the cooling water spray.

The SBC process (figure 3.5) produced a single billet by placing volume of molten metal, contained in a mould, within a moving magnetic field. It electromagnetically stirred the melt to remelt and fragment the dendrite arms which began to grow at the start of solidification. Solidification was initiated by the cooling water spray inside the rotating magnetic field zone of the motor stator.

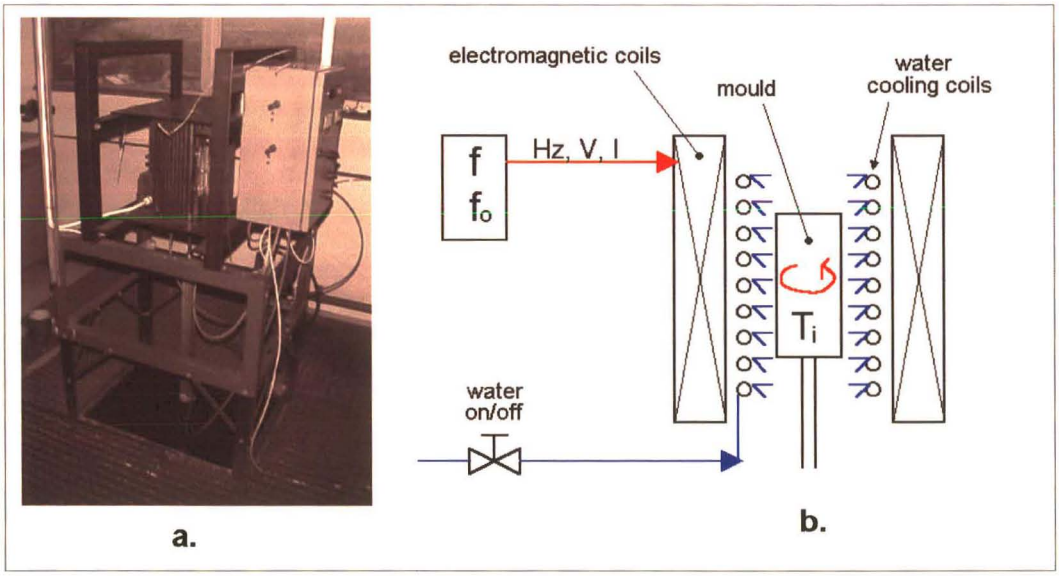

Figure 3.5 **a.** The Single Billet Caster apparatus.

b. Schematic of the SBC apparatus.

The working temperature range in which to form the discrete primary grains by means of stirring was from 615 ^{0}C to approximately 605 ^{0}C.[1] Within this range, a fast cooling rate was applied in order to keep the grain size as small as possible. This also induced a supercooled condition in the melt and formed a large number of nucleation sites.

The factors used in SBC unit (figure 3.5 b.), involved in the formation of the fine grained, equiaxed primary phase, were the line frequency (f), the base frequency (f_0), and the temperature at which the cooling rate was applied, which was called the initiation temperature (T_i).

The line frequency controlled the angular velocity at which the rotating magnetic fields travelled, hence, the stirring speed of the melt. The base frequency indirectly controlled the voltage and current flowing through the inductors of the stator (i.e. the strength of the rotating magnetic field), hence, the stirring strength induced into the melt.

The stirring action of the melt induced the shear rate which was required to remelt and fragment the dendrite arms. Thus, the combination of line frequency, (f), and the base frequency, (f_0), indirectly represented the magnitude of the shear rate.

3.2.1.2 The Electrical Inductor Coils

Of the two systems (i.e. the axial and tangential stirrer), the tangential stirrer was more suitable in terms of lower power consumption, lower frequency requirements, and the already assembled inductor coils in the form of a three phase induction motor stator.

No power ratings required of the stirring coils were revealed through the literature survey. However, current ratings were given and also the physical size of the units could be determined by the sizes of the mould. Combining these two parameters and comparing them with a specifications table (Appendix A1) of available 3 phase, 2 pole induction motors, a suitable unit was selected.

A WEG three phase induction motor stator with a 15 kW, 30 Amp rating (figure 3.6) was selected. Two poles were required due to the magnetic field patterns which increased stirring effectiveness. Stirring had to be symmetric over the stirring region to prevent large discrepancies of microstructure in the form of coalesced primary grains and dead zones where the mushy metal had become strongly viscous in low shear regions.[1, 30]

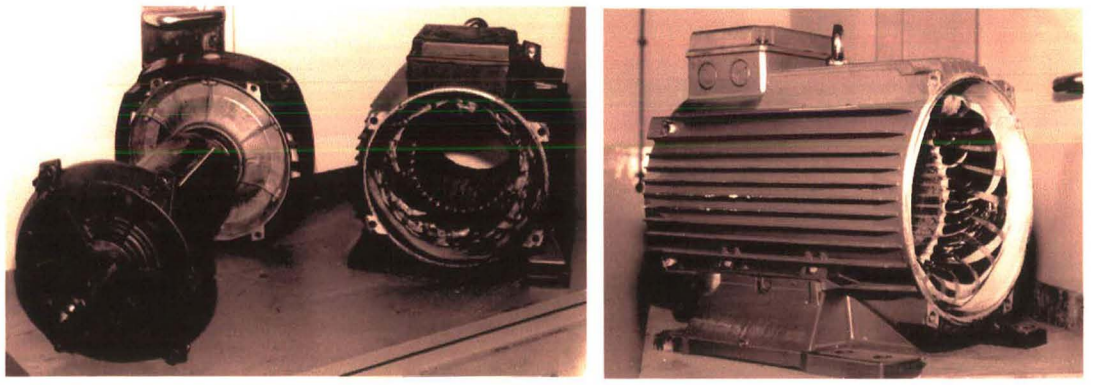

a. b.

Figure 3.6 **a.** The 15 kW induction motor used in the SBC apparatus in exploded form. **b.** The stator showing the windings.

3.2.1.3 The Power Source

A variable speed AC motor drive from AC Technology Corporation, MC 1000 series (figure 3.7), was used to power the induction stirrer. This unit controlled the shear rate by adjusting the line frequency and the line voltage. The control unit had the same power rating as the induction motor, i.e.15 kW and 30 Amps, with a line frequency output range from 0 to 120 Hz. The line frequency set the rotational speed of the electromagnetic field.

Since the rotational speed of induction motors was controlled by the line frequency, it was the only process factor that could be adjusted by the operator via the touchpad (figure 3.7). The voltage and current supplied to the induction stator were automatically controlled to suit the line frequency set by the operator. This prevented the chance of saturating the field coils and overloading them. In the event of an overloaded condition, the unit automatically

tripped off and cut the electrical supply to the field coils, so there was no possibility of destroying the stator in the event of an overloaded condition.

Figure 3.7 The variable speed AC motor drive.

Description of the AC motor drive unit operation

The stator was a set of three electrical windings held stationary in the motor stator housing. The arrangement of the stator coils and the presence of three phase AC voltage gave rise to a rotating magnetic field. The speed at which the magnetic field rotated was known as the synchronous speed of the stator. Synchronous speed was a function of the frequency at which the voltage was alternating and the number of poles in the stator windings.

Equation 3.1 gives the relation between synchronous speed, frequency, and the number of poles[31]:

$$S_s = 120 \cdot \frac{f}{p} \quad \ldots (3.1)$$

where:

S_s = Synchronous speed (rpm)

f = frequency (Hz)

p = number of poles

The strength of the magnetic field in the stator was proportional to the amplitude of the voltage at a given frequency. When operated below base (rated) speed, the stator operated in the range of "constant torque" (figure 3.8). Constant torque output was obtained by maintaining a constant ratio between voltage amplitude (Volts) and frequency (Hertz). For 50 Hz motors rated at 380 Vac, the value for this V/Hz ratio was 7.6. Operating with this V/Hz ratio generally yielded optimum torque capability. *Operating at a lower ratio value resulted in lower torque and power capability. Operating at higher ratio values would cause the stator to overheat.* Most standard stators are capable of providing full torque output from 3 to 60 Hz.[31]

If the frequency applied to the stator was increased while the voltage remained constant, torque capability would decrease as speed increased. This would cause the horsepower capability of the stator to remain approximately constant. Stators run in this mode when operated above base speed, where drive output voltage was limited by the input line voltage. This operating range was known as the "constant horsepower" range (figure 3.4). The typical maximum range for constant horsepower was from 60 to 140 Hz. Figure 3.4 depicts the operating characteristics of a typical AC induction stator with a 60 Hz base speed.[31]

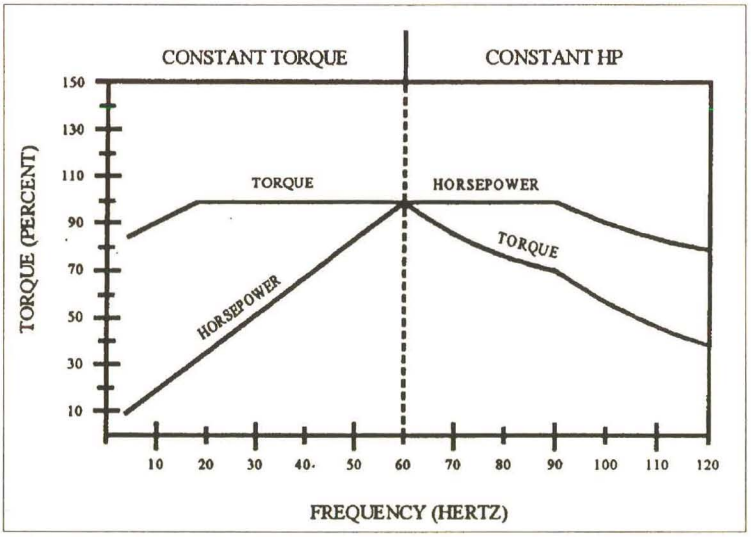

Figure 3.8 Output characteristics with respect to frequency of the AC motor drive unit. [31]

The AC motor drive settings such as the base frequency and overload protection parameters were manually programmed via a touchpad on the unit. The line frequency could be manually controlled via the same keypad, remotely controlled by an externally wired rheostat or computer controlled by control software via a PC interface.[31]

Setup of the AC motor drive unit for experimental purposes

Since the AC motor drive applied power to a 3 phase induction motor stator without the rotor, the coils became saturated and the controller tripped off during the stirring operation to prevent overheating. The base frequency was thus raised to reduce the V/Hz ratio, therefore the power rating applied to the stator was reduced. This allowed the motor drive unit to operate continuously throughout the line frequency range from 0 to 120 Hz during the stirring process. (The higher the line frequency, the higher the power rating applied to the stator.)

The minimum base frequency, which allowed continuous operation of the controller up to 120 Hz line frequency, was 140 Hz. The maximum base frequency setting allowed by the control unit was 360 Hz. Therefore the power rating of the control unit could be set from full rating corresponding to 140 Hz base frequency, down to the lower rating corresponding to the 360 Hz base frequency.

3.2.1.4 The Mould

The mould was used to contain the molten metal for the SBC process and had to posses certain properties.

a) It had to be non-magnetic (i.e. have low magnetic permeability) so as not to shield the magnetic field from the molten metal to be stirred.

b) It had to have low electrical conductivity to reduce losses, due to eddy currents induced in the mould walls, by the induction stirrer.

c) It had to have sufficient thermal conductivity to allow adequate heat transfer for cooling of the melt.

d) It had to be resistant to molten metal wetting its surface, thus preventing the metal adhering to or corroding it.

Suitable materials which displayed these above properties were copper, stainless steels, graphite and ceramics. None of these materials displayed the best of all the above properties so a compromise had to be reached.

Copper had excellent electrical and thermal conductivities which meant high losses would be incurred due to eddy currents. However the heat transfer efficiency would have been high. It was non-magnetic so there was little shielding of the magnetic field. Its non-wetting properties were also good provided the mould was kept chilled at all times whilst the melt was in contact, otherwise the copper was dissolved into the aluminium if the mould was allowed to reach a high temperature.

Stainless steel had fair electrical and thermal conductivities so eddy current losses were reduced however the heat transfer had a reduced efficiency. Non-wetting properties were fair and non-magnetic properties, good (if austenitic stainless steel was used).

Graphite had good electrical and fair thermal conductivities so eddy current losses were high and heat transfer efficiency was fair. Non-wetting and non-magnetic properties were excellent.

Ceramics had poor electrical and thermal conductivities so eddy current losses were low and heat transfer efficiency, low. Non-magnetic properties were excellent and non-wetting properties, fair.

There were a few other factors to consider over and above the properties discussed above:

* Copper and graphite were both very expensive to purchase.
* In terms of heat transfer efficiency, the metal and graphite moulds were satisfactory.
* The ceramic material had poor thermal shock resistance and was prone to cracking.
* Metal and graphite were machinable therefore the moulds could be easily manufactured as desired.

The stainless steel material offered the best compromise for use as the mould material when the physical properties and logistical factors above were considered.

The design of the mould used in this experiment was carefully considered. The aim of the experiment was to test the effect of the three process factors, line frequency, base frequency and initiation temperature on the formation of a discrete, fine grained microstructure. The casting quality of the billet (i.e. shrinkage pores) were of no consequence to the formation of the discrete, fine grained microstructure. Shrinkage pores were the result of the phase change of the liquid metal to solid. The experiment focussed on the formation of the primary phase grains and the shrinkage occurred independent of whether the primary phase was modified or not. It was immaterial to consider shrinkage as a factor in the formation of the discrete, fine grained primary phase microstructure.

Therefore there was no need to focus on controlling the shrinkage porosity with the use of complicated moulds incorporating compression devices or risers. Instead, a simple tube type mould with end caps was used merely as a vessel in which to introduce the molten metal to a rotating magnetic field. Also, using a separate mould to test these factors saved on the wear and tear of the split moulds, used to produce the SBC billets (Chapter 3.3), which consumed considerable cost and time to produce.

The test mould (figure 3.9) was simply a short length of stainless steel tube of 50mm diameter and 100 mm in length. It was capped at both ends with a pouring spout at the top cap and a threaded hole in the bottom cap. It was then attached onto the SBC unit's pneumatic ram which positioned the mould inside the stirring space of the stator. Molten aluminium was poured from a crucible into the mould spout via a sheet metal funnel, previously inserted into the spout.

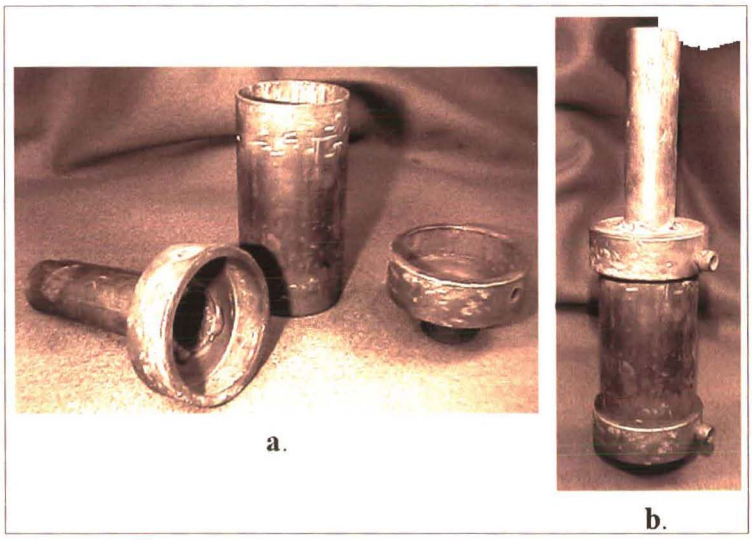

Figure 3.9 **a.** The exploded view of the test mould showing the end caps and tube.
b. The assembled test mould.

3.2.1.5 The Preheat and Melting Furnace

The purpose of the furnace (figure 3.10) was to preheat the mould and stabilise its temperature to that of the melt temperature before being transferred to the SBC apparatus for casting of the billet.

An external furnace was used to preheat the mould to a casting start temperature since an internal furnace, situated within the stirring inductors, hindered the cooling rate. High cooling rates were needed to produce the desired fine grained micro structure and fine eutectic.

The furnace was also used to melt the primary aluminium in A5 size, SiC ceramic crucibles. The melt temperature selected was 675 ^{0}C.

The furnace was a oven type, resistive furnace constructed by KILN CONTRACTS (Cape Town), model HTF 035. It had a 3.5 kW rating and was controlled by a standard P.I.D setpoint controller manufactured by the Canadian Instrumentation Company.

Figure 3.10 Resistive furnace used to preheat mould prior to casting.

3.2.2 Design of the Experiment to Achieve a Fine Grained, Equiaxed Primary Phase

The Taguchi method was used to design the experiment since it offered a good experimental efficiency and determined a percentage contribution of the each of the selected factors to the end result. An optimum condition could also be determined as well as the expected result at the optimum condition.

3.2.2.1 Parameters Selected for the Taguchi Experiment Design

The factors chosen dealt with the control of the fundamental process parameters of the MHD process. The line frequency (f) and base frequency (f_0) influenced the shear rate and the initiation temperature (T_i) influenced the cooling rate. The chemistry of the alloy was kept constant to restrict the variables that could influence the production of a fine grained, equiaxed primary phase to those that were controllable process factors. Therefore, the influence of the process factors would be specific to A356.2.

The experiment had three factors and each were chosen to be tested at three levels each (i.e. the endpoints of their range and a midpoint) as shown in table 3.1, to improve the experimental resolution. The line frequency (f) levels ranged from the minimum frequency that maintained vigorous liquid stirring to the maximum frequency setting allowed by the AC motor drive unit. The minimum level of line frequency was determined by visual experiment. The base frequency (f_0) levels range was outlined in Chapter 3.2.1.3. The initiation temperature levels ranged from a temperature just below the liquidus (Chapter 4.1) to the minimum working temperature that allowed fluid motion (Chapter 3.2.1.1). The minimum working temperature was also determined by visual experiment.

3.2.2.2 The Taguchi Experiment Design

The Taguchi method used an L_9 orthogonal array to perform an experiment with three factors at three levels each. The orthogonal array (OA) associated with this layout showed that there would be 9 trial runs for the experiment. A traditional experimental design using a full factorial method would have needed 3^3 (or 27) trial runs. Clearly, there was a considerable saving in time and effort in running the experiment with the Taguchi method of orthogonal arrays.

Table 3.1 The list of factors used in the primary phase formation experiment and the three levels at which each were tested.

		1	2	3
A	base frequency (Hz)	360	220	140
B	line frequency (Hz)	20	70	120
C	slow/fast $T_{transition}$ (°C)	615	608	605

The descriptive table was constructed according to the Taguchi experimental design methodology for L_9 OAs[26]. This table described the experimental conditions for each trial run of the experiment and is shown in table 3.2.

Table 3.2 The L_9 descriptive table detailing the experimental trials for the primary phase formation experiment.

DESCRIPTIVE TABLE trial #	A base freq	B line freq	C T_i	Result
1	360	20	615	
2	360	70	608	
3	360	120	605	
4	220	20	608	
5	220	70	605	
6	220	120	615	
7	140	20	605	
8	140	70	615	
9	140	120	608	

The L_9 experiment was run according to the settings of each factor at each trial run as shown in the descriptive table (table 3.2). After each trial run, the result was recorded in the appropriate column. (e.g. trial 1 was run with the base frequency set at 360Hz, line frequency at 20 Hz and the initiation temperature at 615 ^{0}C.)

3.2.3 Analytical Techniques Used to Quantify Primary Phase Morphology

The quality of the billets could be assessed in terms of microstructure (in as cast and reheated condition), rheology and mechanical properties.[1] The most practical way to test the quality of the primary phase morphology was to examine the microstructure and perform selected measurements of the primary phase grains.

Microstructural examination was performed on images of the as cast specimens using an image analysis software package capable of calculating the grain size and shape factor of the grains. The shape factor tested for the circular shape of the primary phase grain. The shape factor was 1 for a perfect circle and less than 1 for a non circular shape.

The procedure for analysing the images of the microstructures started with a digital image from an image capturing system attached to an inverted microscope. The captured image was then analysed on an image analysis software system, the Kontron Elektronik Imaging System KS300. The image was processed in a particular manner to clearly define the primary phase grain boundaries for the software to determine the attributes of shape factor and grain size thereof.

Solving an image analysis problem proceeded according to the following general steps. (A detailed macro for the Kontron KS300 is shown in the Appendix A2).

Image acquisition: The images were loaded from a storage media or acquired with a video camera.

Grey image processing: Images were enhanced with a range of image processing functions such as contrast enhancement, smoothing, edge improvements, grey morphology and image arithmetic. (figure 3.11)

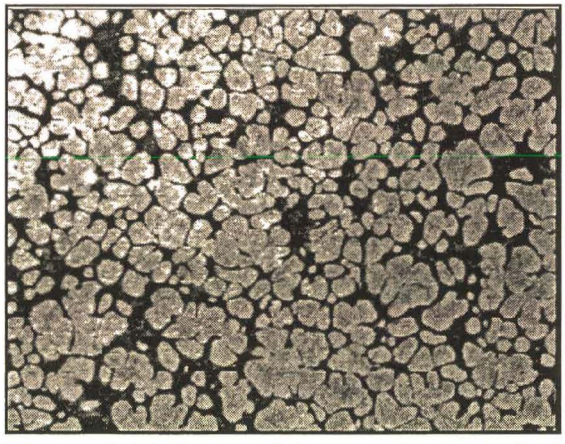

Figure 3.11 Captured image which has had contrast enhancement performed to define the difference between the phases more clearly.

Segmentation: Regions or phases could be detected and separated from their environment on the basis of their grey values. This process created a binary image from the grey scale or true colour image as shown in figure 3.12.

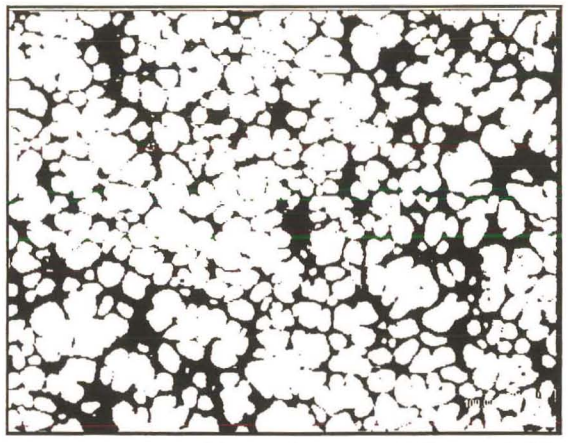

Figure 3.12 A binary image of figure 3.11, after a threshold operation, distinctly showing the primary phase grains.

Binary image processing: Binary image processing can improve segmentation results. This included arithmetic operations, filling holes or filtering on the basis of size as shown in figures 3.13, 3,14, 3.15 and 3.16.

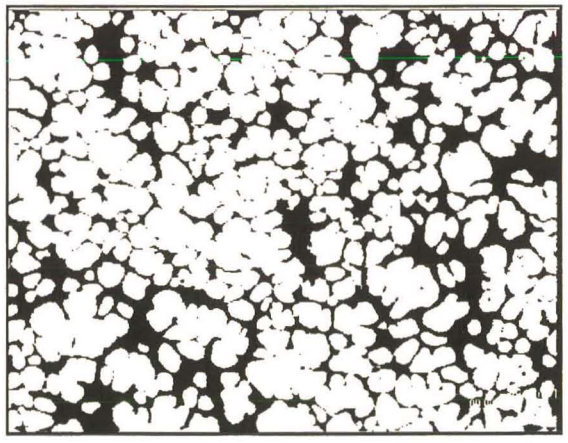

Figure 3.13 The binary image after scrapping the very small white areas, too small to be considered as primary phase grains.

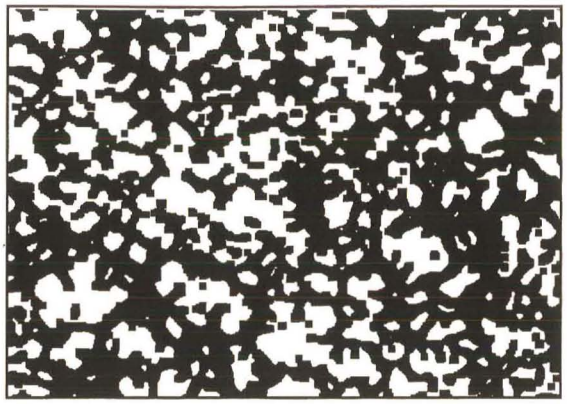

Figure 3.14 An ultimate erosion operation reduced primary grains, separating thin borders between them, without erasing the grains completely.

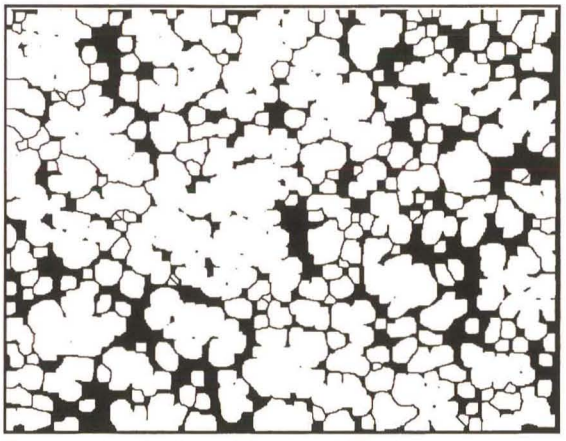

Figure 3.15 An ultimate dilation operation reformed the grains without allowing the close grains to merge; a separating line of background pixels remained between the grains.

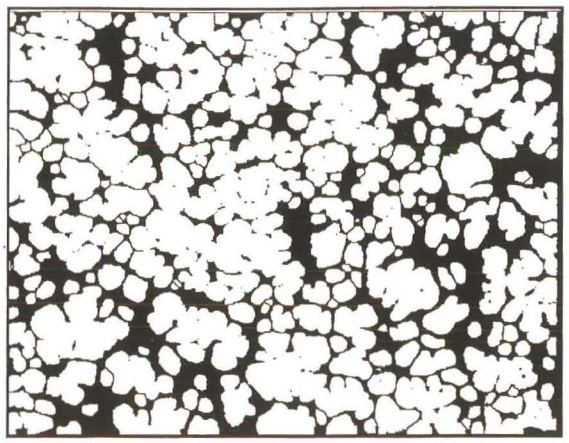

Figure 3.16 Figure 3.12 and figure 3.15 combined with a binary AND boolean operation.

Measurement: There were two kinds of measurements: field specific measurements which used the entire image and region specific measurements applied to the individual regions of an image. In this case, a region represented a primary phase grain, therefore measurements were region specific. This group also included point measurements such as length, angle, and count.

Region measurements used were DCIRCLE[32] and FCIRCLE[32] where:

$$DCIRCLE = \sqrt{\frac{4 \cdot AREAF}{\pi}} \quad \ldots (3.2)$$

1. DCIRCLE was the diameter of a circle with an equivalent area of the measured grain as calculated by formula 3.2 . Figure 3.17 shows graphically how the DCIRCLE was determined.

2. FCIRCLE was the form factor of the measured grain calculated by the formula 3.3. Figure 3.18 shows that FCIRCLE is the quotient of the diameter of a circle derived from the area of the grain and the diameter of a circle derived from the perimeter of the grain.

$$FCIRCLE = \frac{4 \cdot \pi \cdot AREAF}{PERIMCROFT^2} \quad \ldots (3.3)$$

where:

AREAF[32] is the area of the filled grain.

PERIMCROFT[32] is the Crofton perimeter of the grain.

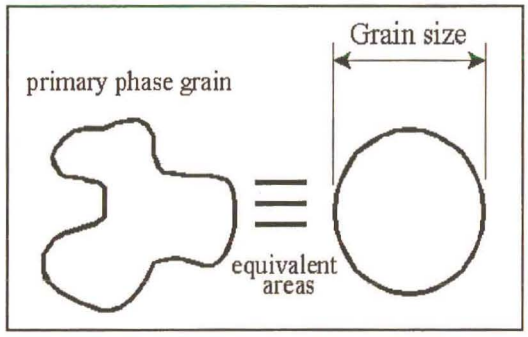

Figure 3.17 Graphical representation of the derivation of DCIRCLE as the grain size.

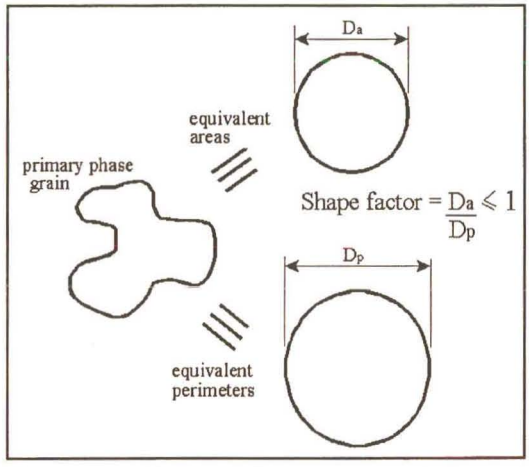

Figure 3.18 Graphical representation of the derivation of FCIRCLE as the shape factor.

The results obtained from the measurement were stored in a temporary database for evaluation.

Evaluation: The measurement results could be listed, represented in various graphics and evaluated statistically. In this case, the measurement results were imported into a Quattro Pro spreadsheet as shown in the Appendix A3.

The Taguchi method, as discussed in the primary phase formation experiment, required a vector of results (i.e. 1 x n array; n being the no. of trial runs) to be inserted into the descriptive table for analysis (table 3.2). However, to test the appearance of the fine grained, equiaxed primary phase grains, both the grain size and shape factor had to be

considered. This resulted in a 2 x n array of results which could not be incorporated into the Taguchi method of analysis.

Therefore a vector result needed to be created from the vector results of shape factor, FCIRCLE, and grain size, DCIRCLE. Shape factor was a dimensionless number, ranging from 0 to 1 where 1 represents a perfect circle. Grain size was represented as the diameter of a circle with the corresponding area of the grain measured and had the linear unit micrometres. Since the object of the experiment was to create a fine grain microstructure, the smaller grained results were desired. However, the shape of the grain had an influence on the grain size result since it is the area of the grain that was used for the purpose of determining grain size.

If two grains were compared (figure 3.19), where both had the same area but one grain had a circular shape and the other had a rosette shape, the results would show that the two grains were the same size but the shape factor would be different. The circular grain would have a shape factor tending towards 1 while the rosette grain would have a shape factor, for example, in the region of 0.5. If the grain size was divided by the shape factor, a new grain size would be produced showing that the circular grain remained the same size and the rosette grain doubled in size. Since the experiment was looking for the finest, equiaxed grains (i.e. the smallest and most round grains), the rosette grain would be rejected and the circular grain accepted on the basis of the smallest, new grain size.

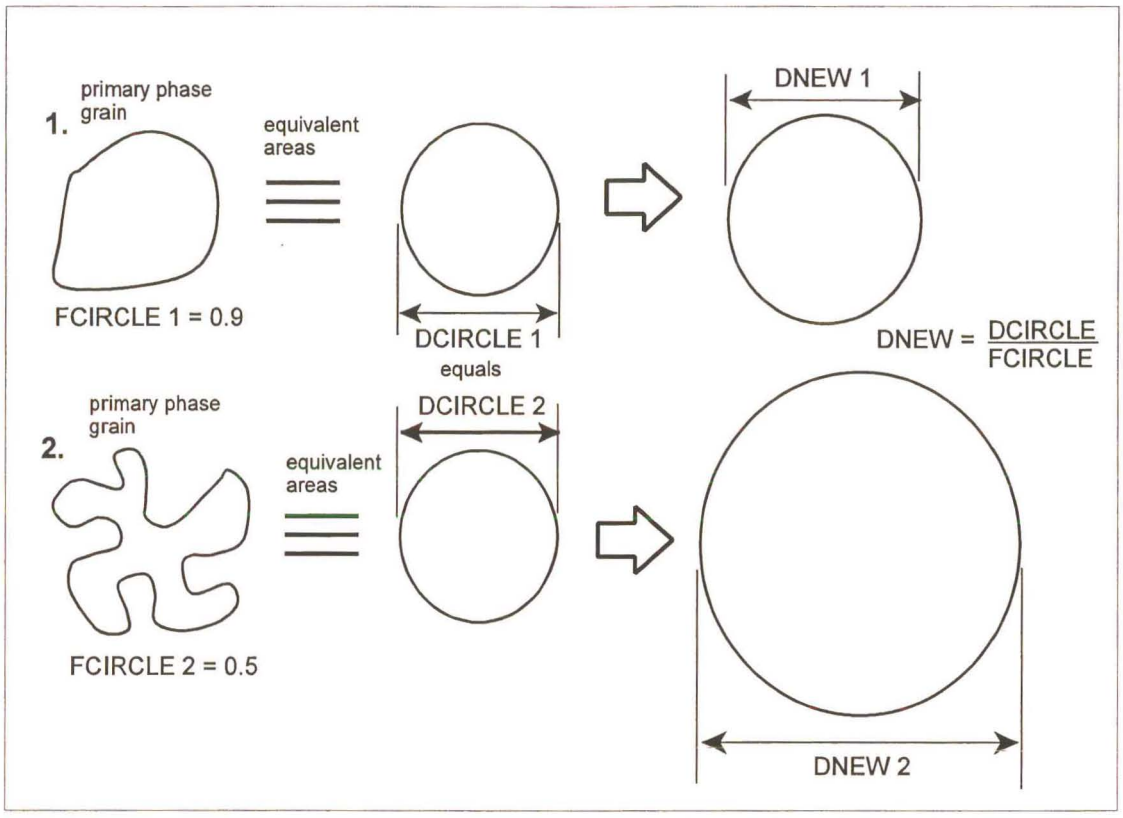

Figure 3.19 Illustrating the differences in DNEW of different shape factored primary phase grains which have equivalent areas and therefore equivalent grain sizes.

3.2.4 ANOVA Analysis

The ANOVA (Analysis of Variance) analysis was a statistical investigation into the characteristics of the results obtained from the experiment. It determined the influence of each process factor towards the outcome of the result by giving a quantified indication to the process factors involved in the experiment. In so doing, the most important process factor was highlighted. This method was used as a tool to indicate which process factor required the most control to achieve repeatable results.

The D_{NEW} results, determined from the image analysis data evaluation, were entered into their respective positions in the results column of the descriptive table (table 3.2). The ANOVA analysis (Appendix A4) was applied to the results column to obtain percentage contribution of the process factors towards the outcome of D_{NEW}. A percentage contribution of error was also determined and this represented the amount of experimental error.

3.2.5 Optimum Condition Verification

The optimum condition was the settings of all the process factors which yielded an optimum result, i.e. D_{NEW}. This condition could be determined following the ANOVA analysis and used to predict the optimum value of D_{NEW}.

Two experimental trial runs were performed using the optimum condition. If the results were consistent then the experiment could be considered to be repeatable. If the results compared to the predicted value, within error limits, then the integrity of the experiment could be verified. If not, a form of pooling had to be performed to incorporate the influence of insignificant process factors into the error term.[26]

The process of pooling adjusted the values of the percentage contribution of the remaining process factors and also the value of the predicted optimum result. Pooling also had the effect of inflating the error, thereby bringing closer the comparison of the actual optimum result to the predicted optimum result. Pooling was repeated until the actual optimum results compared to the predicted optimum result, within error limits.

3.3 Establishment of Cooling Conditions for A Fine Eutectic Phase Formation

The aim of this experiment was to determine the cooling conditions required to form the fine eutectic phase.

The procedure involved heating approximately 1 cm^3 blocks of the 356.2 aluminium alloy to 620 ^{0}C, above the liquidus temperature of the alloy. The samples were contained in small ceramic crucibles with a thermocouple immersed into the molten liquid. The crucible of molten liquid was then taken out of the furnace and allowed to aircool to 600 - 590 ^{0}C. The whole crucible was then immersed into the different quenching/cooling media. The cooling media included air at room temperature and furnace temperature, oil at room temperature and at approximately 180 ^{0}C, and water at room temperature and 100 ^{0}C.

3.3.1 Experimental Apparatus Description

The furnace that was used as the mould preheat furnace (figure 3.10) was used to preheat the samples to 620 ^{0}C.

Small 5 cm^{3} ceramic crucibles were used to contain the samples of liquid metal for quenching.

Glass beakers of 250 cm^{3} capacity were used to hold the different types of quenching media.

A Fluke 52 K/J digital thermometer and a K-type stainless steel sheath (1.5mm dia.) was used to monitor the temperature of the sample prior to quenching.

3.3.2 Evaluation of Results

The quenched samples were then mounted, polished and etched with a 5% HF solution. A Nikon Epiphot inverted light microscope was used to subjectively examine the texture of the eutectic phase.

3.4 Confirmation of Optimum Parameters for Casting SBC Billets

The aim of this experiment was to combine the results of the primary phase formation and eutectic phase formation and use them to cast semi solid feedstock with the split mould incorporating a riser.

3.4.1 Experimental Apparatus Description

3.4.1.1 The SBC System

The SBC system that was used for this experiment was the same that was used for the primary phase formation experiment (Chapter 3.2.1.1). The difference was the type of mould used.

3.4.1.2 The Split Mould and Riser

The mould design was determined after an evolution of many ideas and experiments which included the use ceramic tube moulds, stainless steel tube moulds, parallel and taper bore tube moulds, moving end plugs and chill plugs.

The split mould (figure 3.20) and riser system was designed to produce billets with no shrinkage pores and to ease the extraction of billets from the mould. It was a tube that was split along the length into two equal halves with a split riser top and a whole bottom cup (figure 3.16 b.). Once the melt had solidified, the two tube halves could be prised apart to release the billet. The riser was incorporated onto the mould to feed liquid metal to the casting during solidification as the material shrunk due to the phase change from solidification.

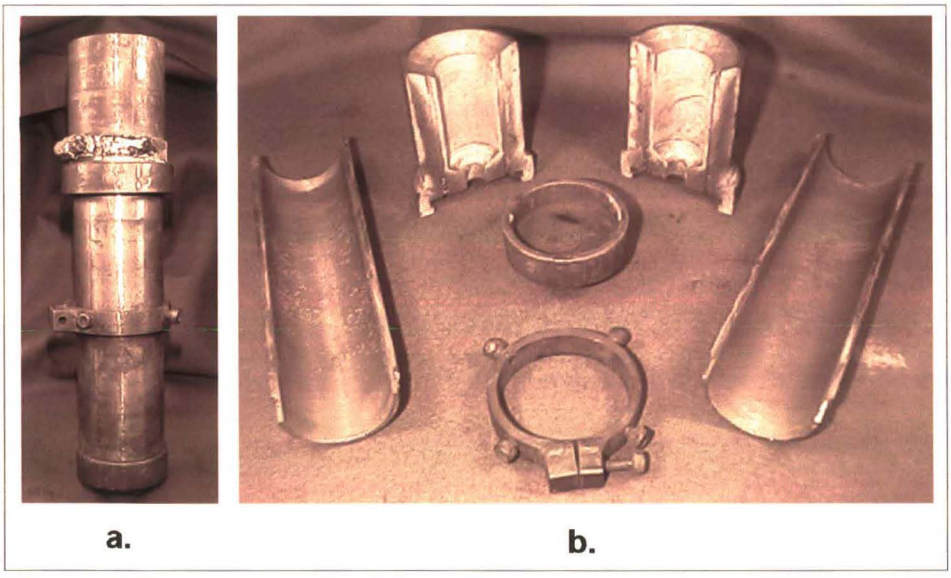

Figure 3.20 **a.** Assembled SBC split mould.
b. Exploded form of the split mould and split riser system.

3.4.2 Parameters Selected for SBC Billet Casting

The optimum condition was used for casting the SBC billets. These process factor levels were used to investigate whether the optimum process factors could be transferred to a different type of mould to that used in the primary phase formation experiment.

A further test was performed using the line frequency of 50 Hz as the stirring frequency and adjusting the base frequency to compensate for the change in stirring power. This was done to investigate if the national grid frequency was sufficient to use as the stirring frequency thereby saving on the cost of a frequency source should further research or development be required in this field.

The parameters used for the casting of SBC billets are shown in table 3.3. Trial SBC 1 used the optimum parameters determined from the Taguchi experiment. Trials SBC 2 to SBC 4 had constant line frequencies set at 50 Hz and the base frequency settings were altered. The initiation temperature of 615 ^{0}C was constant throughout. The load and voltage (V) values were recorded from the AC motor drive unit during the actual experiment.

Table 3.3 The process factor levels for base frequency, line frequency and initiation temperature used in the SBC billet casting trials.

Trial	f_0	f	T_i	load	V
SBC1	220	70	615		
SBC2	220	50	615		
SBC3	200	50	615		
SBC4	180	50	615		

3.4.3 Evaluation of Results

Samples were cut out of the centre of each billet cast and then mounted, polished and etched with a 5% HF solution. A Nikon Epiphot inverted light microscope was used to

subjectively examine the microstructure morphology and texture. The samples were also subjectively compared to the Taguchi experiment optimum results.

3.5 Cooling Rate Measurements in the Moulds

This experiment was performed to determine the actual temperature conditions of the melt during the Taguchi primary phase formation and the SBC billet casting experiments. A good primary phase morphology and eutectic phase texture were achieved during these experiments so the cooling rates experienced needed to be quantified for future reference.

Cooling rates before and after the T_i in the Taguchi experiments were measured, i.e. the slow and fast cooling rates. Temperature profiles of the whole casting cycle of the optimum Taguchi and SBC experiments were also performed.

3.5.1 Experimental Apparatus Description

The apparatus used was the same as those used for the primary phase formation and the SBC billet casting experiments. A temperature measurement and data logging system was used in addition to the SBC apparatus.

3.5.1.1 The Temperature Measurement and Logging System

Two K-type, stainless steel sheathed (1.5 mm dia.) thermocouples were used to measure the temperature of the moulds at two different heights, equidistant about the centre height of the billet.

For the Taguchi experiment, the thermocouples were inserted into the test mould through the pouring spout (figure 3.21 a). The thermocouple tips were placed approximately 50 mm apart within the mould cavity (figure 3.21 b).

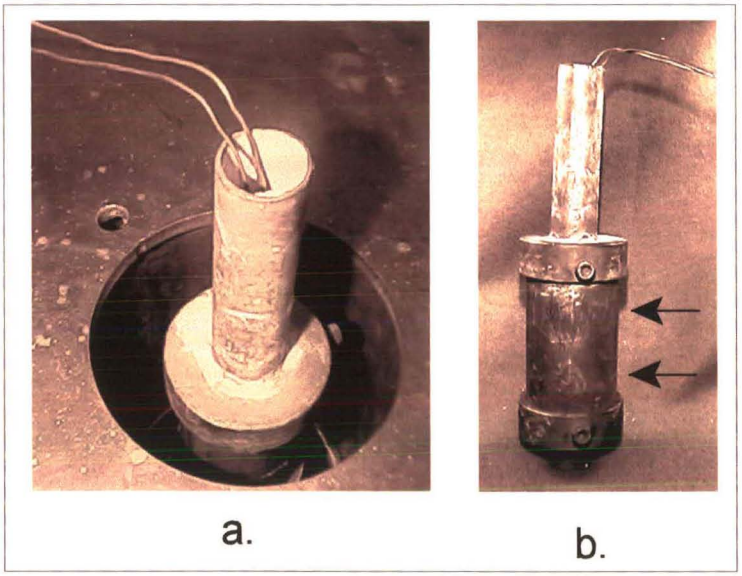

Figure 3.21 **a.** Thermocouple entry into the Taguchi experiment test mould.
b. Approximate positions of the thermocouple tips are shown by the arrows.

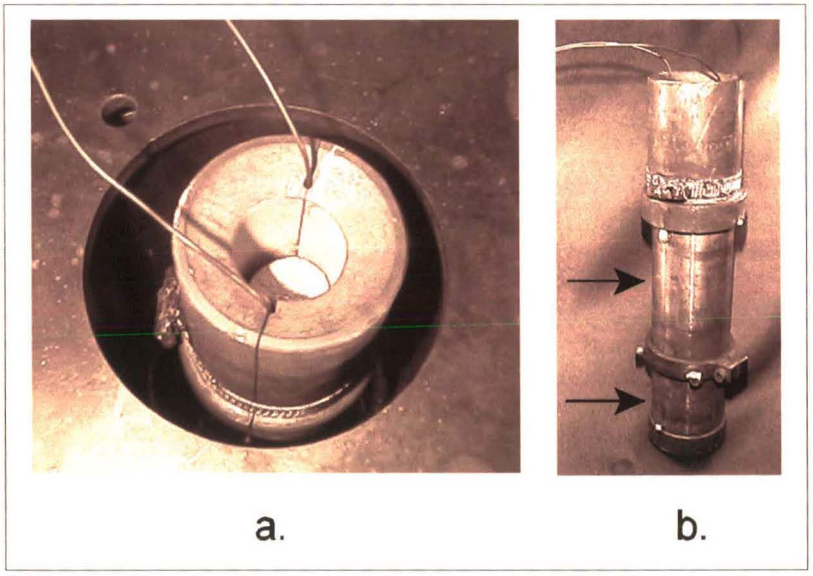

Figure 3.22 **a.** Thermocouple entry into the SBC mould used during the SBC cooling rate measurement.
b. Approximate positions of the thermocouple tips are shown by the arrows.

For the SBC billet casting trial, the thermocouples were inserted through the air vents of the split mould riser top into the mould cavity (figure 3.22 a). The thermocouple tips were spaced approximately 100 mm apart within the mould cavity (figure 3.22 b).

Each thermocouple was measured using the PC temperature logging system (figure 3.3) used for the material characterisation experiments (Chapter 3.1).

3.5.2 Analysis of Results

The logged temperature data was retrieved from the LABVIEW sampling program and imported into a Quattro Pro spreadsheet. Graphs were produced in Quattro Pro using the data for each cooling experiment.

3.6 Evaluation of Cast SBC Billets

One means of evaluating the quality of the SBC billet material was to compare the microstructure to that of commercially available feedstock. Commercial feedstock is acceptable in terms of quality since it is used in semi solid forming. If the SBC material showed a similar morphology to the commercial feedstock after reheating, then the SBC material could be considered suitable for Semi Solid Metal (SSM) forming.

Commercial feedstock was obtained from Pechiney, France and SAG, Austria. When the as cast microstructures of the SBC billet, Pechiney strand and SAG strand were compared (figure 3.23), the SBC billet showed a larger, rounder discrete primary phase grain than the commercial alloys which showed a finer, more rosette shaped primary phase grain.

The aim of this experiment was to determine the reheated microstructure of the SBC, Pechiney and SAG material to compare the SBC to the commercial feedstock reheated microstructures. If the SBC material showed similar microstructural characteristics to the reheated commercial alloys, then the SBC material could be considered suitable for SSM forming.

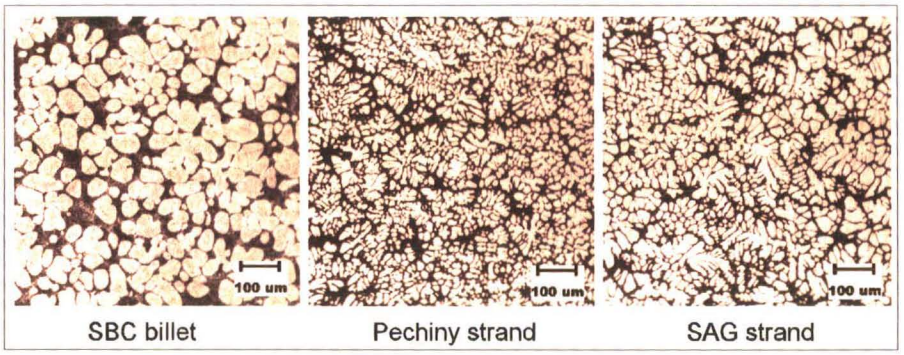

Figure 3.23 Comparisons of the as cast microstructures of the research material from the SBC billet and the commercially available material from Pechiney and SAG.

3.6.1 Experimental Apparatus Description

The samples were a block material of approximately 1 cm x 1cm x 1cm dimensions and were contained in small 5 cm^3 ceramic crucibles.

They were heated in the resistive furnace (figure 3.10) used for the primary phase formation experiment (Chapter 3.2.1.5). The furnace controller was connected to a K- type Stainless steel sheath (3mm dia.) thermocouple which was situated along the floor of the furnace (figure 3.25 and 3.26 a.) to ensure tight control of the temperature in the same area where the samples were heated.

3.6.1.1 Reheating Temperature Profile Measurement

A trial run was performed to determine the heating conditions for the reheating experiment and to visualise the temperature profile of the samples as they were being reheated. One sample was used with a thermocouple inserted (figure 3.24 b.) which was positioned in the furnace in the vicinity of the controller thermocouple (figure 3.25). The sample's thermocouple was measured by the Fluke 52 K/J thermometer (figure 3.24 a) using a K-type stainless steel sheath (1.5mm dia.) thermocouple.

3.6.1.2 Reheating Experiment Layout

Five samples each of the SBC, Pechiny and SAG material were placed in rows spaced evenly on the furnace floor (figure 3.26). The furnace controller thermocouple was placed centrally on the furnace floor.

3.6.2 Parameters Selected for Reheating Trials

3.6.2.1 Reheating Temperature Profile Measurement

A furnace temperature of 590 ^{0}C was established to heat the sample beyond the eutectic transformation to 580 ^{0}C within 20 minutes. A temperature profile was recorded by manually noting the temperature every 30 seconds from the Fluke thermometer.

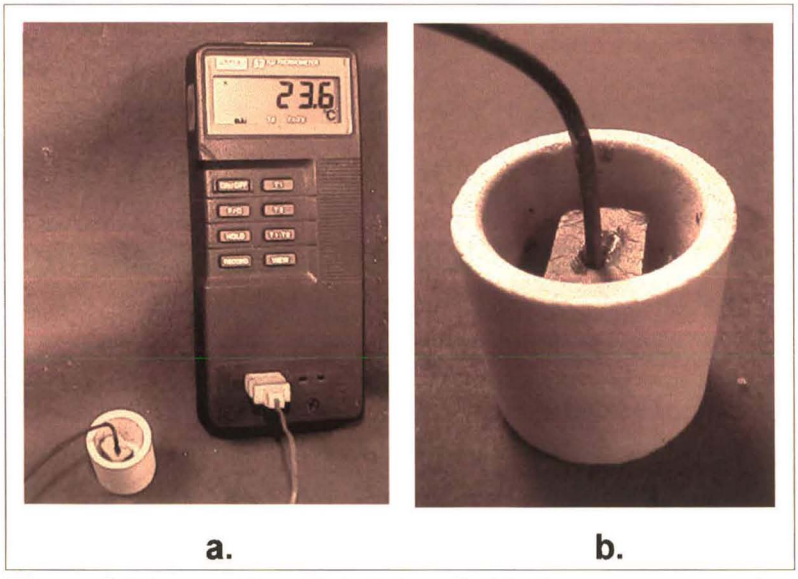

Figure 3.24 **a.** The digital handheld thermometer used to measure the temperature of a trial reheat sample. **b.** View of the thermocouple inserted into the trial reheat sample.

3.6.2.2 Reheating Experiment

The experiment was performed by simultaneously inserting 5 samples of each material, from room temperature, into the furnace which was preheated to 590 ^{0}C. One sample of each material was removed for quenching in water every 5 minutes.

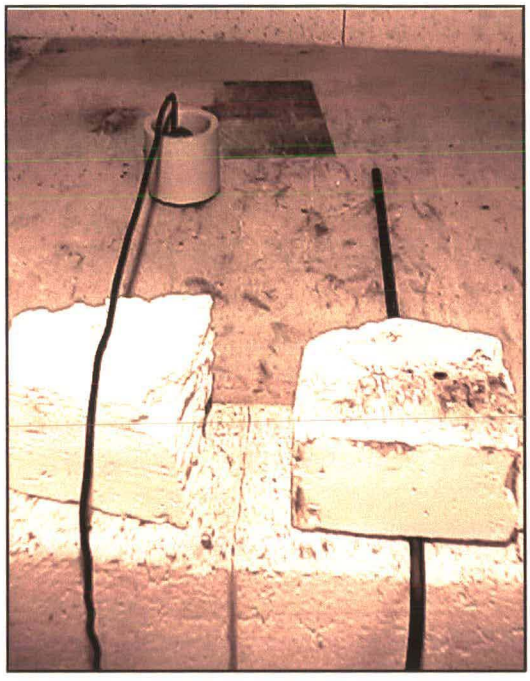

Figure 3.25 Layout of the trial reheat temperature measurement experiment.

3.6.3 Evaluation of Results

The reheating temperature profile was plotted on a graph using Quattro Pro.

All the reheat samples were mounted, polished and etched with a 5% HF solution and examined with the Nikon Epiphot inverted light microscope.

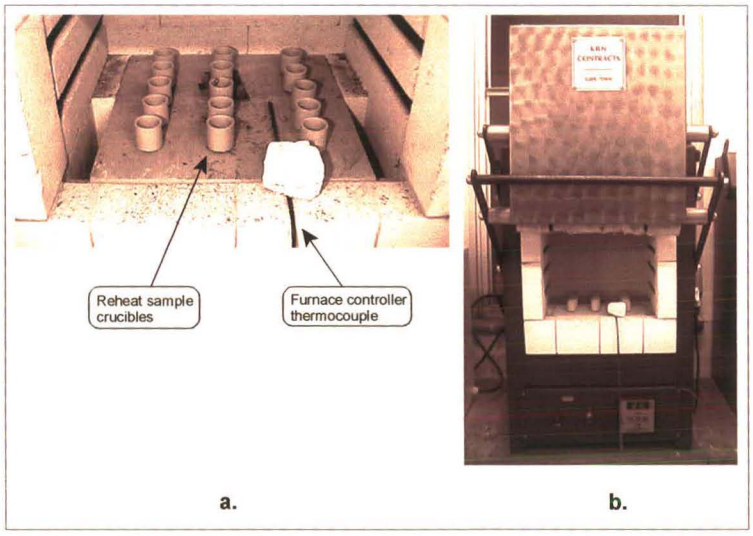

Figure 3.26 **a.** Layout of the reheat sample crucibles in the furnace with the indicated position of the furnace controller thermocouple.

b. The furnace used for the reheat experiment.

CHAPTER 4

4 Results and Discussion

4.1 Material Characterisation

4.1.1 Chemical composition

Table 4.1 Results of the chemical analyses with the average of the three analyses. The nominal composition is given for comparison.

Element	% (Alusaf)	% (PDC)	% (SLS)	% (Average)	Nominal Specifications[6] (A356.0)	
Al	Balance	92.2900	Balance	Balance	Balance	
Si	7.25	7.28	7.47	7.33	6.5 to 7.5	
Mg	0.26	0.22	0.25	0.24	0.25 to 0.45	
Cu	0.0000	0.0020	<0.0100	<0.0100	0.2000 max	
Zn	0.0040	0.0060	<0.0100	<0.0100	0.1000 max	
Mn	0.0050	0.0000	<0.0100	<0.0100	0.1000 max	
Fe	0.1080	0.1030	0.0500	0.0870	0.2000 max	
Ti	0.1130	0.0540	0.0600	0.0757	0.2000 max	
Sr	0.0385	0.0297	0.0330	0.0337	< 0.05 max	Total < 0.15 max
Na	0.0002	0.0006		0.0004	< 0.05 max	
Ca	0.0007	0.0010		0.0009	< 0.05 max	
P	0.0004			0.0004	< 0.05 max	
Pb		0.0000	<0.0100	<0.0100	< 0.05 max	
Cr		0.0010	<0.0100	<0.0100	< 0.05 max	
Sn		0.0020	<0.0100	<0.0100	< 0.05 max	
Ni		0.0030	<0.0100	<0.0100	< 0.05 max	

4.1.2 Microstructure

Figure 4.1 shows the microstructure of a sample from the as received material supplied by Alusaf. The microstructure showed a fine dendritic primary phase with a very fine textured eutectic. These characteristics could be attributed to the high cooling rate of the DC process as well as the use of titanium and strontium as a grain refiner and eutectic modifier respectively, as indicated by chemical composition results (table 4.1).

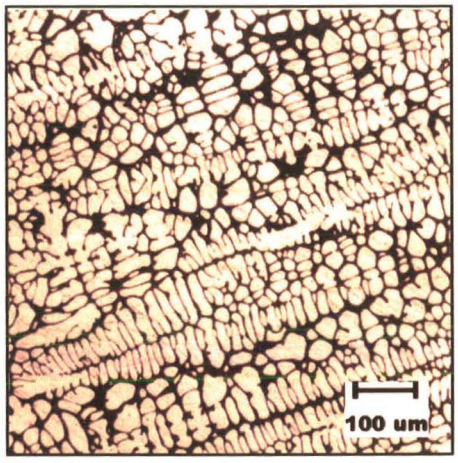

Figure 4.1 Microstructure of the as received material.

4.1.3 Temperature Profiles

Figures 4.2 and 4.3 show the heating and cooling profiles, respectively, obtained from the temperature profile experiment. The solidus, eutectic transformation and liquidus temperatures (table 4.2) were obtained from their respective temperature profiles using the DTA curve (figures 4.2, 4.3). For the cooling rate used during the cooling profile measurement the undercooling was about 4 ^{0}C for the liquidus temperature and 2 ^{0}C for both the eutectic transformation and solidus temperatures. For the experiments involving the modification of the primary phase to the SSM microstructure, the temperature range in which the primary phase may be modified during cooling is therefore from 617 ^{0}C to578 ^{0}C.

Table 4.2 Solidus and liquidus temperature determined from the temperature profile experiments. The nominal values are provided for comparison.

	Heating profile (^{0}C)	Cooling profile (^{0}C)	Nominal[6] (A356.0) (^{0}C)
Solidus temperature	572	570	555
Eutectic transformation	580	578	
Liquidus temperature	621	617	615

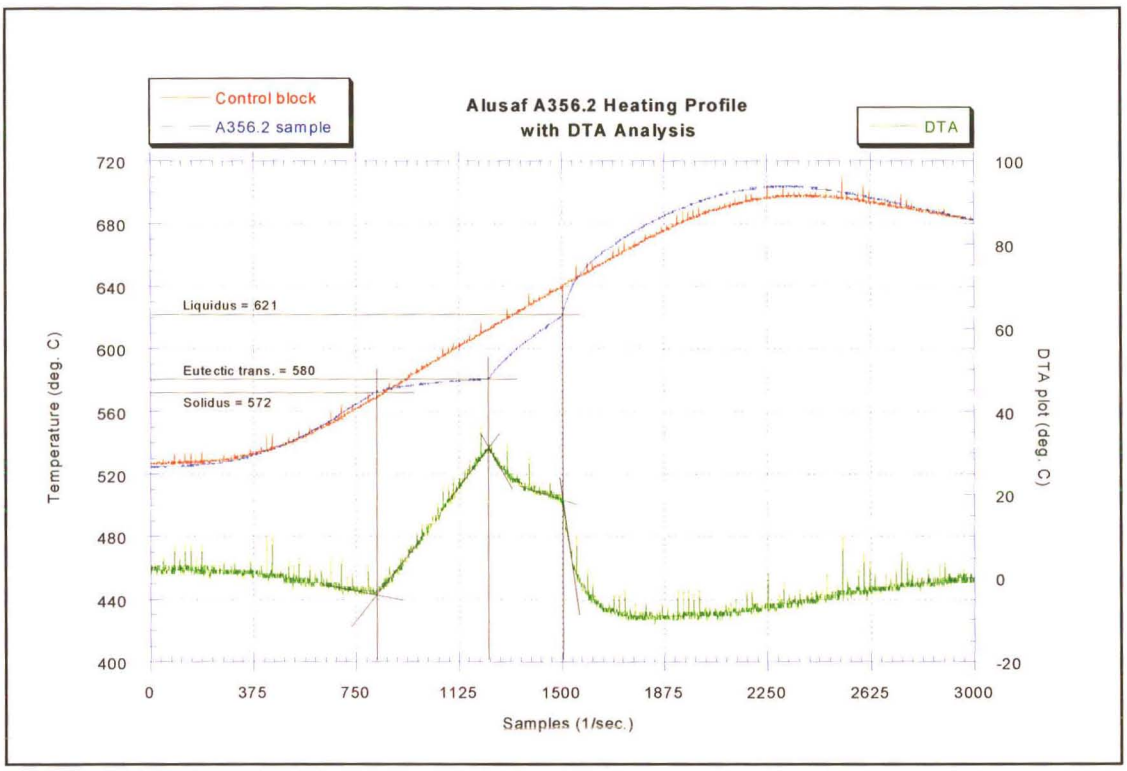

Figure 4.2 Heating profile for A356.2 with DTA analysis.

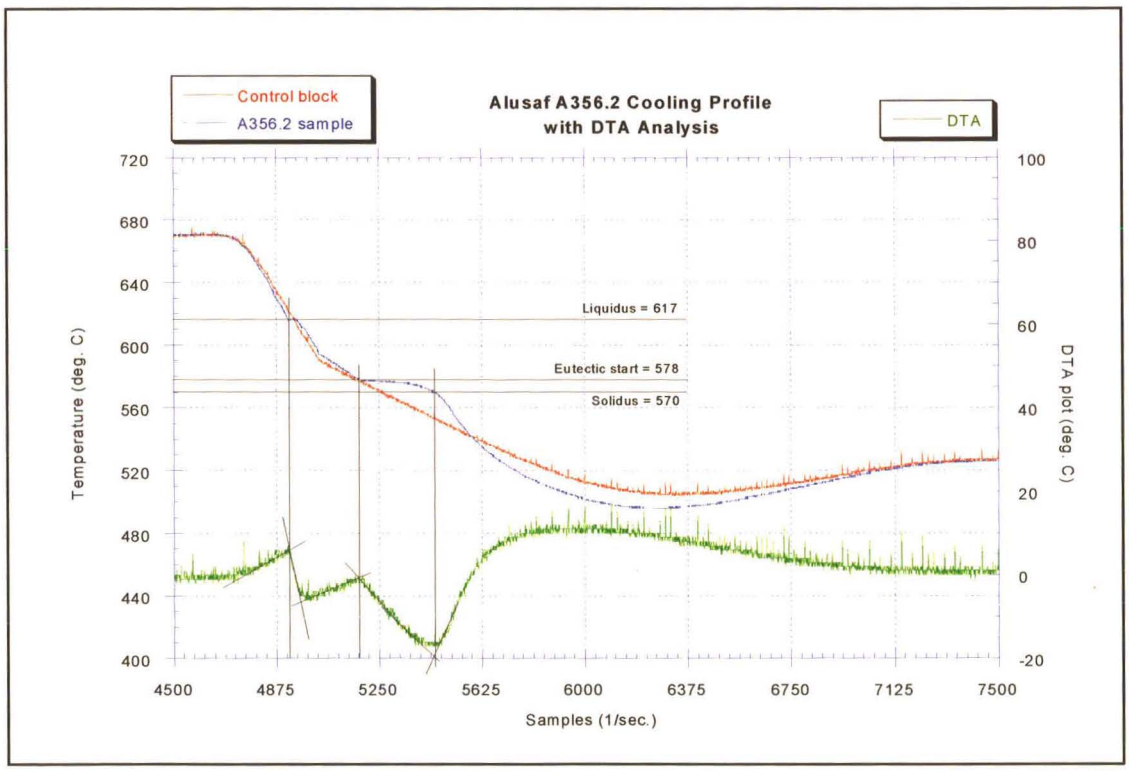

Figure 4.3 Cooling profile for A356.2 with DTA analysis.

4.2 Primary Phase Formation

Figure 4.4 shows the microstructures obtained as a result of the L_9 experiment as defined by the descriptive table shown in table 4.3. The values shown in the results column are those of D_{NEW}, determined from the results of the image processing (Appendix A1). DCIRCLE and FCIRCLE were measured. DNEW was the corrected DCIRCLE taking the shape of the grain into account.

The results in table 4.3 showed that the D_{NEW} value ranges from 55.33 to 133.74 μm. When the levels of the factors were grouped according to results showing similar characteristic trends (i.e. there were groups of three large grains, medium grains and small grains), it was evident that a pattern was developed. Gathering the three largest results, (133.74, 124.42 & 98.39 μm), it was evident that the temperature, at which the high cooling rate was initiated (T_i), 605 ^{0}C was common to the group. Similarly, for the three medium size grains (78.03, 74.61, 89.00), T_i was 608 ^{0}C; and for the three small size grains (59.25, 55.33, 65.54), T_i was 615 ^{0}C. This indicated that the T_i factor has the greatest effect on the outcome since it showed a definite relationship whereby the higher values of T_i yielded smaller grain sizes. It was difficult to classify the other two factors, base frequency and line frequency, into groups whereby the characteristic trends of the result corresponded to similar trends amongst the factor levels.

4.2.1 Results of the ANOVA Analysis

The results of the Taguchi ANOVA analysis (table 4.4) showed the degrees of freedom (f), the sum of squares (S),the variance (V), the F-value of the statistical F-distribution (F) and the Percentage contribution (P) of each factor as well as the error involved in the experiment (refer to the Appendix A2). The f, S, and V values were used in the calculation of the percentage contributions (P). The F value was used as an aid to determine the optimum condition of the experiment, which will be covered in a later section.

The contributions of base frequency, line frequency and initiation temperature were 8.0%, 3.5% and 86.5% respectively towards the end result. The influence of the initiation

temperature's (T_i) contribution was confirmed by the ANOVA analysis. The contributions of the base frequency and the line frequency were relatively low when compared to the contribution of that of the initiation temperature. This was the reason that no characteristic trends in the results could be found when compared to similar trends in the factor levels.

Considering that the working range of the transition temperature was from 615 ^{0}C to 605 ^{0}C, and that its contribution, as determined by the Taguchi analysis, was 86.5 %, the control of this factor was of extreme importance in the process of producing semi solid feedstock. The working range of the stirring factors did not show a great effect towards the process of semi solid feedstock production, although they were necessary for the degeneration of the dendritic branches (see Chapter 4.2.2.2). Since the line frequency was only tested over the range of 0 - 120 Hz, the effect of this variable may or may not differ if higher frequencies were used.

The chemistry of the alloy was kept constant for all experimental trials. Therefore the results would reflect the influence of the process factors specific to the A356.2 alloy. The influence of the alloy chemistry, towards the production of a fine grained, equiaxed primary phase, was not included (Chapter 3.2.2.1) and was beyond the scope of this investigation.

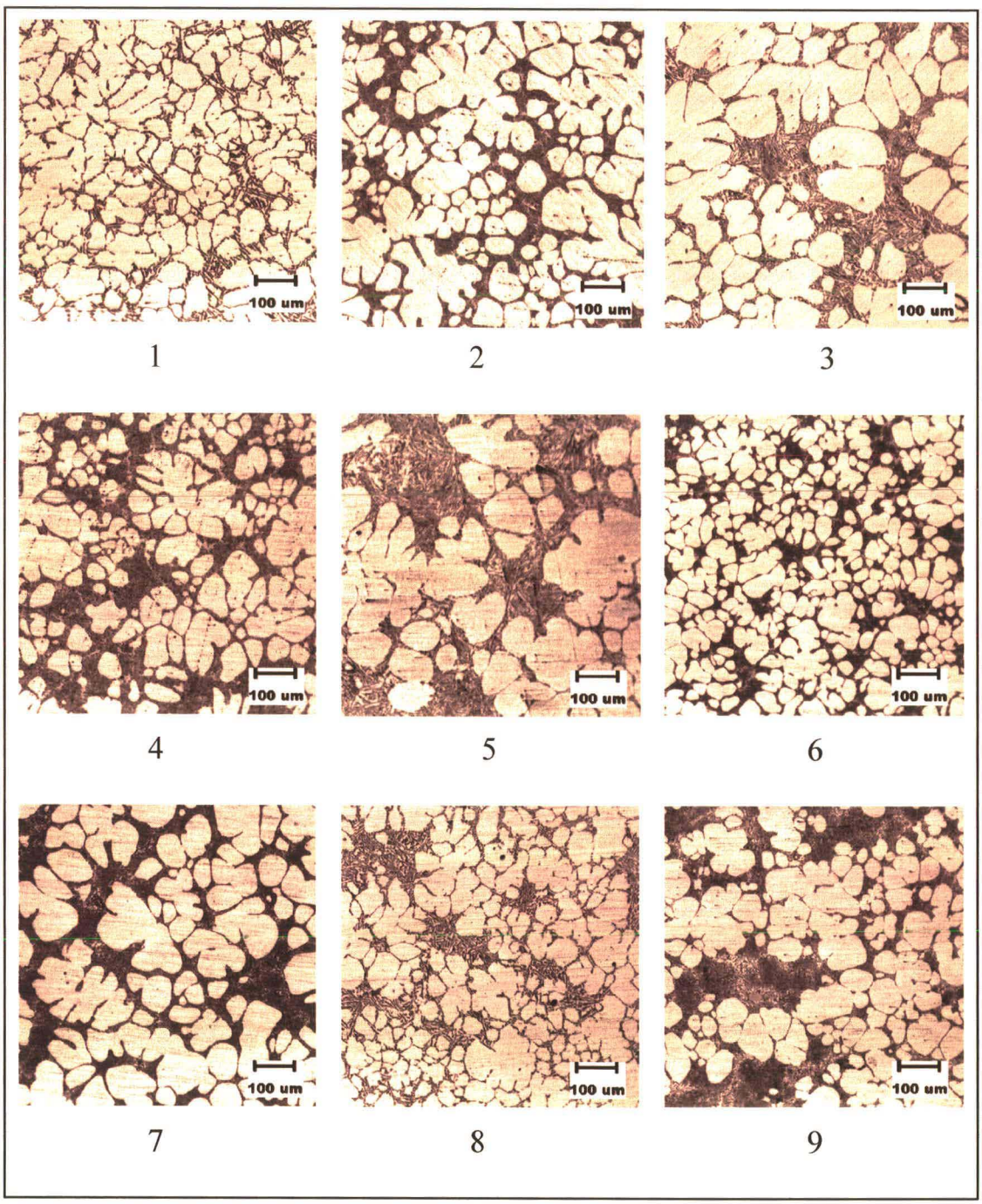

Figure 4.4 Microstructures obtained from the billets cast for the Taguchi L_9 experiment. The numbers below the figures denote the experiment trial number performed on the billet.

Table 4.3 The descriptive table (top) with the D_{NEW} results determined from the image analysis results.

DESCRIPTIVE TABLE	A base freq	B line freq	C $T_{initiation}$	Result D_{NEW} (μm)
1	360	20	615	59.25
2	360	70	608	76.03
3	360	120	605	133.74
4	220	20	608	74.61
5	220	70	605	98.39
6	220	120	615	55.33
7	140	20	605	124.42
8	140	70	615	65.54
9	140	120	608	89.00

Table 4.4 The results of the ANOVA analysis with the percentage contribution (P) towards the outcome of the primary phase grain appearance. Symbols f, S, V and F represent degrees of freedom, sum of squares, variance and the statistical F value respectively. Refer to Appendix A3.

Factors	f	S	V	F	P
A (base frequency)	2	494.305	247.152	3.952	8.0%
B (stir frequency)	2	218.200	109.100	1.744	3.5%
C ($T_{initiation}$)	2	5346.489	2673.244	42.754	86.5%
error	2	125.049	62.524	1	2.0%
Total	8	6184.045			100.0%

4.2.2 Optimum Condition Verification

Once the effect of the various factors had been determined and the most critical factors deduced, the optimum condition of the settings of the various factors could be determined. For this, a plot of the average effects helped to visualise the effects of the factors on the outcome.

Figure 4.5 shows the plot of the average effects with the factors marked A, B, C for base frequency, line frequency and initiation temperature respectively. The average effect was the average of the results wherever a particular factor's level appeared during the experiment. The plot of the average effects, for a particular factor, joined the average effects of each level.

The range over which each plot covered was a measure of each factors' contribution towards the end result. The transition temperature plot covered the largest range with the base frequency and line frequency plots covering very much smaller ranges; the line frequency had the smallest range of all the plots. This observation corresponded to the percentage contributions of each factor as shown in the ANOVA analysis in table 4.4.

The average effects plot also helped to determine the optimum condition of the experiment. The optimum condition required in this experiment was a minima since the requirement of the result was to have as small and round a grain as possible. This was portrayed by an "as small as possible" value of D_{NEW}. For each factor in the average effects plot, the smallest average effect was chosen to give the optimum condition. In this case, the A2, B2 and C1 average effects were selected. Therefore the best possible combination of the factors were a base frequency of 220 Hz, a line frequency of 70 Hz and an initiation temperature of 615 ^{0}C.

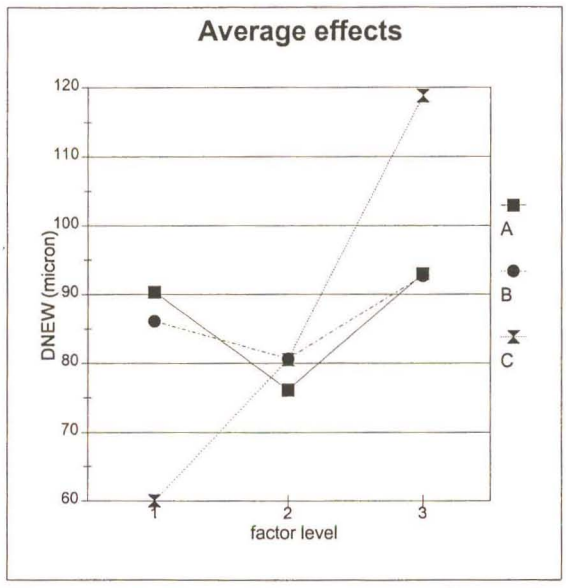

Figure 4.5 Plot of the average effects for each of the factors involved in the L_9 experiment.

To test the integrity of the experiment, a confirmation run was performed using the above optimum values, the results of which were compared to an estimated optimum result. The estimated optimum result was calculated using eqution 4.1.[26]

$$Opt.Cond.= \overline{T} + (A2 - \overline{T}) + (B2 - \overline{T}) + (C1 - \overline{T}) \quad \ldots \textbf{(4.1)}$$

where:

$\overline{T}$ = Grand average of all the results

A2 = average effect of level 2 of base frequency

B2 = average effect of level 2 of line frequency

C1 = average effect of level 1 of transition temperature

The estimated result for this condition was 43.84 μm.

Two confirmation experimental runs were performed to confirm if the results were repeatable. The two results from these two runs were 55.31 μm and 54.73 μm. This confirmed the repeatability of the experiment but these results were somewhat larger than

the estimated result,43.84 μm, by some 11 μm. The percentage error between predicted result and actual result was:

$$prediction.error = 1 - \frac{43.84}{\frac{55.31+54.73}{2}} = 1 - 0.797 \equiv 20\% \quad \ldots (4.2)$$

All the results discussed thus far are summarised in table 4.5.

Table 4.5 Summary of results determined for the optimum condition verification.

Average Effects	A1	90.34
	A2	76.11
	A3	92.99
	B1	86.09
	B2	80.65
	B3	92.69
	C1	60.04
	C2	80.55
	C3	118.85
Smallest value	A2	76.11
	B2	80.65
	C1	60.04
Grand average		86.48
Optimum	min	43.84
Opt. confirmation	1	55.31
	2	54.73

However, if one observes an experimental run which yielded a similar result to that of the confirmation run, (i.e. experiment 6 in the descriptive table yielded a DNEW of 55.33 μm), there was one factor that differed from the optimum condition determined from the average effects graph. Base frequency and initiation temperature were the same between experiment 6 and the optimum condition and the line frequency differed by 50 Hz; 120 Hz for experiment 6 and 70 Hz for the optimum condition. Considering the fact that the line frequency contributes only 3.5 % towards the end result, this factor was insignificant and

experiment 6 could be considered a close gauge for the optimum condition. This was the experiment which yielded the smallest result of D_{NEW}. Viewed in this respect, the optimum confirmation runs confirmed the integrity of the experiment since the results thereof were equivalent to the experiment 6 result. Figure 4.6 shows the microstructures obtained from the optimum confirmation runs. When these are compared to experiment 6 (figure 4.4), they show a similarity in morphology with a fine equiaxed, discrete primary phase microstucture. This visual comparison further supported the argument that experiment 6 was close to the optimum condition since there was no discernable difference between that and the optimum confirmation microstructures.

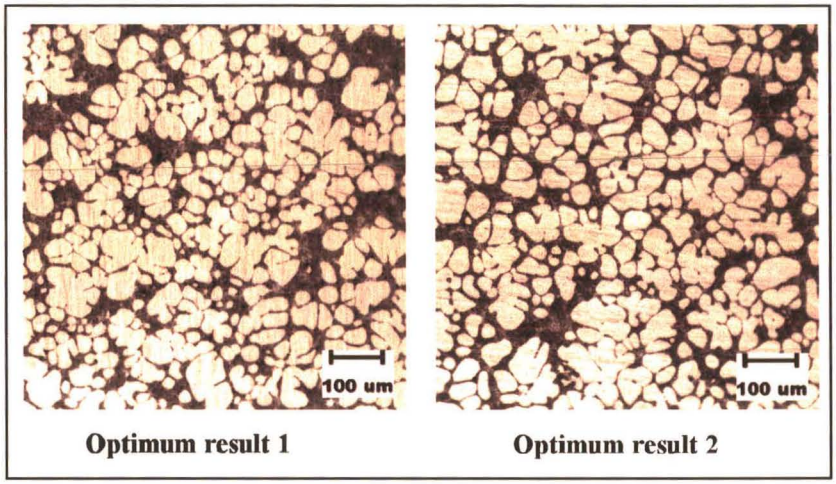

Figure 4.6 Microstructures obtained from the billets cast with the optimum condition settings.

4.2.2.1 Pooling of Insignificant Factors

When the contribution of a factor was small, the sum of squares, S, for that factor was combined with the error sum of squares. This process of disregarding the contribution of a selected factor and subsequently adjusting the contributions of the other factors, was known as pooling. Pooling was usually accomplished by starting with the smallest sum of squares and continuing with the ones having successively larger effects.[26]

Pooling was recommended when a factor was determined to be insignificant by performing a test of significance against the error term at a desired confidence interval. A general

guideline for when to pool was obtained by comparing the error degree of freedom (f) with the total of the factors' degrees of freedom. Taguchi recommended pooling factors until the error degree of freedom was approximately half the total degree of freedom of the experiment.[24] A more technical approach would be to test the significance of a factor's influence (i.e. percentage contribution) and pool all factor influences below the 90 % confidence interval [26].

Taguchi's guideline for pooling requires a start with the smallest main effect and successively includes larger effects, until the total pooled degrees of freedom (DOF) equals approximately half of the total DOF.

The larger DOF for the error term, as a result of pooling, increases the confidence interval of the significant factors [24]. By pooling, the error term was increased and in comparison, the other factors appeared less influential. The greater the number of factors pooled, the worse the unpooled factors' effects look.

When the DOF of the error term was sufficiently large , the error variance represented the degree of inter-experiment error. When the error DOF was small or zero, small factor effects were successively pooled to form a large error term (pooling up strategy). The factors and interactions, that were then significant in comparison with the larger magnitude of the error term, were now influential. This strategy tended to highlight the helpful (or significant) factors. A large error DOF naturally resulted when trial conditions were repeated and standard analysis was performed. When the error DOF was large, pooling may not have been necessary. Therefore, one could repeat the experiment and avoid pooling but, to repeat all the trial conditions just for the error term may not have been practical [26].

The next step in Taguchi's guideline for pooling was to perform a test of significance (1-confidence interval). Generally, a confidence interval between 90% and 99% was recommended. However, if the confidence level was below 90 %, then it was common practice to pool the factor [26].

The percentage contribution of the error variance, as shown in table 4.2, was 2% . The DOF of the error variance was 2 whereas the total DOF of the experiment was 8. The prediction error (equation 4.2), which gave an indication of the experimental error, is 20 %. The fact that the error DOF was not approximately half of the total DOF, and also, the error variance did not corelate to the experimental error, suggested that the error DOF was not large enough and that pooling was necessary. The error variance would then represent the degree of inter experimental error and the significant factors would be highlighted when compared with the larger magnitude of the error term.

Pooling Up Strategy

The results (table 4.4) showed that the error DOF was 2 and the total DOF was 8. Pooling the factor with the lowest significance, B, revised the following:

$$f_e = 8 - (2 + 2) = 4$$

$$S_e = 6184.0459 - (494.3059 + 5346.4893) = 343.2507$$

$$V_e = \frac{343.2507}{4} = 85.8127$$

$$F_A = \frac{247.1530}{85.8127} = 2.8801$$

$$F_C = \frac{2673.2447}{85.8127} = 31.1521$$

$$S'_A = 494.3059 - (85.8127 \times 2) = 322.6805$$

$$S'_C = 5346.4893 - (85.8127 \times 2) = 5174.8639$$

$$P'_A = \frac{322.6805}{6184.0459} = 0.052 \equiv 5.2\%$$

$$P'_C = \frac{5174.8639}{6184.0459} = 0.837 \equiv 83.7\%$$

$$P_e' = 100 - (5.2 + 83.7) = 11.1\%$$

The error DOF became half that of the total DOF, therefore the pooling up strategy was complete. The percentage contribution of the error became 11.1%, whereas previously without pooling, it was 2 %.

Since factor B was considered insignificant, the optimum equation (4.3) was revised according to Taguchi principles. [26]

$$Opt.Cond. = \overline{T} + (A2 - \overline{T}) + (C1 - \overline{T}) \quad \ldots \textbf{(4.3)}$$

$$Opt.Cond. = 86.48 + (76.11 - 86.48) + (60.04 - 86.48) = 49.67\mu m$$

$$prediction.error = 1 - \frac{49.67}{\frac{55.31 + 54.73}{2}} = 1 - 0.903 \equiv 9.7\%$$

The prediction error of 9.7% after the pooling up strategy fell within the error variance of 11.1% so the error variance represented the degree of inter-experiment error. The predicted grain size fell within the error margin, when compared to the actual grain size achieved at optimum settings. This verified the integrity of the experiment and showed that the effects factors C and A contributed 83.7% and 5.2% respectively. The effect of factor B was small enough to be absorbed into the inter-experimental error and thus did not significantly contribute towards the result outcome. The transition temperature was the most effective factor in delivering the discrete, fine grained primary phase to which the effect electromagnetic stirring strength gave a small contribution. The electromagnetic stirring speed (i.e. line frequency) was insignificant in delivering the final result and could be considered as part of experimental error.

Test of Significance Pooling

The next factor to consider for pooling was factor A since its effect contributed 5.2% towards the end result. It was the next least contributing effect towards the end result.

Variance ratio (F_A value) = 2.8801

DOF of factor A = 2

DOF of error term = 4

confidence level % = 90

F-table value = 4.3246

Since the F_A value was smaller than the F-table value, factor A should be pooled.[26] The following were revised:

$$f_e = 8 - (2) = 6$$

$$S_e = 6184.0459 - (5346.4893) = 837.5566$$

$$V_e = \frac{837.5566}{6} = 139.5927$$

$$F_c = \frac{2673.2447}{139.5927} = 19.1503$$

$$S_C^{'} = 5174.8639 - (139.5927 \times 6) = 4337.3077$$

$$P_C^{'} = \frac{4337.3077}{6184.0459} = 0.701 \equiv 70.1\%$$

$$P_e^{'} = 100 - 70.1 = 29.9\%$$

Similarly, the optimum condition equation (4.4) was revised.

$$Opt.Cond. = \overline{T} + (C1 - \overline{T}) \quad \textbf{... (4.4)}$$

$$Opt.Cond. = 86.48 + (60.04 - 86.48) = 60.04\,\mu m$$

$$prediction.error = \frac{60.04}{\frac{55.31 + 54.73}{2}} - 1 = 1.091 - 1 \equiv 9.1\%$$

The prediction error remained approximately the same and the optimum condition (i.e. the grain size) increased to 60.05 μm. Performing this extra step in pooling by testing the significance did not yield any more useful information that could not be determined from the previously performed pooling up strategy.

4.2.2.2 Pooling strategy confirmation

The Taguchi method of pooling insignificant factors had shown that factor B, line frequency (f), was an insignificant factor from the pooling up strategy. It had also shown that factor A, base frequency (f_0), was an insignificant factor from the test of significance pooling. In the latter case, factor B was already pooled into the error term. According to the test of significance pooling method, both A and B were considered insignificant for producing a fine grained, equiaxed primary phase. The prediction error for both pooling methods were approximately the same so the correct pooling strategy could not be determined by comparing the error of the pooling strategy with the actual error calculated from the ANOVA analysis.

Therefore, it was unclear if the factors influencing the stirring were at all necessary to produce a fine grained, equiaxed primary phase. A confirmation experiment was conducted to determine if the stirring factors were at all needed to produce the desired outcome of the microstructure. The SBC system was used to cast billets at the optimum conditions, one without stirring applied and another with stirring applied.

Results showed that the unstirred billet had a fine dendritic grained microstructure and the stirred billet had a fine grained, equiaxed microstructure (figure 4.7). It was evident that stirring had an influence towards the desired microstructure. Therefore, the pooling up strategy was the correct pooling technique to use for determining the prediction error.

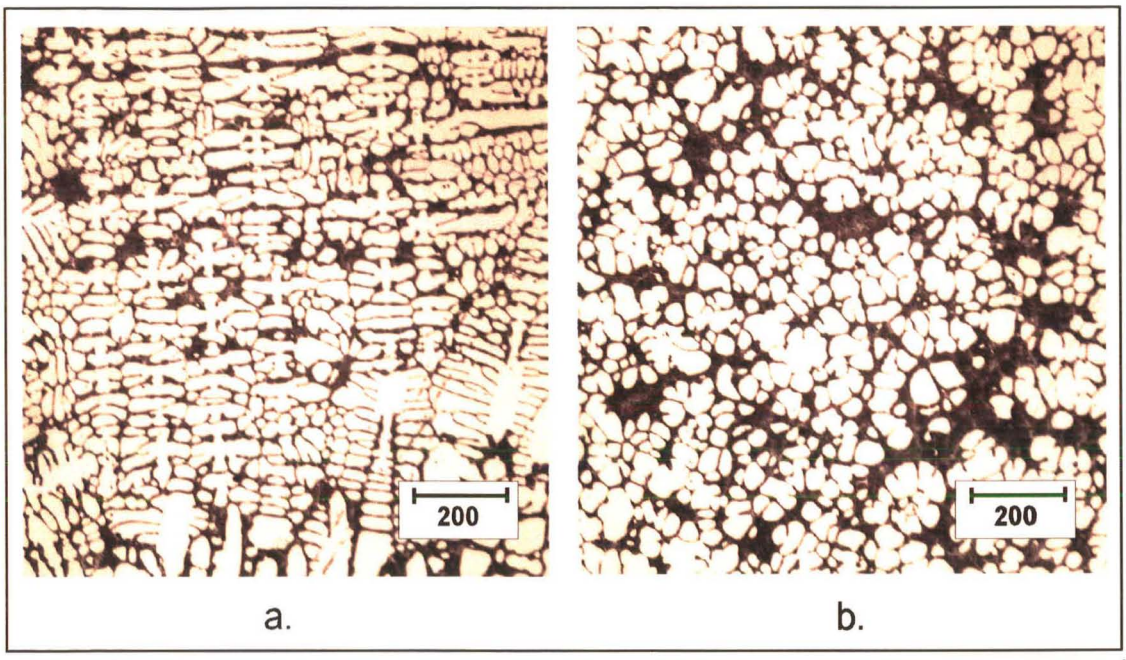

Figure 4.7 Microstructures obtained from billets cast using the SBC system with $T_i = 620\ ^0C$ and **a.** with no stirring and **b.** with stirring at f = 70 Hz and $f_0 = 220$ Hz.

4.3 Eutectic Phase Formation

This experiment determined the cooling conditions necessary to create a fine textured eutectic phase. Since the eutectic phase was the last to solidify when the solidus temperature was reached, the texture was dependant on the cooling rate of the melt as it crossed the solidus temperature. Basically, the higher the cooling rate across this temperature, the finer the texture.

Figure 4.8 shows the results from quenching the samples in the different media, as described by the caption of each figure.

An interesting characteristic common to all the microstructures (figure 4.8) was that the dendrite arm spacings were approximately equal. This was due to the samples all being cooled at the same rate in air to 600 ^{0}C, where nucleation had already started at 615 ^{0}C. Therefore the grain growth conditions were the same for each sample until 600 ^{0}C. This was deliberately done to confirm that eutectic phase formation was independent of nucleation and growth of the primary phase.

Starting with the air cooled samples, the eutectic phase showed very coarse silicon particles with the furnace cooled sample having a coarser texture of the two. This was due to a lower heat transfer coefficient in the hot air. The water cooled samples had a fine texture, however only the cold water quenched sample had an acceptable texture for the eutectic phase. The hot water quench sample had evidence of coarse silicon particles due to the lower heat transfer coefficient of the hot water. The oil cooled samples did not have an acceptable texture although both had an equivalent level of silicon particle coarseness which suggested an equivalent heat transfer coefficient between hot and cold oil. Of all the quenching media above, only the cold water showed a high enough heat transfer rate to form a fine textured eutectic phase.

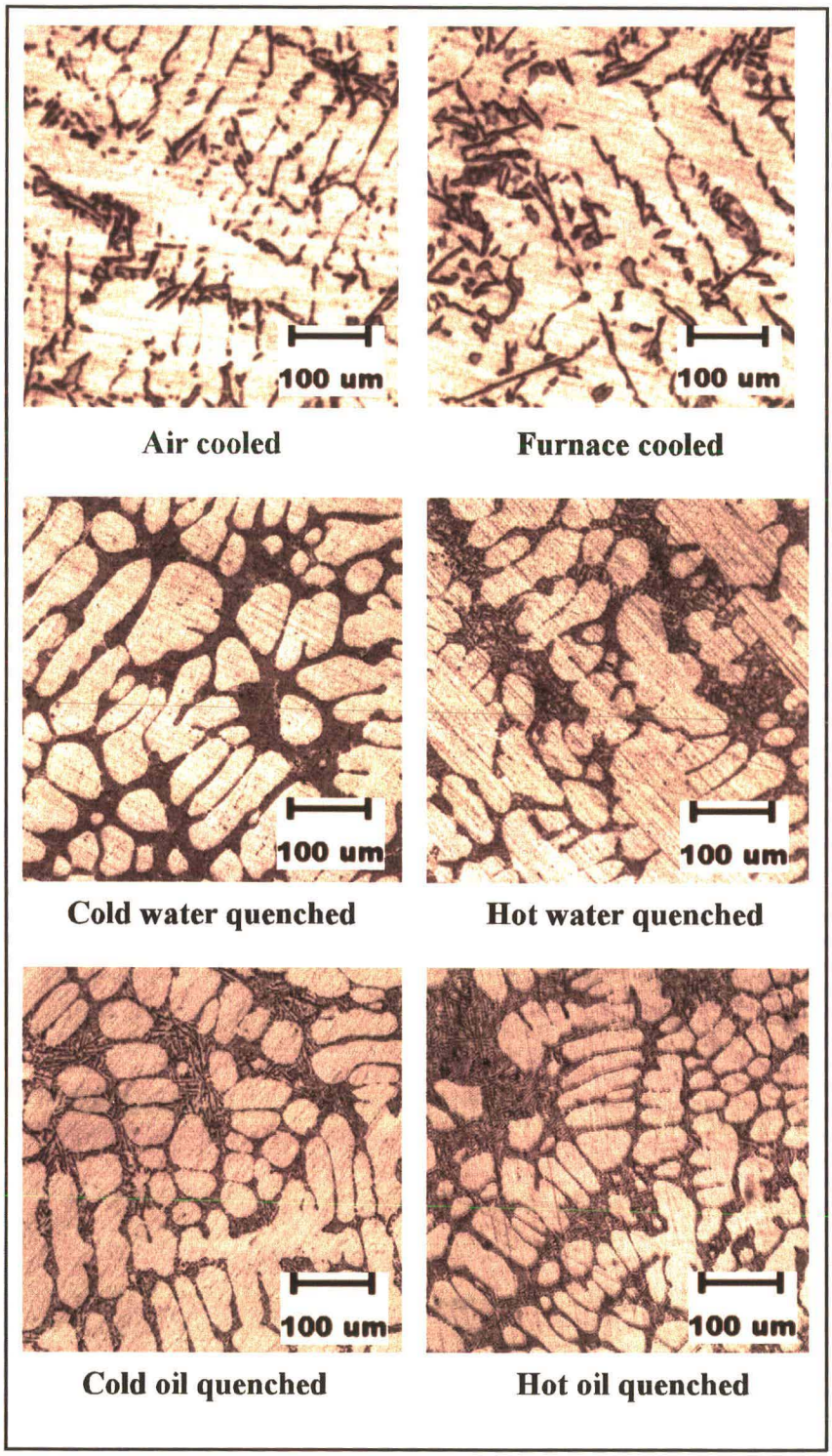

Figure 4.8 Eutectic texture formations as a result of the cooling/quenching media noted below each figure.

4.4 Single Billet Caster Billets

The Single Billet Caster (SBC) billets were all cast using the split mould/ riser system which produced a billet of 50 mm diameter by 200 mm length with no macro shrinkage pores (figure 4.9). The process parameters were transferred from the optimum condition derived from the Taguchi experiment for the primary phase formation (Chapter 4.2.2). Table 4.6 summarizes the factor settings used for the SBC casting trials and figure 4.10 shows the microstructures which resulted from those settings.

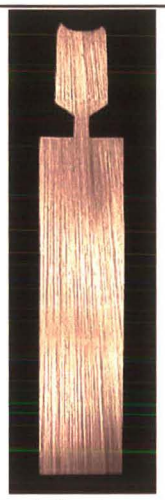

Figure 4.9 A sectioned SBC billet showing the absence of shrinkage pores.

In figure 4.10, SBC 1 shows the microstructure obtained from the SBC billet cast with the optimum parameters of f_0 = 220 Hz, f = 70 Hz, and T_i = 615 ^{0}C. The primary phase grain structure showed a fine grained, equiaxed morphology. However, there appeared to be quite a variance in the grain size. This was anticipated to be as a result of the weakened electromagnetic field strength supplied to the melt due to the thicker mould wall of the SBC mould. The Taguchi test mould had a mould wall thickness of 1.6mm whereas the SBC mould had a wall thickness of 6mm. This extra thickness of the SBC mould would have reduced the effectiveness of the electromagnetic field.

To increase the effective strength of the electromagnetic field, the base frequency had to be reduced to increase the V/Hz ratio of the frequency controller. Thus for the same line frequency setting, the voltage supplied to the controller would increase thereby increasing the power supplied to the electromagnetic coils. The voltages recorded from the SBC 2 to SBC 4 trials (table 4.6) confirmed this reasoning.

Since the line frequency only contributed 3.5% towards the outcome of the fine grained, equiaxed primary phase, it was decided to reduce this setting from 70 Hz to 50 Hz, which is standard line frequency of the national grid. This was done for the sake of further research into this field to show that the line frequency need not be altered from the national grid supply and thus save on the cost of a variable frequency power source.

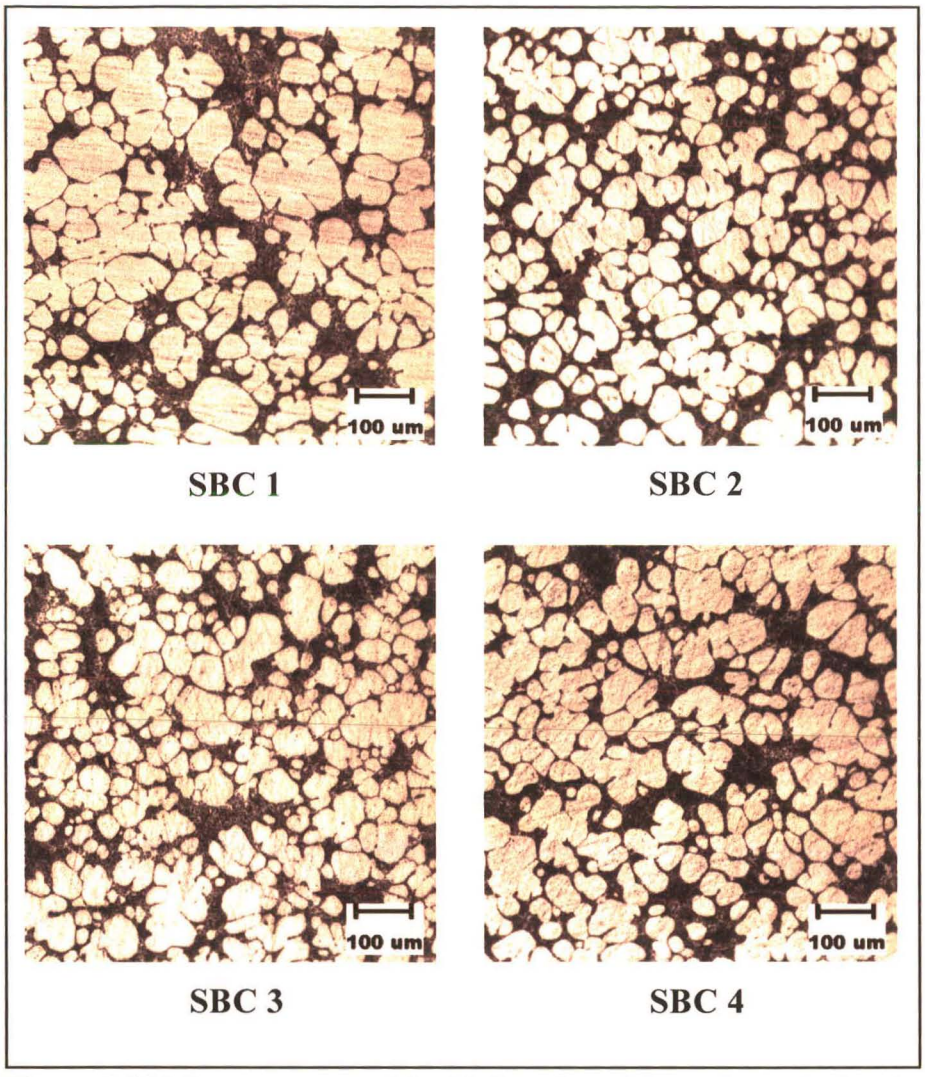

Figure 4.10 Microstructures of the SBC casting trials performed using the parameters listed in table 4.6.

Table 4.6 Summary of the line frequency and base frequency settings used for the SBC casting trials with the resulting load and voltage values measured by the AC motor drive unit.

Trial	f_0	f	T_i	load	V
S B C 1	220	70	615	46%	134
S B C 2	220	50	615	44%	102
S B C 3	200	50	615	51%	110
S B C 4	180	50	615	60%	120

Reducing the line frequency to 50 Hz (for SBC 2 to 4, figure4.10) seemed to have improved the primary phase morphology, when compared to the optimum condition (SBC 1, figure 4.10). Successively reducing the base frequency, from 220 Hz to 180 Hz (SBC 2 to 4), to increase the stirring strength did not have a visual effect on improving on the primary phase morphology. The successive increase in the stator load from 44 % in SBC 2 to 51 % in SBC 3 and finally to 60 % in SBC 4 reflected this increase in stirring strength.

In fact, the appearance in SBC 3 (figure 4.10) showed quite a variance in grain size while SBC 2 and 4 (figure 4.10) showed a more uniform primary phase appearance. The primary phase morphology was varying independent of the successive changes in the stirring strength, although on the whole, it remained a fine grained, equiaxed morphology.

An explanation for the variance in the above results could be derived from the findings of the primary phase formation and the eutectic phase formation experiments. The primary phase formation experiments had shown that the temperature conditions had the largest influence towards the outcome of the primary phase morphology. The slightest variation in these conditions would likely cause a noticeable change in the results. The eutectic phase formation experiments have shown that different cooling rates through the eutectic phase result in different eutectic phase textures. The higher the cooling rate, the finer the eutectic phase texture.

Referring to SBC 1 to 4 (figure 4.10), the eutectic phases did not show a consistent texture. SBC 1 and 3 show a coarser eutectic phase texture and also show a variance in the primary phase grain size. The coarser eutectic indicates that the cooling rate was slightly slower compared to that in SBC 2 and 4. In all likelihood, the temperature conditions were different for SBC 1 and 3. Since the temperature conditions had a significant influence toward the outcome of the primary phase morphology, it was likely that this was the cause of the variations in the grains size in SBC 1 and 3.

4.5 Cooling Rate Measurements

Since the effective temperature range for forming the equiaxed, discrete primary phase was between 615 ^{0}C and 605 ^{0}C, the cooling rate graphs (figure 4.11, 4.13, 4.15) for three different experimental conditions are shown with the temperature ranging from 620 ^{0}C to 600 ^{0}C.

Figure 4.12 and 4.14 show the temperature profile of the complete casting process starting with the preheated mould temperature and ending with a completely chilled mould for the two different casting processes used in this research, the Taguchi experiment casting and the Single Billet Caster (SBC) casting. In both these graphs, the profiles displayed similar characteristics.

The flat portion between 400 and 500 ^{0}C was the mould preheat temperature followed by a sharp rise to approximately 675 ^{0}C when the molten aluminium was poured into the mould. The drop in temperature that followed the peak was the molten aluminium cooling down while the mould absorbed the heat energy thereof. The sudden levelling of the profile thereafter occurred when the stirring unit was switched on. The arrest of the temperature drop at this point was due to the electromagnetic energy input into the mould from the inductor coils which arrested the heat flow out of the mould thus maintaining the temperature. Also, the latent heat of formation was given off as the solid began to form in the melt thus creating more heat energy which needed to be dissipated over and above that of the energy input from the inductor coils. Shortly after the electromagnetic coils had been activated, the cooling water was switched on and the temperature profile then dropped down through the solidification range of the melt.

For the following graphs (figure 4.11, 4.13, 4.15), the cooling rate (CR) was measured by measuring the gradient between the endpoints where the profile intercepted the temperatures 615 ^{0}C and 605 ^{0}C. Also, if the cooling rate increased between these endpoints, the gradient of the asymptote which passed through the inflexion point of the profile was calculated. If there was a difference between the temperature profiles of T_{top}

and T_{bottom}, (i.e. temperature of the top thermocouple and temperature of the bottom thermocouple respectively), their respective gradients as discussed above were calculated. This comprehensive analysis gave a better feel for the range of cooling rates experienced by the whole billet and a suitable average cooling rate could be determined.

The factor T_i was the temperature at which the cooling water was switched on thereby increasing the cooling rate of the melt from a slow cooling rate to a fast cooling rate. The slow cooling rate before T_i is shown in figure 4.11.

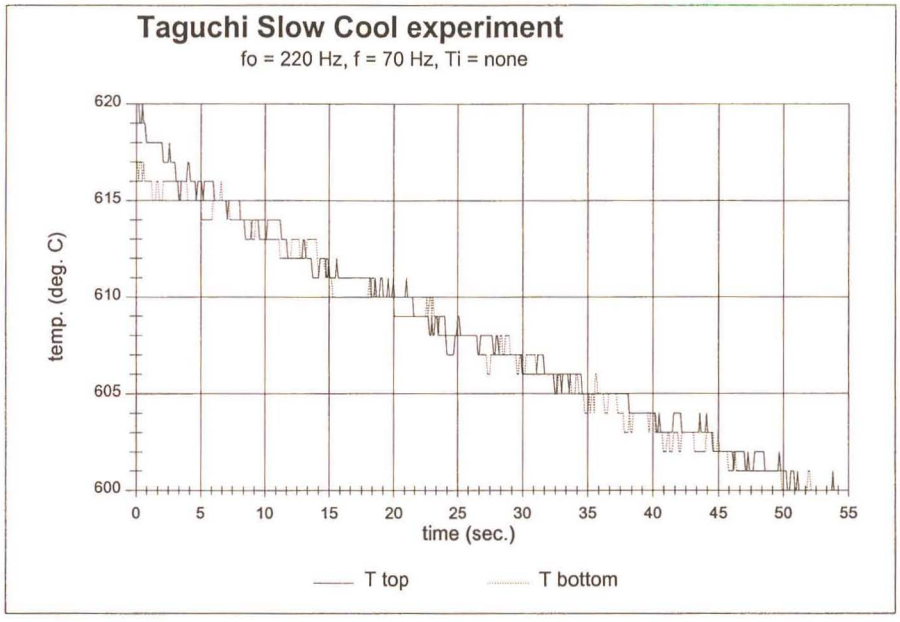

Figure 4.11 Cooling rate profile of the slow cooling rate during the Taguchi experiment.

The difference between T_{top} and T_{bottom} in the slow cooling profile of figure 4.11 was negligible and the gradient was constant between the endpoints so the cooling rate was uniform throughout the billet. The cooling rate for this situation was:

$$CR = \frac{615-605}{6-35} = -0.345\,{}^{\circ C}/_{sec} \equiv -20.7\,{}^{\circ C}/_{min}$$

Figure 4.12 shows the cooling profile of the casting made during the Taguchi experiment with the optimum conditions of the factors applied. The difference between T_{top} and T_{bottom} during solidification was negligible between 620 ^{0}C and 605 ^{0}C, however the cooling profile did not maintain a constant gradient between the endpoints as shown in figure 4.13. Thus two gradients were calculated showing the cooling rate between the endpoints (CR_{endpts}) and the cooling rate of the steepest gradient within the range of the endpoints (CR_{max}).

$$CR_{endpts} = \frac{615-605}{29.5-34.75} = -1.905\,{}^{0}C/_{sec} \equiv -114\,{}^{0}C/_{min}$$

$$CR_{max} = \frac{615-605}{32-35} = -4.667\,{}^{0}C/_{sec} \equiv -280\,{}^{0}C/_{min}$$

Figures 4.14 and 4.15 showed the temperature profiles of the SBC castings made with the same optimum values determined from the Taguchi experiment. The temperature profile between the endpoints showed both a difference in T_{top} and T_{bottom} and a changing gradient in the cooling rate. Below are the CR_{endpts} and CR_{max} values for both T_{top} and T_{bottom}.

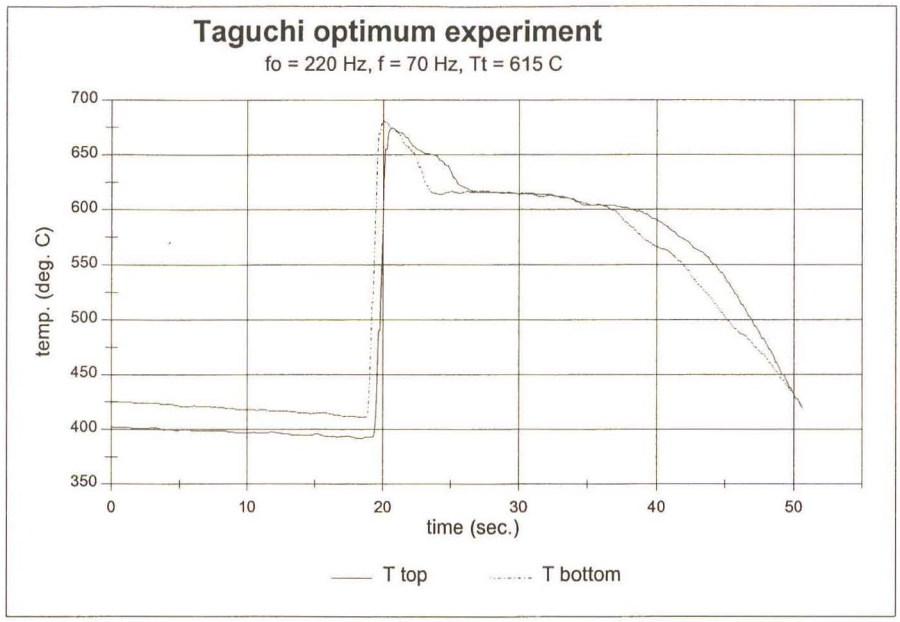

Figure 4.12 Temperature profile of the Taguchi experiment performed with the optimum settings. The whole casting cycle from metal pouring to complete solidification is shown.

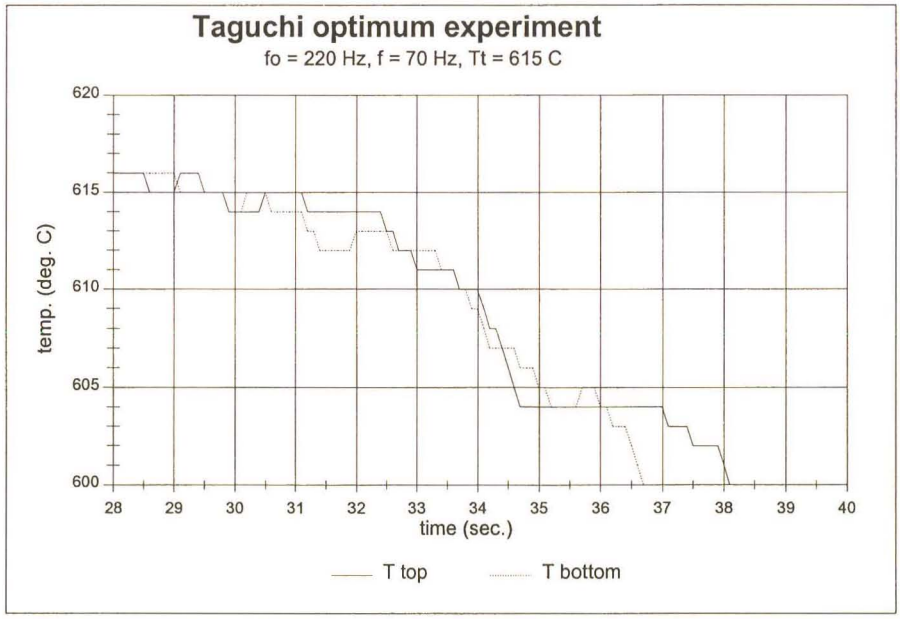

Figure 4.13 The cooling rate profile portion of figure 4.8 from the liquidus temperature to the temperature at which the slurry stops turning at 604 ^{0}C.

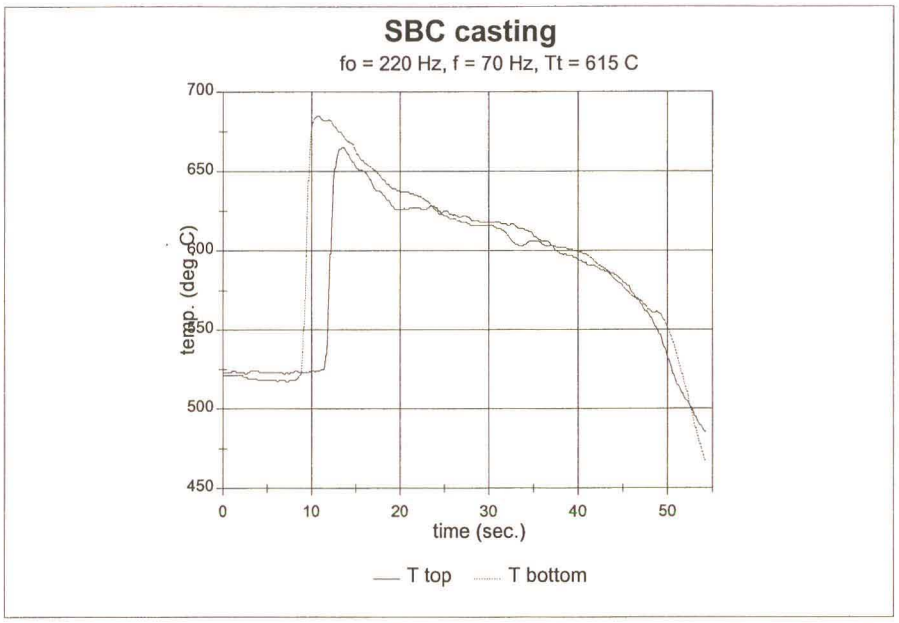

Figure 4.14 Temperature profile of the SBC casting performed at the optimum setting determined from the Taguchi experiment. The whole casting cycle from metal pouring to solidification is shown.

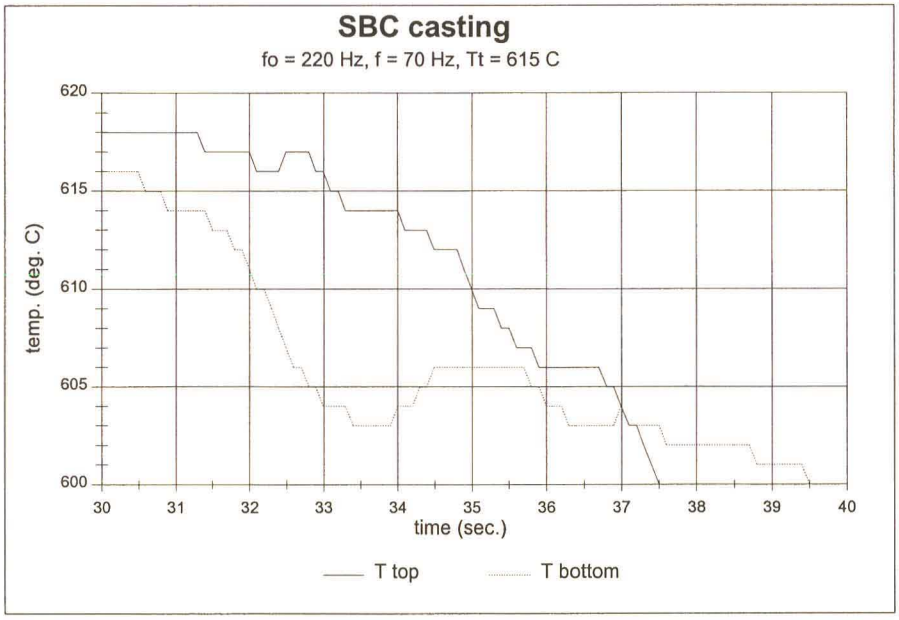

Figure 4.15 The cooling rate profile portion of figure 4.10 from the liquidus temperature to the temperature at which the slurry stops turning at approximately 605 ^{0}C.

For T_{top}:

$$CR_{endpts} = \frac{615-605}{33.2-36.8} = -2.778\ ^{0}C/_{sec} \equiv -167\ ^{0}C/_{min}$$

$$CR_{max} = \frac{618-601}{33-37} = -4.25\ ^{0}C/_{sec} \equiv -255\ ^{0}C/_{min}$$

For T_{bottom}:

$$CR_{endpts} = \frac{615-605}{30.6-32.8} = -4.545\ ^{0}C/_{sec} \equiv -273\ ^{0}C/_{min}$$

$$CR_{max} = \frac{617-604}{31-33} = -6.5\ ^{0}C/_{sec} \equiv -390\ ^{0}C/_{min}$$

The difference in the T_{top} and T_{bottom} temperatures (figure 4.15) may be explained by the fact that the thermocouples were spaced further apart than was the case in the Taguchi experiment. Also, the SBC mould was twice as long as the mould used for the Taguchi experiment and the effect of directional solidification was more pronounced. This also explained why the T_{bottom} cooling rates in figure 4.15 were higher than those of T_{top}. The directional solidification mechanism started from the bottom of the billet and moved upwards. The cooling water used to chill the mould also flowed down the sides of the mould so the bottom of the mould was in contact with water for a longer period of time than the top of the mould. Hence the faster cooling rate at the bottom of the mould.

Referring to the temperature profiles in figures 4.13 and 4.15, two characteristics differ between the Taguchi experiment and the Single Billet Caster.

Firstly, the mould preheat temperatures differed, where the Taguchi experiment mould started at approximately 400 ^{0}C and the SBC mould started at approximately 525 ^{0}C. Both were preheated in the same furnace set at 675 ^{0}C and then transferred to the stirring apparatus. Heat energy in the moulds were dissipated during the transfer of the moulds from furnace to apparatus. However, the mass of the Taguchi experiment mould was far less than that of the Single Billet Caster mould, having a wall thickness of approximately 1.6mm and a length of 100mm. The Single Billet Caster mould had a wall thickness of 6mm and was 200mm in length. The Single Billet Caster mould therefore contained more heat energy within and dropped in temperature slower than the Taguchi experiment mould over the same time period taken during the transfer.

Secondly, the time period from when the melt was poured into the mould until the billet cooled down to 500 ^{0}C was longer for the SBC process. This time period was approximately 25 seconds for the Taguchi experiment process and approximately 42 seconds for the SBC process. Again this can be explained by the bigger mass of the SBC mould and also the larger mass of the billet therein. This larger mass contained more heat energy, which under the heat flow conditions within the stirring unit, took a longer period of time to dissipate than the Taguchi experiment process under the same conditions.

4.6 Reheating Characteristics

Figure 4.16 shows the reheating profile of an A356.2 sample of similar proportions to those samples actually reheated and analysed this experiment. The furnace was set to 590 ^{0}C and the size of the sample was a cube with approximately 1cm sides.

Figure 4.16 shows three distinct gradients. The first gradient was very steep and ended in the region of 5 minutes from the time the sample was inserted into the furnace from room temperature. This first gradient represented the heating rate of the sample while it was totally solid.

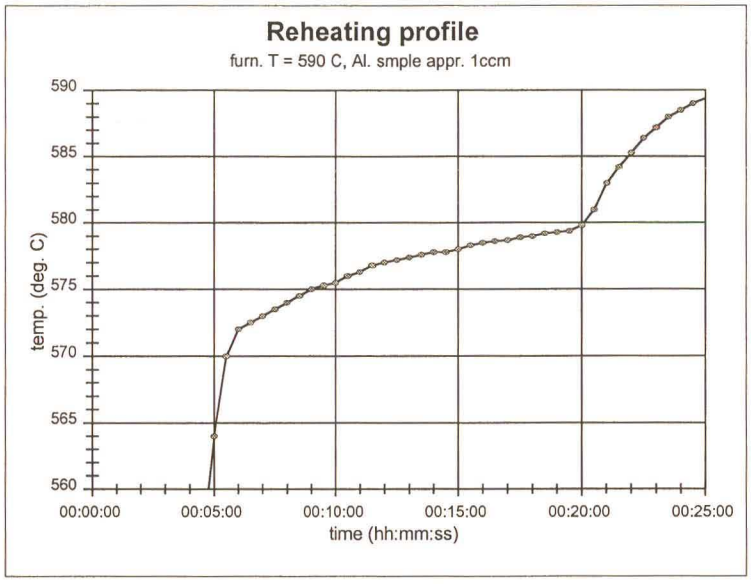

Figure 4.16 The reheating profile of A356.2 up to a temperature of 590 ^{0}C.

The second gradient showed a much reduced heating rate from that of the first gradient. This shallower gradient represented the phase change of the eutectic phase in the metal over the temperature range of 572 ^{0}C to 579 ^{0}C. The heating rate was reduced during this phase because extra heat energy was absorbed by the material to transform into the higher energy state of a liquid phase.

The third gradient increased dramatically again since the eutectic phase had been fully transformed to the liquid phase. The remainder of the solid phase, the primary phase,

would have remelted during this gradient until all was fully transformed into liquid at 615 ^{0}C. However, the furnace was set to 590 ^{0}C thus the gradient tapered off strongly near this temperature due to the low temperature difference between sample and furnace.

Figure 4.17 shows the microstructural evolution of samples from a SBC cast billet. The samples were exposed to the same furnace conditions as the reheated sample used in measuring the reheating profile above. In figure 4.17, f0 represents a sample in the as cast condition prior to reheating. The reheated samples (f1, f2, f3, f4, f5) were quenched at 5 minute intervals; starting with sample f1 (figure 4.17).

After 5 minutes of reheating, the temperature of sample f1 (figure 4.17) had reached approximately 564 ^{0}C (refer to reheating curve, figure 4.16). The eutectic phase showed signs of coarsening. The primary phase remained unchanged. After 10 minutes, the temperature of sample f2 (figure 4.17) had reached approximately 576 ^{0}C (refer to reheating curve, figure 4.16). The silicon particles in the eutectic phase had coalesced to form globules between the primary phase grains. The primary phase grains had also begun to coalesce and the primary grains had become larger.

After 15 minutes the temperature of sample f3 (figure 4.17) had reached approximately 578 ^{0}C (refer to reheating curve, figure 4.16). The sample showed that the eutectic phase had fully transformed and the primary phase grains had spheroidised completely to a grain size of approximately 100 μm. The samples f4 and f5 (figure 4.17), which had been reheated for 20 minutes and 25 minutes respectively, had reached a temperature of approximately 580 ^{0}C and 589 ^{0}C respectively (refer to reheating curve, figure 4.16). There was no noticeable change in the eutectic and primary phases compared to f3. There were, however, signs of fine dendritic primary phase present in the eutectic regions. This was due to the primary phase beginning to remelt and dissolve into the liquid phase and upon quenching, the dissolved primary phase precipitated as a fine dendritic grain. Sample f5 showed signs of more fine dendritic grains than that of sample f4. This was due to the higher temperature reached by sample f5. Hence, there would be more dissolved primary phase in sample f5 prior to quenching.

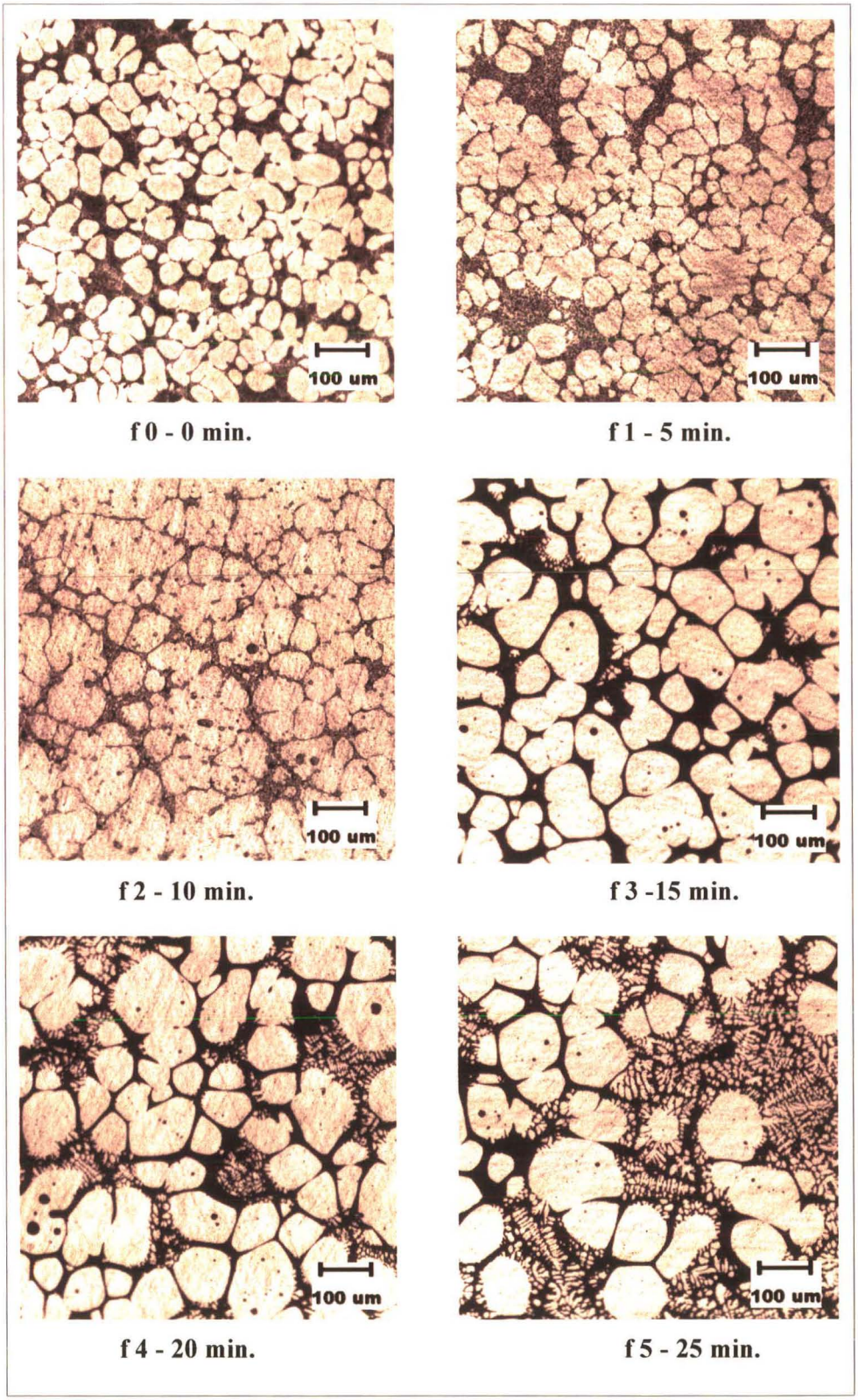

Figure 4.17 Microstructures of reheated samples of SBC material. Samples were quenched after the reheating times indicated below each figure.

Figure 4.18 shows the microstructural evolution of the commercially available semi solid feedstock supplied by Pechiney. The reheating conditions for samples p1, p2, p3, p4 and p5 (figure 4.18) were identical to those of samples f1 to f5 (figure 4.17). So the temperatures at which the samples were quenched were 564, 576, 578, 580 and 589 ^{0}C respectively. The characteristic features of each of the samples p0 to p5 were similar to the features already described for samples f0 to f5. The microstructural evolution was thus the same as for the SBC material. The only exception was that the primary phase grain size was a lot smaller in the as cast condition, prior to reheating than that of the SBC material. The final grain size of the Pechiney material after full eutectic transformation looked similar to the final grain size of the SBC material.

Figure 4.19 shows the microstructural evolution of the commercially available semi solid feedstock supplied by SAG. Again, the reheating conditions were identical to that of the SBC material reheating tests. Thus, the temperatures from which s1, s2, s3, s4 and s5 (figure 4.19) were quenched were the same as mentioned for samples f1 to f5 (figure 4.17).

Observing the microstructures of f3, p3 and s3 samples, one notices that the grain sizes were all similar at approximately 100 to 120 μm. This was despite the fact that the as cast grain sizes (f0, p0, s0) were quite different between the SBC and commercial alloys.

There was a distinct change of morphology in both the primary and eutectic phase at the 10 minute interval of f2, p2 and s2. The primary phase grains coalesced and suddenly grew in size. The silicon in the eutectic phase had also coalesced into small globules. It seemed that the α phase present in the eutectic phase had diffused to the primary phase grains and contributed to their sudden growth.

A distinct feature of the reheated commercial alloys was the trapped eutectic in the primary phase grains. This was a result of the rosette shaped grains closing up small regions of eutectic as the primary grain arms coalesced to form the larger, final primary grains after reheating. The SBC material was largely free of trapped eutectic in the primary phase grains due to the primary grains being larger and nearly globular prior to reheating. This meant that there was less movement of primary phase material and less coalescence of primary phase grains to trap the eutectic phase during transformation.

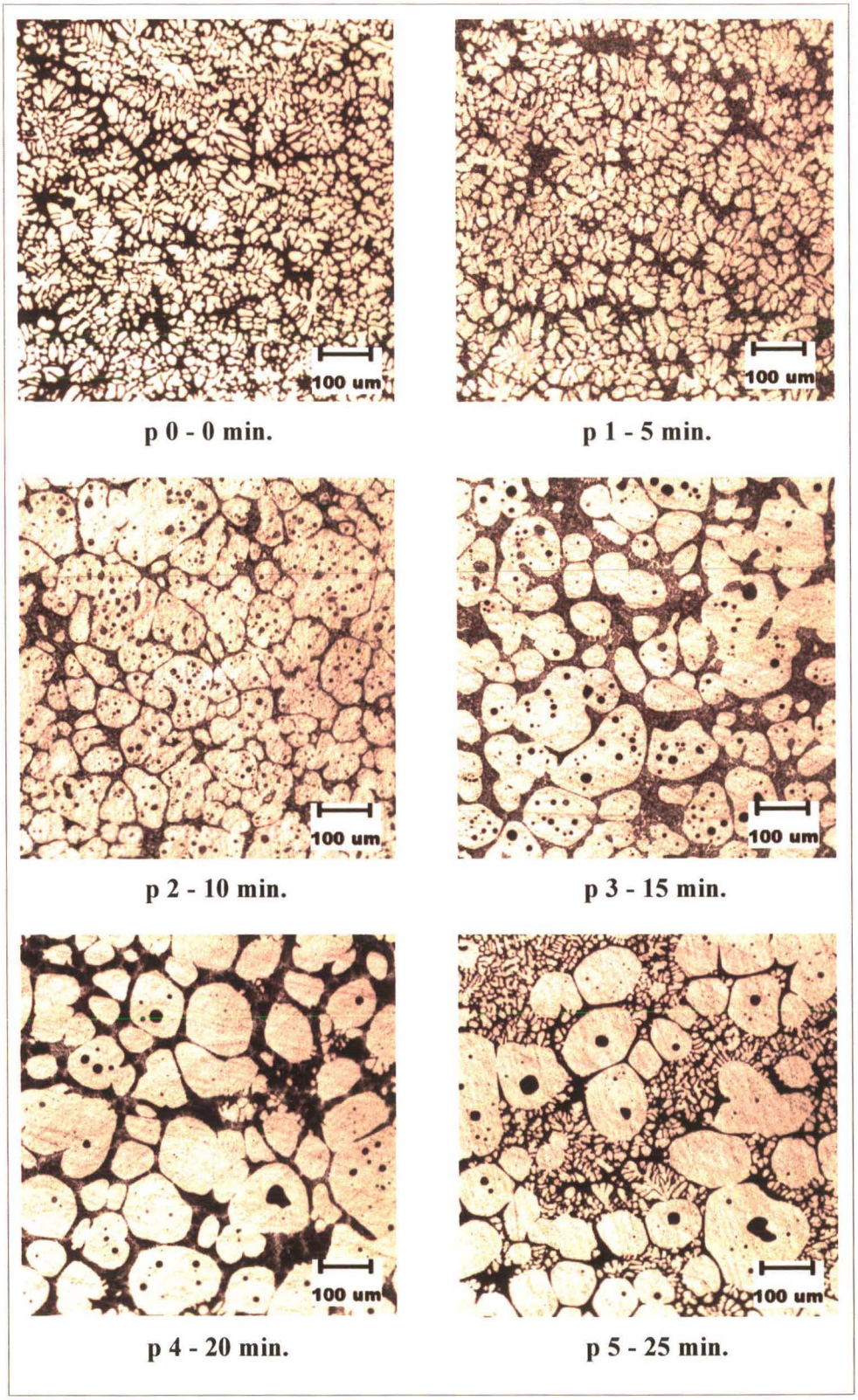

Figure 4.18 Microstructures of reheated samples of Pechiney material. Samples were quenched after the reheating times indicated below each figure.

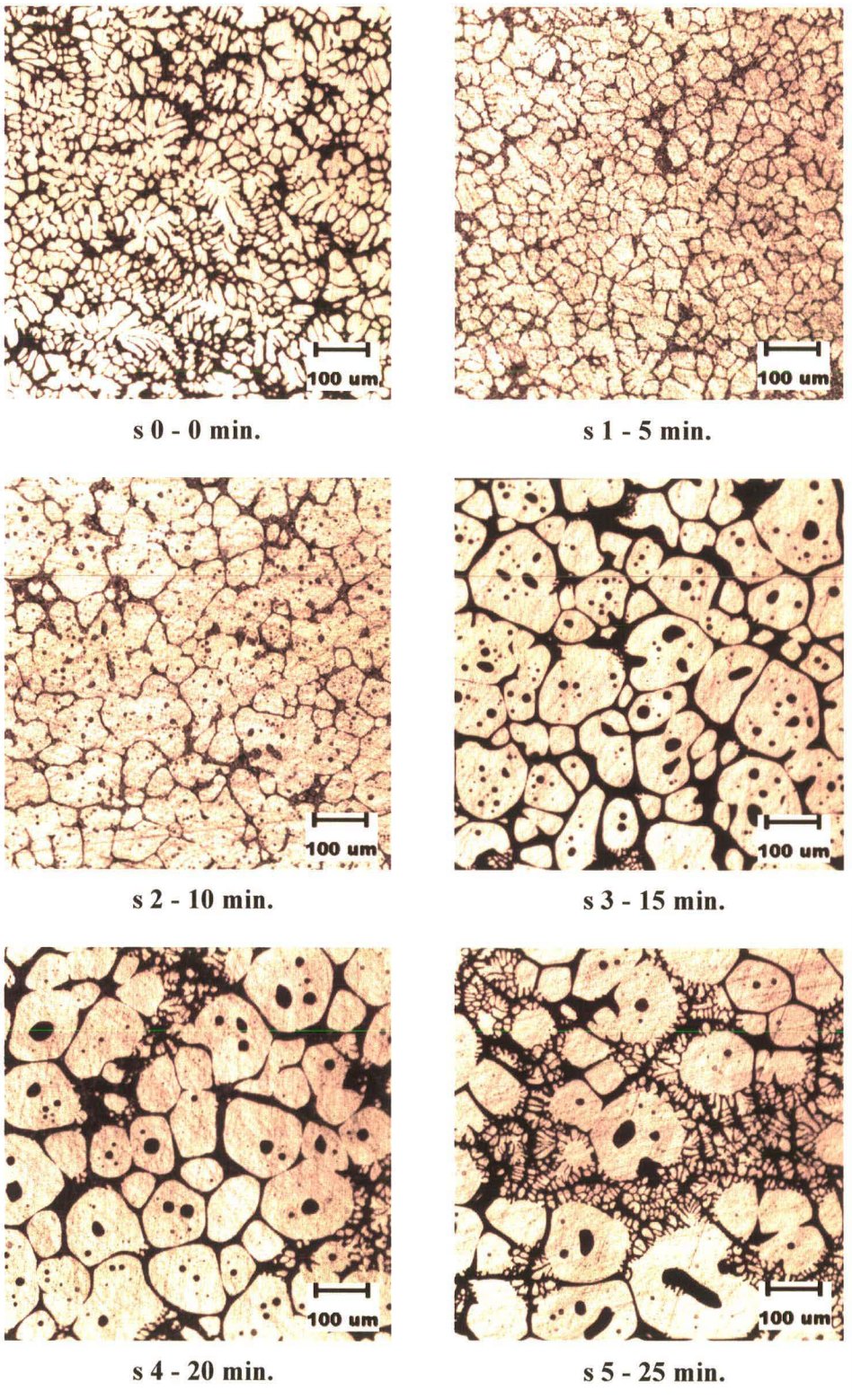

Figure 4.19 Microstructures of the reheated samples of SAG material. Samples were quenched after the reheating times indicated below each figure.

Figure 4.20 shows the appearance of the ground and polished surfaces of the reheated samples of the SBC, Pechiney and SAG feedstock. The SBC feedstock (figure 4.20) had small pores all over the surface which had the appearance of gas pores due to their smooth inside surfaces and spherical shape. This gas could have resulted from hydrogen absorption during melting and/or turbulence during mould filling. Upon reheating, the pores would be exaggerated due to the trapped gas expanding with heat.

The commercial feedstock, Pechiney and SAG (figure 4.20), showed surfaces free of pores. This was due to the fact that these materials were continuously cast strand. Material produced by the continuous casting method had less porosity than chill cast material since the directional freezing mechanism forced gas to the interface,[33] between the liquid and solid metal, during casting.

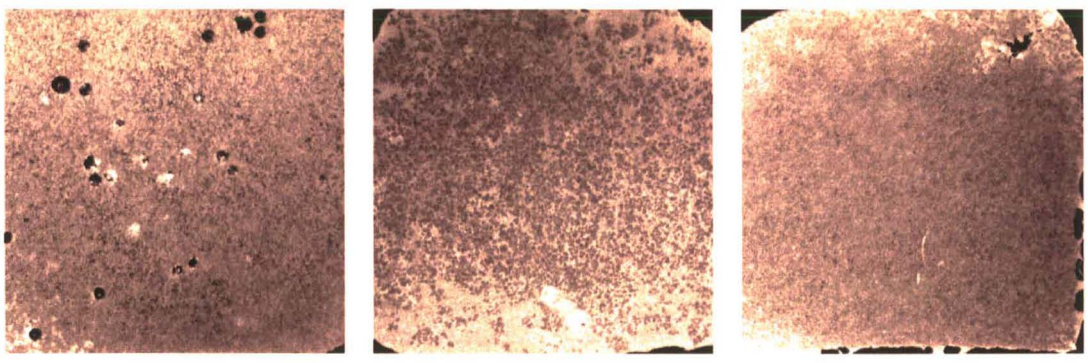

Figure 4.20 Appearance of the polished surfaces of the reheated samples of each of the materials indicated.

4.7 Summary of Results

A billet with a fine grained, equiaxed primary phase and a fine textured eutectic phase was produced using the SBC system with the MHD stirrer. The process parameters, shear rate and solidification rate were controlled and monitored indirectly by experimenting with the base frequency, and line frequency of the motor stator and the temperature of the melt at which the cooling water spray was initiated.

The Taguchi method was used to achieve the aim of determining the influence of the SBC process factors on the formation of the SSM microstructure. The Taguchi method was also used to show the optimum settings of the levels of process factors used in the experiment as well as the estimated value of D_{NEW} at this condition. The optimum estimated value was verified by performing further trial runs at the optimum settings. This produced results that were repeatable and within error limits of the estimated optimum value, thus confirming the integrity of the experiment. Further deductions have been summarized from the following sections.

4.7.1 Material characterisation

1. Chemical analysis showed that the raw material was within the nominal specification of A356.0.
2. The microstructure confirmed the use of grain refiner and modifiers due to evidence of a fine grain primary phase and a fine textured eutectic.
3. The DTA analysis on the cooling profile showed a liquidus temperature of 617 ^{0}C, a solidus temperature of 570 ^{0}C and the start of eutectic transformation at 578 ^{0}C.

4.7.2 Primary Phase Formation

1. T_i had the greatest influence over the formation of the appropriate primary phase where the factors governing the shear rate had very little influence. This implied that inhibiting excessive grain growth by high solidification rates of the melt had a far greater influence in achieving the fine grained, equiaxed primary phase than

attempting to increase the remelting and fragmentation rate of the dendrites through a high shear rate.

2. The calculation of the D_{NEW} was effective in combining two characteristics, grain size and shape factor of the primary phase, into one result for use in optimizing the process factors.
3. Confirmation runs at the optimum setting derived from the Taguchi analysis showed a repeatable result. There was an indiscernible difference in the microstructure of the optimum condition when compared to an experimental trial run with similar process settings. The only process setting different was that of the line frequency. This factor contributed a very small percentage towards the outcome of the result and this visual comparison confirmed this.
4. The result of the optimum condition showed an error of 20 % between the predicted optimum result and the actual optimum result. The least significant factor, f (line frequency), was offsetting the value of the estimated optimum result and had to be pooled into the error term.
5. The process factors governing the shear rate were insignificant when compared to the process factor governing the cooling rate. However, they were necessary to remelt and degenerate the dendrites as they formed during solidification.
6. The chemistry of the alloy was kept constant throughout the investigation to restrict the variables to controllable process factors. The influence of the chemistry of the alloy A356.2 was beyond the scope of this investigation.

4.7.3 Eutectic Phase Formation

Water quenching was the only media from the selection of air, water and oil that provided sufficient heat transfer to create a fine textured eutectic phase.

4.7.4 Single Billet Caster Billets

1. The SBC billets showed similar microstructures when cast with the same process factor settings as the optimum condition castings from the Taguchi experiment.
2. The variance in the primary phase grain size and shape in the SBC billets were

evidence of the effects of slightly different temperature conditions in casting the billets.

4.7.5 Cooling Rate Measurements

1. During the Taguchi experiment, the cooling rate of the melt changed from 20.7 ^{0}C/min to approximately 200 ^{0}C/min at the initiation of cooling water (T_i).
2. The SBC casting temperature profiles showed slower cooling times through the semi solid forming temperature region when compared to the Taguchi experiment cooling times. This was due to the larger mass of liquid aluminium containing more superheat and also the thicker mould walls of the SBC mould restricting heat flow outwards to the cooling water.

4.7.6 Reheating Characteristics

1. The SBC microstructure in the as cast condition differed from those of the commercial alloys in the as cast condition. The SBC microstructure had a larger, rounder primary phase morphology while the commercial alloys had a finer, rosette shaped primary phase morphology. This was due to the higher cooling rates experienced in the continuous casting of the commercial alloys.
2. There was little discernable difference between the primary phase morphology of SBC material microstructure and the commercial alloy microstructure in the reheated state, except that the commercial alloy had a noticeable amount of trapped eutectic in the primary phase grains. The trapped eutectic in the commercial alloys was the result of the rosette grains, from the as cast condition, trapping pockets of eutectic as the primary phase grain arms coalesced into larger, rounder grains.

CHAPTER 5

5 Conclusions

1. The temperature of the melt at which the fast cooling rate was initiated had the most significant influence in the formation of a fine grained, equiaxed primary phase. The fast cooling rate had to be initiated at a melt temperature of 615 ^{0}C, which was specific to A356.2.

2. The process factors influencing the shear rate, base frequency and line frequency, had very little influence on the primary phase morphology although they were necessary to remelt and fragment the dendrites during the semi solid forming region.

3. This investigation was specific to A356.2. The influence of the process factors as well the optimum condition towards the formation of a fine grained, equiaxed primary phase was specific to the production method and alloy used. The influence of the latter variables was beyond the scope of this investigation.

4. The morphology of the reheated microstructures of the compared feedstock did not depend on the morphology of the as cast microstructure. As long as the as cast micostructure showed fine grained, equiaxed primary phase grains, they evolved to an equilibrium condition which showed similar characteristics when the commercial and research alloys were compared. However, the quality of the reheated microstructure, in terms of the exclusion of trapped eutectic, was dependant on the on the as cast microstructure.

A1 Three Phase Motor Data

THREE - PHASE MOTOR WINDING DATA - ELECTRICAL ENGINEERING - WEG MOTORES LTDA.

2 Poles 50 Hz 380 V Line.: STANDARD

CÓPIA CONTROLADA

C/G = COILS PER GROUP G/P = GROUPS PER PHASE CON = CONNECTION INS = INSULATION Io = NO LOAD CURRENT Po = NO LOAD OUTPUT

RATED OUTPUT		FRAME SIZE	BARS WIRES	TURNS		PITCH						C/G	G/P	CON	NUMBER OF LAYERS	INTERNAL CONNECTION	LENGHT OF STACK	STATOR DATA			INS	Io	Po
HP	KW			Z1	Z2	P1	P2	P3	P4	P5	P6							NUMB. SLOTS	INSIDE DIAMETER	OUTSIDE DIAMETER			
0.75	0.55	71	1 x 0.450 + x	92		10	12					2	2	Y	SINGLE	SERIES	60	24	56.00	110.00	B	0.76	70
1.50	1.10	80	1 x 0.630 + x	64		10	12					2	2	Y	SINGLE	SERIES	80	24	62.00	122.00	B	1.35	130
2.00	1.50	90S	1 x 0.800 + x	60		10	12					2	2	Y	SINGLE	SERIES	75	24	75.00	140.00	B	1.35	150
3.00	2.20	90L	2 x 0.670 + x	49		10	12					2	2	Y	SINGLE	SERIES	85	24	75.00	140.00	B	1.90	220
4.00	3.00	100L	1 x 0.850 + x	66		10	12					2	2	T	SINGLE	SERIES	110	24	92.50	160.00	B	2.10	250
5.00	4.00	112M	1 x 0.750 + 1 x 0.710	41		14	16	18				3	2	T	SINGLE	SERIES	95	36	100.00	182.00	B	3.15	350
7.50	5.50	132S	2 x 0.800 + x	32		14	16	18				3	2	T	SINGLE	SERIES	110	36	125.00	220.00	B	3.80	430
10.00	7.50	132S	1 x 0.800 + 2 x 0.750	28		14	16	18				3	2	T	SINGLE	SERIES	130	36	125.00	220.00	B	4.00	500
12.50	9.30	132M	2 x 0.750 + x	45		14	16	18				3	2	T	SINGLE	PARALLEL	150	36	125.00	220.00	B	6.00	600
15.00	11.00	160M	3 x 0.950 + 1 x 0.900	23		14	16	18				3	2	T	SINGLE	SERIES	130	36	140.00	240.00	B	6.30	650
20.00	15.00	160M	3 x 1.060 + 1 x 1.000	19		14	16	18				3	2	T	SINGLE	SERIES	180	36	140.00	240.00	B	5.40	700
25.00	18.50	160L	2 x 0.950 + 1 x 0.900	31		14	16	18				3	2	T	SINGLE	PARALLEL	220	36	140.00	240.00	B	7.00	880
30.00	22.00	180M	3 x 1.320 + 1 x 1.180	7		16						6	2	T	TWO	SERIES	200	36	175.00	283.00	B	8.00	1100
40.00	30.00	200L	2 x 1.320 + 4 x 1.180	6		9	11	13	15	17	19	6	2	T	TWO	SERIES	230	36	185.00	315.00	B	13.00	1700
50.00	37.00	200L	6 x 1.180 + 2 x 1.320	5		9	11	13	15	17	19	6	2	T	TWO	SERIES	250	36	185.00	315.00	B	20.00	2000
60.00	45.00	225S/M	8 x 1.320 + x	4		15	17	19	21			4	4	T	TWO	SERIES	220	48	220.00	380.00	B	20.00	3525
75.00	55.00	250S/M	5 x 1.320 + x	7	6	18	20	22	24			4	4	T	TWO	PARALLEL	260	48	220.00	380.00	B	25.00	3580
100.00	75.00	280S/M	17 x 1.320 + x	3		17	19	21	23			4	4	T	TWO	SERIES	230	48	280.00	480.00	B	32.00	4400
125.00	90.00	280S/M	21 x 1.320 + x	3		13	15	17	19			4	4	T	TWO	SERIES	270	48	280.00	480.00	B	35.00	4900
175.00	132.00	315S/M	34 x 1.320 + x	2		18	20	22	24			4	4	T	TWO	SERIES	350	48	280.00	480.00	F	49.00	5400
200.00	150.00	315S/M	21 x 1.320 + x	4	3	14	16	18	20			4	4	T	TWO	PARALLEL	450	48	280.00	480.00	F	62.00	5000
250.00	185.00	315S/M	24 x 1.320 + x	3		18	20	22	24			4	4	T	TWO	PARALLEL	450	48	280.00	480.00	F	80.00	4480

EXECUTED.: EDINEI CHECKED.: EMERSON REALESED.: DATE..: 13/11/95 REV.: 00

A2 Kontron KS300 Image Analysis Macro

Macro C:\KS300\Conf\Macros\fred50.mcr

```
imgdelete 1
Gclear 0
! imgload "a:\19_ la_50.tif.",1
MSsetgeom
MSmarker 1,100.00,0.00,570,479,14,1,2      {sets the scale}
Gmerge 1,255                               { merges scale onto the image}
iimgdisplay 1
MSsetframe
! Dislev 1,2,173,255,1                     {prompts to set threshold}
imgdisplay 2
binscrap 2,3,0,100,0                       {cleans image - scraps small areas}
imgdisplay 3
binuerode 3,4,7,3                          {ultimate erode operation}
imgdisplay 4
binudilate 4,5,7,4                         {ultimate dilate operation - leaves single
                                           pixel line between touching particles}
imgdisplay 5
! imgsave 5,"d:\ks300\conf\images\fredla.bmp"
! imgload "d:\ks300\conf\images\fredla.bmp",5
binand 3,5,6                               {combines thresholded & dilated image to
                                           create grains with non touching sides}
imgdisplay 6
dislev 6,7,120,0, 0                        {sets threshold for analysis}
MSsetfeat "REGIONFEAT"                     {defines region features to measure -
                                           FCIRCLE, DCIRCLE, etc}
! MSmeasmask 7,1,"fredla",0,1,10           {automatic measurement of regions}
! datalist "fred1a",0,0                    {creates list of results defined in
                                           REGIONFEAT}
```

A3 Determination and Statistical Analysis of D_{NEW}

After the Taguchi experiment was performed using all the nine experimental conditions described in the experimental procedure, samples from each experiment were cut from the billet and polished. Photographs were taken of the microstructures, one photograph for each experimental trial run. Two digital images were scanned from separate regions of each photograph to obtain an average result for each photograph. The digital images, a and b for each experimental trial run, were then used in the Kontron KS300 image analysis software to determine the grain size and shape factor of each of the primary phase grains in the images. The grain size was measured and labelled DCIRCLE[32] and the shape factor was labelled FCIRCLE[32].

The measured data was imported from the Kontron KS 300 image analysis software into the Quattro Pro spreadsheet. The data imported was a n x 2 array (n being the number of grains measured), with the first column showing the DCIRCLE values for grain size and the second column showing the FCIRCLE values for shape factor.

Page 130 shows the spreadsheet calculations and results derived from the two columns of information imported from sample 1a (i.e. the results from the first of two images grabbed from the photograph of the Taguchi experiment 1 microstructure). These two columns are shown in the first two columns of the spreadsheet and the third column shows the calculated values of DNEW (NOTE: not all the imported and calculated data is shown in the printed pages). DNEW is the division of DCIRCLE by FCIRCLE. The following three columns show DCIRCLE, FCIRCLE and DNEW sorted into ascending order respectively. The Quattro Pro numerical analysis tool, Descriptive Statistics, was applied on the latter three columns. The results of these statistical analyses are shown under the bold headings of DCIRCLE, FCIRCLE and DNEW.

Below the Descriptive Statistical analyses are the tables and graphs of the frequency distributions of DCIRCLE, FCIRCLE and DNEW. The frequency distribution tables were generated by applying the @FREQDIST command of Quattro Pro over the sorted columns of DCIRCLE, FCIRCLE and DNEW. The graphs were generated using the data of the

@FREQDIST results.

The last column on the extreme right shows the macro code that was used to perform all the operations described above. All the operations were applied to all the other Taguchi experiment results and those results are shown in the pages following 1a up to opt2.

The average values from the Descriptive Statistical analysis of DNEW were chosen to represent the results for the Taguchi Analysis of Variance (ANOVA)[26]. The statistical analysis of DCIRCLE and FCIRCLE were done for interest.

Sample 1a.

DCIRCLE	FCIRCLE	DNEW
20.99	0.43	48.81395
21.06	0.49	42.97959
22.56	0.73	30.90411
21.89	0.72	30.40278
23.21	0.59	39.33898
25.82	0.89	29.01124
29.58	0.85	34.8
18.98	0.38	49.94737
35.11	0.85	41.30588
34.55	0.73	47.32877
40.65	0.75	54.2
66.13	0.58	114.0172
37.44	0.73	51.28767
18.74	0.59	31.76271
51.5	0.72	71.52778
24.7	0.84	29.40476
26.39	0.54	48.87037
27.56	0.81	34.14815
65.95	0.56	117.7679
59.14	0.68	86.97059
25.12	0.89	28.22472
26.11	0.74	35.28378
32.32	0.47	68.76596
34.16	0.77	44.36364
33.72	0.74	45.56757
47.78	0.68	70.26471
48.92	0.59	82.91525
23.78	0.53	44.86792
62.97	0.49	128.5102
40.87	0.77	53.07792
3.86	0.85	4.541176
24.64	0.69	35.71014
43.72	0.7	62.45714
57.95	0.73	79.38356
77.49	0.48	161.4375
42.58	0.8	53.225
42.26	0.72	58.69444
30.57	0.79	38.6962
29.83	0.79	37.75949
75.07	0.51	147.1961
60.66	0.5	121.32
48.34	0.84	75.53125
18.42	0.82	22.46341
52.64	0.67	78.56716
19.29	0.71	27.16901
25.59	0.52	49.21154
23.59	0.79	29.86076
48.62	0.7	69.45714
59.22	0.63	94
23.66	0.82	28.85366
26.28	0.71	37.01408
23.34	0.78	29.92308
18.28	0.77	23.71429
76.4	0.45	169.7778
39.31	0.79	49.75949
43.51	0.64	67.98438
60.58	0.6	100.9667
35.19	0.79	44.5443
29.33	0.79	37.12658
24.64	0.78	31.58974
28.51	0.7	40.72857
30.72	0.79	38.88608
39.91	0.72	55.43056
40.35	0.73	55.27397
20.76	0.89	23.34831
24.22	0.51	47.49412
48.52	0.76	63.84211
20.49	0.94	21.79787
109.23	0.29	376.6552
32.65	0.63	51.8254
58.08	0.64	90.75
56.41	0.53	106.434
27.01	0.79	34.18987
25.42	0.91	27.93407
34.03	0.7	48.61429
21.27	0.52	40.90385
26.05	0.72	36.18056
31.91	0.75	42.54667
28.51	0.86	33.15116
18.98	0.31	61.22581
67.53	0.51	132.4118
64.53	0.76	84.90789
44.26	0.68	65.08824
59.49	0.62	95.95161
15.53	0.54	28.75926
43.95	0.79	55.63291
17.76	0.4	44.4
19.52	0.87	22.43678
38.31	0.76	50.40789
43.2	0.61	70.81967
59.94	0.5	119.88
20.92	0.65	32.18462
58.05	0.53	109.5283
60.61	0.81	99.36066
30.33	0.53	36.54217
22.03	0.71	31.02817
21.13	0.71	29.76056
39.5	0.68	58.08824
15.53	0.69	22.50725
52.7	0.71	74.22535
18.82	0.32	58.8125
19.14	0.43	44.51163
23.59	0.76	31.03947
43.31	0.78	55.52564
58.92	0.47	125.3617
50.24	0.71	70.76056
23.21	0.57	40.7193
29.33	0.58	50.56897
26.62	0.79	33.6962
25.59	0.54	47.38889
49.62	0.69	71.91304
27.87	0.61	45.68852
35.23	0.75	46.97333
18.82	0.66	28.51515
51.44	0.74	69.51351
26.11	0.79	33.05063
18.98	0.68	27.91176
11.18	0.59	18.94915
34.07	0.7	48.67143
30.03	0.79	38.01266
16.37	0.51	32.09804
58.97	0.77	76.58442
58.64	0.54	108.5926
29.13	0.77	37.83117
36.31	0.67	54.19403
18.34	0.86	21.32558
14.33	0.6	23.88333
57.59	0.56	102.8393
10.64	0.71	14.98592
40.83	0.67	60.9403
34.38	0.83	41.42169
27.66	0.8	34.575
25.88	0.58	44.62069
32.92	0.78	42.20513
3.86	0.75	5.146667
18.18	0.54	33.66667
34.07	0.87	39.16092
44.32	0.7	63.31429
49.44	0.69	71.65217
47.03	0.58	81.08621
39	0.8	48.75
23.47	0.43	54.5814
24.88	0.76	32.73684
81.99	0.36	227.75
31.77	0.69	46.04348
49.53	0.78	63.5
13.59	0.81	16.77778
14.02	0.87	16.11494
44.56	0.71	62.76056
21.34	0.46	46.3913
58.92	0.7	84.17143
49.5	0.74	66.89189
20.56	0.69	29.7971
69.12	0.5	138.24
33.32	0.61	54.62295
31.1	0.74	42.02703
72.36	0.7	103.3714
79.72	0.53	150.4151
17.17	0.44	39.02273
3.45	0.26	4.21
3.45	0.28	4.54
3.45	0.29	4.79
3.86	0.31	5.15
3.86	0.32	6.43
3.86	0.32	7.84
10.06	0.34	14.99
10.64	0.34	15.72
10.91	0.35	16.11
11.18	0.35	16.78
11.18	0.36	18.16
11.83	0.36	18.95
11.95	0.37	19.94
12.2	0.38	20.61
13.36	0.39	21.24
13.36	0.4	21.33
13.48	0.4	21.82
13.59	0.41	22.14
13.8	0.42	22.44
14.02	0.43	22.46
14.33	0.43	22.51
14.33	0.43	22.53
15.24	0.43	22.54
15.34	0.43	22.59
15.43	0.44	22.87
15.53	0.44	23.21
15.53	0.45	23.22
15.72	0.46	23.24
15.72	0.46	23.35
15.81	0.46	23.71
16.28	0.47	23.88
16.37	0.47	24.13
16.46	0.47	24.42
16.46	0.47	24.66
16.64	0.48	24.77
16.73	0.48	24.90
16.9	0.49	25.88
16.99	0.49	26.14
17.17	0.49	26.23
17.25	0.49	26.36
17.34	0.49	26.45
17.34	0.5	26.53
17.76	0.5	27.00
18.18	0.5	27.10
18.26	0.5	27.10
18.26	0.51	27.14
18.34	0.51	27.17
18.34	0.51	27.27
18.42	0.51	27.27
18.74	0.51	27.71
18.74	0.51	27.91
18.82	0.51	27.93
18.82	0.51	27.99
18.9	0.52	28.22
18.98	0.52	28.30
18.98	0.52	28.30
18.98	0.52	28.47
19.14	0.52	28.52
19.29	0.52	28.76
19.44	0.53	28.85
19.52	0.53	28.92
19.67	0.53	29.01
19.75	0.53	29.39
19.82	0.53	29.40
19.97	0.54	29.48
20.49	0.54	29.76
20.56	0.54	29.80
20.63	0.54	29.83
20.78	0.54	29.86
20.78	0.54	29.92
20.92	0.54	30.33
20.99	0.54	30.40
20.99	0.54	30.49
21.06	0.54	30.63
21.13	0.55	30.90
21.27	0.55	31.03
21.34	0.56	31.04
21.41	0.56	31.16
21.48	0.56	31.36
21.48	0.56	31.49
21.69	0.56	31.59
21.82	0.56	31.70
21.89	0.57	31.76
22.03	0.57	31.97
22.23	0.57	32.09
22.3	0.57	32.10
22.43	0.58	32.18
22.56	0.58	32.57
22.56	0.58	32.74
22.56	0.58	33.05
22.82	0.58	33.15
22.82	0.58	33.24
22.89	0.58	33.27
22.95	0.58	33.41
23.21	0.59	33.54
23.21	0.59	33.67
23.21	0.59	33.70
23.34	0.59	33.82
23.34	0.59	33.83
23.47	0.59	33.89
23.47	0.59	33.89
23.59	0.59	34.06
23.59	0.59	34.15
23.66	0.6	34.18
23.66	0.6	34.19
23.72	0.6	34.38
23.72	0.6	34.80
23.78	0.6	34.86
24.03	0.61	34.97
24.09	0.61	35.00
24.15	0.61	35.28
24.22	0.61	35.71
24.34	0.61	35.77
24.46	0.61	36.18
24.52	0.61	36.54
24.64	0.62	36.56
24.64	0.62	36.98
24.7	0.63	37.01
24.88	0.63	37.13
25	0.63	37.31
25.06	0.63	37.32
25.12	0.64	37.54
25.24	0.64	37.76
25.42	0.64	37.83
25.42	0.64	38.01
25.42	0.64	38.12
25.53	0.64	38.12
25.59	0.64	38.22
25.59	0.64	38.24
25.65	0.65	38.70
25.71	0.65	38.89
25.82	0.65	38.98
25.88	0.65	39.02
25.99	0.65	39.11
26.05	0.65	39.16
26.11	0.66	39.34
26.11	0.66	39.35
26.11	0.66	39.54
26.11	0.66	40.01
26.28	0.66	40.18
26.28	0.66	40.70
26.39	0.67	40.72
26.45	0.67	40.73
26.62	0.67	40.90
26.73	0.67	41.09
27.01	0.67	41.17
27.06	0.67	41.31
27.28	0.67	41.42
27.28	0.67	41.54
27.5	0.67	41.62
27.61	0.68	42.03
27.66	0.68	42.04
27.66	0.68	42.21
27.67	0.68	42.40
28.25	0.68	42.55
28.51	0.68	42.90
28.51	0.68	42.93
28.77	0.68	42.98
29.13	0.68	43.22

DCIRCLE/micron		FCIRCLE		DNEW	
Mean	35.9353	Mean	0.6719	Mean	57.9500
Standard Error	0.9686	Standard Error	0.0072	Standard Error	2.2570
Median	32.1150	Median	0.7000	Median	46.2258
Mode	26.1100	Mode	0.7100	Mode	NA
Standard Deviation	18.3774	Standard Deviation	0.1368	Standard Deviation	42.8239
Variance	337.7301	Variance	0.0187	Variance	1833.8859
Kurtosis	1.2508	Kurtosis	-0.0725	Kurtosis	12.7544
Skewness	1.0371	Skewness	-0.6746	Skewness	2.9362
Range	105.7800	Range	0.6800	Range	372.4479
Minimum	3.4500	Minimum	0.2600	Minimum	4.2073
Maximum	109.2300	Maximum	0.9400	Maximum	376.6552
Sum	12936.7100	Sum	241.9000	Sum	20861.9990
Count	360.0000	Count	360.0000	Count	360.0000
Confidence Level(0.9	1.8984	Confidence Level(0.9	0.0141	Confidence Level(0.9	4.4237

BIN	FREQUECNY	BIN	FREQUECNY	BIN	FREQUECNY
10	6	0.05	0	10	6
20	59	0.1	0	20	7
30	101	0.15	0	30	57
40	68	0.2	0	40	68
50	57	0.25	0	50	64
60	33	0.3	3	60	49
70	17	0.35	7	70	27
80	11	0.4	7	80	20
90	3	0.45	10	90	11
100	3	0.5	18	100	12
110	2	0.55	31	110	10
120	0	0.6	32	120	4
130	0	0.65	27	130	4
140	0	0.7	50	140	5
150	0	0.75	59	150	1
160	0	0.8	64	160	2
170	0	0.85	29	170	2
180	0	0.9	21	180	1
190	0	0.95	2	190	1
200	0	1	0	200	1
	0		0		8

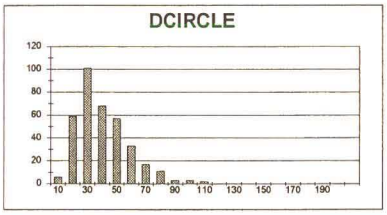

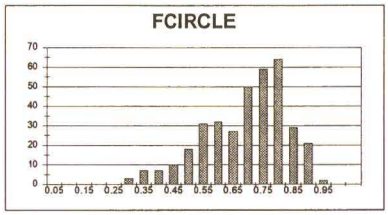

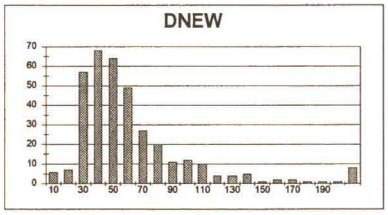


```
{SelectBlock C1)
{PutCell2 "DNEW")
{SelectBlock C2)
{PutCell2 "+A2..A361/B2..B361")
{SelectBlock A2..B361)
{EditCopy)
{SelectBlock E2)
{EditPaste)
{SelectBlock C2)
{BlockValues C2;O2)
{SelectBlock C3..G361)
{EditCopy)
{SelectBlock G3)
{EditPaste)
{SelectBlock E2..E361)
{Sort.Block "E2..E361")
{Sort.Type Top to bottom}
{Sort.Heading 0)
{Sort.Key_1 "E2")
{Sort.Key_2 ""}
{Sort.Key_3 ""}
{Sort.Key_4 ""}
{Sort.Key_5 ""}
{Sort.BlankCellsFirst 0)
{Sort.Data Numbers First)
{Sort.PreviousSorts -1)
{Sort.Go)
{SelectBlock F2..F361)
{Sort.Block "F2..F361")
{Sort.Type Top to bottom}
{Sort.Heading 0)
{Sort.Key_1 "F2")
{Sort.Key_2 ""}
{Sort.Key_3 ""}
{Sort.Key_4 ""}
{Sort.Key_5 ""}
{Sort.BlankCellsFirst 0)
{Sort.Data Numbers First)
{Sort.PreviousSorts -1)
{Sort.Go)
{SelectBlock G2..G361)
{Sort.Block "G2..G361")
{Sort.Type Top to bottom}
{Sort.Heading 0)
{Sort.Key_1 "G2")
{Sort.Key_2 ""}
{Sort.Key_3 ""}
{Sort.Key_4 ""}
{Sort.Key_5 ""}
{Sort.BlankCellsFirst 0)
{Sort.Data Numbers First)
{Sort.PreviousSorts -1)
{Sort.Go)
{Selproperty Numeric_Format,"Fixed;2;South Africa")
{SelectBlock A1..C1)
{EditCopy)
{SelectBlock E1)
{EditPaste)

{SelectBlock I1)
{DESCR "E1..E361";I1;C;"1";"1";"0";"0";"95%")
{SelectBlock K1)
{DESCR "F1..F361";K1;C;"1";"1";"0";"0";"95%")
{SelectBlock M1)
{DESCR "G1..G361";M1;C;"1";"1";"0";"0";"95%")
{SelectBlock I19)
{PutCell2 "BIN")
{SelectBlock J19)
{PutCell2 "FREQUENCY")
{SelectBlock I19..J19)
{EditCopy)
{SelectBlock (K19..L19;M19..N19);M19)
{EditPaste)
{SelectBlock I20)
{PutCell2 "10")
{SelectBlock I21)
{PutCell2 "20")
{SelectBlock I20..I39)
{SpeedFill)
{EditCopy)
{SelectBlock M20)
{EditPaste)
{SelectBlock K20)
{PutCell2 "0.05")
{SelectBlock K21)
{PutCell2 "0.1")
{SelectBlock K20..K39)
{SpeedFill)
{SelectBlock J20)
{PutCell2 "@FREQDIST(E2..E361,I20..I39)")
{SelectBlock L20)
{PutCell2 "@FREQDIST(F2..F361,K20..K39)")
{SelectBlock N20)
{PutCell2 "@FREQDIST(G2..G361,M20..M39)")
{SelectBlock J20..J40)
{GraphNew Chart2)
{Series.Data_Range 1;(J20..J40);1)
{Series.Go)
{FloatCreate Graph;H42;940;220;N59;960;240;Chart2)
{FloatSize H42;940;220;N62;960;240)
{Series.Data_Range XAxisLabelSeries;I20..I40)
{Series.Data_Range 1;J20..J40;1)
{Series.Go)
{GraphSettings.Type "Bar;Bar")
{GraphSettings.Titles DCIRCLE;"","","")
{EditCopy)
{SelectBlock I64)
{EditPaste)
{SelectBlock I85)
{EditPaste)
{SelectFloat Inserted3)
{Series.Data_Range XAxisLabelSeries;K20..K40)
{Series.Data_Range 1;L20..L40;1)
{Series.Go)
{GraphSettings.Titles FCIRCLE;"","","")
{SelectFloat Inserted4)
{Series.Data_Range XAxisLabelSeries;M20..M40)
{Series.Data_Range 1;N20..N40;1)
{Series.Go)
{GraphSettings.Titles DNEW;"","","")

{Selproperty Numeric_Format,"Fixed;4;South Africa")
{SelectBlock L)
{Selproperty Numeric_Format,"Fixed;4;South Africa")
{SelectBlock J)
{Selproperty Numeric_Format,"Fixed;4;South Africa")
{SelectBlock J20..J40)
{Selproperty Numeric_Format,"General;4;South Africa")
{SelectBlock L20..L40)
{Selproperty Numeric_Format,"General;4;South Africa")
{SelectBlock N20..N40)
{Selproperty Numeric_Format,"General;4;South Africa")
{SelectBlock J)
{Selproperty Column_Width,"Auto Width;;1")
{SelectBlock L)
{Selproperty Column_Width,"Auto Width;;1")
{SelectBlock N)
{Selproperty Column_Width,"Auto Width;;1")
{SelectBlock O1)
```

Sample 1b.

DCIRCLE	FCIRCLE	DNEW
4.23	0.68	6.220588
3.45	0.51	6.764706
24.15	0.84	28.75
30.38	0.79	38.4557
28.51	0.68	41.92647
29.73	0.84	35.39286
38.96	0.68	57.29412
24.64	0.91	27.07692
33.37	0.78	42.78205
33.28	0.73	45.58904
28.56	0.83	34.40964
34.81	0.8	43.5125
56.78	0.65	87.35385
43	0.76	56.57895
29.63	0.77	38.48052
71.06	0.41	173.3659
29.43	0.6	49.05
26.28	0.76	34.57895
51.09	0.79	64.67089
62.16	0.65	95.63077
76.83	0.53	144.9623
42.79	0.69	62.01449
28.25	0.57	49.5614
58.23	0.77	75.62338
11.7	0.7	16.71429
20.34	0.74	27.48649
24.22	0.64	37.84375
27.06	0.55	49.2
31.44	0.81	38.81481
29.33	0.7	41.9
42.09	0.54	77.94444
61.13	0.57	107.4912
28.25	0.83	34.03614
34.68	0.79	43.89873
50.09	0.69	72.5942
50.33	0.71	70.88732
33.77	0.78	43.29487
27.98	0.82	34.12195
4.23	0.54	7.833333
22.69	0.73	31.08219
54.04	0.61	88.59016
34.81	0.78	44.62821
72.42	0.46	157.4348
45.39	0.63	72.04762
26.11	0.82	31.84146
59.72	0.58	102.9655
23.02	0.94	24.48936
43.13	0.69	62.50725
31.39	0.55	57.07273
40.79	0.78	52.29487
32.96	0.82	40.19512
28.35	0.85	33.35294
5.18	0.93	5.569892
99.08	0.55	125.6
22.56	0.94	24
7.91	0.5	15.82
43.44	0.72	60.33333
30.67	0.76	40.35526
50.3	0.78	64.48718
3.45	0.72	4.791667
87	0.52	128.8462
57.41	0.61	94.11475
68.69	0.5	137.38
56.2	0.65	86.46154
3.45	0.95	3.631579
41.73	0.73	57.16438
29.73	0.84	35.39286
35.27	0.76	46.40789
3.86	0.57	6.77193
31.95	0.79	40.44304
23.34	0.76	30.71053
68.49	0.56	122.3036
19.14	0.85	22.51765
47.85	0.65	73.61538
58.71	0.71	82.69014
43.95	0.59	74.49153
39.19	0.72	54.43056
52.13	0.65	80.2
31.95	0.83	38.49398
22.03	0.74	29.77027
30.77	0.73	42.15068
32.14	0.82	39.19512
34.85	0.76	45.85526
28.92	0.75	38.56
32.92	0.83	39.66265
47.91	0.81	59.14815
20.34	0.67	30.35821
59.09	0.7	84.41429
23.97	0.7	34.24286
95.5	0.37	258.1081
33.32	0.74	45.02703
46.26	0.76	60.86842
38.66	0.83	46.57831
58.99	0.51	115.6667
38.11	0.7	54.44286
52.87	0.64	82.60938
31.39	0.7	44.84286
32.78	0.78	42.02564
26.51	0.83	31.93976
41.94	0.65	64.52308
29.48	0.87	33.88506
44.73	0.78	57.34615
52.1	0.75	69.46667
36.15	0.73	49.52055
21.2	0.71	29.85915
45.42	0.76	59.76316
55.67	0.65	85.64615
6.46	1	6.46
32.05	0.92	34.83696
26.39	0.53	49.79245
81.64	0.47	173.7021
48.71	0.67	72.70149
73.67	0.58	127.0172
23.53	0.87	27.04598
37.17	0.73	50.91781
28.56	0.86	33.2093
37.88	0.8	47.35
37.44	0.75	49.92
29.33	0.84	34.91667
24.88	0.76	32.73684
25.76	0.81	31.80247
43.82	0.79	55.46835
30.48	0.79	38.58228
33.23	0.72	46.15278
24.82	0.88	28.20455
38.77	0.72	53.84722
43.82	0.83	52.79518
98.31	0.26	378.1154
7.72	0.54	14.2963
25.42	0.83	30.62651
87.89	0.5	175.78
26.9	0.85	31.64706
20.92	0.91	22.98901
30.86	0.75	41.14667
94.85	0.37	256.3514
61.24	0.66	92.78788
45.49	0.65	69.98462
24.09	0.83	29.0241
52.02	0.74	70.2973
19.97	0.67	29.80597
23.72	0.9	26.35556
28.51	0.81	35.19753
21.62	0.79	27.36709
61.63	0.62	99.40323
43.13	0.77	56.01299
17.93	0.68	26.36765
41.16	0.69	59.65217
38.5	0.73	52.73973
22.69	0.64	35.45313
51.76	0.6	86.26667
66.47	0.62	107.2097
23.84	0.89	26.78652
21.2	0.75	28.26667
52.84	0.68	77.70588
39.76	0.78	50.97436
46.33	0.57	81.2807
42.47	0.64	66.35938
54.75	0.78	70.19231
44.73	0.84	53.25
3.45	0.26	3.63
3.45	0.3	4.79
3.45	0.32	4.79
3.45	0.35	5.57
3.86	0.37	6.22
4.23	0.37	6.46
4.23	0.39	6.76
5.18	0.41	6.77
6.22	0.44	7.83
6.46	0.46	12.44
6.9	0.46	13.80
7.72	0.47	14.30
7.91	0.47	15.82
11.7	0.49	16.71
14.74	0.49	22.48
14.84	0.49	22.52
17.93	0.5	22.99
18.58	0.5	23.80
19.14	0.5	24.00
19.21	0.5	24.13
19.52	0.5	24.16
19.67	0.5	24.49
19.97	0.5	24.69
20.05	0.51	25.81
20.27	0.51	25.90
20.34	0.52	26.36
20.34	0.52	26.37
20.34	0.52	26.68
20.85	0.53	26.68
20.92	0.53	26.79
20.92	0.53	26.95
21.13	0.53	27.00
21.2	0.53	27.05
21.2	0.54	27.08
21.34	0.54	27.18
21.48	0.54	27.36
21.55	0.54	27.37
21.62	0.54	27.49
22.03	0.55	28.20
22.56	0.55	28.25
22.56	0.55	28.27
22.69	0.56	28.35
22.69	0.56	28.75
22.95	0.57	29.02
23.02	0.57	29.77
23.21	0.57	29.80
23.34	0.57	29.81
23.53	0.57	29.86
23.53	0.57	30.36
23.53	0.57	30.56
23.72	0.58	30.63
23.84	0.58	30.71
23.84	0.58	31.08
23.84	0.58	31.20
23.97	0.58	31.36
24.09	0.58	31.65
24.09	0.59	31.70
24.15	0.59	31.80
24.15	0.59	31.84
24.22	0.6	31.94
24.64	0.6	32.03
24.82	0.6	32.35
24.88	0.61	32.74
25.42	0.61	33.21
25.78	0.61	33.35
25.88	0.61	33.89
26.11	0.61	34.04
26.28	0.62	34.12
26.28	0.62	34.24
26.39	0.62	34.41
26.51	0.62	34.56
26.84	0.62	34.58
26.9	0.63	34.64
26.95	0.63	34.92
27.06	0.63	35.20
27.98	0.64	35.34
28.19	0.64	35.39
28.25	0.64	35.39
28.25	0.64	35.45
28.35	0.64	35.68
28.4	0.64	36.67
28.46	0.64	37.24
28.51	0.64	37.43
28.51	0.64	37.47
28.56	0.65	37.81
28.56	0.65	37.84
28.92	0.65	37.84
28.97	0.65	37.87
29.33	0.65	38.10
29.33	0.65	38.27
29.33	0.65	38.33
29.38	0.65	38.46
29.43	0.65	38.48
29.48	0.65	38.49
29.63	0.65	38.56
29.73	0.65	38.58
29.73	0.66	38.81
30.03	0.66	39.20
30.13	0.66	39.66
30.23	0.66	39.82
30.33	0.67	40.20
30.36	0.67	40.36
30.48	0.67	40.36
30.48	0.67	40.44
30.67	0.68	40.80
30.77	0.68	41.09
30.86	0.68	41.15
30.91	0.68	41.27
31.1	0.68	41.74
31.39	0.68	41.86
31.39	0.68	41.90
31.44	0.69	41.93
31.58	0.69	42.03
31.95	0.69	42.11
31.95	0.69	42.11
32	0.69	42.15
32.05	0.69	42.30
32.05	0.7	42.40
32.14	0.7	42.78
32.19	0.7	42.89
32.23	0.7	42.91
32.6	0.7	43.08
32.65	0.7	43.29
32.65	0.7	43.29
32.69	0.7	43.36
32.78	0.71	43.51
32.87	0.71	43.72
32.92	0.71	43.84
32.96	0.71	43.90
33.05	0.71	44.63
33.23	0.71	44.84
33.23	0.71	45.03
33.28	0.71	45.06
33.32	0.71	45.39
33.37	0.72	45.48
33.37	0.72	45.59
33.77	0.72	45.70
33.81	0.72	45.86
33.94	0.72	46.15
33.99	0.72	46.41
34.29	0.72	46.42
34.68	0.72	46.58
34.76	0.72	46.63
34.81	0.72	46.72
34.81	0.72	47.00
34.85	0.72	47.35
35.27	0.72	47.57
35.44	0.72	47.63
35.82	0.72	47.80
36.15	0.72	48.25
36.15	0.72	48.36
36.19	0.73	48.46
36.19	0.73	49.05
36.19	0.73	49.07
36.44	0.73	49.18
36.52	0.73	49.20
36.56	0.73	49.23
36.92	0.73	49.26
37.17	0.73	49.52

DCIRCLE/micron		FCIRCLE		DNEW	
Mean	38.9171	Mean	0.7061	Mean	60.5573
Standard Error	1.0208	Standard Error	0.0072	Standard Error	2.6966
Median	36.1900	Median	0.7300	Median	49.0592
Mode	3.4500	Mode	0.7200	Mode	4.7917
Standard Deviation	17.8562	Standard Deviation	0.1267	Standard Deviation	47.1712
Variance	318.8453	Variance	0.0161	Variance	2225.1219
Kurtosis	3.6757	Kurtosis	0.4838	Kurtosis	26.2500
Skewness	1.1310	Skewness	-0.6878	Skewness	4.0656
Range	137.6200	Range	0.7400	Range	466.6018
Minimum	3.4500	Minimum	0.2600	Minimum	3.6316
Maximum	141.0700	Maximum	1.0000	Maximum	470.2333
Sum	11906.6200	Sum	216.6700	Sum	18530.5335
Count	306.0000	Count	306.0000	Count	306.0000
Confidence Level(0	2.0007	Confidence Level(0	0.0142	Confidence Level(0	5.2852

BIN	FREQUENCY	BIN	FREQUENCY	BIN	FREQUENCY
10	13	0.05	0	10	9
20	10	0.1	0	20	5
30	74	0.15	0	30	34
40	86	0.2	0	40	52
50	52	0.25	0	50	63
60	40	0.3	2	60	39
70	15	0.35	2	70	19
80	8	0.4	3	80	24
90	4	0.45	2	90	19
100	3	0.5	14	100	9
110	0	0.55	18	110	8
120	0	0.6	21	120	5
130	0	0.65	34	130	5
140	0	0.7	29	140	2
150	1	0.75	56	150	1
160	0	0.8	56	160	2
170	0	0.85	44	170	1
180	0	0.9	14	180	4
190	0	0.95	10	190	0
200	0	1	1	200	0
	0		0		5

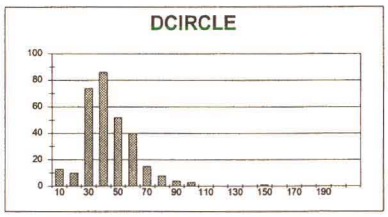

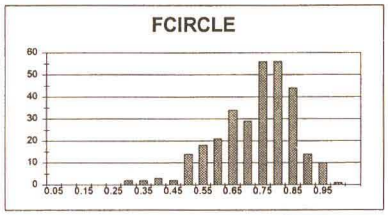

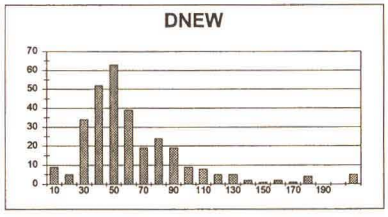


```
{SelectBlock C1}
{PutCell2 "DNEW"}
{SelectBlock C2}
{PutCell2 "+A2..A307/B2..B307"}
{SelectBlock A2..B307}
{EditCopy}
{SelectBlock E2}
{EditPaste}
{SelectBlock C2}
{BlockValues C2;G2}
{SelectBlock C3..C307}
{EditCopy}
{SelectBlock G3}
{EditPaste}
{SelectBlock E2..E307}
{Sort.Block "E2..E307"}
{Sort.Type Top to bottom}
{Sort.Heading 0}
{Sort.Key_1 "E2"}
{Sort.Key_2 ""}
{Sort.Key_3 ""}
{Sort.Key_4 ""}
{Sort.Key_5 ""}
{Sort.BlankCellsFirst 0}
{Sort.Data Numbers First}
{Sort.PreviousSorts -1}
{Sort.Go}
{SelectBlock F2..F307}
{Sort.Block "F2..F307"}
{Sort.Type Top to bottom}
{Sort.Heading 0}
{Sort.Key_1 "F2"}
{Sort.Key_2 ""}
{Sort.Key_3 ""}
{Sort.Key_4 ""}
{Sort.Key_5 ""}
{Sort.BlankCellsFirst 0}
{Sort.Data Numbers First}
{Sort.PreviousSorts -1}
{Sort.Go}
{SelectBlock G2..G307}
{Sort.Block "G2..G307"}
{Sort.Type Top to bottom}
{Sort.Heading 0}
{Sort.Key_1 "G2"}
{Sort.Key_2 ""}
{Sort.Key_3 ""}
{Sort.Key_4 ""}
{Sort.Key_5 ""}
{Sort.BlankCellsFirst 0}
{Sort.Data Numbers First}
{Sort.PreviousSorts -1}
{Sort.Go}
{Selproperty Numeric_Format;"Fixed;2;South Africa"}
{SelectBlock A1..C1}
{EditCopy}
{SelectBlock E1}
{EditPaste}
{SelectBlock I1}
{DESCR "E1..E307";I1;C;"1";"1";"0";"0";"95%"}
{SelectBlock K1}
{DESCR "F1..F307";K1;C;"1";"1";"0";"0";"95%"}
{SelectBlock M1}
{DESCR "G1..G307";M1;C;"1";"1";"0";"0";"95%"}
{SelectBlock I19}
{PutCell2 "Bin"}
{SelectBlock J19}
{PutCell2 "FREQUENCY"}
{SelectBlock I19..J19}
{EditCopy}
{SelectBlock (K19..L19;M19..N19);M19}
{EditPaste}
{SelectBlock I20}
{PutCell2 "10"}
{SelectBlock I21}
{PutCell2 "20"}
{SelectBlock I20..I39}
{SpeedFill}
{EditCopy}
{SelectBlock M20}
{EditPaste}
{SelectBlock K20}
{PutCell2 "0.05"}
{SelectBlock K21}
{PutCell2 "0.1"}
{SelectBlock K20..K39}
{SpeedFill}
{SelectBlock J20}
{PutCell2 "@FREQDIST(E2..E307,I20..I39)"}
{SelectBlock L20}
{PutCell2 "@FREQDIST(F2..F307,K20..K39)"}
{SelectBlock N20}
{PutCell2 "@FREQDIST(G2..G307,M20..M39)"}
{SelectBlock J20..J40}
{GraphNew Chart5}
{Series.Data_Range 1;(J20..J40);1}
{Series.Go}
{FloatCreate Graph;H42;840;220;N59;960;240;Chart5}
{FloatSize H42;840;220;N62;960;240}
{Series.Data_Range XAxisLabelSeries;I20..I40}
{Series.Data_Range 1;J20..J40;1}
{Series.Go}
{GraphSettings.Type "Bar;Bar"}
{GraphSettings.Titles DCIRCLE;"";"";"";""}
{EditCopy}
{SelectBlock I64}
{EditPaste}
{SelectBlock I85}
{EditPaste}
{SelectFloat Inserted6}
{Series.Data_Range XAxisLabelSeries;K20..K40}
{Series.Data_Range 1;L20..L40;1}
{Series.Go}
{GraphSettings.Titles FCIRCLE;"";"";"";""}
{SelectFloat Inserted7}
{Series.Data_Range XAxisLabelSeries;M20..M40}
{Series.Data_Range 1;N20..N40;1}
{Series.Go}
{GraphSettings.Titles DNEW;"";"";"";""}
{SelectBlock 1b:J}
{Selproperty Numeric_Format;"Fixed;4;South Africa"}
{SelectBlock 1b:L}
{Selproperty Numeric_Format;"Fixed;4;South Africa"}
{SelectBlock 1b:N}
{Selproperty Numeric_Format;"Fixed;4;South Africa"}
{SelectBlock J20..J40}
{Selproperty Numeric_Format;"General;4;South Africa"}
{SelectBlock L20..L40}
{Selproperty Numeric_Format;"General;4;South Africa"}
{SelectBlock N20..N40}
{Selproperty Numeric_Format;"General;4;South Africa"}
{SelectBlock 1b:J}
{Selproperty Column_Width;"Auto Width;;1"}
{SelectBlock 1b:L}
{Selproperty Column_Width;"Auto Width;;1"}
{SelectBlock 1b:N}
{Selproperty Column_Width;"Auto Width;;1"}
{SelectBlock O1}
```

Sample 2a.

DCIRCLE	FCIRCLE	DNEW
23.08	0.81	28.49383
39.65	0.8	49.5625
29.02	0.62	46.80645
27.66	0.79	35.01266
22.63	0.76	29.77632
37.84	0.94	40.25532
22.5	0.86	26.16279
23.91	0.55	43.47273
37.4	0.86	43.48837
25.59	0.64	39.98438
38.5	0.89	43.25843
22.5	0.71	31.69014
59.59	0.82	72.67073
40.13	0.89	45.08989
43.37	0.79	54.89873
16.64	0.45	36.97778
31.25	0.86	36.33721
45.97	0.76	60.48684
22.63	0.86	26.31395
4.23	0.51	8.294118
88.78	0.43	206.4651
22.43	0.9	24.92222
24.46	0.83	29.46988
25.82	0.95	27.17895
54.78	0.75	73.04
63.84	0.45	141.8667
23.28	0.95	24.50526
51.41	0.88	58.42045
24.15	0.88	27.44318
33.14	0.86	38.53488
58.74	0.58	101.2759
18.01	0.93	19.36559
85.21	0.58	146.9138
37.52	0.8	46.9
31.06	0.85	36.54118
33.1	0.81	40.8642
20.92	0.8	26.15
52.62	0.66	79.72727
47.35	0.91	52.03297
48.09	0.81	59.37037
199.57	0.31	643.7742
29.63	0.83	35.6988
45.97	0.84	54.72619
27.96	0.82	34.12195
17.76	0.33	53.81818
26.28	0.9	29.2
57.59	0.69	83.46377
13.48	0.7	19.25714
43.24	0.79	54.73418
57.79	0.77	75.05195
69.04	0.57	121.1228
14.84	0.41	36.19512
60.31	0.74	81.5
27.33	0.75	36.44
92.56	0.32	289.25
24.88	0.49	50.77551
25.06	0.67	37.40299
26.28	0.56	46.92857
28.09	0.8	35.1125
28.46	0.95	29.95789
164.96	0.26	634.4615
83.26	0.72	115.6389
45.88	0.88	52.13636
46.87	0.65	72.10769
44.89	0.8	56.1125
28.92	0.86	33.62791
70.04	0.6	116.7333
38.89	0.74	52.55405
17.34	0.66	26.27273
21.27	0.66	32.22727
48.98	0.92	53.23913
18.9	0.78	24.23077
62.73	0.9	69.7
39.61	0.89	44.50562
104.39	0.57	183.1404
26.22	0.9	29.13333
35.4	0.9	39.33333
25.24	0.95	26.56842
27.66	0.87	31.7931
39.65	0.8	49.5625
46.07	0.81	56.87654
29.48	0.89	33.1236
40.54	0.88	46.06818
58.46	0.88	66.43182
18.01	0.87	20.70115
116.8	0.46	253.913
41.73	0.71	58.77465
20.49	0.76	26.96053
45.88	0.8	57.35
38.66	0.78	49.5641
20.34	0.8	25.425
21.82	0.95	22.75789
50.89	0.79	64.41772
37	0.84	44.04762
35.11	0.91	38.58242
197.69	0.25	790.76
42.47	0.86	49.38372
89.1	0.47	189.5745
23.21	0.92	25.22826
52.7	0.81	65.06173
44.12	0.92	47.95652
38.31	0.78	49.11538
43.31	0.67	64.64179
31.67	0.76	41.67105
26.62	0.53	50.22642
39.91	0.89	44.8427
33.68	0.84	40.09524
18.26	0.92	19.84783
25.42	0.55	46.21818
42.82	0.66	64.87879
84.4	0.7	120.5714
25.53	0.86	29.66605
25.99	0.82	31.69512
112.95	0.85	132.8824
53.21	0.8	66.5125
70.15	0.81	86.60494
138.05	0.34	406.0294
43.1	0.8	53.875
20.56	0.68	29.7971
36.31	0.85	42.71765
24.22	0.88	27.52273
22.76	0.88	25.86364
27.87	0.87	32.03448
27.98	0.91	30.74725
37.13	0.73	50.86301
24.22	0.9	26.91111
27.23	0.94	28.96809
30.77	0.84	36.63095
44.12	0.83	53.15663
25.99	0.81	32.08642
104.19	0.56	186.0536
30.96	0.88	35.18182
41.23	0.85	48.50588
19.14	0.83	23.06024
71.35	0.83	85.96386
23.97	0.79	30.34177
23.47	0.91	25.79121
32.92	0.86	38.27907
44.53	0.77	57.83117
26.72	0.77	37.2987
28.66	0.7	40.94286
34.38	0.89	38.62921
48.46	0.69	70.23188
29.33	0.89	32.95506
49.29	0.84	58.67857
44.19	0.82	53.89024
35.19	0.87	40.44828
28.25	0.82	34.45122
25.3	0.96	26.35417
31.81	0.83	38.3253
21.48	0.85	25.27059

DCIRCLE	FCIRCLE	DNEW
3.86	0.2	5.46
5.46	0.25	7.57
5.46	0.25	8.29
7.91	0.26	11.63
11.57	0.28	15.35
13.48	0.29	18.69
14.02	0.31	19.26
14.12	0.32	19.37
14.84	0.33	19.85
16.64	0.34	20.70
17.08	0.41	21.72
17.34	0.42	21.95
17.76	0.43	22.35
17.76	0.45	22.76
18.01	0.45	23.06
18.01	0.45	23.14
18.26	0.46	23.36
18.66	0.47	24.23
18.9	0.48	24.51
19.14	0.49	24.83
20.34	0.5	24.92
20.34	0.51	25.23
20.49	0.51	25.27
20.56	0.52	25.43
20.63	0.52	25.79
20.7	0.53	25.86
20.92	0.55	26.15
21.27	0.55	26.16
21.48	0.56	26.27
21.62	0.56	26.31
21.96	0.57	26.35
22.43	0.57	26.57
22.5	0.58	26.91
22.5	0.58	26.96
22.63	0.59	27.18
22.63	0.6	27.24
22.63	0.61	27.42
22.76	0.62	27.44
22.76	0.64	27.52
23.08	0.64	28.49
23.21	0.64	28.65
23.28	0.65	28.97
23.34	0.66	29.13
23.47	0.66	29.20
23.91	0.66	29.47
23.97	0.66	29.69
24.15	0.66	29.78
24.22	0.67	29.80
24.22	0.67	29.96
24.46	0.67	30.34
24.58	0.68	30.75
24.64	0.68	31.21
24.82	0.69	31.69
24.88	0.69	31.70
25.06	0.69	31.79
25.24	0.69	32.02
25.3	0.7	32.03
25.42	0.7	32.09
25.53	0.7	32.23
25.59	0.71	32.91
25.65	0.71	32.96
25.82	0.71	33.12
25.96	0.72	33.18
25.99	0.73	33.36
26.22	0.74	33.54
26.28	0.74	33.63
26.28	0.74	33.78
26.62	0.74	34.12
27.23	0.75	34.12
27.33	0.75	34.15
27.66	0.75	34.45
27.66	0.76	34.86
27.87	0.76	35.01
27.96	0.76	35.05
27.96	0.76	35.11
28.03	0.76	35.18
28.09	0.76	35.50
28.09	0.77	35.58
28.25	0.77	35.70
28.3	0.77	35.94
28.46	0.78	36.20
28.66	0.78	36.34
28.66	0.78	36.44
28.72	0.78	36.54
28.82	0.79	36.63
28.92	0.79	36.75
29.02	0.79	36.98
29.02	0.79	37.30
29.33	0.79	37.40
29.48	0.79	38.28
29.53	0.8	38.33
29.63	0.8	38.40
30.77	0.8	38.41
30.91	0.8	38.53
30.96	0.8	38.58
31.06	0.8	38.63
31.25	0.8	39.33
31.58	0.8	39.98
31.67	0.8	40.10
31.72	0.8	40.26
31.81	0.8	40.45
31.91	0.81	40.62
31.95	0.81	40.86
32.6	0.81	40.91
32.92	0.81	40.94
33.1	0.81	41.13
33.14	0.81	41.67
33.14	0.81	42.72
33.41	0.81	43.26
33.68	0.81	43.47
33.81	0.81	43.47
34.38	0.82	43.49
35.11	0.82	44.01
35.19	0.82	44.05
35.23	0.82	44.51
35.4	0.82	44.84
35.65	0.82	45.07
36.19	0.83	45.09
36.31	0.83	46.07
37	0.83	46.22
37.13	0.83	46.81
37.4	0.83	46.90
37.52	0.83	46.93
37.84	0.83	47.96
38.31	0.83	48.51
38.31	0.84	49.12
38.5	0.84	49.38
38.66	0.84	49.56
38.89	0.84	49.56
39.61	0.84	49.56
39.65	0.84	50.23
39.65	0.84	50.23
39.91	0.85	50.78
40.13	0.85	50.86
40.54	0.85	51.54
41.08	0.85	52.03
41.23	0.85	52.14
41.69	0.85	52.31
41.73	0.85	52.55
42.19	0.86	52.84
42.26	0.86	53.16
42.37	0.86	53.24
42.47	0.86	53.82
42.82	0.86	53.86
43.1	0.86	53.89
43.24	0.86	54.05
43.31	0.86	54.73
43.37	0.86	54.73
44.12	0.86	54.90
44.12	0.86	55.54
44.19	0.86	55.86
44.53	0.87	56.11
44.56	0.87	56.88
44.89	0.87	57.35
44.99	0.87	57.75
45.88	0.87	57.83
45.88	0.87	58.42
45.97	0.87	58.68
45.97	0.88	58.77

DCIRCLE/micron		FCIRCLE		DNEW	
Mean	41.6198	Mean		0.7582	Mean	71.3852
Standard Error	2.1137	Standard Error		0.0115	Standard Error	8.0446
Median	33.1000	Median		0.8100	Median	41.1250
Mode	22.6300	Mode		0.8600	Mode	49.5625
Standard Deviation	30.7026	Standard Deviation		0.1671	Standard Deviation	116.8550
Variance	942.6497	Variance		0.0279	Variance	13655.1009
Kurtosis	10.7548	Kurtosis		1.3620	Kurtosis	30.2802
Skewness	2.9561	Skewness		-1.3625	Skewness	5.1929
Range	195.7100	Range		0.8000	Range	981.5900
Minimum	3.8600	Minimum		0.2000	Minimum	5.4600
Maximum	199.5700	Maximum		1.0000	Maximum	987.0500
Sum	8781.7700	Sum		159.9800	Sum	15062.2715
Count	211.0000	Count		211.0000	Count	211.0000
Confidence Level(0	4.1427	Confidence Level(0		0.0225	Confidence Level(0	15.7672

BIN	FREQUENCY	BIN	FREQUENCY	BIN	FREQUENCY
10	4	0.05	0	10	3
20	16	0.1	0	20	6
30	72	0.15	0	30	40
40	41	0.2	1	40	49
50	36	0.25	2	50	32
60	16	0.3	3	60	30
70	5	0.35	4	70	11
80	3	0.4	0	80	10
90	6	0.45	6	90	5
100	1	0.5	5	100	1
110	2	0.55	7	110	2
120	2	0.6	8	120	2
130	1	0.65	6	130	3
140	1	0.7	17	140	2
150	0	0.75	12	150	2
160	1	0.8	30	160	0
170	1	0.85	38	170	0
180	0	0.9	46	180	0
190	0	0.95	24	190	3
200	3	1	2	200	0
	0		0		10

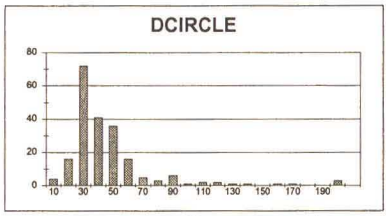

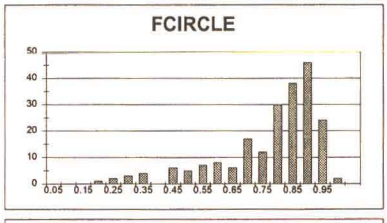

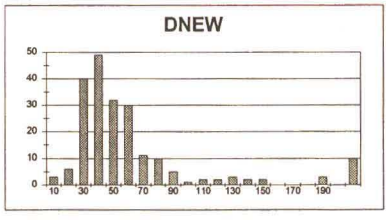


```
{SelectBlock C1}
{PutCell2 "DNEW"}
{SelectBlock C2}
{PutCell2 "=A2..A212/B2..B212"}
{SelectBlock A2..B212}
{EditCopy}
{SelectBlock E2}
{EditPaste}
{SelectBlock C2}
{BlockValues C2;G2}
{SelectBlock C3..C212}
{EditCopy}
{SelectBlock G3}
{EditPaste}
{SelectBlock E2..E212}
{Sort.Block "E2..E212"}
{Sort.Type Top to bottom}
{Sort.Heading 0}
{Sort.Key_1 "E2"}
{Sort.Key_2 ""}
{Sort.Key_3 ""}
{Sort.Key_4 ""}
{Sort.Key_5 ""}
{Sort.BlankCellsFirst 0}
{Sort.Data Numbers First}
{Sort.PreviousSorts -1}
{Sort.Go}
{SelectBlock F2..F212}
{Sort.Block "F2..F212"}
{Sort.Type Top to bottom}
{Sort.Heading 0}
{Sort.Key_1 "F2"}
{Sort.Key_2 ""}
{Sort.Key_3 ""}
{Sort.Key_4 ""}
{Sort.Key_5 ""}
{Sort.BlankCellsFirst 0}
{Sort.Data Numbers First}
{Sort.PreviousSorts -1}
{Sort.Go}
{SelectBlock G2..G212}
{Sort.Block "G2..G212"}
{Sort.Type Top to bottom}
{Sort.Heading 0}
{Sort.Key_1 "G2"}
{Sort.Key_2 ""}
{Sort.Key_3 ""}
{Sort.Key_4 ""}
{Sort.Key_5 ""}
{Sort.BlankCellsFirst 0}
{Sort.Data Numbers First}
{Sort.PreviousSorts -1}
{Sort.Go}
{Selproperty Numeric_Format,"Fixed;2;South Africa"}
{SelectBlock A1..C1}
{EditCopy}
{SelectBlock E1}
{EditPaste}
{SelectBlock I1}
{DESCR "E1..E212",I1;C;"1","1","0","0","95%"}
{SelectBlock K1}
{DESCR "F1..F212",K1;C;"1","1","0","0","95%"}
{SelectBlock M1}
{DESCR "G1..G212",M1;C;"1","1","0","0","95%"}
{SelectBlock I19}
{PutCell2 "Bin"}
{SelectBlock J19}
{PutCell2 "FREQUENCY"}
{SelectBlock I19..J19}
{EditCopy}
{SelectBlock (K19..L19;M19..N19);M19}
{EditPaste}
{SelectBlock I20}
{PutCell2 "10"}
{SelectBlock I21}
{PutCell2 "20"}
{SelectBlock I20..I39}
{SpeedFill}
{EditCopy}
{SelectBlock M20}
{EditPaste}
{SelectBlock K20}
{PutCell2 "0.05"}
{SelectBlock K21}
{PutCell2 "0.1"}
{SelectBlock K20..K39}
{SpeedFill}
{SelectBlock J20}
{PutCell2 "@FREQDIST(E2..E212,I20..I39)"}
{SelectBlock L20}
{PutCell2 "@FREQDIST(F2..F212,K20..K39)"}
{SelectBlock N20}
{PutCell2 "@FREQDIST(G2..G212,M20..M39)"}
{SelectBlock J20..J40}
{GraphNew Chart8}
{Series.Data_Range 1;(J20..J40);1}
{Series.Go}
{FloatCreate Graph;H42;940;220;N59;960;240;Chart8}
{FloatSize H42;940;220;N62;960;240}
{Series.Data_Range XAxisLabelSeries;I20..I40}
{Series.Data_Range 1;J20..J40;1}
{Series.Go}
{GraphSettings.Type "Bar;Bar"}
{GraphSettings.Titles DCIRCLE,"","","",""}
{EditCopy}
{SelectBlock I64}
{EditPaste}
{SelectBlock I85}
{EditPaste}
{SelectFloat Inserted9}
{Series.Data_Range XAxisLabelSeries;K20..K40}
{Series.Data_Range 1;L20..L40;1}
{Series.Go}
{GraphSettings.Titles FCIRCLE,"","","",""}
{SelectFloat Inserted10}
{Series.Data_Range XAxisLabelSeries;M20..M40}
{Series.Data_Range 1;N20..N40;1}
{Series.Go}
{GraphSettings.Titles DNEW,"","","",""}
{SelectBlock 2a:J}
{Selproperty Numeric_Format,"Fixed;4;South Africa"}
{SelectBlock 2a:L}
{Selproperty Numeric_Format,"Fixed;4;South Africa"}
{SelectBlock 2a:N}
{Selproperty Numeric_Format,"Fixed;4;South Africa"}
{SelectBlock J20..J40}
{Selproperty Numeric_Format,"General;4;South Africa"}
{SelectBlock L20..L40}
{Selproperty Numeric_Format,"General;4;South Africa"}
{SelectBlock N20..N40}
{Selproperty Numeric_Format,"General;4;South Africa"}
{SelectBlock 2a:J}
{Selproperty Column_Width,"Auto Width;;1"}
{SelectBlock 2a:L}
{Selproperty Column_Width,"Auto Width;;1"}
{SelectBlock 2a:N}
{Selproperty Column_Width,"Auto Width;;1"}
{SelectBlock O1}
```

Sample 2b.

DCIRCLE	FCIRCLE	DNEW
22.43	0.9	24.92222
22.1	0.79	27.97468
30.08	0.89	33.79775
49.59	0.72	68.875
24.52	0.62	39.54839
34.59	0.8	43.2375
62.45	0.62	100.7258
17.85	0.77	23.18182
19.52	0.73	26.73973
42.68	0.69	61.85507
55.93	0.67	83.47761
37.92	0.91	41.67033
33.14	0.8	41.425
37.84	0.66	57.33333
40.13	0.78	51.44872
33.41	0.74	45.14865
37.8	0.81	46.66667
33.28	0.88	37.81818
16.9	0.83	20.36145
36.23	0.91	39.81319
105.29	0.4	263.225
25.65	0.81	31.66667
23.97	0.84	28.53571
23.91	0.78	30.65385
25.76	0.86	29.95349
70.19	0.83	84.56627
25.12	0.47	53.44681
36.19	0.87	41.5977
24.58	0.75	32.77333
41.55	0.75	55.4
44.22	0.77	57.42857
59.52	0.71	83.83099
24.09	0.87	27.68966
53.74	0.75	71.65333
31.29	0.78	40.11538
27.93	0.61	45.78689
43.65	0.76	57.43421
20.99	0.78	26.91026
35.74	0.73	48.9589
24.88	0.63	39.49206
76.38	0.47	162.5106
28.09	0.82	34.2561
41.44	0.78	53.12821
34.25	0.62	55.24194
18.98	0.74	25.64865
53.65	0.61	87.95082
48.62	0.75	64.82667
37.68	0.76	49.57895
51.62	0.63	81.93651
47.85	0.93	51.45161
132.99	0.42	316.6429
101.5	0.44	230.6818
23.28	0.71	32.78873
33.9	0.8	42.375
102.36	0.36	284.3333
15.81	0.51	31
39.72	0.75	52.96
26.62	0.84	31.69048
42.72	0.72	59.33333
25.24	0.94	26.85106
31.01	0.91	34.07692
57.41	0.83	69.16867
46.36	0.77	60.20779
63.44	0.66	96.12121
18.42	0.78	23.61538
26.95	0.87	30.97701
22.69	0.79	28.72152
66.13	0.67	98.59701
11.05	0.58	19.05172
136.63	0.32	426.9688
25.59	0.86	29.75581
24.52	0.91	26.94505
38.23	0.74	51.66216
42.33	0.7	60.47143
108.86	0.45	241.9111
22.69	0.89	25.49438
65.34	0.66	99
21.89	0.7	31.27143
48.16	0.69	69.7971
49.2	0.74	66.48649
21.62	0.94	23
25.24	0.71	35.5493
59.89	0.7	85.55714
23.08	0.74	31.18919
59.27	0.79	75.02532
33.54	0.79	42.4557
68.56	0.69	99.36232
60.66	0.65	93.32308
101.15	0.5	202.3
71.74	0.56	128.1071
28.97	0.63	45.98413
24.15	0.92	26.25
45.81	0.84	54.53571
39.88	0.69	57.50725
39.5	0.77	51.2987
24.34	0.91	26.74725
34.07	0.76	44.82895
36.64	0.81	45.23457
26.95	0.56	48.125
36.72	0.84	43.71429
25.65	0.89	28.82022
20.41	0.85	24.01176
23.78	0.86	27.65116
25.18	0.85	29.62353
16.46	0.78	21.10256
14.02	0.89	15.75281
24.46	0.93	26.30108
28.97	0.87	33.29885
24.22	0.87	27.83908
45.22	0.71	63.69014
29.18	0.75	38.90667
30.57	0.9	33.96667
22.36	0.77	29.03896
41.8	0.73	57.26027
28.3	0.91	31.0989
22.16	0.64	34.625
38.19	0.79	48.34177
43.85	0.9	48.72222
39.04	0.82	47.60976
20.34	0.85	23.92941
49.74	0.58	85.75862
26.95	0.82	32.86585
31.2	0.72	43.33333
19.37	0.78	24.83333
25.94	0.48	54.04167
20.19	0.75	26.92
12.44	0.7	17.77143
61.22	0.78	78.48718
23.72	0.73	32.49315
27.5	0.75	36.66667
24.76	0.86	28.7907
19.9	0.7	28.42857
27.77	0.8	34.7125
26.84	0.77	34.85714
65.08	0.46	141.4783
29.08	0.84	34.61905
41.73	0.87	47.96552
30.72	0.84	36.57143
23.78	0.9	26.42222
34.72	0.78	44.51282
32.78	0.86	38.11628
31.34	0.78	40.17949
31.15	0.75	41.53333
34.33	0.66	52.01515
16.37	0.8	20.4625
40.68	0.84	48.42857
56.25	0.61	92.21311
18.5	0.53	34.90566
94.15	0.7	134.5
18.42	0.89	20.69663
44.56	0.79	56.40506
21.06	0.61	34.52459
45.35	0.77	58.8961
19.37	0.71	27.28169
33.77	0.77	43.85714
15.91	0.82	19.40244
38.08	0.76	49.82051
32	0.73	43.83562
26.22	0.55	47.67273

DCIRCLE	FCIRCLE	DNEW
3.45	0.12	3.63
11.05	0.13	15.63
12.44	0.19	15.75
14.02	0.32	17.77
14.54	0.36	19.01
14.64	0.39	19.05
15.81	0.4	19.40
15.91	0.42	20.36
16.37	0.44	20.46
16.46	0.45	20.70
16.9	0.46	20.97
17.85	0.47	21.10
18.42	0.47	23.00
18.42	0.48	23.03
18.42	0.5	23.18
18.5	0.51	23.62
18.74	0.51	23.98
18.9	0.51	24.01
18.98	0.52	24.34
19.06	0.53	24.80
19.29	0.53	24.83
19.37	0.54	24.92
19.37	0.55	25.23
19.52	0.55	25.49
19.9	0.56	25.65
20.05	0.56	26.25
20.19	0.58	26.30
20.19	0.58	26.42
20.19	0.61	26.74
20.34	0.61	26.75
20.41	0.61	26.78
20.99	0.61	26.85
21.06	0.61	26.91
21.27	0.61	26.92
21.62	0.62	26.93
21.89	0.62	26.95
22.1	0.62	27.28
22.18	0.62	27.65
22.36	0.63	27.69
22.43	0.63	27.84
22.69	0.63	27.97
22.69	0.64	28.43
22.76	0.65	28.44
22.82	0.65	28.54
22.89	0.66	28.72
22.89	0.66	28.79
23.08	0.66	28.82
23.21	0.66	28.97
23.28	0.67	29.04
23.53	0.67	29.51
23.72	0.67	29.54
23.78	0.67	29.62
23.78	0.69	29.76
23.91	0.69	29.95
23.97	0.69	29.97
24.03	0.69	30.13
24.09	0.7	30.65
24.15	0.7	30.98
24.22	0.7	31.00
24.34	0.7	31.10
24.46	0.7	31.19
24.52	0.7	31.25
24.52	0.71	31.27
24.58	0.71	31.67
24.76	0.71	31.69
24.88	0.71	32.49
25.12	0.71	32.51
25.18	0.72	32.77
25.24	0.72	32.79
25.24	0.72	32.83
25.59	0.72	32.87
25.65	0.72	32.92
25.65	0.73	33.30
25.76	0.73	33.80
25.88	0.73	33.97
25.94	0.73	34.08
26.22	0.73	34.26
26.56	0.73	34.36
26.62	0.74	34.52
26.67	0.74	34.62
26.67	0.74	34.63
26.84	0.74	34.71
26.95	0.74	34.80
26.95	0.74	34.86
26.95	0.75	34.91
27.5	0.75	35.55
27.77	0.75	35.87
27.93	0.75	36.04
27.98	0.75	36.20
28.09	0.75	36.52
28.3	0.75	36.57
28.61	0.75	36.61
28.97	0.75	36.67
28.97	0.76	37.13
29.08	0.76	37.82
29.18	0.76	38.12
29.58	0.76	38.83
29.58	0.76	38.91
30.08	0.76	39.49
30.57	0.77	39.55
30.72	0.77	39.81
30.86	0.77	40.12
31.01	0.77	40.18
31.15	0.77	41.43
31.2	0.77	41.53
31.29	0.77	41.60
31.34	0.77	41.67
32	0.77	41.67
32.78	0.77	42.37
32.92	0.77	42.46
33.14	0.78	42.49
33.28	0.78	43.24
33.41	0.78	43.33
33.54	0.78	43.58
33.68	0.78	43.71
33.77	0.78	43.84
33.9	0.78	43.86
33.99	0.78	44.51
34.07	0.78	44.83
34.25	0.78	45.15
34.33	0.78	45.23
34.59	0.78	45.44
34.72	0.78	45.79
35.74	0.79	45.96
36.19	0.79	46.67
36.23	0.79	47.61
36.64	0.79	47.67
36.72	0.79	47.97
37.68	0.79	48.12
37.8	0.79	48.34
37.84	0.79	48.43
37.92	0.8	48.72
38.08	0.8	48.82
38.11	0.8	48.86
38.11	0.8	48.96
38.19	0.8	49.27
38.23	0.8	49.58
38.35	0.8	51.30
39.04	0.8	51.45
39.5	0.81	51.45
39.53	0.81	51.66
39.68	0.81	52.02
39.72	0.81	52.56
40.13	0.82	52.93
40.68	0.82	52.96
41.44	0.82	53.13
41.55	0.82	53.45
41.73	0.82	54.04
41.8	0.83	54.54
42.33	0.83	55.24
42.37	0.83	55.40
42.68	0.84	56.41
42.72	0.84	57.26
43.1	0.84	57.33
43.65	0.84	57.43
43.85	0.84	57.43
44.22	0.84	57.51
44.29	0.84	57.52
44.56	0.85	58.90

DCIRCLE/mforon		FCIRCLE		DNEW	
Mean	41.4891	Mean	0.7413	Mean	84.6664
Standard Error	2.5185	Standard Error	0.0101	Standard Error	16.3427
Median	31.2900	Median	0.7700	Median	41.5977
Mode	18.4200	Mode	0.7800	Mode	NA
Standard Deviation	36.5832	Standard Deviation	0.1470	Standard Deviation	237.3907
Variance	1338.3280	Variance	0.0216	Variance	56354.3575
Kurtosis	25.5136	Kurtosis	2.9812	Kurtosis	65.7593
Skewness	4.4518	Skewness	-1.4487	Skewness	7.9116
Range	296.5900	Range	0.8300	Range	2332.9518
Minimum	3.4500	Minimum	0.1200	Minimum	3.6316
Maximum	300.0400	Maximum	0.9500	Maximum	2336.5833
Sum	8754.2000	Sum	156.4100	Sum	17864.6197
Count	211.0000	Count	211.0000	Count	211.0000
Confidence Level(0	4.9361	Confidence Level(0	0.0198	Confidence Level(0	32.0310

BIN	FREQUENCY	BIN	FREQUENCY	BIN	FREQUENCY
10	1	0.05	0	10	1
20	24	0.1	0	20	6
30	73	0.15	2	30	48
40	45	0.2	1	40	46
50	27	0.25	0	50	36
60	12	0.3	0	60	23
70	9	0.35	1	70	12
80	4	0.4	3	80	3
90	2	0.45	3	90	9
100	3	0.5	5	100	7
110	5	0.55	9	110	1
120	0	0.6	4	120	0
130	0	0.65	16	130	1
140	3	0.7	18	140	1
150	0	0.75	31	150	1
160	0	0.8	46	160	1
170	0	0.85	26	170	3
180	0	0.9	27	180	0
190	0	0.95	19	190	1
200	0	1	0	200	0
	3		0		11

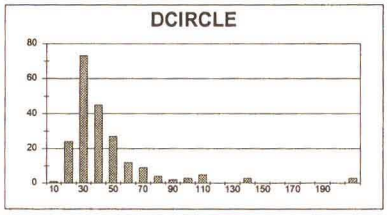

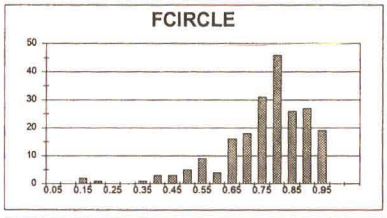

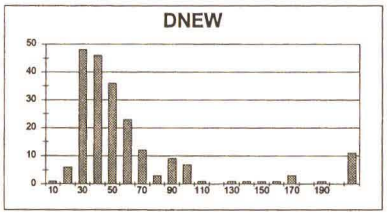


```
(SelectBlock C1)
(PutCell2 "DNEW")
(SelectBlock C2)
(PutCell2 "=A2..A212/B2..B212")
(SelectBlock A2..B212)
(EditCopy)
(SelectBlock E2)
(EditPaste)
(SelectBlock C2)
(BlockValues C2;G2)
(SelectBlock C3..C212)
(EditCopy)
(SelectBlock G3)
(EditPaste)
(SelectBlock E2..E212)
(Sort.Block "E2..E212")
(Sort.Type Top to bottom)
(Sort.Heading 0)
(Sort.Key_1 "E2")
(Sort.Key_2 "")
(Sort.Key_3 "")
(Sort.Key_4 "")
(Sort.Key_5 "")
(Sort.BlankCellsFirst 0)
(Sort.Data Numbers First)
(Sort.PreviousSorts -1)
(Sort.Go)
(SelectBlock F2..F212)
(Sort.Block "F2..F212")
(Sort.Type Top to bottom)
(Sort.Heading 0)
(Sort.Key_1 "F2")
(Sort.Key_2 "")
(Sort.Key_3 "")
(Sort.Key_4 "")
(Sort.Key_5 "")
(Sort.BlankCellsFirst 0)
(Sort.Data Numbers First)
(Sort.PreviousSorts -1)
(Sort.Go)
(SelectBlock G2..G212)
(Sort.Block "G2..G212")
(Sort.Type Top to bottom)
(Sort.Heading 0)
(Sort.Key_1 "G2")
(Sort.Key_2 "")
(Sort.Key_3 "")
(Sort.Key_4 "")
(Sort.Key_5 "")
(Sort.BlankCellsFirst 0)
(Sort.Data Numbers First)
(Sort.PreviousSorts -1)
(Sort.Go)
(Setproperty Numeric_Format,"Fixed;2;South Africa")
(SelectBlock A1..C1)
(EditCopy)
(SelectBlock E1)
(EditPaste)
(SelectBlock I1)
(DESCR "E1..E212";I1;C;"1";"1";"0";"0";"95%")
(SelectBlock K1)
(DESCR "F1..F212";K1;C;"1";"1";"0";"0";"95%")
(SelectBlock M1)
(DESCR "G1..G212";M1;C;"1";"1";"0";"0";"95%")
(SelectBlock I19)
(PutCell2 "BIN")
(SelectBlock J19)
(PutCell2 "FREQUENCY")
(SelectBlock I19..J19)
(EditCopy)
(SelectBlock (K19..L19;M19..N19);M19)
(EditPaste)
(SelectBlock I20)
(PutCell2 "10")
(SelectBlock I21)
(PutCell2 "20")
(SelectBlock I20..I39)
(SpeedFill)
(EditCopy)
(SelectBlock M20)
(EditPaste)
(SelectBlock K20)
(PutCell2 "0.05")
(SelectBlock K21)
(PutCell2 "0.1")
(SelectBlock K20..K39)
(SpeedFill)
(SelectBlock J20)
(PutCell2 "@FREQDIST(E2..E212,I20..I39)")
(SelectBlock L20)
(PutCell2 "@FREQDIST(F2..F212,K20..K39)")
(SelectBlock N20)
(PutCell2 "@FREQDIST(G2..G212,M20..M39)")
(SelectBlock J20..J40)
(GraphNew Chart11)
(Series.Data_Range 1;{J20..J40};1)
(Series.Go)
(FloatCreate Graph;H42;940,220;N59;960;240,Chart11)
(FloatSize H42;940;220;N62;960;240)
(Series.Data_Range XAxisLabelSeries;I20..I40)
(Series.Data_Range 1;J20..J40;1)
(Series.Go)
(GraphSetItngs.Type "Bar;Bar")
(GraphSetItngs.Titles DCIRCLE;"";"";"";"")
(EditCopy)
(SelectBlock I64)
(EditPaste)
(SelectBlock I85)
(EditPaste)
(SelectFloat Inserted12)
(Series.Data_Range XAxisLabelSeries;K20..K40)
(Series.Data_Range 1;L20..L40;1)
(Series.Go)
(GraphSetItngs.Titles FCIRCLE;"";"";"";"")
(SelectFloat Inserted13)
(Series.Data_Range XAxisLabelSeries;M20..M40)
(Series.Data_Range 1;N20..N40;1)
(Series.Go)
(GraphSetItngs.Titles DNEW,"","","","")
(SelectBlock 2b:J)
(Selproperty Numeric_Format,"Fixed;4;South Africa")
(SelectBlock 2b:L)
(Selproperty Numeric_Format,"Fixed;4;South Africa")
(SelectBlock 2b:N)
(Selproperty Numeric_Format,"Fixed;4;South Africa")
(SelectBlock J20..J40)
(Selproperty Numeric_Format,"General;4;South Africa")
(SelectBlock L20..L40)
(Selproperty Numeric_Format,"General;4;South Africa")
(SelectBlock N20..N40)
(Selproperty Numeric_Format,"General;4;South Africa")
(SelectBlock 2b:J)
(Selproperty Column_Width,"Auto Width;;1")
(SelectBlock 2b:L)
(Selproperty Column_Width,"Auto Width;;1")
(SelectBlock 2b:N)
(Selproperty Column_Width,"Auto Width;;1")
(SelectBlock O1)
```

Sample 3a.

DCIRCLE	FCIRCLE	DNEW
4.23	0.43	9.837209
4.23	0.62	6.822581
4.56	0.45	10.13333
3.45	0.72	4.791667
4.23	0.33	8.294118
26.73	0.84	31.82143
45.09	0.74	60.93243
4.88	0.72	6.777778
3.86	0.67	5.761194
47.22	0.71	66.50704
77.31	0.7	110.4429
24.64	0.77	32
96.63	0.41	235.6829
20.56	0.82	25.07317
44.19	0.79	55.93671
38.56	0.84	45.92857
24.34	0.8	30.425
26.05	0.58	44.91378
17.25	0.42	41.07143
25.47	0.88	28.94318
26.67	0.8	33.3375
3.45	0.95	3.631579
27.71	0.56	49.48214
101.46	0.46	220.5652
71.62	0.59	121.3898
51.85	0.66	78.56061
123.59	0.39	316.8974
23.84	0.72	33.11111
24.34	0.95	25.62105
24.94	0.87	28.66667
87.48	0.63	138.8571
90.25	0.63	143.254
64.21	0.67	95.83582
207.03	0.25	828.12
88.9	0.68	130.7353
37.13	0.76	48.85526
32.46	0.87	37.31034
13.25	0.57	23.24561
85.28	0.66	129.2121
33.72	0.73	46.19178
68.93	0.76	90.69737
107.11	0.6	178.5167
55.64	0.58	95.93103
37.56	0.82	45.80488
27.93	0.8	34.9125
19.82	0.81	24.46914
76.87	0.75	102.4933
34.59	0.77	44.92208
5.98	0.42	14.2381
46.13	0.8	57.6625
37.84	0.72	52.55556
146.88	0.3	489.6
75.78	0.69	109.8261
3.86	0.75	5.146667
25.06	0.81	30.93827
215.3	0.21	1025.238
46.49	0.79	58.8481
11.95	0.66	18.10606
111.55	0.58	192.3276
40.61	0.77	52.74026
65.31	0.75	87.08
113.13	0.65	174.0462
372.06	0.15	2480.4
3.45	0.72	4.791667
26.67	0.72	38.11111
49.92	0.75	66.56
107.1	0.62	172.7419
61.2	0.75	81.6
35.23	0.41	85.92683
3.86	0.75	5.146667
134.85	0.33	408.6364
80.63	0.66	122.1667
77.72	0.66	117.7576
58.13	0.69	84.24638
28.19	0.85	33.16471
115.24	0.8	144.05
52.79	0.65	81.21538
83.18	0.43	193.4419
49.13	0.7	70.18571
105.36	0.63	167.2381
97.94	0.48	204.0417

DCIRCLE	FCIRCLE	DNEW
3.45	0.15	3.63
3.45	0.21	4.79
3.45	0.25	4.79
3.86	0.3	5.15
3.86	0.33	5.15
3.86	0.39	5.76
4.23	0.41	6.78
4.23	0.41	6.82
4.23	0.42	8.29
4.56	0.42	9.84
4.88	0.43	10.13
5.98	0.43	14.24
11.95	0.45	18.11
13.25	0.46	23.25
17.25	0.48	24.47
19.82	0.51	25.07
20.56	0.56	25.62
23.84	0.57	28.67
24.34	0.58	28.94
24.34	0.58	30.43
24.64	0.58	30.94
24.94	0.59	31.82
25.06	0.6	32.00
25.47	0.62	33.11
26.05	0.62	33.16
26.67	0.63	33.34
26.73	0.63	34.91
27.71	0.63	37.31
27.93	0.65	41.07
28.19	0.65	44.91
32.46	0.66	44.92
33.72	0.66	45.80
34.59	0.66	45.93
35.23	0.66	46.19
37.13	0.66	48.86
37.56	0.67	49.48
37.84	0.67	52.56
38.56	0.68	52.74
40.61	0.69	55.94
44.19	0.69	57.66
45.09	0.7	58.85
46.13	0.7	60.93
46.49	0.71	66.51
47.22	0.72	66.56
49.13	0.72	70.19
49.92	0.72	78.56
51.85	0.72	81.22
52.79	0.72	81.60
55.64	0.72	84.25
56.13	0.73	85.93
61.2	0.74	87.08
63.44	0.75	88.11
64.21	0.75	90.70
65.31	0.75	95.84
68.93	0.75	95.93
71.62	0.75	102.49
75.78	0.75	109.83
76.87	0.76	110.44
77.31	0.76	117.76
77.72	0.77	121.39
80.63	0.77	122.17
83.18	0.77	129.21
85.28	0.79	130.74
87.48	0.79	138.86
88.9	0.8	143.25
90.25	0.8	144.05
96.63	0.8	167.24
97.94	0.8	172.74
101.46	0.8	174.05
105.36	0.81	178.52
107.1	0.81	192.33
107.11	0.82	192.44
111.55	0.82	204.04
113.13	0.84	220.57
115.24	0.84	235.66
123.59	0.85	316.90
134.85	0.87	408.64
146.88	0.87	489.60
207.03	0.88	828.12
215.3	0.95	1025.24
372.06	0.95	2480.40

DCIRCLE/micron		FCIRCLE		DNEW	
Mean	58.2274	Mean	0.6588	Mean	135.7099
Standard Error	6.2564	Standard Error	0.0187	Standard Error	34.1523
Median	45.0900	Median	0.7000	Median	58.8481
Mode	3.4500	Mode	0.7200	Mode	4.7917
Standard Deviation	56.3075	Standard Deviation	0.1680	Standard Deviation	307.3703
Variance	3170.5400	Variance	0.0282	Variance	94476.5080
Kurtosis	11.7696	Kurtosis	0.6771	Kurtosis	43.8424
Skewness	2.7203	Skewness	-0.9673	Skewness	6.1536
Range	368.6100	Range	0.8000	Range	2476.7684
Minimum	3.4500	Minimum	0.1500	Minimum	3.6316
Maximum	372.0600	Maximum	0.9500	Maximum	2480.4000
Sum	4716.4200	Sum	53.3800	Sum	10992.5000
Count	81.0000	Count	81.0000	Count	81.0000
Confidence Level(0.9	12.2623	Confidence Level(0.9	0.0366	Confidence Level(0.9	66.9372

BIN	FREQUENCY	BIN	FREQUENCY	BIN	FREQUENCY
10	12	0.05	0	10	10
20	4	0.1	0	20	3
30	14	0.15	1	30	6
40	8	0.2	0	40	9
50	8	0.25	2	50	8
60	4	0.3	1	60	5
70	5	0.35	1	70	3
80	5	0.4	1	80	2
90	5	0.45	7	90	6
100	3	0.5	2	100	3
110	4	0.55	1	110	2
120	3	0.6	7	120	2
130	1	0.65	7	130	3
140	1	0.7	12	140	2
150	1	0.75	15	150	2
160	0	0.8	12	160	0
170	0	0.85	7	170	1
180	0	0.9	3	180	3
190	0	0.95	2	190	0
200	0	1	0	200	2
	3		0		9

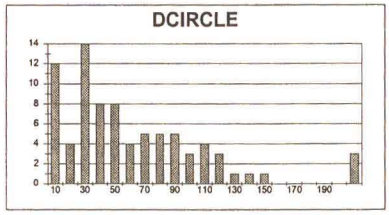

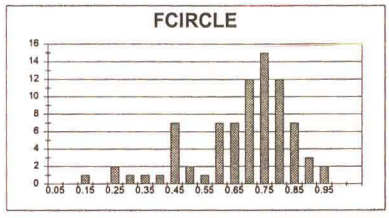

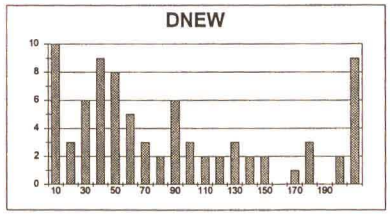


```
{SelectBlock C1}
{PutCell2 "DNEW"}
{SelectBlock C2}
{PutCell2 "=A2..A82/B2..B82"}
{SelectBlock A2..B82}
{EditCopy}
{SelectBlock E2}
{EditPaste}
{SelectBlock C2}
{BlockValues C2;G2}
{SelectBlock C3..C212}
{EditCopy}
{SelectBlock G3}
{EditPaste}
{SelectBlock E2..E82}
{Sort.Block "E2..E82"}
{Sort.Type Top to bottom}
{Sort.Heading 0}
{Sort.Key_1 "E2"}
{Sort.Key_2 ""}
{Sort.Key_3 ""}
{Sort.Key_4 ""}
{Sort.Key_5 ""}
{Sort.BlankCellsFirst 0}
{Sort.Data Numbers First}
{Sort.PreviousSorts -1}
{Sort.Go}
{SelectBlock F2..F82}
{Sort.Block "F2..F82"}
{Sort.Type Top to bottom}
{Sort.Heading 0}
{Sort.Key_1 "F2"}
{Sort.Key_2 ""}
{Sort.Key_3 ""}
{Sort.Key_4 ""}
{Sort.Key_5 ""}
{Sort.BlankCellsFirst 0}
{Sort.Data Numbers First}
{Sort.PreviousSorts -1}
{Sort.Go}
{SelectBlock G2..G82}
{Sort.Block "G2..G82"}
{Sort.Type Top to bottom}
{Sort.Heading 0}
{Sort.Key_1 "G2"}
{Sort.Key_2 ""}
{Sort.Key_3 ""}
{Sort.Key_4 ""}
{Sort.Key_5 ""}
{Sort.BlankCellsFirst 0}
{Sort.Data Numbers First}
{Sort.PreviousSorts -1}
{Sort.Go}
{Selproperty Numeric_Format,"Fixed;2;South Africa"}
{SelectBlock A1..C1}
{EditCopy}
{SelectBlock E1}
{EditPaste}
{SelectBlock I1}
{DESCR "E1..E82";I1;C;"1";"1";"0";"0";"95%"}
{SelectBlock K1}
{DESCR "F1..F82";K1;C;"1";"1";"0";"0";"95%"}
{SelectBlock M1}
{DESCR "G1..G82";M1;C;"1";"1";"0";"0";"95%"}
{SelectBlock I19}
{PutCell2 "BIN"}
{SelectBlock J19}
{PutCell2 "FREQUENCY"}
{SelectBlock I19..J19}
{EditCopy}
{SelectBlock (K19..L19;M19..N19);M19}
{EditPaste}
{SelectBlock I20}
{PutCell2 "10"}
{SelectBlock I21}
{PutCell2 "20"}
{SelectBlock I20..I39}
{SpeedFill}
{EditCopy}
{SelectBlock M20}
{EditPaste}
{SelectBlock K20}
{PutCell2 "0.05"}
{SelectBlock K21}
{PutCell2 "0.1"}
{SelectBlock K20..K39}
{SpeedFill}
{SelectBlock J20}
{PutCell2 "@FREQDIST(E2..E82,I20..I39)"}
{SelectBlock L20}
{PutCell2 "@FREQDIST(F2..F82,K20..K39)"}
{SelectBlock N20}
{PutCell2 "@FREQDIST(G2..G82,M20..M39)"}
{SelectBlock J20..J40}
{GraphNew Chart14}
{Series.Data_Range 1;(J20..J40);1}
{Series.Go}
{FloatCreate Graph;H42;940;220;N59;960;240;Chart14}
{FloatSize H42;940;220;N62;960;240}
{Series.Data_Range XAxisLabelSeries;I20..I40}
{Series.Data_Range 1;J20..J40;1}
{Series.Go}
{GraphSettings.Type "Bar;Bar"}
{GraphSettings.Titles DCIRCLE;"";"";""}
{EditCopy}
{SelectBlock I64}
{EditPaste}
{SelectBlock I85}
{EditPaste}
{SelectFloat Inserted15}
{Series.Data_Range XAxisLabelSeries;K20..K40}
{Series.Data_Range 1;L20..L40;1}
{Series.Go}
{GraphSettings.Titles FCIRCLE;"";"";""}
{SelectFloat Inserted16}
{Series.Data_Range XAxisLabelSeries;M20..M40}
{Series.Data_Range 1;N20..N40;1}
{Series.Go}
{GraphSettings.Titles DNEW;"";"";""}
{SelectBlock 3a:J}
{Selproperty Numeric_Format,"Fixed;4;South Africa"}
{SelectBlock 3a:L}
{Selproperty Numeric_Format,"Fixed;4;South Africa"}
{SelectBlock 3a:N}
{Selproperty Numeric_Format,"Fixed;4;South Africa"}
{SelectBlock J20..J40}
{Selproperty Numeric_Format,"General;4;South Africa"}
{SelectBlock L20..L40}
{Selproperty Numeric_Format,"General;4;South Africa"}
{SelectBlock N20..N40}
{Selproperty Numeric_Format,"General;4;South Africa"}
{SelectBlock 3a:J}
{Selproperty Column_Width,"Auto Width;;1"}
{SelectBlock 3a:L}
{Selproperty Column_Width,"Auto Width;;1"}
{SelectBlock 3a:N}
{Selproperty Column_Width,"Auto Width;;1"}
{SelectBlock O1}
```

Sample 3b.

DCIRCLE	FCIRCLE	DNEW
70.11	0.61	114.9344
57.74	0.77	74.98701
25.82	0.61	42.32787
27.98	0.77	36.33766
22.16	0.71	31.21127
25.06	0.81	30.93827
85.5	0.65	131.5385
106.37	0.75	141.8267
116.61	0.51	228.6471
61.53	0.52	118.3269
205.72	0.32	642.875
130.65	0.67	195
67.2	0.7	96
111.32	0.65	171.2615
61.68	0.79	78.07595
53.68	0.82	65.46341
118.52	0.55	215.4909
56.86	0.67	84.86567
32.42	0.77	42.1039
134.42	0.5	268.84
54.64	0.81	67.45679
27.28	0.62	44
159.11	0.35	454.6
117.55	0.48	244.8958
57.15	0.67	85.29851
48.52	0.78	62.20513
55.13	0.78	70.67949
73.71	0.46	160.2391
10.77	0.65	16.56923
78.44	0.83	94.50602
33.46	0.8	41.825
164.43	0.21	783
105.99	0.81	130.8519
88.2	0.76	116.0526
156.98	0.48	327.0417
56.2	0.54	104.0741
16.99	0.8	21.2375
111.51	0.74	150.6892
13.14	0.36	36.5
84.1	0.77	109.2208
51.56	0.79	65.26582
101.39	0.46	220.413
193.71	0.4	484.275
23.91	0.53	45.11321
32.42	0.75	43.22667
53.46	0.79	80.32911
140.03	0.23	608.8261
56.33	0.8	70.4125
22.63	0.76	29.77632
40.02	0.7	57.17143
35.36	0.85	41.6
23.72	0.82	28.92683
44.29	0.88	50.32955
46.65	0.84	55.53571
50.18	0.74	67.81081
76.48	0.54	141.6296
38.11	0.75	50.81333
38.08	0.7	54.4
76.33	0.69	110.6232
43.72	0.85	51.43529
27.66	0.68	40.67647
87.26	0.42	207.7619
116.69	0.66	176.803
81.69	0.4	204.225
83.86	0.63	101.3651
48	0.59	81.35593
172.69	0.35	493.4
89.12	0.77	89.78623
16.09	0.3	53.63333
48.16	0.75	64.21333
83.46	0.81	103.037
67.2	0.65	103.3846
85.59	0.63	135.8571
26.28	0.77	34.12987
69.47	0.59	117.7458
44.56	0.69	64.57971
40.46	0.68	59.5
38.5	0.72	53.47222
77.64	0.77	100.8312
54.04	0.81	66.71605
35.49	0.75	47.32
20.63	0.59	34.9661
24.4	0.92	26.52174
38.35	0.76	50.46053
36.27	0.85	42.67059
133.09	0.27	492.9259
85.38	0.74	88.35135
46.1	0.77	59.87013
83.28	0.66	126.1818
113.44	0.35	324.1143
46.87	0.84	55.79762

DCIRCLE	FCIRCLE	DNEW
10.77	0.21	16.57
13.14	0.23	21.24
16.09	0.27	26.52
16.99	0.3	28.93
20.63	0.32	29.78
22.16	0.35	30.94
22.63	0.35	31.21
23.72	0.35	34.13
23.91	0.36	34.97
24.4	0.4	36.34
25.06	0.4	36.50
25.82	0.42	40.88
26.28	0.46	41.60
27.28	0.46	41.83
27.66	0.48	42.10
27.98	0.48	42.33
32.42	0.5	42.67
32.42	0.51	43.23
33.46	0.52	44.00
35.36	0.53	45.11
35.49	0.54	47.32
36.27	0.54	50.33
38.08	0.55	50.46
38.11	0.59	50.81
38.35	0.59	51.44
38.5	0.59	53.47
40.02	0.61	53.63
40.46	0.61	54.40
43.72	0.62	55.54
44.29	0.63	55.80
44.56	0.63	57.17
46.1	0.65	59.50
46.65	0.65	59.87
46.87	0.65	62.21
48	0.65	64.21
48.16	0.66	64.58
48.52	0.66	65.27
50.18	0.67	65.46
51.56	0.67	66.72
53.68	0.67	67.46
54.04	0.68	67.81
54.64	0.68	70.41
55.13	0.69	70.68
56.2	0.69	74.99
56.33	0.7	78.08
56.86	0.7	80.33
57.15	0.7	81.36
57.74	0.71	84.87
61.53	0.72	85.30
61.68	0.74	88.35
63.46	0.74	89.77
63.86	0.74	94.51
65.38	0.75	96.00
67.2	0.75	100.83
67.2	0.75	101.37
69.12	0.75	103.04
69.47	0.75	103.38
70.11	0.76	104.07
73.71	0.76	109.22
76.33	0.76	110.62
76.48	0.77	114.93
77.64	0.77	116.05
78.44	0.77	117.75
81.69	0.77	118.33
83.28	0.77	126.18
83.46	0.77	130.85
84.1	0.77	131.54
85.5	0.77	135.86
85.59	0.78	141.63
87.26	0.78	141.83
88.2	0.79	150.69
101.39	0.79	160.24
105.99	0.79	171.26
106.37	0.8	176.80
111.32	0.8	195.00
111.51	0.8	204.23
113.44	0.81	207.76
116.61	0.81	215.49
116.69	0.81	220.41
117.55	0.81	228.65
118.52	0.81	244.90
130.65	0.82	268.84
133.09	0.82	324.11
134.42	0.83	327.04
140.03	0.84	454.60
156.98	0.84	484.28
159.11	0.85	492.93
164.43	0.85	493.40
172.69	0.85	608.83
193.71	0.88	642.86
205.72	0.92	783.00

DCIRCLE/micron		FCIRCLE		DNEW	
Mean	68.62363	Mean	0.658132	Mean	131.7752
Standard Error	4.469264	Standard Error	0.017365	Standard Error	15.19113
Median	56.86	Median	0.7	Median	80.32911
Mode	32.42	Mode	0.77	Mode	NA
Standard Deviation	42.63407	Standard Deviation	0.16565	Standard Deviation	144.9141
Variance	1817.664	Variance	0.02744	Variance	21000.1
Kurtosis	0.994935	Kurtosis	0.106581	Kurtosis	6.766207
Skewness	1.14555	Skewness	-0.96358	Skewness	2.552451
Range	194.95	Range	0.71	Range	766.4308
Minimum	10.77	Minimum	0.21	Minimum	16.56923
Maximum	205.72	Maximum	0.92	Maximum	783
Sum	6244.75	Sum	59.89	Sum	11991.54
Count	91	Count	91	Count	91
Confidence Level(0.9	8.759597	Confidence Level(0.9	0.034034	Confidence Level(0.9	29.77406

BIN	FREQUE	BIN	FREQUE	BIN	FREQUENCY
10	0	0.05	0	10	0
20	4	0.1	0	20	1
30	12	0.15	0	30	4
40	10	0.2	0	40	6
50	11	0.25	2	50	10
60	11	0.3	2	60	12
70	9	0.35	4	70	8
80	8	0.4	3	80	4
90	8	0.45	1	90	6
100	0	0.5	5	100	2
110	3	0.55	6	110	6
120	7	0.6	3	120	5
130	0	0.65	9	130	1
140	3	0.7	12	140	3
150	1	0.75	10	150	2
160	2	0.8	19	160	1
170	1	0.85	13	170	1
180	1	0.9	1	180	2
190	0	0.95	1	190	0
200	1	1	0	200	1
	1		0		16

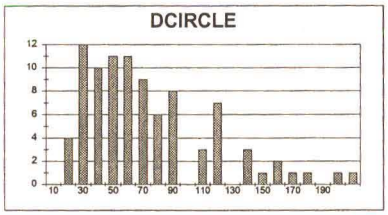

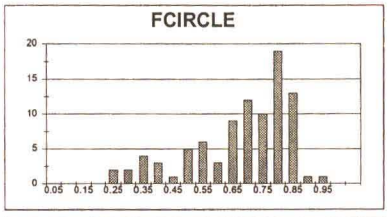

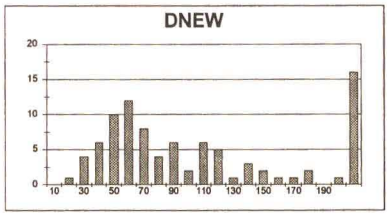


```
{SelectBlock C1}
{PutCell2 "DNEW"}
{SelectBlock C2}
{PutCell2 "=A2..A92/B2..B92"}
{SelectBlock A2..B92}
{EditCopy}
{SelectBlock E2}
{EditPaste}
{SelectBlock C2}
{BlockValues C2;G2}
{SelectBlock C3..C92}
{EditCopy}
{SelectBlock G3}
{EditPaste}
{SelectBlock E2..E92}
{Sort.Block "E2..E92"}
{Sort.Type Top to bottom}
{Sort.Heading 0}
{Sort.Key_1 "E2"}
{Sort.Key_2 ""}
{Sort.Key_3 ""}
{Sort.Key_4 ""}
{Sort.Key_5 ""}
{Sort.BlankCellsFirst 0}
{Sort.Data Numbers First}
{Sort.PreviousSorts -1}
{Sort.Go}
{SelectBlock F2..F92}
{Sort.Block "F2..F92"}
{Sort.Type Top to bottom}
{Sort.Heading 0}
{Sort.Key_1 "F2"}
{Sort.Key_2 ""}
{Sort.Key_3 ""}
{Sort.Key_4 ""}
{Sort.Key_5 ""}
{Sort.BlankCellsFirst 0}
{Sort.Data Numbers First}
{Sort.PreviousSorts -1}
{Sort.Go}
{SelectBlock G2..G92}
{Sort.Block "G2..G92"}
{Sort.Type Top to bottom}
{Sort.Heading 0}
{Sort.Key_1 "G2"}
{Sort.Key_2 ""}
{Sort.Key_3 ""}
{Sort.Key_4 ""}
{Sort.Key_5 ""}
{Sort.BlankCellsFirst 0}
{Sort.Data Numbers First}
{Sort.PreviousSorts -1}
{Sort.Go}
{Selproperty Numeric_Format,"Fixed;2;South Africa"}
{SelectBlock A1..C1}
{EditCopy}
{SelectBlock E1}
{EditPaste}
{SelectBlock I1}
{DESCR "E1..E92";I1,C,"1","1","0","0","95%"}
{SelectBlock K1}
{DESCR "F1..F92";K1,C,"1","1","0","0","95%"}
{SelectBlock M1}
{DESCR "G1..G92";M1,C,"1","1","0","0","95%"}
{SelectBlock I19}
{PutCell2 "BIN"}
{SelectBlock J19}
{PutCell2 "FREQUENCY"}
{SelectBlock I19..J19}
{EditCopy}
{SelectBlock (K19..L19;M19..N19),M19}
{EditPaste}
{SelectBlock I20}
{PutCell2 "10"}
{SelectBlock I21}
{PutCell2 "20"}
{SelectBlock I20..I39}
{SpeedFill}
{EditCopy}
{SelectBlock M20}
{EditPaste}
{SelectBlock K20}
{PutCell2 "0.05"}
{SelectBlock K21}
{PutCell2 "0.1"}
{SelectBlock K20..K39}
{SpeedFill}
{SelectBlock J20}
{PutCell2 "@FREQDIST(E2..E92,I20..I39)"}
{SelectBlock L20}
{PutCell2 "@FREQDIST(F2..F92,K20..K39)"}
{SelectBlock N20}
{PutCell2 "@FREQDIST(G2..G92,M20..M39)"}
```

Sample 4a.

DCIRCLE	FCIRCLE	DNEW
12.06	0.7	17.25714
4.56	0.57	8
21.62	0.8	27.025
5.46	0.55	9.927273
22.82	0.59	38.67797
12.91	0.44	29.34091
27.98	0.89	31.4382
27.17	0.85	31.99471
28.66	0.86	33.32558
26.73	0.84	31.82143
21.48	0.72	29.83333
31.46	0.61	51.60656
61.49	0.49	125.4898
11.44	0.42	27.2381
10.91	0.74	14.74324
34.68	0.63	55.04762
37.04	0.87	42.57471
63.53	0.75	84.70667
56.7	0.57	99.47368
23.53	0.7	33.61429
26.11	0.85	30.71765
28.92	0.82	35.26829
19.37	0.64	30.26563
38.81	0.65	59.70769
25.71	0.94	27.35106
61.27	0.5	122.54
31.48	0.91	34.59341
49.53	0.58	85.39655
50.83	0.81	62.75309
23.4	0.58	40.34483
23.72	0.93	25.50538
16.82	0.54	31.14815
69.55	0.42	165.5952
57.82	0.65	88.95385
32.87	0.86	38.22093
66.98	0.52	128.8077
4.23	0.39	10.84615
16.73	0.6	27.88333
126.14	0.35	360.4
18.82	0.78	24.12821
21.62	0.76	28.44737
19.9	0.73	27.26027
18.34	0.81	22.64198
39.15	0.86	45.52326
32.42	0.74	43.81081
31.15	0.8	38.9375
24.15	0.88	27.44318
34.59	0.84	41.17857
38.23	0.76	50.30263
30.18	0.5	60.36
26.56	0.82	32.39024
17.08	0.84	20.33333
56.81	0.74	76.77027
37.92	0.44	86.18182
135.44	0.41	330.3415
23.84	0.87	27.4023
49.8	0.62	80.32258
42.16	0.78	54.05128
98.71	0.46	214.587
27.01	0.68	39.72059
31.44	0.76	41.36842
34.89	0.7	49.84286
12.44	0.52	23.92308
21.27	0.83	25.62651
32.87	0.77	42.68831
29.93	0.84	35.63095
10.21	0.5	20.42
23.28	0.85	27.38824
79.5	0.77	103.2468
15.04	0.65	23.13846
73.97	0.5	147.94
29.38	0.8	36.725
30.48	0.87	35.03448
57.56	0.74	77.78378
19.29	0.76	24.73077
3.45	0.72	4.791667
47.85	0.78	61.34615
29.68	0.82	36.19512
106.8	0.47	227.234
26.22	0.79	33.18987
24.09	0.88	27.375
88.67	0.79	112.2405
40.97	0.73	56.12329
36.48	0.65	56.12308
27.98	0.8	34.975
21.62	0.86	25.13953
19.67	0.86	22.87209
25.3	0.88	28.75
43.75	0.68	64.33824
28.35	0.87	32.58621
44.69	0.75	59.58667
35.86	0.94	38.14894
18.34	0.81	22.64198
35.02	0.81	43.23457
41.91	0.72	58.20833
51.15	0.72	71.04167
23.84	0.72	33.11111
38.54	0.77	50.05195
67.77	0.75	90.36
21.82	0.72	30.30556
46.23	0.71	65.11268
34.07	0.78	43.67949
49.07	0.72	68.15278
43.85	0.89	49.26966
51.44	0.71	72.4507
44.86	0.77	58.25974
54.2	0.73	74.24658
19.06	0.85	22.42353
170.37	0.22	774.4091
23.53	0.82	28.69512
18.5	0.72	25.69444
20.99	0.59	35.57627
68.45	0.75	91.26667
18.5	0.62	29.83871
75.25	0.59	127.5424
115.96	0.34	341.0588
29.58	0.78	37.92308
24.88	0.67	37.13433
119.75	0.57	210.0877
25.82	0.65	39.72308
5.46	0.67	8.149254
21.96	0.88	24.95455
28.82	0.73	39.47945
27.06	0.86	31.46512
18.5	0.8	23.125
26.22	0.65	40.33846
20.27	0.6	33.78333
31.29	0.87	35.96552
18.58	0.87	21.35632
137.76	0.34	405.1765
179.89	0.19	946.7895
26.62	0.92	28.93478
27.82	0.81	34.34568
40.24	0.79	50.93671
22.5	0.87	25.86207
32.14	0.7	45.91429
21.06	0.79	26.65823
44.22	0.8	55.275
28.14	0.86	32.72093
17.51	0.6	29.18333
24.4	0.94	25.95745
45.29	0.81	55.91358
32.46	0.81	40.07407
50.24	0.67	74.98507
28.25	0.8	35.3125
19.52	0.8	24.4
26.22	0.57	46
19.52	0.87	22.43678
21.34	0.87	24.52874
45.02	0.62	72.6129
116.82	0.4	297.05
82.74	0.55	150.4364
134.83	0.28	481.5357
25.94	0.91	28.50549
26.34	0.78	33.76923
5.46	0.32	17.0625
42.12	0.84	50.14286
23.53	0.72	32.68056
36.84	0.75	49.12
3.45	0.19	4.79
4.23	0.19	6.82
4.23	0.22	7.24
4.56	0.28	8.00
4.56	0.32	8.15
4.88	0.34	8.68
5.46	0.34	9.93
5.46	0.35	10.85
5.46	0.35	12.51
6.68	0.38	14.74
6.68	0.39	17.06
10.21	0.39	17.13
10.91	0.39	17.26
11.44	0.4	17.88
12.08	0.4	18.40
12.44	0.41	18.99
12.68	0.42	19.23
12.91	0.42	20.33
13.25	0.42	20.42
13.36	0.44	20.55
13.48	0.44	21.36
14.23	0.44	21.68
14.74	0.45	22.42
15.04	0.45	22.44
15.62	0.46	22.64
15.91	0.46	22.64
16.73	0.47	22.87
16.82	0.49	23.13
17.08	0.49	23.14
17.51	0.5	23.92
18.34	0.5	23.92
18.34	0.5	24.13
18.34	0.5	24.30
18.5	0.5	24.40
18.5	0.5	24.53
18.5	0.51	24.73
18.58	0.51	24.88
18.58	0.52	24.95
18.66	0.52	25.14
18.82	0.52	25.19
19.06	0.53	25.51
19.21	0.53	25.63
19.29	0.53	25.69
19.37	0.53	25.72
19.44	0.54	25.72
19.52	0.55	25.74
19.52	0.55	25.66
19.6	0.57	25.96
19.67	0.57	26.04
19.75	0.57	26.11
19.82	0.57	26.33
19.9	0.58	26.53
20.27	0.58	26.66
20.41	0.58	26.75
20.63	0.58	26.78
20.63	0.59	27.03
20.85	0.59	27.24
20.92	0.59	27.26
20.99	0.59	27.35
21.06	0.6	27.37
21.27	0.6	27.38
21.27	0.6	27.39
21.34	0.61	27.40
21.41	0.62	27.44
21.48	0.62	27.44
21.48	0.62	27.68
21.62	0.62	27.88
21.62	0.62	28.34
21.62	0.62	28.45
21.89	0.62	28.51
21.82	0.62	28.56
21.82	0.62	28.70
21.96	0.63	28.75
22.03	0.63	28.93
22.16	0.63	29.07
22.5	0.63	29.18
22.63	0.64	29.34
22.63	0.64	29.79
22.69	0.65	29.83
22.82	0.65	29.84
22.82	0.65	30.15
22.89	0.65	30.27
22.95	0.65	30.31
23.21	0.65	30.34
23.28	0.65	30.72
23.28	0.65	30.79
23.4	0.66	31.05
23.47	0.66	31.15
23.53	0.66	31.43
23.53	0.67	31.44
23.53	0.67	31.47
23.72	0.67	31.59
23.84	0.67	31.82
23.84	0.67	31.96
23.84	0.67	32.18
23.91	0.68	32.27
24.09	0.68	32.39
24.15	0.68	32.59
24.22	0.68	32.68
24.28	0.68	32.72
24.34	0.68	32.92
24.4	0.68	33.11
24.64	0.69	33.19
24.64	0.69	33.21
24.76	0.69	33.33
24.88	0.69	33.38
24.94	0.69	33.57
25.3	0.7	33.61
25.47	0.7	33.77
25.71	0.7	33.78
25.82	0.7	34.01
25.86	0.71	34.12
25.94	0.71	34.35
26.11	0.71	34.59
26.22	0.71	34.64
26.22	0.71	34.98
26.22	0.72	35.03
26.34	0.72	35.27
26.39	0.72	35.31
26.51	0.72	35.58
26.56	0.72	35.63
26.62	0.72	35.88
26.67	0.72	35.97
26.73	0.72	36.20
27.01	0.72	36.39
27.06	0.72	36.43
27.17	0.72	36.73
27.23	0.72	36.87
27.82	0.73	37.13
27.98	0.73	37.32
27.98	0.73	37.92
27.98	0.73	38.15
28.14	0.73	38.22
28.25	0.73	38.42
28.35	0.74	38.63
28.4	0.74	38.68
28.66	0.74	38.76
28.72	0.74	38.94
28.82	0.74	39.34
28.92	0.75	39.46
29.36	0.75	39.72
29.46	0.75	39.72
29.58	0.75	39.74
29.68	0.75	40.07
29.88	0.75	40.34
29.93	0.75	40.34
30.18	0.76	40.52
30.23	0.76	40.53
30.33	0.76	40.80
30.38	0.76	40.90
30.48	0.76	41.17
30.57	0.77	41.18
30.62	0.77	41.26
31.15	0.77	41.37
31.29	0.77	41.78
31.29	0.77	42.24
31.44	0.77	42.57
31.48	0.77	42.69
31.48	0.77	42.72

DCIRCLE/micron		FCIRCLE		DNEW	
Mean	37.82701	Mean	0.701609	Mean	68.11724
Standard Error	1.851314	Standard Error	0.00971	Standard Error	6.89969
Median	27.98	Median	0.73	Median	37.92308
Mode	5.46	Mode	0.72	Mode	22.64198
Standard Deviation	29.90689	Standard Deviation	0.15687	Standard Deviation	111.4679
Variance	894.5419	Variance	0.024608	Variance	12425.09
Kurtosis	6.86239	Kurtosis	0.345387	Kurtosis	39.44595
Skewness	2.418702	Skewness	-0.86497	Skewness	5.734601
Range	186.47	Range	0.75	Range	994.7873
Minimum	3.45	Minimum	0.19	Minimum	4.791667
Maximum	189.92	Maximum	0.94	Maximum	999.5789
Sum	9872.85	Sum	183.12	Sum	17778.6
Count	261	Count	261	Count	261
Confidence Level(0.9	3.628509	Confidence Level(0.9	0.019031	Confidence Level(0.9	13.52314

BIN	FREQUE	BIN	FREQUE	BIN	FREQUENCY
10	11	0.05	0	10	7
20	41	0.1	0	20	10
30	94	0.15	0	30	63
40	41	0.2	2	40	83
50	24	0.25	1	50	29
60	13	0.3	1	60	26
70	11	0.35	5	70	9
80	6	0.4	6	80	10
90	3	0.45	9	90	9
100	1	0.5	11	100	4
110	4	0.55	12	110	1
120	4	0.6	15	120	2
130	1	0.65	24	130	4
140	4	0.7	25	140	1
150	0	0.75	35	150	3
160	0	0.8	38	160	1
170	0	0.85	30	170	1
180	2	0.9	35	180	1
190	1	0.95	12	190	2
200	0	1	0	200	0
	0		0		15

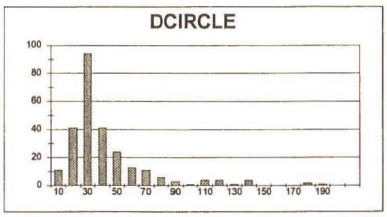

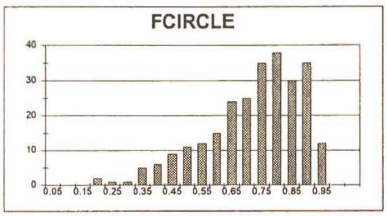

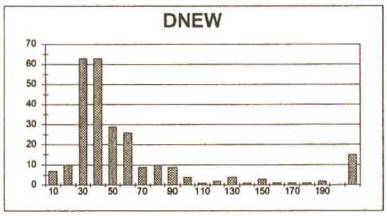


```
{SelectBlock C1}
{PutCell2 "DNEW"}
{SelectBlock C2}
{PutCell2 "=A2..A262/B2..B262"}
{SelectBlock A2..B262}
{EditCopy}
{SelectBlock E2}
{EditPaste}
{SelectBlock C2}
{BlockValues C2;G2}
{SelectBlock C3..C262}
{EditCopy}
{SelectBlock G3}
{EditPaste}
{SelectBlock E2..E262}
{Sort.Block "E2..E262"}
{Sort.Type Top to bottom}
{Sort.Heading 0}
{Sort.Key_1 "E2"}
{Sort.Key_2 ""}
{Sort.Key_3 ""}
{Sort.Key_4 ""}
{Sort.Key_5 ""}
{Sort.BlankCellsFirst 0}
{Sort.Data Numbers First}
{Sort.PreviousSorts -1}
{Sort.Go}
{SelectBlock F2..F262}
{Sort.Block "F2..F262"}
{Sort.Type Top to bottom}
{Sort.Heading 0}
{Sort.Key_1 "F2"}
{Sort.Key_2 ""}
{Sort.Key_3 ""}
{Sort.Key_4 ""}
{Sort.Key_5 ""}
{Sort.BlankCellsFirst 0}
{Sort.Data Numbers First}
{Sort.PreviousSorts -1}
{Sort.Go}
{SelectBlock G2..G262}
{Sort.Block "G2..G262"}
{Sort.Type Top to bottom}
{Sort.Heading 0}
{Sort.Key_1 "G2"}
{Sort.Key_2 ""}
{Sort.Key_3 ""}
{Sort.Key_4 ""}
{Sort.Key_5 ""}
{Sort.BlankCellsFirst 0}
{Sort.Data Numbers First}
{Sort.PreviousSorts -1}
{Sort.Go}
{Selproperty Numeric_Format,"Fixed;2;South Africa"}
{SelectBlock A1..C1}
{EditCopy}
{SelectBlock E1}
{EditPaste}
{SelectBlock I1}
{DESCR "E1..E262",I1,C,"1","1","0","0","95%"}
{SelectBlock K1}
{DESCR "F1..F262",K1,C,"1","1","0","0","95%"}
{SelectBlock M1}
{DESCR "G1..G262",M1,C,"1","1","0","0","95%"}
{SelectBlock I19}
{PutCell2 "BIN"}
{SelectBlock J19}
{PutCell2 "FREQUENCY"}
{SelectBlock I19..J19}
{EditCopy}
{SelectBlock (K19..L19;M19..N19);M19}
{EditPaste}
{SelectBlock I20}
{PutCell2 "10"}
{SelectBlock I21}
{PutCell2 "20"}
{SelectBlock I20..I39}
{SpeedFill}
{EditCopy}
{SelectBlock M20}
{EditPaste}
{SelectBlock K20}
{PutCell2 "0.05"}
{SelectBlock K21}
{PutCell2 "0.1"}
{SelectBlock K20..K39}
{SpeedFill}
{SelectBlock J20}
{PutCell2 "@FREQDIST(E2..E262,I20..I39)"}
{SelectBlock L20}
{PutCell2 "@FREQDIST(F2..F262,K20..K39)"}
{SelectBlock N20}
{PutCell2 "@FREQDIST(G2..G262,M20..M39)"}
{SelectBlock J20..J40}
{GraphNew Chart20}
{Series.Data_Range 1;(J20..J40);1}
{Series.Go}
{FloatCreate Graph;H42;940;220;N59;960;240;Chart20}
{FloatSize H42;940;220;N62;960;240}
{Series.Data_Range XAxisLabelSeries;I20..I40}
{Series.Data_Range 1;J20..J40;1}
{Series.Go}
{GraphSettings.Type "Bar;Bar"}
{GraphSettings.Titles DCIRCLE,"","","",""}
{EditCopy}
{SelectBlock I64}
{EditPaste}
{SelectBlock I85}
{EditPaste}
{SelectFloat Inserted21}
{Series.Data_Range XAxisLabelSeries;K20..K40}
{Series.Data_Range 1;L20..L40;1}
{Series.Go}
{GraphSettings.Titles FCIRCLE,"","","",""}
{SelectFloat Inserted22}
{Series.Data_Range XAxisLabelSeries;M20..M40}
{Series.Data_Range 1;N20..N40;1}
{Series.Go}
{GraphSettings.Titles DNEW,"","","",""}
{SelectBlock 4a:J}
{Selproperty Numeric_Format,"Fixed;4;South Africa"}
{SelectBlock 4a:L}
{Selproperty Numeric_Format,"Fixed;4;South Africa"}
{SelectBlock 4a:N}
{Selproperty Numeric_Format,"Fixed;4;South Africa"}
{SelectBlock J20..J40}
{Selproperty Numeric_Format,"General;4;South Africa"}
{SelectBlock L20..L40}
{Selproperty Numeric_Format,"General;4;South Africa"}
{SelectBlock N20..N40}
{Selproperty Numeric_Format,"General;4;South Africa"}
{SelectBlock 4a:J}
{Selproperty Column_Width,"Auto Width;;1"}
{SelectBlock 4a:L}
{Selproperty Column_Width,"Auto Width;;1"}
{SelectBlock 4a:N}
{Selproperty Column_Width,"Auto Width;;1"}
{SelectBlock O1}
```

Sample 4b.

DCIRCLE	FCIRCLE	DNEW
4.88	0.82	5.95122
25.59	0.84	30.46429
26.22	0.91	28.81319
4.23	0.51	8.294118
23.4	0.88	26.59091
22.76	0.85	26.77647
38.5	0.74	52.02703
27.77	0.64	43.39063
43.75	0.63	69.44444
26.39	0.86	30.68605
25	0.54	46.2963
24.03	0.82	29.30488
31.25	0.78	40.0641
24.46	0.78	31.35897
33.94	0.94	36.10638
24.76	0.86	28.7907
20.7	0.84	24.64286
3.86	0.85	4.541176
21.34	0.73	29.23288
26.84	0.89	30.1573
13.91	0.39	35.66667
42.72	0.69	61.91304
23.34	0.62	37.64516
92.56	0.41	225.8049
21.41	0.77	27.80519
63.7	0.86	74.06977
22.63	0.77	29.38961
50.54	0.62	81.51613
147.93	0.44	336.2045
30.82	0.9	34.24444
86.39	0.51	169.3922
21.48	0.79	27.18987
27.93	0.86	32.47674
22.76	0.62	36.70968
15.14	0.58	26.10345
44.36	0.69	64.26866
30.08	0.85	35.38824
27.06	0.81	33.40741
20.78	0.78	26.64103
42.09	0.92	45.75
130.43	0.5	260.86
53.32	0.84	63.47619
30.18	0.58	52.03448
39.31	0.78	50.39744
3.86	0.6	6.433333
18.74	0.38	49.31579
258.56	0.3	861.8667
71.53	0.68	105.1912
32.14	0.64	50.21875
25.3	0.71	35.6338
93.6	0.51	183.5294
70.57	0.81	87.12346
43.41	0.73	59.46575
18.42	0.72	25.58333
40.5	0.86	47.09302
15.81	0.78	20.80263
133.5	0.51	261.7647
68.12	0.8	85.15
94.88	0.53	179.0189
66.73	0.79	84.46835
30.82	0.9	34.24444
16.46	0.59	27.89831
45.91	0.68	67.51471
60.02	0.82	73.19512
4.88	0.52	9.384615
27.81	0.58	47.60345
79.1	0.77	102.7273
4.56	0.52	8.769231
3.45	0.72	4.791667
20.78	0.69	23.34831
14.02	0.31	45.22581
32.46	0.94	34.53191
25.59	0.93	27.51613
93.6	0.53	176.6038
70.82	0.51	138.8627
61.41	0.76	80.80263
54.94	0.58	94.72414
33.59	0.71	47.30986
47.31	0.61	77.55738
63.06	0.62	101.7097
40.87	0.62	65.91935
85.35	0.58	147.1552
21.62	0.92	23.5
109.15	0.46	237.2826
41.62	0.79	52.68354
19.67	0.8	24.5875
30.67	0.81	37.8642
28.35	0.68	32.21591
206.98	0.22	940.8182
97	0.51	190.1961
25.65	0.94	27.28723
34.94	0.8	43.675
35.32	0.79	44.70886
30.67	0.85	36.08235
35.53	0.85	41.8
26.05	0.93	28.01075
25.88	0.92	28.13043
54.45	0.67	81.26866
44.12	0.74	59.62162
39.5	0.71	55.6338
134.59	0.24	560.7917
51.88	0.76	68.26316
23.91	0.81	29.51852
30.91	0.78	39.62821
67.95	0.59	115.1695
79.7	0.74	107.7027
262.51	0.22	1193.227
20.78	0.94	22.10638
37.8	0.78	48.46154
38.96	0.83	46.93976
58.43	0.69	84.68116
23.15	0.94	24.62766
17.68	0.77	22.96104
31.77	0.87	36.51724
21.13	0.86	24.56977
35.06	0.83	42.24096
62.87	0.66	95.25758
41.94	0.82	51.14634
25.12	0.68	36.54545
42.82	0.72	59.47222
63.21	0.45	140.4667
174.93	0.32	546.6563
4.56	0.8	5.7
58.69	0.6	97.81667
20.78	0.76	27.34211
48.49	0.83	58.42169
35.02	0.84	41.69048
41.98	0.65	64.58462
50.45	0.83	60.78313
23.53	0.92	25.57609
35.82	0.71	50.4507
46.2	0.77	60
62.16	0.58	107.1724
27.77	0.93	29.86022
50.18	0.76	66.02632
31.77	0.85	37.37647
21.69	0.78	27.80769
5.46	0.67	8.149254
33.23	0.89	37.33708
25.59	0.86	29.75581
24.52	0.6	40.86667
19.97	0.73	27.35616
17.6	0.43	40.93023
23.15	0.86	26.9186
20.12	0.71	28.33803
81.24	0.69	117.7391
24.76	0.77	32.15584
33.59	0.79	42.51899
44.83	0.74	60.58108
37.96	0.79	48.05063
18.5	0.54	34.25926
41.16	0.47	87.57447
16	0.91	17.58242
78.52	0.41	191.5122
47.09	0.73	64.50685
29.18	0.58	50.31034
40.28	0.67	60.1194
4.56	0.72	6.333333
45.16	0.65	69.47692

DCIRCLE	FCIRCLE	DNEW
3.45	0.22	4.54
3.45	0.22	4.79
3.86	0.24	5.07
3.86	0.3	5.70
4.23	0.31	5.95
4.56	0.32	6.33
4.56	0.34	6.43
4.56	0.36	8.15
4.88	0.38	8.29
4.88	0.39	8.77
5.46	0.41	9.38
13.91	0.41	17.58
14.02	0.41	20.80
15.14	0.43	22.11
15.81	0.44	22.96
16	0.45	23.35
16.46	0.46	23.50
17.6	0.47	24.57
17.68	0.49	24.59
18.42	0.5	24.63
18.5	0.5	24.64
18.74	0.51	25.34
19.67	0.51	25.58
19.97	0.51	25.58
20.12	0.51	26.10
20.27	0.51	26.59
20.63	0.51	26.64
20.7	0.52	26.78
20.78	0.52	26.92
20.78	0.53	27.19
20.78	0.53	27.29
20.78	0.53	27.34
21.13	0.54	27.36
21.34	0.54	27.52
21.41	0.54	27.81
21.48	0.58	27.81
21.62	0.58	27.84
21.69	0.58	27.90
21.69	0.58	28.01
22.63	0.58	28.13
22.76	0.58	28.17
22.76	0.58	28.34
23.15	0.59	28.55
23.15	0.59	28.65
23.34	0.6	28.79
23.4	0.6	28.81
23.53	0.6	29.19
23.91	0.61	29.23
24.03	0.62	29.30
24.46	0.62	29.39
24.52	0.62	29.52
24.76	0.62	29.76
24.76	0.62	29.86
25	0.63	30.16
25.06	0.64	30.25
25.06	0.64	30.46
25.12	0.65	30.69
25.3	0.65	31.36
25.59	0.66	32.16
25.59	0.66	32.22
25.59	0.67	32.48
25.65	0.67	33.41
25.65	0.67	34.24
25.88	0.68	34.24
26.05	0.68	34.26
26.22	0.68	34.53
26.39	0.69	35.39
26.51	0.69	35.63
26.62	0.69	35.87
26.67	0.69	36.08
26.84	0.7	36.11
27.06	0.71	36.52
27.44	0.71	36.71
27.61	0.71	37.34
27.77	0.71	37.38
27.77	0.71	37.56
27.93	0.71	37.65
28.35	0.72	37.96
29.18	0.72	39.63
30.08	0.72	40.06
30.18	0.72	40.87
30.67	0.72	40.93
30.67	0.73	41.69
30.82	0.73	41.80
30.82	0.73	42.24
30.91	0.73	42.52
31.06	0.73	43.39
31.25	0.74	43.68
31.44	0.74	44.71
31.77	0.74	44.91
31.77	0.74	45.23
32.14	0.74	45.75
32.46	0.76	46.30
33.23	0.76	46.94
33.59	0.76	47.09
33.59	0.76	47.31
33.94	0.76	47.60
34.94	0.77	48.05
35.02	0.77	48.46
35.06	0.77	49.32
35.32	0.77	50.22
35.53	0.77	50.31
35.82	0.77	50.40
37.8	0.77	50.45
37.96	0.77	51.14
38.43	0.78	51.15
38.5	0.78	52.03
38.96	0.78	52.03
39.31	0.78	52.66
39.5	0.78	55.63
40.28	0.78	56.82
40.5	0.78	57.52
40.87	0.79	58.23
41.16	0.79	58.42
41.62	0.79	58.95
41.94	0.79	59.47
41.98	0.79	59.47
42.09	0.79	59.62
42.72	0.8	60.00
42.82	0.8	60.12
43.03	0.8	60.39
43.41	0.8	60.58
43.75	0.8	60.78
43.75	0.81	61.91
44.12	0.81	63.48
44.36	0.81	64.29
44.69	0.81	64.51
44.83	0.82	64.58
45.16	0.82	65.92
45.91	0.82	66.03
46.2	0.82	67.51
47.09	0.83	68.26
47.31	0.83	69.44
48.49	0.83	69.48
50.18	0.83	71.25
50.45	0.84	73.20
50.54	0.84	74.07
51.88	0.84	77.56
53.26	0.84	77.97
53.32	0.85	80.80
54.45	0.85	81.27
54.94	0.85	81.52
56.6	0.85	84.47
58.43	0.85	84.68
58.69	0.85	85.15
60.02	0.86	87.12
61.41	0.86	87.57
62.16	0.86	94.72
62.87	0.86	95.26
63.06	0.86	97.82
63.21	0.86	100.49
63.7	0.86	101.71
66.73	0.86	102.73
67.95	0.87	105.19
68.12	0.88	107.17
70.57	0.88	107.70
70.82	0.88	113.20
71.53	0.88	115.17
78.52	0.89	117.74

DCIRCLE/micron		FCIRCLE		DNEW	
Mean	43.36542	Mean	0.709089	Mean	81.10086
Standard Error	2.852389	Standard Error	0.012402	Standard Error	10.62399
Median	31.77	Median	0.74	Median	44.91429
Mode	20.78	Mode	0.77	Mode	34.24444
Standard Deviation	38.16236	Standard Deviation	0.165931	Standard Deviation	142.1394
Variance	1456.366	Variance	0.027533	Variance	20203.6
Kurtosis	13.10003	Kurtosis	0.149233	Kurtosis	33.3472
Skewness	3.137565	Skewness	-0.81901	Skewness	5.397052
Range	259.06	Range	0.72	Range	1188.686
Minimum	3.45	Minimum	0.22	Minimum	4.541176
Maximum	262.51	Maximum	0.94	Maximum	1193.227
Sum	7762.41	Sum	126.39	Sum	14517.05
Count	179	Count	179	Count	179
Confidence Level(0	5.590579	Confidence Level(0	0.024308	Confidence Level(0	20.82265

BIN	FREQUE	BIN	FREQUE	BIN	FREQUENCY
10	11	0.05	0	10	11
20	13	0.1	0	20	1
30	55	0.15	0	30	41
40	31	0.2	0	40	26
50	24	0.25	3	50	21
60	11	0.3	1	60	19
70	10	0.35	3	70	15
80	6	0.4	3	80	5
90	3	0.45	6	90	8
100	6	0.5	5	100	3
110	1	0.55	14	110	6
120	0	0.6	12	120	3
130	0	0.65	11	130	0
140	3	0.7	13	140	1
150	1	0.75	21	150	2
160	0	0.8	31	160	0
170	0	0.85	22	170	1
180	1	0.9	19	180	2
190	0	0.95	15	190	1
200	0	1	0	200	2
	3		0		11

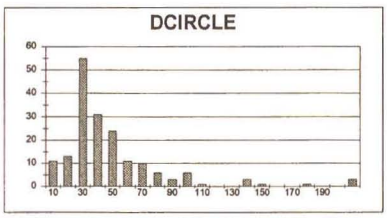

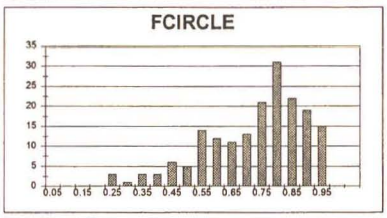

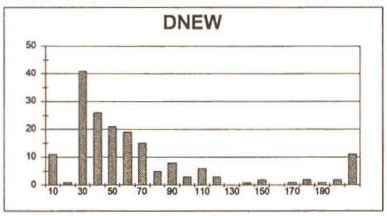


```
{SelectBlock C1}
{PutCell2 "DNEW"}
{SelectBlock C2}
{PutCell2 "=A2..A180/B2..B180"}
{SelectBlock A2..B160}
{EditCopy}
{SelectBlock E2}
{EditPaste}
{SelectBlock C2}
{BlockValues C2;G2}
{SelectBlock C3..C180}
{EditCopy}
{SelectBlock G3}
{EditPaste}
{SelectBlock E2..E180}
{Sort, Block "E2..E180"}
{Sort, Type Top to bottom}
{Sort, Heading 0}
{Sort, Key_1 "E2"}
{Sort, Key_2 ""}
{Sort, Key_3 ""}
{Sort, Key_4 ""}
{Sort, Key_5 ""}
{Sort, BlankCellsFirst 0}
{Sort, Data Numbers First}
{Sort, PreviousSorts -1}
{Sort, Go}
{SelectBlock F2..F180}
{Sort, Block "F2..F180"}
{Sort, Type Top to bottom}
{Sort, Heading 0}
{Sort, Key_1 "F2"}
{Sort, Key_2 ""}
{Sort, Key_3 ""}
{Sort, Key_4 ""}
{Sort, Key_5 ""}
{Sort, BlankCellsFirst 0}
{Sort, Data Numbers First}
{Sort, PreviousSorts -1}
{Sort, Go}
{SelectBlock G2..G180}
{Sort, Block "G2..G180"}
{Sort, Type Top to bottom}
{Sort, Heading 0}
{Sort, Key_1 "G2"}
{Sort, Key_2 ""}
{Sort, Key_3 ""}
{Sort, Key_4 ""}
{Sort, Key_5 ""}
{Sort, BlankCellsFirst 0}
{Sort, Data Numbers First}
{Sort, PreviousSorts -1}
{Sort, Go}
{Selproperty Numeric_Format,"Fixed,2;South Africa"
{SelectBlock A1..C1}
{EditCopy}
{SelectBlock E1}
{EditPaste}
{SelectBlock I1}
{DESCR "E1..E180";I1;C;"1";"1";"0";"0";"95%"}
{SelectBlock K1}
{DESCR "F1..F180";K1;C;"1";"1";"0";"0";"95%"}
{SelectBlock M1}
{DESCR "G1..G180";M1;C;"1";"1";"0";"0";"95%"}
{SelectBlock I19}
{PutCell2 "BIN"}
{SelectBlock J19}
{PutCell2 "FREQUENCY"}
{SelectBlock I19..J19}
{EditCopy}
{SelectBlock (K19..L19,M19..N19);M19}
{EditPaste}
{SelectBlock I20}
{PutCell2 "10"}
{SelectBlock I21}
{PutCell2 "20"}
{SelectBlock I20..I39}
{SpeedFill}
{EditCopy}
{SelectBlock M20}
{EditPaste}
{SelectBlock K20}
{PutCell2 "0.05"}
{SelectBlock K21}
{PutCell2 "0.1"}
{SelectBlock K20..K39}
{SpeedFill}
{SelectBlock J20}
{PutCell2 "@FREQDIST(E2..E180,I20..I39)"}
{SelectBlock L20}
{PutCell2 "@FREQDIST(F2..F180,K20..K39)"}
{SelectBlock N20}
{PutCell2 "@FREQDIST(G2..G180,M20..M39)"}
```

Sample 5a.

DCIRCLE	FCIRCLE	DNEW
4.56	0.45	10.13333
3.45	0.72	4.791667
20.41	0.83	24.59036
18.58	0.75	24.77333
27.17	0.87	31.22989
28.03	0.51	54.96078
16	0.72	22.22222
4.56	0.63	7.238095
19.75	0.28	70.53571
83.39	0.46	181.2826
55.91	0.7	79.87143
5.72	0.32	17.875
18.9	0.83	22.77108
17.51	0.68	25.75
6.46	0.54	11.96296
49.23	0.77	63.93506
3.45	0.95	3.631579
8.09	0.43	18.81395
7.11	0.37	19.21622
4.23	0.49	8.632653
7.11	0.72	9.875
117.6	0.77	152.7273
17.6	0.39	45.12821
146.27	0.39	375.0513
17.43	0.81	21.51852
6.22	0.43	14.46512
34.03	0.81	42.01235
4.23	0.54	7.833333
42.79	0.69	62.01449
18.82	0.69	27.27536
71.83	0.43	167.0465
22.5	0.56	40.17857
38.66	0.83	46.57831
4.88	0.49	9.959184
140.44	0.49	286.6122
13.8	0.48	28.75
4.88	0.82	5.95122
3.45	0.82	4.207317
9.76	0.73	13.36986
17.93	0.5	35.86
60.88	0.67	90.86567
39.23	0.64	61.29687
17.76	0.71	25.01408
61.82	0.69	89.5942
41.44	0.69	60.05797
44.93	0.62	72.46774
41.16	0.65	63.32308
38.11	0.71	53.67606
26.84	0.82	32.73171
28.66	0.52	55.11538
31.25	0.73	42.80822
200.44	0.45	445.4222
25.18	0.8	31.475
20.56	0.61	33.70492
15.14	0.59	25.66102
64.02	0.76	84.23684
50.12	0.62	80.83871
61.75	0.67	92.16418
10.49	0.76	13.80263
3.45	0.82	4.207317
49.29	0.6	82.15
4.23	0.62	6.822581
18.82	0.89	21.14607
34.76	0.76	45.73684
5.46	0.26	21
4.88	0.91	5.362637
49.16	0.72	68.27778
16.46	0.72	22.86111
106.37	0.72	147.7361
22.5	0.52	43.26923
25.59	0.53	48.28302
281.44	0.16	1759
71.1	0.66	107.7273
3.86	0.6	6.433333
32.09	0.86	37.31395
21.82	0.53	41.16981
52.16	0.79	66.02532
26.05	0.7	37.21429
57.79	0.69	83.75362
32.46	0.76	42.71053
27.17	0.65	41.8
16.19	0.75	21.58667
70.76	0.47	150.5532
23.28	0.83	28.04819
554.7	0.2	2773.5
33.85	0.8	42.3125
60.73	0.62	97.95161
4.23	1	4.23
3.45	1	3.45
11.57	0.48	24.10417
47.28	0.7	67.54286
42.16	0.65	64.86154
12.68	0.74	17.13514
11.05	0.47	23.51064
24.09	0.8	30.1125
136.4	0.38	358.9474
58.56	0.72	81.33333
231.02	0.51	452.9804
66.84	0.42	159.1429

DCIRCLE	FCIRCLE	DNEW
3.45	0.16	3.45
3.45	0.2	3.63
3.45	0.26	4.21
3.45	0.28	4.21
3.45	0.32	4.23
3.86	0.37	4.79
4.23	0.38	5.36
4.23	0.39	5.95
4.23	0.39	6.43
4.23	0.42	6.82
4.56	0.43	7.24
4.56	0.43	7.83
4.88	0.43	8.63
4.88	0.45	9.88
4.88	0.45	9.96
5.46	0.46	10.13
5.72	0.47	11.96
6.22	0.47	13.37
6.46	0.48	13.80
7.11	0.48	14.47
7.11	0.49	17.14
8.09	0.49	17.88
9.76	0.49	18.81
10.49	0.5	19.22
11.05	0.51	21.00
11.57	0.51	21.15
12.68	0.52	21.52
13.8	0.52	21.59
15.14	0.53	22.22
16	0.53	22.77
16.19	0.54	22.86
16.46	0.54	23.51
17.43	0.56	24.10
17.51	0.59	24.59
17.6	0.6	24.77
17.76	0.6	25.01
17.93	0.61	25.66
18.58	0.62	25.75
18.82	0.62	27.25
18.82	0.62	28.05
18.9	0.62	28.75
19.75	0.63	30.11
20.41	0.64	31.23
20.56	0.65	31.48
21.82	0.65	32.73
22.5	0.65	33.70
22.5	0.66	35.86
23.28	0.67	37.21
24.09	0.67	37.31
25.18	0.68	40.18
25.59	0.69	41.17
26.05	0.69	41.80
26.84	0.69	42.01
27.17	0.69	42.31
27.17	0.69	42.71
28.03	0.7	42.81
28.66	0.7	43.27
31.25	0.7	45.13
32.09	0.71	45.74
32.46	0.71	46.58
33.85	0.72	48.28
34.03	0.72	53.68
34.76	0.72	54.96
38.11	0.72	55.12
38.66	0.72	60.06
38.23	0.72	61.30
41.16	0.72	62.01
41.44	0.73	63.32
42.16	0.73	63.94
42.79	0.74	64.86
44.93	0.75	66.03
47.28	0.75	67.54
49.16	0.76	68.28
49.23	0.76	70.54
49.29	0.76	72.47
50.12	0.76	79.87
52.16	0.77	80.84
55.91	0.77	81.33
57.79	0.79	82.15
58.56	0.8	83.75
60.73	0.8	84.24
60.88	0.8	89.59
61.75	0.81	90.87
61.82	0.81	92.16
64.02	0.82	97.95
66.84	0.82	107.73
70.76	0.82	147.74
71.1	0.82	150.55
71.83	0.83	152.73
83.39	0.83	159.14
106.37	0.83	167.05
117.6	0.83	181.28
136.4	0.86	286.61
140.44	0.87	358.95
146.27	0.89	375.05
200.44	0.91	445.42
231.02	0.95	452.98
281.44	1	1759.00
554.7	1	2773.50

DCIRCLE/micron		FCIRCLE		DNEW	
Mean	44.22495	Mean	0.640505	Mean	108.0423
Standard Error	7.012997	Standard Error	0.017336	Standard Error	33.25168
Median	25.18	Median	0.68	Median	40.17857
Mode	3.45	Mode	0.72	Mode	4.207317
Standard Deviation	89.77844	Standard Deviation	0.172487	Standard Deviation	330.85
Variance	4869.031	Variance	0.029752	Variance	109461.7
Kurtosis	30.43314	Kurtosis	-0.05251	Kurtosis	49.37069
Skewness	4.852186	Skewness	-0.45789	Skewness	6.762763
Range	551.25	Range	0.84	Range	2770.05
Minimum	3.45	Minimum	0.16	Minimum	3.45
Maximum	554.7	Maximum	1	Maximum	2773.5
Sum	4378.27	Sum	63.41	Sum	10696.19
Count	99	Count	99	Count	99
Confidence Level(0.9	13.74522	Confidence Level(0.9	0.033977	Confidence Level(0.9	65.17209

BIN	FREQUE	BIN	FREQUE	BIN	FREQUENCY
10	23	0.05	0	10	15
20	19	0.1	0	20	9
30	15	0.15	0	30	17
40	9	0.2	2	40	8
50	9	0.25	0	50	12
60	5	0.3	2	60	3
70	6	0.35	1	70	9
80	3	0.4	4	80	3
90	1	0.45	6	90	6
100	0	0.5	9	100	3
110	1	0.55	8	110	1
120	1	0.6	4	120	0
130	0	0.65	10	130	0
140	1	0.7	12	140	0
150	2	0.75	14	150	1
160	0	0.8	10	160	3
170	0	0.85	10	170	1
180	0	0.9	3	180	0
190	0	0.95	2	190	1
200	0	1	2	200	0
	4		0		7

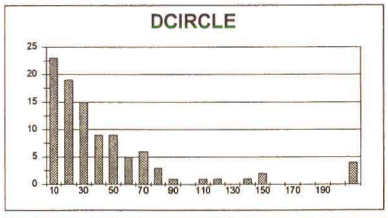

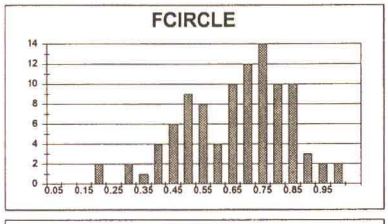

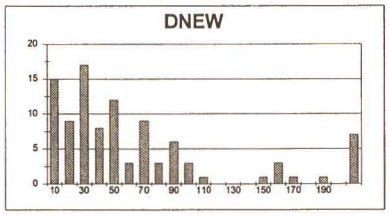


```
{SelectBlock C1}
{PutCell2 "DNEW"}
{SelectBlock C2}
{PutCell2 "=A2..A100/B2..B100"}
{SelectBlock A2..B100}
{EditCopy}
{SelectBlock E2}
{EditPaste}
{SelectBlock C2}
{BlockValues C2;G2}
{SelectBlock C3..C100}
{EditCopy}
{SelectBlock G3}
{EditPaste}
{SelectBlock E2..E100}
{Sort.Block "E2..E100"}
{Sort.Type Top to bottom}
{Sort.Heading 0}
{Sort.Key_1 "E2"}
{Sort.Key_2 ""}
{Sort.Key_3 ""}
{Sort.Key_4 ""}
{Sort.Key_5 ""}
{Sort.BlankCellsFirst 0}
{Sort.Data Numbers First}
{Sort.PreviousSorts -1}
{Sort.Go}
{SelectBlock F2..F100}
{Sort.Block "F2..F100"}
{Sort.Type Top to bottom}
{Sort.Heading 0}
{Sort.Key_1 "F2"}
{Sort.Key_2 ""}
{Sort.Key_3 ""}
{Sort.Key_4 ""}
{Sort.Key_5 ""}
{Sort.BlankCellsFirst 0}
{Sort.Data Numbers First}
{Sort.PreviousSorts -1}
{Sort.Go}
{SelectBlock G2..G100}
{Sort.Block "G2..G100"}
{Sort.Type Top to bottom}
{Sort.Heading 0}
{Sort.Key_1 "G2"}
{Sort.Key_2 ""}
{Sort.Key_3 ""}
{Sort.Key_4 ""}
{Sort.Key_5 ""}
{Sort.BlankCellsFirst 0}
{Sort.Data Numbers First}
{Sort.PreviousSorts -1}
{Sort.Go}
{Selproperty Numeric_Format;"Fixed;2;South Africa")
{SelectBlock A1..C1}
{EditCopy}
{SelectBlock E1}
{EditPaste}
{SelectBlock I1}
{DESCR "E1..E100";I1;C;"1";"1";"0";"0";"95%"}
{SelectBlock K1}
{DESCR "F1..F100";K1;C;"1";"1";"0";"0";"95%"}
{SelectBlock M1}
{DESCR "G1..G100";M1;C;"1";"1";"0";"0";"95%"}
{SelectBlock I19}
{PutCell2 "BIN"}
{SelectBlock J19}
{PutCell2 "FREQUENCY"}
{SelectBlock I19..J19}
{EditCopy}
{SelectBlock (K19..L19;M19..N19);M19}
{EditPaste}
{SelectBlock I20}
{PutCell2 "10"}
{SelectBlock I21}
{PutCell2 "20"}
{SelectBlock I20..I39}
{SpeedFill}
{EditCopy}
{SelectBlock M20}
{EditPaste}
{SelectBlock K20}
{PutCell2 "0.05"}
{SelectBlock K21}
{PutCell2 "0.1"}
{SelectBlock K20..K39}
{SpeedFill}
{SelectBlock J20}
{PutCell2 "@FREQDIST(E2..E100,I20..I39)"}
{SelectBlock L20}
{PutCell2 "@FREQDIST(F2..F100,K20..K39)"}
{SelectBlock N20}
{PutCell2 "@FREQDIST(G2..G100,M20..M39)"}
{SelectBlock J20..J40}
{GraphNew Chart26}
{Series.Data_Range 1;(J20..J40);1}
{Series.Go}
{FloatCreate Graph;H42;940,220;N59;960,240,Chart26}
{FloatSize H42;940,220;N62;960,240}
{Series.Data_Range XAxisLabelSeries;I20..I40}
{Series.Data_Range 1;J20..J40;1}
{Series.Go}
{GraphSettings.Type "Bar;Bar"}
{GraphSettings.Titles DCIRCLE;"";"";"";""}
{EditCopy}
{SelectBlock I64}
{EditPaste}
{SelectBlock I85}
{EditPaste}
{SelectFloat Inserted27}
{Series.Data_Range XAxisLabelSeries;K20..K40}
{Series.Data_Range 1;L20..L40;1}
{Series.Go}
{GraphSettings.Titles FCIRCLE;"";"";"";""}
{SelectFloat Inserted28}
{Series.Data_Range XAxisLabelSeries;M20..M40}
{Series.Data_Range 1;N20..N40;1}
{Series.Go}
{GraphSettings.Titles DNEW;"";"";"";""}
{SelectBlock 5a:J}
{Selproperty Numeric_Format;"Fixed;4;South Africa")
{SelectBlock 5a:L}
{Selproperty Numeric_Format;"Fixed;4;South Africa")
{SelectBlock 5a:N}
{Selproperty Numeric_Format;"Fixed;4;South Africa")
{SelectBlock J20..J40}
{Selproperty Numeric_Format;"General;4;South Africa")
{SelectBlock L20..L40}
{Selproperty Numeric_Format;"General;4;South Africa")
{SelectBlock N20..N40}
{Selproperty Numeric_Format;"General;4;South Africa")
{SelectBlock 5a:J}
{Selproperty Column_Width;"Auto Width;;1")
{SelectBlock 5a:L}
{Selproperty Column_Width;"Auto Width;;1")
{SelectBlock 5a:N}
{Selproperty Column_Width;"Auto Width;;1")
{SelectBlock O1}
```

Sample 5b.

DCIRCLE	FCIRCLE	DNEW
3.86	1	3.86
10.49	0.72	14.56944
46.97	0.72	65.23611
3.86	0.6	6.433333
9.45	0.72	13.125
3.45	0.82	4.207317
4.88	0.49	9.959184
14.44	0.34	42.47059
22.69	0.89	25.49438
10.77	0.28	38.46429
4.23	0.76	5.565789
16.64	0.54	30.81481
19.82	0.58	34.17241
80.8	0.55	146.9091
47.41	0.75	63.21333
4.23	0.8	5.2875
5.98	0.48	12.45833
3.45	0.68	5.073529
4.56	0.72	6.333333
26.51	0.77	34.42857
7.11	0.6	11.85
54.64	0.65	84.06154
4.88	0.58	8.413793
21.76	0.88	24.72727
12.8	0.33	38.78788
50.36	0.75	67.14667
5.46	0.67	8.149254
4.23	1	4.23
5.98	0.56	10.67857
105.43	0.47	224.3191
73.46	0.66	111.303
55.83	0.68	82.10294
23.15	0.59	39.23729
4.56	0.72	6.333333
3.45	0.72	4.791667
9.45	0.35	27
4.23	0.62	6.822581
31.72	0.89	35.64045
31.06	0.76	40.86842
3.45	0.95	3.631579
4.23	0.68	6.220588
3.45	0.82	4.207317
5.72	0.68	8.411765
14.54	0.38	38.26316
45.39	0.63	72.04762
73.71	0.7	105.3
26.56	0.62	42.83871
32.32	0.58	54.77966
66.55	0.54	123.2407
4.23	0.56	7.553571
4.56	0.93	4.903226
74.45	0.63	118.1746
58.59	0.81	72.33333
64.3	0.64	100.4688
90.28	0.65	138.8923
14.94	0.43	34.74419
305.33	0.17	1796.059
413.08	0.19	2174.105
146.71	0.44	333.4318
15.14	0.4	37.85
6.22	0.39	15.94872
36.15	0.71	50.91549
12.08	0.34	35.52941
3.86	0.51	7.568627
43.99	0.7	62.84286
47.88	0.68	70.41176
5.18	0.6	8.633333
53.82	0.54	99.66667
22.16	0.54	41.03704
5.46	0.6	9.1
61.78	0.76	81.28947
25.12	0.86	29.2093
60.02	0.69	86.98551
27.06	0.89	30.40449
69.27	0.65	106.5692
28.72	0.51	56.31373
30.33	0.73	41.54795
23.53	0.75	31.37333
13.03	0.34	38.32353
41.73	0.69	60.47826
24.88	0.89	27.95506
15.58	0.7	26.54286
3.45	0.72	4.791667
72.44	0.61	118.7541
62.64	0.59	106.1695
3.86	0.51	7.568627
5.46	0.48	11.375
27.5	0.79	34.81013
21.82	0.5	43.64
148.17	0.5	296.34
15.14	0.42	36.04762
123.59	0.6	205.9833
75.03	0.56	133.9821
12.56	0.5	25.12
23.53	0.76	30.96053
23.15	0.74	31.28378
31.91	0.8	39.8875
34.55	0.69	50.07246
29.56	0.88	33.61364
4.23	0.9	4.7
49.29	0.64	77.01563
49.77	0.7	71.1
5.72	0.24	23.83333
21.2	0.29	73.10345
12.56	0.34	36.94118
14.23	0.33	43.12121
3.86	0.67	5.761194
37.72	0.67	56.29851
40.72	0.76	53.57895
70.53	0.51	138.2941
18.98	0.64	29.65625
46.1	0.73	63.15068
26.11	0.6	43.51667
50.42	0.67	75.25373
26.67	0.56	47.625
27.12	0.58	46.75862
9.29	0.35	26.54286
22.69	0.75	30.25333
19.52	0.53	36.83019
298.8	0.37	807.5676
22.16	0.63	35.1746
3.45	0.17	3.63
3.45	0.19	3.86
3.45	0.24	4.21
3.45	0.28	4.21
3.45	0.29	4.23
3.45	0.33	4.70
3.86	0.33	4.79
3.86	0.34	4.79
3.86	0.34	4.90
3.86	0.34	5.07
3.86	0.34	5.29
4.23	0.35	5.57
4.23	0.35	5.76
4.23	0.37	6.22
4.23	0.38	6.33
4.23	0.39	6.33
4.23	0.4	6.43
4.23	0.42	6.82
4.56	0.43	7.55
4.56	0.44	7.57
4.56	0.47	7.57
4.88	0.48	8.15
4.88	0.48	8.41
5.18	0.49	8.41
5.46	0.5	8.63
5.46	0.5	9.10
5.46	0.5	9.96
5.72	0.51	10.68
5.72	0.51	11.38
5.98	0.51	11.85
5.98	0.51	12.46
6.22	0.53	13.13
7.11	0.54	14.57
9.29	0.54	15.95
9.45	0.54	23.83
9.45	0.54	24.73
10.49	0.55	25.12
10.77	0.56	25.49
12.08	0.56	26.54
12.56	0.56	26.54
12.56	0.56	27.00
12.8	0.58	27.96
13.03	0.58	29.21
14.23	0.58	29.66
14.44	0.59	30.25
14.54	0.59	30.40
14.94	0.59	30.81
15.14	0.6	30.96
15.14	0.6	31.28
16.64	0.6	31.37
18.58	0.6	33.61
18.98	0.6	34.17
19.52	0.6	34.43
19.82	0.61	34.74
21.2	0.62	34.81
21.76	0.62	35.17
21.82	0.63	35.53
22.16	0.63	35.64
22.16	0.63	36.05
22.69	0.64	36.83
22.69	0.64	36.94
23.15	0.64	37.85
23.15	0.65	38.26
23.53	0.65	38.32
23.53	0.65	38.46
24.88	0.66	38.79
25.12	0.67	39.24
26.11	0.67	39.89
26.51	0.67	40.87
26.56	0.67	41.04
26.67	0.68	41.55
27.06	0.68	42.47
27.12	0.68	42.84
27.5	0.68	43.12
28.72	0.68	43.52
29.56	0.69	43.64
30.33	0.69	46.76
31.06	0.69	47.63
31.72	0.7	50.07
31.91	0.7	50.92
32.32	0.7	53.58
34.55	0.7	54.76
36.15	0.71	56.30
37.72	0.72	56.31
40.72	0.72	60.48
41.73	0.72	62.84
43.99	0.72	63.15
45.39	0.72	63.21
46.1	0.72	65.24
46.97	0.72	67.15
47.41	0.73	70.41
47.88	0.73	71.10
49.29	0.74	72.05
49.77	0.75	72.33
50.36	0.75	73.10
50.42	0.75	75.25
53.82	0.75	77.02
54.64	0.76	81.29
55.83	0.76	82.10
58.59	0.76	84.06
60.02	0.76	86.99
61.78	0.76	99.67
62.64	0.77	100.47
64.3	0.79	105.30
66.55	0.8	106.17
69.27	0.8	106.57
70.53	0.81	111.30
72.44	0.82	118.17
73.46	0.82	118.75
73.71	0.86	123.24
74.45	0.88	133.98
75.03	0.88	138.29
80.8	0.89	138.89
90.28	0.89	146.91
105.43	0.89	205.98
123.59	0.89	224.32
146.71	0.9	296.34
148.17	0.93	333.43
298.8	0.95	807.57
305.33	1	1796.06
413.08	1	2174.11

DCIRCLE/micron		FCIRCLE		DNEW	
Mean	37.80579	Mean	0.622397	Mean	88.73654
Standard Error	5.168453	Standard Error	0.015728	Standard Error	23.90321
Median	22.69	Median	0.64	Median	36.94118
Mode	4.23	Mode	0.72	Mode	4.207317
Standard Deviation	56.85298	Standard Deviation	0.173003	Standard Deviation	262.9353
Variance	3232.261	Variance	0.02993	Variance	69134.96
Kurtosis	22.10684	Kurtosis	-0.07386	Kurtosis	47.6648
Skewness	4.261812	Skewness	-0.31739	Skewness	6.721475
Range	409.63	Range	0.83	Range	2170.474
Minimum	3.45	Minimum	0.17	Minimum	3.631579
Maximum	413.08	Maximum	1	Maximum	2174.105
Sum	4574.5	Sum	75.31	Sum	10737.12
Count	121	Count	121	Count	121
Confidence Level(0	10.12998	Confidence Level(0	0.030825	Confidence Level(0	46.84943

BIN	FREQUE	BIN	FREQUE	BIN	FREQUENCY
10	36	0.05	0	10	27
20	18	0.1	0	20	7
30	22	0.15	0	30	10
40	8	0.2	2	40	24
50	10	0.25	1	50	10
60	6	0.3	2	60	6
70	6	0.35	8	70	6
80	6	0.4	4	80	7
90	1	0.45	3	90	4
100	1	0.5	7	100	1
110	1	0.55	10	110	4
120	0	0.6	16	120	3
130	1	0.65	12	130	1
140	0	0.7	17	140	3
150	2	0.75	15	150	1
160	0	0.8	9	160	0
170	0	0.85	3	170	0
180	0	0.9	8	180	0
190	0	0.95	2	190	0
200	0	1	2	200	0
	3		0		7

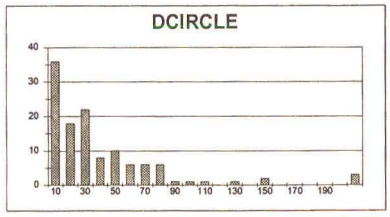

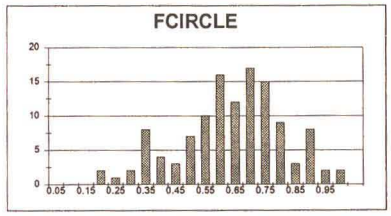

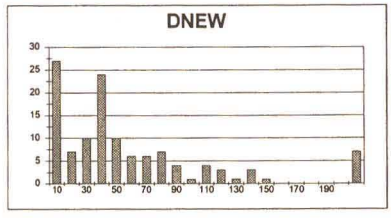


```
{SelectBlock C1}
{PutCell2 "DNEW"}
{SelectBlock C2}
{PutCell2 "=A2..A122/B2..B122"}
{SelectBlock A2..B122}
{EditCopy}
{SelectBlock E2}
{EditPaste}
{SelectBlock C2}
{BlockValues C2;G2}
{SelectBlock C3..C212}
{EditCopy}
{SelectBlock G3}
{EditPaste}
{SelectBlock E2..E122}
{Sort.Block "E2..E122"}
{Sort.Type Top to bottom}
{Sort.Heading 0}
{Sort.Key_1 "E2"}
{Sort.Key_2 ""}
{Sort.Key_3 ""}
{Sort.Key_4 ""}
{Sort.Key_5 ""}
{Sort.BlankCellsFirst 0}
{Sort.Data Numbers First}
{Sort.PreviousSorts -1}
{Sort.Go}
{SelectBlock F2..F122}
{Sort.Block "F2..F122"}
{Sort.Type Top to bottom}
{Sort.Heading 0}
{Sort.Key_1 "F2"}
{Sort.Key_2 ""}
{Sort.Key_3 ""}
{Sort.Key_4 ""}
{Sort.Key_5 ""}
{Sort.BlankCellsFirst 0}
{Sort.Data Numbers First}
{Sort.PreviousSorts -1}
{Sort.Go}
{SelectBlock G2..G122}
{Sort.Block "G2..G122"}
{Sort.Type Top to bottom}
{Sort.Heading 0}
{Sort.Key_1 "G2"}
{Sort.Key_2 ""}
{Sort.Key_3 ""}
{Sort.Key_4 ""}
{Sort.Key_5 ""}
{Sort.BlankCellsFirst 0}
{Sort.Data Numbers First}
{Sort.PreviousSorts -1}
{Sort.Go}
{SelProperty Numeric_Format,"Fixed;2;South Africa"}
{SelectBlock A1..C1}
{EditCopy}
{SelectBlock E1}
{EditPaste}
{SelectBlock I1}
{DESCR "E1..E122";I1;C;"1";"1";"0";"0";"95%"}
{SelectBlock K1}
{DESCR "F1..F122";K1;C;"1";"1";"0";"0";"95%"}
{SelectBlock M1}
{DESCR "G1..G122";M1;C;"1";"1";"0";"0";"95%"}
{SelectBlock I19}
{PutCell2 "BIN"}
{SelectBlock J19}
{PutCell2 "FREQUENCY"}
{SelectBlock I19..J19}
{EditCopy}
{SelectBlock (K19..L19;M19..N19);M19}
{EditPaste}
{SelectBlock I20}
{PutCell2 "10"}
{SelectBlock I21}
{PutCell2 "20"}
{SelectBlock I20..I39}
{SpeedFill}
{EditCopy}
{SelectBlock M20}
{EditPaste}
{SelectBlock K20}
{PutCell2 "0.05"}
{SelectBlock K21}
{PutCell2 "0.1"}
{SelectBlock K20..K39}
{SpeedFill}
{SelectBlock J20}
{PutCell2 "@FREQDIST(E2..E122,I20..I39)"}
{SelectBlock L20}
{PutCell2 "@FREQDIST(F2..F122,K20..K39)"}
{SelectBlock N20}
{PutCell2 "@FREQDIST(G2..G122,M20..M39)"}
```

Sample 6a.

DCIRCLE	FCIRCLE	DNEW
13.03	0.5	26.06
9.29	0.68	13.66176
23.59	0.67	35.20896
17.6	0.77	22.85714
30.62	0.88	34.79545
23.91	0.78	30.65385
27.71	0.87	31.85057
15.81	0.47	33.6383
20.05	0.81	24.75309
28.97	0.8	36.2125
23.08	0.68	33.94118
29.63	0.82	36.13415
16.37	0.41	39.92683
39.68	0.68	58.35294
19.14	0.75	25.52
25.59	0.41	62.41463
25.36	0.91	27.86813
18.26	0.81	22.54321
83.96	0.48	174.9167
28.82	0.92	31.32609
37.52	0.78	48.10256
34.64	0.93	37.24731
36.56	0.71	51.49296
61.1	0.53	115.283
26.05	0.67	38.8806
47.25	0.81	58.33333
51.24	0.87	58.89655
46.26	0.59	78.40678
21.2	0.55	38.54545
84.68	0.48	176.4167
39.87	0.55	72.49091
18.1	0.82	22.07317
50.42	0.58	86.93103
6.22	0.43	14.46512
27.17	0.43	63.18605
38.85	0.69	56.30435
4.56	0.52	8.769231
21.76	0.81	26.8642
24.15	0.79	30.56962
26.11	0.79	33.05063
21.62	0.82	26.36585
37.72	0.72	52.38889
27.77	0.89	31.20225
18.9	0.65	29.07692
21.55	0.85	25.35294
63.37	0.77	82.2987
35.74	0.73	48.9589
17.68	0.78	22.66667
37.17	0.78	47.65385
15.04	0.6	25.06667
41.34	0.76	54.39474
18.01	0.76	23.69737
13.8	0.73	18.90411
23.91	0.59	40.52542
44.76	0.78	58.69474
36.78	0.75	49.01333
97.34	0.36	270.3889
56.07	0.68	82.45588
27.23	0.65	41.89231
71.45	0.69	103.5507
25.99	0.86	30.22093
38.39	0.7	54.84286
27.93	0.52	53.71154
20.99	0.67	31.32836
14.84	0.66	22.48485
44.39	0.85	52.22353
36.64	0.8	45.8
71.62	0.61	117.4098
3.86	0.75	5.146667
38.89	0.73	53.27397
19.97	0.62	32.20968
27.12	0.87	31.17241
28.09	0.83	33.84337
35.36	0.76	46.52632
21.2	0.77	27.53247
37.13	0.81	45.83951
62.8	0.72	87.22222
24.52	0.84	29.19048
33.32	0.81	41.1358
39.12	0.86	44.45455
71.66	0.49	146.2449
53.43	0.57	93.73684
64.05	0.54	118.6111
7.32	0.76	9.631579
122.44	0.27	453.4815
3.45	0.6	5.75
28.25	0.79	35.75949
20.78	0.77	26.98701
23.84	0.74	32.21622
4.23	0.68	6.220588
25.76	0.83	31.03614
16.09	0.64	25.14063
4.88	0.52	9.384615
25.99	0.91	28.56044
75.66	0.47	160.9787
29.53	0.9	33.14444
23.84	0.87	27.4023
22.43	0.42	53.40476
24.46	0.9	27.17778
14.54	0.62	23.45161
18.18	0.91	19.97802
5.98	0.64	9.34375
31.25	0.9	34.72222
18.9	0.78	24.23077
19.82	0.74	26.78378
38.58	0.59	65.38983
23.08	0.83	27.80723
18.74	0.83	22.57831
23.34	0.88	26.52273
44.49	0.83	53.60241
88.53	0.47	189
96.04	0.38	226.4211
33.99	0.79	43.02532
34.98	0.82	42.65854
42.47	0.74	57.39189
32.83	0.86	38.17442
36.8	0.8	46
20.63	0.82	25.15854
23.97	0.77	31.12987
21.48	0.84	25.57143
124.73	0.49	254.551
38.43	0.82	46.86585
33.37	0.93	35.88172
52.33	0.72	72.68056
47.75	0.67	71.26866
40.06	0.8	50.075
23.53	0.65	27.68235
27.12	0.95	28.54737
45.75	0.69	66.30435
19.97	0.93	21.47312
51.15	0.62	82.5
53.18	0.78	68.17949
21.48	0.92	23.34783
24.52	0.74	33.13514
49.16	0.86	57.16279
25.88	0.72	35.94444
46.93	0.76	61.75
3.86	0.6	6.433333
31.53	0.76	41.48684
68.45	0.47	145.6383
45.42	0.77	58.98701
25.76	0.94	27.40426
52.67	0.79	66.67089
54.18	0.56	96.75
35.06	0.85	41.24706
5.46	0.47	11.61702
20.99	0.83	25.28916
31.72	0.87	36.45977
27.93	0.91	30.69231
25.76	0.8	32.2
45.78	0.72	63.58333
99.58	0.4	248.95
43.85	0.82	53.47561
47.66	0.68	70.08824
28.09	0.81	34.67901
26.62	0.73	36.46575
25.36	0.91	27.86813
18.1	0.83	21.80723
34.33	0.84	40.86905

DCIRCLE	FCIRCLE	DNEW
3.45	0.24	3.86
3.86	0.27	5.15
3.86	0.27	5.75
3.86	0.29	6.22
4.23	0.33	6.43
4.23	0.36	8.00
4.56	0.36	8.29
4.56	0.38	8.77
4.56	0.39	9.34
4.88	0.39	9.38
5.46	0.4	9.63
5.98	0.4	10.13
5.98	0.4	11.62
6.22	0.4	13.66
6.68	0.41	14.47
7.32	0.41	16.70
9.29	0.42	17.52
13.03	0.43	17.99
13.8	0.43	18.90
14.54	0.45	19.98
14.54	0.45	20.24
14.84	0.47	20.33
15.04	0.47	21.14
15.43	0.47	21.30
15.62	0.47	21.47
15.81	0.47	21.81
16.09	0.48	22.07
16.19	0.48	22.10
16.37	0.48	22.15
17.08	0.49	22.48
17.6	0.49	22.48
17.68	0.49	22.54
17.68	0.49	22.58
17.68	0.5	22.64
17.76	0.5	22.67
18.01	0.51	22.86
18.1	0.51	23.06
18.1	0.52	23.35
18.18	0.52	23.42
18.26	0.52	23.45
18.42	0.52	23.70
18.42	0.52	23.90
18.66	0.52	24.23
18.74	0.53	24.75
18.9	0.53	24.78
18.9	0.53	25.07
18.98	0.54	25.12
19.14	0.55	25.14
19.37	0.55	25.16
19.6	0.55	25.29
19.67	0.55	25.35
19.82	0.56	25.52
19.97	0.56	25.54
19.97	0.56	25.57
20.05	0.56	26.06
20.63	0.57	26.12
20.7	0.57	26.37
20.78	0.57	26.40
20.99	0.57	26.52
20.99	0.58	26.69
21.06	0.59	26.70
21.2	0.59	26.78
21.2	0.59	26.86
21.2	0.6	26.95
21.41	0.6	26.99
21.48	0.6	26.99
21.48	0.6	27.04
21.55	0.61	27.18
21.62	0.61	27.20
21.76	0.61	27.35
21.76	0.61	27.40
21.76	0.62	27.40
22.1	0.62	27.53
22.3	0.62	27.68
22.36	0.63	27.81
22.43	0.63	27.87
22.43	0.64	27.87
22.69	0.64	27.96
23.08	0.65	28.24
23.08	0.65	28.55
23.34	0.65	28.56
23.53	0.65	28.56
23.59	0.65	28.57
23.59	0.66	28.75
23.72	0.66	28.77
23.84	0.67	29.06
23.84	0.67	29.19
23.91	0.67	29.65
23.91	0.67	29.81
23.97	0.67	29.83
24.03	0.67	30.07
24.03	0.68	30.22
24.15	0.68	30.25
24.15	0.68	30.44
24.46	0.68	30.57
24.46	0.68	30.59
24.52	0.68	30.65
24.52	0.68	30.69
24.76	0.68	30.72
24.82	0.69	31.04
24.82	0.69	31.09
24.88	0.69	31.13
25.06	0.69	31.17
25.18	0.69	31.20
25.3	0.7	31.33
25.36	0.7	31.33
25.36	0.7	31.38
25.42	0.7	31.66
25.59	0.71	31.74
25.65	0.71	31.85
25.71	0.71	32.10
25.76	0.72	32.13
25.76	0.72	32.20
25.76	0.72	32.21
25.88	0.72	32.22
25.88	0.72	32.59
25.99	0.72	32.77
25.99	0.72	33.05
25.99	0.72	33.06
26.05	0.72	33.14
26.11	0.72	33.14
26.11	0.73	33.27
26.28	0.73	33.31
26.46	0.73	33.53
26.45	0.73	33.64
26.62	0.73	33.84
27.06	0.73	33.90
27.12	0.73	33.91
27.12	0.73	33.94
27.17	0.73	34.40
27.23	0.73	34.52
27.23	0.74	34.68
27.44	0.74	34.72
27.61	0.74	34.75
27.61	0.74	34.80
27.71	0.74	34.90
27.71	0.74	35.21
27.77	0.75	35.22
27.77	0.75	35.76
27.87	0.75	35.88
27.93	0.75	35.94
27.93	0.76	35.99
28.09	0.76	36.08
28.09	0.76	36.13
28.14	0.76	36.21
28.25	0.76	36.21
28.51	0.76	36.46
28.82	0.76	36.47
28.92	0.76	36.79
28.92	0.77	37.03
28.97	0.77	37.04
28.97	0.77	37.25
29.28	0.77	37.37
29.33	0.77	38.12
29.63	0.77	38.17
29.83	0.77	38.37
29.93	0.77	38.55
30.03	0.77	38.78
30.08	0.78	38.88

DCIRCLE/micron		*FCIRCLE*		*DNEW*	
Mean	36.05399	Mean	0.734579	Mean	56.1172
Standard Error	1.157451	Standard Error	0.008673	Standard Error	3.223468
Median	30.23	Median	0.78	Median	39
Mode	3.86	Mode	0.82	Mode	27.86813
Standard Deviation	20.73745	Standard Deviation	0.155392	Standard Deviation	57.75317
Variance	430.0417	Variance	0.024147	Variance	3335.428
Kurtosis	3.570305	Kurtosis	0.171517	Kurtosis	28.14602
Skewness	1.544583	Skewness	-0.91129	Skewness	4.512785
Range	129.14	Range	0.76	Range	548.5983
Minimum	3.45	Minimum	0.24	Minimum	3.86
Maximum	132.59	Maximum	1	Maximum	552.4583
Sum	11576.54	Sum	235.8	Sum	18013.62
Count	321	Count	321	Count	321
Confidence Level(0.9	2.268583	Confidence Level(0.9	0.016999	Confidence Level(0.9	6.31788

BIN	FREQUE	BIN	FREQUE	BIN	FREQUENCY
10	17	0.05	0	10	11
20	37	0.1	0	20	9
30	103	0.15	0	30	70
40	67	0.2	0	40	75
50	37	0.25	1	50	39
60	23	0.3	3	60	35
70	12	0.35	1	70	20
80	10	0.4	9	80	14
90	8	0.45	7	90	12
100	3	0.5	14	100	3
110	0	0.55	16	110	4
120	1	0.6	16	120	5
130	2	0.65	16	130	3
140	1	0.7	25	140	1
150	0	0.75	33	150	3
160	0	0.8	42	160	3
170	0	0.85	65	170	1
180	0	0.9	46	180	2
190	0	0.95	23	190	3
200	0	1	4	200	0
	0		0		8

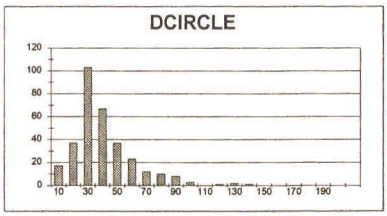

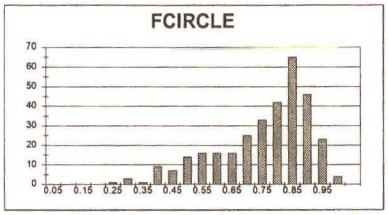

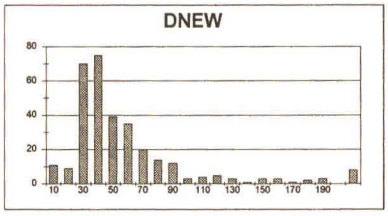


```
{SelectBlock C1)
{PutCell2 "DNEW")
{SelectBlock C2)
{PutCell2 "=A2..A322/B2..B322")
{SelectBlock A2..B322)
{EditCopy)
{SelectBlock E2)
{EditPaste)
{SelectBlock C2)
{BlockValues C2;G2)
{SelectBlock C3..C322)
{EditCopy)
{SelectBlock G3)
{EditPaste)
{SelectBlock E2..E322)
{Sort.Block "E2..E322")
{Sort.Type Top to bottom)
{Sort.Heading 0)
{Sort.Key_1 "E2")
{Sort.Key_2 "")
{Sort.Key_3 "")
{Sort.Key_4 "")
{Sort.Key_5 "")
{Sort.BlankCellsFirst 0)
{Sort.Data Numbers First)
{Sort.PreviousSorts -1)
{Sort.Go)
{SelectBlock F2..F322)
{Sort.Block "F2..F322")
{Sort.Type Top to bottom)
{Sort.Heading 0)
{Sort.Key_1 "F2")
{Sort.Key_2 "")
{Sort.Key_3 "")
{Sort.Key_4 "")
{Sort.Key_5 "")
{Sort.BlankCellsFirst 0)
{Sort.Data Numbers First)
{Sort.PreviousSorts -1)
{Sort.Go)
{SelectBlock G2..G322)
{Sort.Block "G2..G322")
{Sort.Type Top to bottom)
{Sort.Heading 0)
{Sort.Key_1 "G2")
{Sort.Key_2 "")
{Sort.Key_3 "")
{Sort.Key_4 "")
{Sort.Key_5 "")
{Sort.BlankCellsFirst 0)
{Sort.Data Numbers First)
{Sort.PreviousSorts -1)
{Sort.Go)
{Selproperty Numeric_Format,"Fixed;2;South Africa")
{SelectBlock A1..C1)
{EditCopy)
{SelectBlock E1)
{EditPaste)
{SelectBlock I1)
{DESCR "E1..E322";I1;C;"1";"1";"0";"0";"95%")
{SelectBlock K1)
{DESCR "F1..F322";K1;C;"1";"1";"0";"0";"95%")
{SelectBlock M1)
{DESCR "G1..G322";M1;C;"1";"1";"0";"0";"95%")
{SelectBlock I19)
{PutCell2 "BIN")
{SelectBlock J19)
{PutCell2 "FREQUENCY")
{SelectBlock I19..J19)
{EditCopy)
{SelectBlock {K19..L19;M19..N19);M19)
{EditPaste)
{SelectBlock I20)
{PutCell2 "10")
{SelectBlock I21)
{PutCell2 "20")
{SelectBlock I20..I39)
{SpeedFill)
{EditCopy)
{SelectBlock M20)
{EditPaste)
{SelectBlock K20)
{PutCell2 "0.05")
{SelectBlock K21)
{PutCell2 "0.1")
{SelectBlock K20..K39)
{SpeedFill)
{SelectBlock J20)
{PutCell2 "@FREQDIST(E2..E322,I20..I39)")
{SelectBlock L20)
{PutCell2 "@FREQDIST(F2..F322,K20..K39)")
{SelectBlock N20)
{PutCell2 "@FREQDIST(G2..G322,M20..M39)")
{SelectBlock J20..J40)
```

Sample 6b.

DCIRCLE	FCIRCLE	DNEW
3.86	0.49	7.877551
21.34	0.76	28.07895
18.82	0.77	24.44156
4.86	0.46	10.6087
16	0.47	34.04255
5.18	0.46	11.26087
11.7	0.36	32.5
26.22	0.9	29.13333
23.78	0.83	28.6506
25.12	0.94	26.7234
30.86	0.85	36.30588
23.91	0.92	25.98913
52.5	0.6	87.5
28.97	0.82	35.32927
22.69	0.82	27.67073
17.17	0.4	42.925
34.51	0.93	37.10753
33.41	0.92	36.31522
27.28	0.7	38.97143
17.08	0.71	24.05634
61.05	0.54	113.0556
62.71	0.61	102.8033
69.62	0.45	154.7111
30.72	0.93	33.03226
44.12	0.75	58.82667
27.28	0.85	32.09412
45.71	0.62	73.72581
39.42	0.82	48.07317
3.86	0.6	6.433333
53.68	0.72	74.55556
24.09	0.93	25.90323
70.72	0.47	150.4681
29.28	0.89	32.89888
67.24	0.51	131.8431
34.42	0.88	39.11364
19.82	0.78	25.41026
43.34	0.78	55.5641
20.7	0.84	24.64286
31.1	0.86	36.16279
57.33	0.54	106.1667
53.71	0.69	77.84058
32.96	0.81	40.69136
25.36	0.91	27.86813
36.72	0.79	46.48101
37.04	0.8	46.3
27.01	0.85	31.77647
28.97	0.99	29.26263
33.41	0.87	38.4023
27.98	0.85	32.91765
31.67	0.96	47.98485
13.59	0.73	18.61644
38.81	0.85	45.65882
16.62	0.86	19.55814
31.83	0.86	36.77907
15.24	0.73	20.87671
5.98	0.74	8.081081
55.67	0.51	109.1569
4.56	0.72	6.333333
32.37	0.86	37.63953
35.86	0.77	46.57143
23.84	0.8	29.8
25.12	0.94	26.7234
37	0.89	41.57303
24.88	0.93	26.75269
33.81	0.73	46.31507
38.68	0.75	48.90667
36.8	0.72	51.11111
22.23	0.82	27.10976
29.02	0.87	33.35632
41.59	0.75	55.45333
33.19	0.88	37.71591
34.16	0.86	39.72093
30.18	0.86	35.09302
31.25	0.87	35.91954
21.27	0.79	26.92405
16.55	0.86	19.24419
28.35	0.72	39.375
37.84	0.75	50.45333
34.55	0.86	40.17442
26.22	0.88	29.79545
40.94	0.83	49.3253
28.14	0.81	34.74074
93.38	0.38	245.7368
29.96	0.82	36.56098
24.52	0.79	31.03797
25.65	0.95	27
39	0.9	43.33333
19.82	0.74	26.78378
48.22	0.65	74.18462
22.76	0.92	24.73913
24.94	0.82	30.41463
17.68	0.8	22.1
29.13	0.88	33.10227
21.34	0.91	23.45055
23.59	0.72	32.76389
37.6	0.86	43.72093
24.88	0.89	27.95506
54.7	0.69	79.27536
29.78	0.85	35.03529
26.22	0.87	30.13793
15.14	0.84	18.02381
35.78	0.75	47.70667
27.5	0.56	49.10714
28.72	0.82	35.02439
3.45	0.44	7.840909
16.73	0.88	19.01136
6.46	0.7	9.228571
44.12	0.87	50.71264
25.18	0.89	28.29213
40.39	0.81	49.8642
38.04	0.84	45.28571
24.88	0.9	27.64444
45.16	0.73	61.86301
24.76	0.88	28.13636
28.61	0.85	33.65882
21.34	0.8	26.675
39.8	0.88	45.22727
36.31	0.82	44.28049
23.34	0.9	25.93333
39.46	0.81	48.71605
42.37	0.81	52.30864
28.35	0.82	34.57317
110.87	0.27	411
27.71	0.82	33.79268
38.84	0.85	43.34118
32.19	0.68	47.33824
28.56	0.9	31.73333
3.86	1	3.86
21.34	0.66	32.33333
23.28	0.9	25.86667
28.19	0.9	31.32222
53.26	0.84	63.40476
22.16	0.81	27.35802
34.72	0.87	39.90805
51.62	0.5	103.24
38.85	0.68	57.13235
141.01	0.38	371.0789
44.16	0.82	53.85366
54.78	0.57	96.10526
28.97	0.61	47.4918
22.43	0.83	27.0241
37.6	0.75	50.13333
38.43	0.89	43.17978
56.15	0.56	100.2679
28.3	0.87	32.52874
32.92	0.78	42.20513
30.38	0.84	36.16667
33.94	0.84	40.40476
22.16	0.74	29.94595
105.66	0.34	310.7647
83.67	0.37	226.1351
33.68	0.88	38.27273
24.64	0.89	27.68539
25.53	0.91	28.05495
56.94	0.83	68.60241
39.04	0.89	43.86517
36.03	0.87	41.41379
41.44	0.89	46.5618
46.23	0.75	61.64
3.45	0.23	3.86
3.45	0.24	4.21
3.45	0.26	4.79
3.86	0.27	6.33
3.86	0.29	6.43
3.86	0.33	7.51
4.56	0.34	7.84
4.88	0.34	7.88
4.88	0.36	8.08
5.18	0.36	9.23
5.46	0.37	10.61
5.98	0.38	11.26
6.46	0.38	11.62
10.06	0.38	14.08
11.7	0.4	14.79
11.83	0.44	17.68
13.59	0.45	18.02
15.14	0.46	18.62
15.24	0.46	19.01
15.91	0.47	19.24
16	0.47	19.27
16.55	0.47	19.56
16.73	0.48	19.78
16.82	0.49	20.06
17.08	0.5	20.38
17.17	0.5	20.83
17.34	0.5	20.88
17.34	0.51	22.10
17.6	0.51	22.82
17.68	0.53	23.11
17.76	0.53	23.19
17.85	0.54	23.45
17.93	0.54	23.52
18.26	0.54	24.06
18.34	0.55	24.11
18.58	0.55	24.32
18.66	0.56	24.44
18.82	0.56	24.64
19.21	0.57	24.74
19.37	0.57	24.93
19.67	0.57	25.06
19.82	0.58	25.14
19.82	0.58	25.15
19.97	0.6	25.20
20.05	0.6	25.41
20.12	0.6	25.43
20.27	0.61	25.51
20.34	0.61	25.55
20.41	0.61	25.79
20.41	0.61	25.87
20.41	0.62	25.88
20.49	0.62	25.90
20.63	0.62	25.93
20.7	0.64	25.93
21.2	0.64	25.99
21.27	0.64	26.00
21.34	0.65	26.08
21.34	0.65	26.38
21.34	0.65	26.54
21.34	0.65	26.68
21.41	0.65	26.69
21.48	0.66	26.70
21.62	0.66	26.72
21.76	0.66	26.72
22.43	0.66	26.75
22.16	0.66	26.78
22.16	0.66	26.92
22.16	0.66	26.94
22.16	0.68	27.00
22.23	0.68	27.02
22.36	0.68	27.05
22.43	0.68	27.07
22.43	0.68	27.08
22.69	0.69	27.09
22.69	0.69	27.10
22.69	0.69	27.11
22.69	0.69	27.34
22.76	0.69	27.36
22.82	0.69	27.64
22.89	0.7	27.67
22.95	0.7	27.69
23.15	0.7	27.77
23.28	0.7	27.79
23.34	0.7	27.87
23.4	0.7	27.96
23.53	0.71	27.99
23.53	0.71	28.05
23.59	0.71	28.08
23.66	0.71	28.14
23.78	0.72	28.16
23.78	0.72	28.29
23.78	0.72	28.31
23.84	0.72	28.46
23.84	0.72	28.65
23.91	0.72	28.65
23.91	0.72	28.75
24.03	0.72	29.05
24.09	0.72	29.13
24.09	0.73	29.26
24.4	0.73	29.30
24.52	0.73	29.34
24.52	0.73	29.35
24.64	0.73	29.76
24.64	0.73	29.80
24.76	0.73	29.80
24.88	0.73	29.95
24.88	0.73	30.06
24.88	0.74	30.08
24.88	0.74	30.10
24.94	0.74	30.14
24.94	0.74	30.41
25	0.74	30.52
25.06	0.74	30.86
25.12	0.74	30.87
25.12	0.75	31.04
25.18	0.75	31.21
25.24	0.75	31.23
25.3	0.75	31.32
25.3	0.75	31.73
25.36	0.75	31.74
25.53	0.75	31.78
25.59	0.75	32.04
25.65	0.76	32.09
25.82	0.76	32.10
25.94	0.76	32.23
26.17	0.77	32.33
26.22	0.77	32.41
26.22	0.77	32.50
26.22	0.77	32.53
26.26	0.77	32.59
26.45	0.77	32.76
26.56	0.77	32.90
27.01	0.77	32.92
27.28	0.77	33.03
27.28	0.77	33.10
27.5	0.78	33.36
27.55	0.78	33.49
27.55	0.78	33.66
27.71	0.78	33.79
27.98	0.78	34.04
28.03	0.78	34.16
28.09	0.78	34.29
28.14	0.79	34.53
28.19	0.79	34.55
28.25	0.79	34.57
28.3	0.79	34.57
28.35	0.79	34.74
28.35	0.79	35.02
28.35	0.79	35.04
28.4	0.79	35.09
28.56	0.79	35.13
28.61	0.8	35.33
28.72	0.8	35.45
28.97	0.8	35.47
28.97	0.8	35.52
28.97	0.8	35.62
29.02	0.8	35.64
29.13	0.8	35.66
29.28	0.8	35.89

DCIRCLE/micron		FCIRCLE		DNEW	
Mean	35.08523	Mean	0.766437	Mean	54.54843
Standard Error	1.086743	Standard Error	0.007862	Standard Error	3.858437
Median	30.885	Median	0.82	Median	37.04767
Mode	21.34	Mode	0.82	Mode	26.7234
Standard Deviation	20.27292	Standard Deviation	0.146657	Standard Deviation	68.24725
Variance	410.9914	Variance	0.021508	Variance	4657.687
Kurtosis	8.583171	Kurtosis	1.921514	Kurtosis	29.8092
Skewness	2.372594	Skewness	-1.45404	Skewness	5.069112
Range	144.41	Range	0.77	Range	580.5313
Minimum	3.45	Minimum	0.23	Minimum	3.86
Maximum	147.86	Maximum	1	Maximum	584.3913
Sum	12209.66	Sum	266.72	Sum	18982.85
Count	348	Count	348	Count	348
Confidence Level(0	2.129977	Confidence Level(0	0.015409	Confidence Level(0	7.170404

BIN	FREQUE	BIN	FREQUE	BIN	FREQUENCY
10	13	0.05	0	10	10
20	31	0.1	0	20	13
30	122	0.15	0	30	83
40	92	0.2	0	40	95
50	38	0.25	2	50	51
60	24	0.3	3	60	29
70	13	0.35	3	70	16
80	2	0.4	7	80	12
90	3	0.45	2	90	4
100	2	0.5	10	100	5
110	2	0.55	9	110	9
120	2	0.6	10	120	4
130	0	0.65	15	130	1
140	2	0.7	24	140	1
150	2	0.75	37	150	1
160	0	0.8	37	160	2
170	0	0.85	81	170	0
180	0	0.9	78	180	0
190	0	0.95	26	190	0
200	0	1	4	200	0
	0		0		12

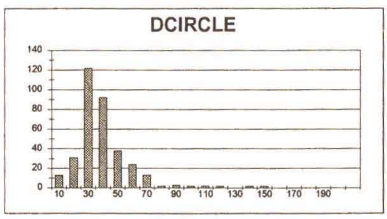

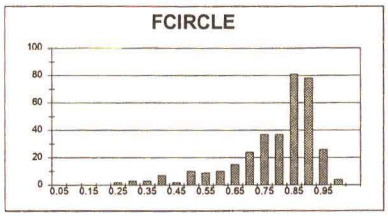

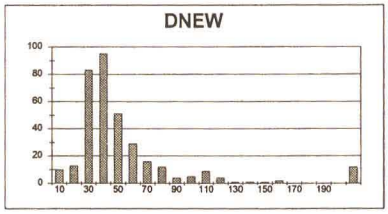


```
{SelectBlock C1}
{PutCell2 "DNEW"}
{SelectBlock C2}
{PutCell2 "=A2..A349/B2..B349"}
{SelectBlock A2..B349}
{EditCopy}
{SelectBlock E2}
{EditPaste}
{SelectBlock C2}
{BlockValues C2;G2}
{SelectBlock C3..C349}
{EditCopy}
{SelectBlock G3}
{EditPaste}
{SelectBlock E2..E349}
{Sort Block "E2..E349"}
{Sort Type Top to bottom}
{Sort Heading 0}
{Sort Key_1 "E2"}
{Sort Key_2 ""}
{Sort Key_3 ""}
{Sort Key_4 ""}
{Sort Key_5 ""}
{Sort BlankCellsFirst 0}
{Sort Data Numbers First}
{Sort PreviousSorts -1}
{Sort Go}
{SelectBlock F2..F349}
{Sort Block "F2..F349"}
{Sort Type Top to bottom}
{Sort Heading 0}
{Sort Key_1 "F2"}
{Sort Key_2 ""}
{Sort Key_3 ""}
{Sort Key_4 ""}
{Sort Key_5 ""}
{Sort BlankCellsFirst 0}
{Sort Data Numbers First}
{Sort PreviousSorts -1}
{Sort Go}
{SelectBlock G2..G349}
{Sort Block "G2..G349"}
{Sort Type Top to bottom}
{Sort Heading 0}
{Sort Key_1 "G2"}
{Sort Key_2 ""}
{Sort Key_3 ""}
{Sort Key_4 ""}
{Sort Key_5 ""}
{Sort BlankCellsFirst 0}
{Sort Data Numbers First}
{Sort PreviousSorts -1}
{Sort Go}
{Setproperty Numeric_Formal;"Fixed;2;South Africa"}
{SelectBlock A1..C1}
{EditCopy}
{SelectBlock E1}
{EditPaste}
{SelectBlock I1}
{DESCR "E1..E349";I1;C;"1";"1";"0";"0";"95%"}
{SelectBlock K1}
{DESCR "F1..F349";K1;C;"1";"1";"0";"0";"95%"}
{SelectBlock M1}
{DESCR "G1..G349";M1;C;"1";"1";"0";"0";"95%"}
{SelectBlock I19}
{PutCell2 "BIN"}
{SelectBlock J19}
{PutCell2 "FREQUENCY"}
{SelectBlock I19..J19}
{EditCopy}
{SelectBlock (K19..L19;M19..N19);M19}
{EditPaste}
{SelectBlock I20}
{PutCell2 "10"}
{SelectBlock I21}
{PutCell2 "20"}
{SelectBlock I20..I39}
{SpeedFill}
{EditCopy}
{SelectBlock M20}
{EditPaste}
{SelectBlock K20}
{PutCell2 "0.05"}
{SelectBlock K21}
{PutCell2 "0.1"}
{SelectBlock K20..K39}
{SpeedFill}
{SelectBlock J20}
{PutCell2 "@FREQDIST(E2..E349,I20..I39)"}
{SelectBlock L20}
{PutCell2 "@FREQDIST(F2..F349,K20..K39)"}
{SelectBlock N20}
{PutCell2 "@FREQDIST(G2..G349,M20..M39)"}
```

Sample 7a.

DCIRCLE	FCIRCLE	DNEW
24.46	0.72	33.97222
51.56	0.79	65.26582
24.03	0.68	35.33824
49.01	0.8	61.2625
22.63	0.92	24.59783
65.27	0.69	94.5942
41.44	0.84	49.33333
48.19	0.71	67.87324
33.14	0.81	40.91358
27.5	0.86	31.97674
67.97	0.84	80.91667
96.6	0.73	132.3288
38.93	0.77	50.55644
29.53	0.86	34.33721
135.02	0.36	375.0556
46.55	0.6	77.58333
54.59	0.69	79.11594
58.97	0.91	64.8022
178	0.29	613.7931
29.88	0.89	33.57303
58.13	0.7	83.04286
57.48	0.76	75.63158
48.25	0.81	59.5679
21.76	0.8	27.2
38.39	0.8	47.9875
26.05	0.85	30.64706
94.97	0.77	123.3377
46.71	0.74	63.12162
79.14	0.73	108.411
29.02	0.8	36.275
68.78	0.86	79.97674
80.63	0.54	149.3148
107.53	0.53	202.8868
54.23	0.9	60.25556
52.28	0.8	65.35
74.39	0.74	100.527
126.35	0.61	207.1311
28.77	0.89	32.32584
100.14	0.55	182.0727
65.36	0.83	78.74699
155.72	0.28	556.1429
85.61	0.55	155.6545
67.22	0.67	100.3284
89.57	0.86	104.1512
20.05	0.89	22.52809
96.11	0.68	141.3382
130.23	0.43	302.8605
106.92	0.84	129.6667
31.95	0.88	36.30682
32.42	0.82	39.53659
20.56	0.91	22.59341
51.01	0.86	59.31395
62.69	0.74	84.71622
32.42	0.82	39.53659
68.18	0.68	129.6765
29.33	0.8	36.6625
68.18	0.79	111.6203
25.18	0.91	27.67033
37.04	0.81	45.7284
127.04	0.34	373.6471
34.07	0.87	39.16092
63.79	0.76	83.93421
162.99	0.4	407.475
58.94	0.82	73.09756
40.72	0.79	51.5443
92.48	0.9	102.7556
52.9	0.85	62.23529
45.06	0.95	47.43158
33.41	0.77	43.38961
81.29	0.68	119.5441
57.56	0.86	65.40909
83.44	0.6	139.0667
117.78	0.61	193.082
60.63	0.63	96.2381
32.74	0.79	41.44304
36.27	0.58	62.53448
113.3	0.53	213.7736
18.98	0.79	24.02532
33.68	0.8	42.1
76.68	0.81	94.66667
66.6	0.66	100.9091
68.25	0.7	97.5
26.51	0.8	33.1375
60.14	0.86	69.93023
53.51	0.84	63.70238
77.89	0.57	136.6491
47.78	0.8	59.725
39.94	0.91	43.89011
52.22	0.84	62.16667
60.98	0.93	65.56989
98.93	0.78	130.1711
74.13	0.84	88.25
107.71	0.75	143.6133
45.62	0.81	60.02469
29.08	0.77	37.76623
94.41	0.53	178.1321
40.5	0.77	52.5974
106.65	0.77	138.5065
33.41	0.84	39.77381
107.67	0.68	158.3382
30.03	0.89	33.74157
27.23	0.69	39.46377
158.45	0.34	466.0294
94.44	0.57	165.6842
18.98	0.28	22.53
20.05	0.29	22.58
20.56	0.34	24.03
21.76	0.34	24.60
22.63	0.36	27.20
24.03	0.4	27.67
24.46	0.43	30.65
25.18	0.53	31.96
26.05	0.53	32.33
26.51	0.53	33.14
27.23	0.54	33.57
27.5	0.55	33.74
28.77	0.55	33.97
29.02	0.57	34.34
29.08	0.57	35.34
29.33	0.58	36.26
29.53	0.6	36.31,
29.88	0.6	36.66
30.03	0.61	37.77
31.95	0.61	39.16
32.42	0.63	39.46
32.42	0.66	39.54
32.74	0.67	39.54
33.14	0.68	39.77
33.41	0.68	40.91
33.41	0.68	41.44
33.68	0.68	42.10
34.07	0.68	43.39
36.27	0.69	43.89
37.04	0.69	45.73
38.39	0.69	47.43
38.93	0.7	47.99
39.94	0.7	49.33
40.5	0.71	50.56
40.72	0.72	51.54
41.44	0.73	52.60
45.06	0.73	59.31
46.55	0.74	59.57
46.71	0.74	59.73
47.78	0.74	60.02
48.19	0.75	60.26
48.25	0.76	61.26
48.62	0.76	62.17
49.01	0.76	62.24
51.01	0.77	62.53
51.56	0.77	63.12
52.22	0.77	63.70
52.28	0.77	64.80
52.9	0.77	65.27
53.51	0.77	65.35
54.23	0.79	65.41
54.59	0.79	65.57
57.48	0.79	67.87
57.56	0.79	69.93
58.13	0.79	73.10
58.97	0.8	75.63
59.94	0.8	77.58
60.14	0.8	78.75
60.63	0.8	79.12
60.98	0.8	79.98
62.69	0.8	80.92
63.79	0.8	83.04
65.27	0.8	83.93
65.36	0.8	84.72
66.6	0.81	88.25
67.22	0.81	94.59
67.97	0.81	94.67
68.25	0.81	96.24
68.78	0.81	97.50
74.13	0.82	100.33
74.39	0.82	100.53
76.68	0.82	100.91
77.89	0.83	102.76
79.14	0.84	104.15
80.63	0.84	108.41
81.29	0.84	111.62
83.44	0.84	119.54
85.61	0.84	123.34
88.18	0.84	129.67
88.18	0.84	129.68
89.57	0.85	130.17
92.48	0.85	132.33
94.41	0.86	136.65
94.44	0.86	138.51
94.97	0.86	139.07
96.11	0.86	141.34
96.6	0.86	143.71
98.93	0.86	149.31
100.14	0.87	155.65
106.65	0.88	158.34
107.53	0.88	165.68
107.67	0.89	178.13
107.71	0.89	182.07
108.92	0.89	193.08
113.3	0.89	202.89
117.78	0.9	207.13
126.35	0.9	213.77
127.04	0.91	302.86
130.23	0.91	373.65
135.02	0.91	375.06
155.72	0.91	407.48
158.45	0.92	466.03
162.99	0.93	556.14
178	0.95	613.79

DCIRCLE/micron		FCIRCLE		DNEW	
Mean	64.07548	Mean	0.740962	Mean	104.316
Standard Error	3.478009	Standard Error	0.014506	Standard Error	10.33855
Median	56.035	Median	0.79	Median	66.72157
Mode	32.42	Mode	0.8	Mode	39.53659
Standard Deviation	35.46587	Standard Deviation	0.147934	Standard Deviation	105.4329
Variance	1258.041	Variance	0.021885	Variance	11116.11
Kurtosis	0.728262	Kurtosis	1.440042	Kurtosis	9.250341
Skewness	1.041406	Skewness	-1.30347	Skewness	2.872409
Range	159.02	Range	0.67	Range	591.265
Minimum	18.98	Minimum	0.28	Minimum	22.52809
Maximum	178	Maximum	0.95	Maximum	613.7931
Sum	6663.85	Sum	77.06	Sum	10848.86
Count	104	Count	104	Count	104
Confidence Level(0.9	6.816772	Confidence Level(0.9	0.028431	Confidence Level(0.9	20.26319

BIN	FREQUE	BIN	FREQUE	BIN	FREQUENCY
10	0	0.05	0	10	0
20	1	0.1	0	20	0
30	17	0.15	0	30	8
40	15	0.2	0	40	18
50	11	0.25	0	50	9
60	13	0.3	2	60	6
70	12	0.35	2	70	15
80	5	0.4	2	80	6
90	7	0.45	1	90	5
100	7	0.5	0	100	4
110	6	0.55	6	110	6
120	2	0.6	5	120	2
130	2	0.65	3	130	3
140	2	0.7	12	140	5
150	0	0.75	8	150	3
160	2	0.8	23	160	2
170	1	0.85	18	170	1
180	1	0.9	15	180	1
190	0	0.95	7	190	1
200	0	1	0	200	1
	0		0		10

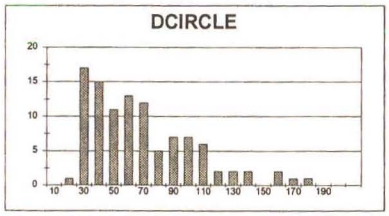

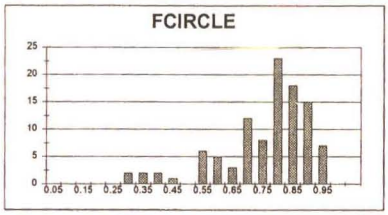

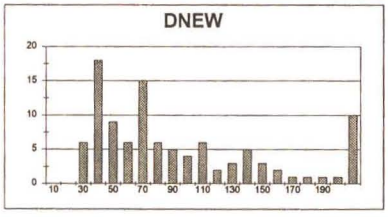


```
(SelectBlock C1)
(PutCell2 "DNEW")
(SelectBlock C2)
(PutCell2 "=A2..A105/B2..B105")
(SelectBlock A2..B105)
(EditCopy)
(SelectBlock E2)
(EditPaste)
(SelectBlock C2)
(BlockValues C2:G2)
(SelectBlock C3..C105)
(EditCopy)
(SelectBlock G3)
(EditPaste)
(SelectBlock E2..E105)
(Sort.Block "E2..E105")
(Sort.Type Top to bottom)
(Sort.Heading 0)
(Sort.Key_1 "E2")
(Sort.Key_2 "")
(Sort.Key_3 "")
(Sort.Key_4 "")
(Sort.Key_5 "")
(Sort.BlankCellsFirst 0)
(Sort.Data Numbers First)
(Sort.PreviousSorts -1)
(Sort.Go)
(SelectBlock F2..F105)
(Sort.Block "F2..F105")
(Sort.Type Top to bottom)
(Sort.Heading 0)
(Sort.Key_1 "F2")
(Sort.Key_2 "")
(Sort.Key_3 "")
(Sort.Key_4 "")
(Sort.Key_5 "")
(Sort.BlankCellsFirst 0)
(Sort.Data Numbers First)
(Sort.PreviousSorts -1)
(Sort.Go)
(SelectBlock G2..G105)
(Sort.Block "G2..G105")
(Sort.Type Top to bottom)
(Sort.Heading 0)
(Sort.Key_1 "G2")
(Sort.Key_2 "")
(Sort.Key_3 "")
(Sort.Key_4 "")
(Sort.Key_5 "")
(Sort.BlankCellsFirst 0)
(Sort.Data Numbers First)
(Sort.PreviousSorts -1)
(Sort.Go)
(SelectBlock A1..C1)
(SetProperty Numeric_Format,"Fixed,2,South Africa")
(SelectBlock A1..C1)
(EditCopy)
(SelectBlock E1)
(EditPaste)
(SelectBlock I1)
(DESCR "E1..E105";I1,C,"1","1","0","0","95%")
(SelectBlock K1)
(DESCR "F1..F105";K1,C,"1","1","0","0","95%")
(SelectBlock M1)
(DESCR "G1..G105";M1,C,"1","1","0","0","95%")
(SelectBlock I19)
(PutCell2 "BIN")
(SelectBlock J19)
(PutCell2 "FREQUENCY")
(SelectBlock I19..J19)
(EditCopy)
(SelectBlock (K19..L19;M19..N19),M19)
(EditPaste)
(SelectBlock I20)
(PutCell2 "10")
(SelectBlock I21)
(PutCell2 "20")
(SelectBlock I20..I39)
(SpeedFill)
(EditCopy)
(SelectBlock M20)
(EditPaste)
(SelectBlock K20)
(PutCell2 "0.05")
(SelectBlock K21)
(PutCell2 "0.1")
(SelectBlock K20..K39)
(SpeedFill)
(SelectBlock J20)
(PutCell2 "@FREQDIST(E2..E105,I20..I39)")
(SelectBlock L20)
(PutCell2 "@FREQDIST(F2..F105,K20..K39)")
(SelectBlock N20)
(PutCell2 "@FREQDIST(G2..G105,M20..M39)")
(SelectBlock J20..J40)
```

Sample 7b.

DCIRCLE	FCIRCLE	DNEW
43.95	0.69	63.69565
64.95	0.9	72.16667
49.5	0.73	67.80822
24.28	0.69	35.18841
73.73	0.84	87.77381
75.56	0.83	91.03614
96.99	0.47	206.3617
29.73	0.79	37.63291
103.84	0.46	225.7391
27.77	0.79	35.1519
32.32	0.83	38.93976
67.29	0.8	84.1125
22.89	0.75	30.52
85.28	0.84	101.5238
123.3	0.42	293.5714
37.76	0.81	46.61728
42.09	0.84	50.10714
118.7	0.44	269.7727
79.1	0.54	146.4815
60.41	0.74	81.63514
101.09	0.83	121.7952
56.75	0.56	101.3393
39.65	0.83	47.77108
23.72	0.93	25.50538
35.65	0.84	42.44048
46.84	0.83	56.43373
24.09	0.73	33
127.13	0.57	223.0351
101	0.66	153.0303
94.41	0.57	165.6316
116.88	0.49	238.5306
29.78	0.75	39.70667
54.83	0.7	78.32857
23.84	0.72	33.11111
74.29	0.85	87.4
25.06	0.87	28.8046
84.17	0.47	179.0851
53.93	0.83	65.60317
19.9	0.74	26.89189
50.3	0.74	67.97297
22.89	0.88	26.01136
73.26	0.84	87.21429
30.08	0.91	33.05495
114.59	0.41	279.4878
89.57	0.66	105.4091
37.56	0.72	52.16667
39.08	0.91	42.94505
73.5	0.69	106.5217
48.71	0.73	66.72603
148.9	0.35	425.4286
34.94	0.89	39.25843
53.49	0.7	76.41429
49.62	0.87	57.03448
66.06	0.62	106.5484
33.59	0.74	45.39189
50.45	0.82	61.52439
3.45	0.72	4.791667
12.32	0.72	17.11111
71.39	0.65	109.8308
27.39	0.89	30.77528
37.52	0.81	46.32099
79.57	0.7	113.6714
23.66	0.68	34.79412
59.82	0.62	96.48387
20.99	0.69	30.42029
32.23	0.8	40.2875
45.91	0.82	55.9878
173.51	0.36	481.9722
31.53	0.92	34.27174
292.91	0.14	2092.214
61.2	0.93	65.80645
52.84	0.82	64.43902
54.75	0.79	69.3038
50.3	0.87	57.81609
147.16	0.38	387.2632
34.89	0.77	45.31169
39.65	0.75	52.86667
163.08	0.42	388.2857
62.33	0.74	84.22973
23.47	0.78	30.08974
64.02	0.72	88.91667
179.67	0.25	718.68
178.72	0.26	687.3846
43.41	0.73	59.46575
46.46	0.85	54.65882
244.6	0.28	873.5714

DCIRCLE	FCIRCLE	DNEW
3.45	0.14	4.79
12.32	0.25	17.11
19.9	0.26	25.51
20.99	0.28	26.01
22.89	0.35	26.89
22.89	0.36	28.80
23.47	0.38	30.09
23.66	0.41	30.42
23.72	0.42	30.52
23.84	0.42	30.78
24.09	0.44	33.00
24.28	0.46	33.05
25.06	0.47	33.11
27.39	0.47	34.27
27.77	0.49	34.79
29.73	0.54	35.15
29.78	0.56	35.19
30.08	0.57	37.63
31.53	0.57	38.94
32.23	0.62	39.26
32.32	0.62	39.71
33.59	0.63	40.29
34.89	0.65	42.44
34.94	0.66	42.95
35.65	0.66	45.31
37.52	0.68	45.39
37.56	0.69	46.32
37.76	0.69	46.62
39.08	0.69	47.77
39.65	0.69	50.11
39.65	0.7	52.17
42.09	0.7	52.87
43.41	0.7	54.66
43.95	0.72	55.99
45.91	0.72	56.43
46.46	0.72	57.03
46.84	0.72	57.82
48.71	0.72	59.47
49.5	0.73	61.52
49.62	0.73	63.70
50.3	0.73	64.44
50.3	0.73	65.81
50.45	0.74	66.73
52.84	0.74	67.81
53.48	0.74	67.97
53.93	0.74	69.30
54.75	0.74	72.17
54.83	0.75	76.41
56.75	0.75	78.33
59.82	0.75	81.64
60.41	0.77	84.11
61.2	0.78	84.23
62.33	0.79	85.60
64.02	0.79	87.21
64.95	0.79	87.40
66.06	0.8	87.77
67.29	0.8	88.92
69.57	0.81	91.04
71.39	0.81	96.48
73.26	0.82	101.34
73.5	0.82	101.52
73.73	0.82	105.41
74.29	0.83	106.52
75.56	0.83	106.55
79.1	0.83	109.83
79.57	0.83	113.67
84.17	0.83	121.80
85.28	0.84	146.48
94.41	0.84	153.03
96.99	0.84	165.63
101	0.84	179.09
101.09	0.84	206.36
103.84	0.85	223.04
114.58	0.85	225.74
116.88	0.87	238.53
118.7	0.87	269.77
123.3	0.87	279.49
127.13	0.88	293.57
147.16	0.89	387.26
148.9	0.89	388.29
163.08	0.9	425.43
173.51	0.91	481.97
178.72	0.91	687.38
179.67	0.92	716.68
244.6	0.93	873.57
292.91	0.93	2092.21

DCIRCLE/micron		FCIRCLE		DNEW	
Mean	66.83477	Mean	0.698953	Mean	144.5281
Standard Error	5.438572	Standard Error	0.019187	Standard Error	28.35213
Median	51.645	Median	0.74	Median	67.26712
Mode	22.89	Mode	0.72	Mode	NA
Standard Deviation	50.43524	Standard Deviation	0.177929	Standard Deviation	262.9268
Variance	2543.713	Variance	0.031659	Variance	69130.53
Kurtosis	5.419047	Kurtosis	0.751004	Kurtosis	36.25798
Skewness	2.069596	Skewness	-1.1497	Skewness	5.414964
Range	289.46	Range	0.79	Range	2067.423
Minimum	3.45	Minimum	0.14	Minimum	4.791667
Maximum	292.91	Maximum	0.93	Maximum	2092.214
Sum	5747.79	Sum	60.11	Sum	12429.41
Count	86	Count	86	Count	86
Confidence Level(0	10.6594	Confidence Level(0	0.037605	Confidence Level(0	55.56916

BIN	FREQUE	BIN	FREQUE	BIN	FREQUENCY
10	1	0.05	0	10	1
20	2	0.1	0	20	1
30	14	0.15	1	30	4
40	14	0.2	0	40	15
50	9	0.25	1	50	8
60	10	0.3	2	60	9
70	8	0.35	1	70	8
80	8	0.4	2	80	3
90	2	0.45	4	90	8
100	2	0.5	4	100	2
110	3	0.55	1	110	6
120	3	0.6	3	120	1
130	2	0.65	4	130	1
140	0	0.7	10	140	0
150	2	0.75	17	150	1
160	0	0.8	7	160	1
170	1	0.85	17	170	1
180	3	0.9	7	180	1
190	0	0.95	5	190	0
200	0	1	0	200	0
	2		0		15

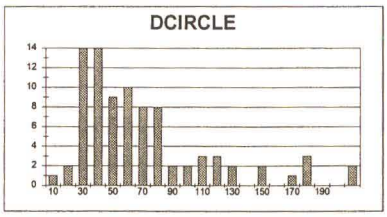

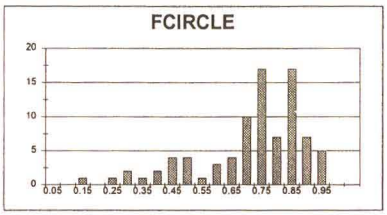

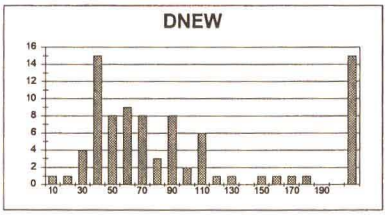


```
{SelectBlock C1}
{PutCell2 "DNEW"}
{SelectBlock C2}
{PutCell2 "=A2..A87/82..B87"}
{SelectBlock A2..B87}
{EditCopy}
{SelectBlock E2}
{EditPaste}
{SelectBlock C2}
{BlockValues C2;G2}
{SelectBlock C3..C212}
{EditCopy}
{SelectBlock G3}
{EditPaste}
{SelectBlock E2..E87}
{Sort.Block "E2..E87"}
{Sort.Type Top to bottom}
{Sort.Heading 0}
{Sort.Key_1 "E2"}
{Sort.Key_2 ""}
{Sort.Key_3 ""}
{Sort.Key_4 ""}
{Sort.Key_5 ""}
{Sort.BlankCellsFirst 0}
{Sort.Data Numbers First}
{Sort.PreviousSorts -1}
{Sort.Go}
{SelectBlock F2..F87}
{Sort.Block "F2..F87"}
{Sort.Type Top to bottom}
{Sort.Heading 0}
{Sort.Key_1 "F2"}
{Sort.Key_2 ""}
{Sort.Key_3 ""}
{Sort.Key_4 ""}
{Sort.Key_5 ""}
{Sort.BlankCellsFirst 0}
{Sort.Data Numbers First}
{Sort.PreviousSorts -1}
{Sort.Go}
{SelectBlock G2..G87}
{Sort.Block "G2..G87"}
{Sort.Type Top to bottom}
{Sort.Heading 0}
{Sort.Key_1 "G2"}
{Sort.Key_2 ""}
{Sort.Key_3 ""}
{Sort.Key_4 ""}
{Sort.Key_5 ""}
{Sort.BlankCellsFirst 0}
{Sort.Data Numbers First}
{Sort.PreviousSorts -1}
{Sort.Go}
{Selproperty Numeric_Format,"Fixed;2;South Africa"}
{SelectBlock A1..C1}
{EditCopy}
{SelectBlock E1}
{EditPaste}
{SelectBlock I1}
{DESCR "E1..E87";I1;C;"1";"1";"0";"0";"95%"}
{SelectBlock K1}
{DESCR "F1..F87";K1;C;"1";"1";"0";"0";"95%"}
{SelectBlock M1}
{DESCR "G1..G87";M1;C;"1";"1";"0";"0";"95%"}
{SelectBlock I19}
{PutCell2 "BIN"}
{SelectBlock J19}
{PutCell2 "FREQUENCY"}
{SelectBlock I19..J19}
{EditCopy}
{SelectBlock (K19..L19,M19..N19),M19}
{EditPaste}
{SelectBlock I20}
{PutCell2 "10"}
{SelectBlock I21}
{PutCell2 "20"}
{SelectBlock I20..I39}
{SpeedFill}
{EditCopy}
{SelectBlock M20}
{EditPaste}
{SelectBlock K20}
{PutCell2 "0.05"}
{SelectBlock K21}
{PutCell2 "0.1"}
{SelectBlock K20..K39}
{SpeedFill}
{SelectBlock J20}
{PutCell2 "@FREQDIST(E2..E87,I20..I39)"}
{SelectBlock L20}
{PutCell2 "@FREQDIST(F2..F87,K20..K39)"}
{SelectBlock N20}
{PutCell2 "@FREQDIST(G2..G87,M20..M39)"}
```

Sample 8a.

DCIRCLE	FCIRCLE	DNEW
29.58	0.81	36.51852
22.82	0.84	27.16667
36.23	0.81	44.7284
22.89	0.56	40.875
71.01	0.63	112.7143
15.53	0.78	19.91026
33.19	0.76	43.67105
23.53	0.79	29.78481
29.02	0.77	37.68831
44.63	0.8	55.7875
76.66	0.46	166.6522
42.33	0.74	57.2027
52.39	0.62	84.5
24.7	0.88	28.06818
23.47	0.54	43.46296
19.21	0.45	42.68889
21.62	0.63	34.31746
22.63	0.5	45.26
28.56	0.81	35.25926
44.46	0.73	60.90411
49.01	0.81	60.50617
33.9	0.77	44.02597
35.61	0.7	50.87143
31.39	0.83	37.81928
31.53	0.81	38.92593
45.84	0.58	79.03448
35.65	0.83	42.95181
60.39	0.71	85.05634
121.34	0.36	337.0556
24.58	0.45	54.62222
26.62	0.9	29.57778
28.56	0.76	37.57895
42.51	0.72	59.04167
48.92	0.7	69.88571
17.85	0.74	24.12162
23.66	0.88	26.88636
30.82	0.86	35.83721
99.59	0.45	221.3111
146.72	0.32	458.5
39.19	0.54	72.57407
44.46	0.71	62.61972
79.35	0.53	149.717
40.24	0.86	46.7907
21.96	0.47	46.7234
4.23	0.51	8.294118
4.88	0.53	9.207547
59.29	0.76	78.01316
32.09	0.73	43.9589
17.93	0.27	66.40741
23.66	0.56	42.25
57.59	0.81	71.09877
48.85	0.65	74.84615
29.26	0.78	37.53846
75.6	0.68	111.1765
25.24	0.55	45.89091
39.68	0.8	49.6
23.4	0.73	32.05479
20.41	0.74	27.58108
45.88	0.69	66.49275
31.29	0.84	37.25
32.87	0.62	40.08537
38.62	0.72	53.63889
48.22	0.67	71.97015
30.96	0.79	39.18987
41.06	0.71	57.85915
23.78	0.89	26.7191
31.29	0.79	39.60759
19.75	0.56	35.26786
55.1	0.89	79.85507
72.36	0.46	157.3043
17.51	0.68	25.75
17.76	0.55	32.29091
4.23	1	4.23
83.5	0.56	149.1071
21.69	0.86	25.22093
5.98	0.3	19.93333
3.45	0.6	5.75
29.78	0.73	40.79452
34.42	0.76	45.28947
25.47	0.86	29.61628
19.67	0.79	24.89873
137.39	0.39	352.2821
13.36	0.57	23.4386
23.97	0.69	34.73913
3.86	1	3.86
18.74	0.77	24.33766
15.14	0.75	20.18667
3.86	0.45	8.577778
15.24	0.54	28.22222
51.73	0.7	73.9
85.7	0.61	140.4918
44.22	0.74	59.75676
15.14	0.75	20.18667
45.39	0.67	67.74627
24.58	0.85	28.91765
53.07	0.6	88.45
4.56	0.48	9.5
20.05	0.5	40.1
27.33	0.78	35.03846
5.72	0.73	7.835616
17.68	0.71	24.90141
45.78	0.58	78.93103
35.19	0.72	48.875
25.82	0.52	49.65385
31.53	0.77	40.94805
3.45	0.95	3.631579
44.66	0.69	64.72464
5.46	0.57	9.578947
63.32	0.66	95.93939
30.38	0.82	37.04878
69.04	0.7	98.62857
5.72	0.44	13
29.53	0.85	34.74118
29.88	0.84	35.57143
28.46	0.86	33.09302
22.63	0.76	29.77632
14.84	0.81	18.32099
13.91	0.29	47.96552
23.78	0.67	35.49254
17.76	0.57	31.15789
17.08	0.66	25.87879
21.41	0.63	33.98413
21.62	0.2	108.1
5.98	0.9	6.644444
21.41	0.72	29.73611
185.79	0.22	844.5
18.9	0.46	41.08696
36.48	0.63	57.90476
41.26	0.75	55.01333
24.7	0.66	37.42424
28.51	0.59	48.32203
32.78	0.81	40.49914
25.3	0.86	29.4186
44.93	0.75	59.90667
65.22	0.68	95.91176
25.88	0.54	47.92593
38.15	0.81	47.09877
38.08	0.7	54.4
32.74	0.59	55.49153
138.81	0.39	355.9231
25.12	0.92	27.30435
24.58	0.47	52.29787
30.33	0.83	36.54217
40.87	0.62	65.91935
20.34	0.62	32.80645
37.64	0.78	48.25641
40.94	0.73	56.08219
36.48	0.68	53.64706
45.12	0.74	60.97297
20.34	0.55	36.98182
19.21	0.57	33.70175
51.67	0.64	80.73438
83.59	0.37	225.9189
19.9	0.47	42.34043
24.22	0.8	30.275
41.3	0.59	70
26.45	0.52	50.86538
20.56	0.78	26.35897
18.74	0.73	25.67123

DCIRCLE	FCIRCLE	DNEW
3.45	0.2	3.63
3.45	0.22	3.86
3.86	0.26	4.23
3.86	0.27	4.90
3.86	0.28	5.75
4.23	0.28	6.22
4.23	0.29	6.43
4.23	0.3	6.64
4.56	0.31	7.84
4.56	0.32	8.00
4.56	0.34	8.29
4.88	0.36	8.58
4.88	0.37	9.21
5.46	0.38	9.50
5.72	0.39	9.58
5.72	0.39	10.04
5.72	0.39	10.91
5.98	0.39	12.51
5.98	0.41	13.00
8.22	0.42	14.08
9.29	0.42	18.32
12.68	0.42	19.91
13.36	0.42	19.93
13.59	0.43	20.19
13.69	0.44	20.19
13.91	0.45	21.04
14.64	0.45	21.39
14.64	0.45	21.86
15.14	0.45	23.44
15.14	0.46	24.00
15.24	0.46	24.12
15.53	0.46	24.29
16	0.47	24.34
17.08	0.47	24.47
17.25	0.47	24.71
17.25	0.48	24.90
17.51	0.48	24.90
17.65	0.49	25.22
17.76	0.49	25.67
17.76	0.5	25.75
17.85	0.5	25.81
17.93	0.5	25.88
18.01	0.51	26.36
18.18	0.52	26.63
18.58	0.52	26.72
18.74	0.52	26.89
18.74	0.53	27.17
18.74	0.53	27.30
18.9	0.54	27.58
19.21	0.54	27.66
19.21	0.54	28.07
19.44	0.54	28.22
19.44	0.54	28.24
19.52	0.54	28.30
19.67	0.55	28.39
19.75	0.55	28.92
19.9	0.55	28.99
20.05	0.55	29.06
20.05	0.55	29.42
20.19	0.56	29.58
20.34	0.56	29.59
20.34	0.56	29.62
20.41	0.56	29.74
20.56	0.56	29.74
20.63	0.56	29.78
21.41	0.57	29.78
21.41	0.57	29.80
21.62	0.57	29.83
21.62	0.57	30.19
21.62	0.57	30.28
21.69	0.57	30.57
21.96	0.57	30.80
22.43	0.57	31.01
22.63	0.57	31.16
22.63	0.57	31.17
22.76	0.57	31.46
22.82	0.58	31.97
22.89	0.58	32.05
23.02	0.58	32.22
23.15	0.59	32.29
23.4	0.59	32.75
23.47	0.59	32.81
23.53	0.59	33.03
23.59	0.59	33.09
23.66	0.59	33.70
23.66	0.6	33.90
23.78	0.6	33.98
23.78	0.6	34.32
23.78	0.6	34.55
23.84	0.61	34.55
23.97	0.61	34.73
23.97	0.61	34.74
24.15	0.62	34.74
24.22	0.62	35.04
24.34	0.62	35.12
24.46	0.62	35.26
24.58	0.63	35.27
24.58	0.63	35.36
24.58	0.63	35.37
24.7	0.63	35.42
24.7	0.63	35.49
24.7	0.64	35.57
24.76	0.64	35.84
25.12	0.65	36.38
25.24	0.65	36.52
25.3	0.65	36.54
25.47	0.65	36.62
25.82	0.66	36.96
25.88	0.66	37.05
26.11	0.66	37.25
26.17	0.66	37.36
26.45	0.66	37.42
26.62	0.67	37.54
26.67	0.67	37.56
26.67	0.67	37.58
26.9	0.67	37.69
27.12	0.67	37.82
27.23	0.67	37.88
27.33	0.68	38.02
27.39	0.68	38.21
27.39	0.68	38.40
27.44	0.68	38.78
27.93	0.68	38.93
27.96	0.68	39.19
28.4	0.68	39.61
28.46	0.69	39.97
28.51	0.69	39.98
28.56	0.69	40.09
28.56	0.69	40.10
28.66	0.69	40.47
29.02	0.69	40.79
29.28	0.69	40.88
29.53	0.69	40.95
29.58	0.7	41.09
29.78	0.7	41.26
29.83	0.7	41.58
29.83	0.7	42.25
29.88	0.7	42.33
30.33	0.7	42.34
30.33	0.7	42.69
30.38	0.71	42.95
30.72	0.71	43.46
30.82	0.71	43.56
30.96	0.71	43.67
31.06	0.71	43.75
31.29	0.71	43.96
31.29	0.72	44.03
31.34	0.72	44.73
31.39	0.72	45.26
31.53	0.72	45.27
31.53	0.72	45.29
31.86	0.72	45.89
32.09	0.72	46.29
32.74	0.73	46.72
32.78	0.73	46.79
32.87	0.73	47.10
32.96	0.73	47.22
33.01	0.73	47.71
33.05	0.73	47.93

DCIRCLE/micron		FCIRCLE		DNEW	
Mean	37.37276	Mean	0.671581	Mean	67.42389
Standard Error	1.705894	Standard Error	0.009572	Standard Error	5.631883
Median	29.83	Median	0.7	Median	41.91512
Mode	3.86	Mode	0.73	Mode	20.18667
Standard Deviation	28.13103	Standard Deviation	0.157862	Standard Deviation	92.88339
Variance	791.3549	Variance	0.02492	Variance	8627.325
Kurtosis	7.54527	Kurtosis	-0.01663	Kurtosis	29.04119
Skewness	2.36722	Skewness	-0.63487	Skewness	4.857559
Range	182.34	Range	0.6	Range	840.8684
Minimum	3.45	Minimum	0.2	Minimum	3.631579
Maximum	185.79	Maximum	1	Maximum	844.5
Sum	10165.39	Sum	182.67	Sum	18339.3
Count	272	Count	272	Count	272
Confidence Level(0	3.343099	Confidence Level(0	0.01876	Confidence Level(0	11.03829

BIN	FREQUE	BIN	FREQUE	BIN	FREQUENCY
10	21	0.05	0	10	15
20	36	0.1	0	20	8
30	81	0.15	0	30	45
40	45	0.2	1	40	59
50	37	0.25	1	50	39
60	17	0.3	6	60	25
70	8	0.35	3	70	21
80	9	0.4	7	80	12
90	4	0.45	11	90	9
100	4	0.5	13	100	6
110	1	0.55	17	110	4
120	0	0.6	30	120	4
130	2	0.65	18	130	3
140	3	0.7	33	140	0
150	1	0.75	36	150	3
160	1	0.8	36	160	1
170	0	0.85	33	170	2
180	0	0.9	20	180	2
190	2	0.95	5	190	0
200	0	1	2	200	0
	0		0		14

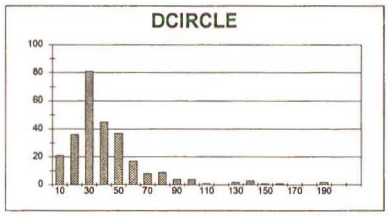

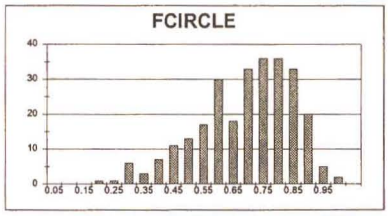

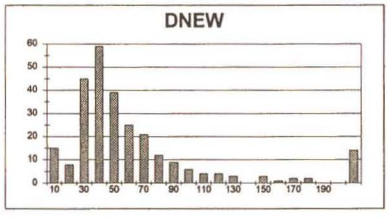


```
{SelectBlock C1}
{PutCell2 "DNEW"}
{SelectBlock C2}
{PutCell2 "=A2..A273/B2..B273"}
{SelectBlock A2..B273}
{EditCopy}
{SelectBlock E2}
{EditPaste}
{SelectBlock C2}
{BlockValues C2;O2}
{SelectBlock C3..C273}
{EditCopy}
{SelectBlock G3}
{EditPaste}
{SelectBlock E2..E273}
{Sort.Block "E2..E273"}
{Sort.Type Top to bottom}
{Sort.Heading 0}
{Sort.Key_1 "E2"}
{Sort.Key_2 ""}
{Sort.Key_3 ""}
{Sort.Key_4 ""}
{Sort.Key_5 ""}
{Sort.BlankCellsFirst 0}
{Sort.Data Numbers First}
{Sort.PreviousSorts -1}
{Sort.Go}
{SelectBlock F2..F273}
{Sort.Block "F2..F273"}
{Sort.Type Top to bottom}
{Sort.Heading 0}
{Sort.Key_1 "F2"}
{Sort.Key_2 ""}
{Sort.Key_3 ""}
{Sort.Key_4 ""}
{Sort.Key_5 ""}
{Sort.BlankCellsFirst 0}
{Sort.Data Numbers First}
{Sort.PreviousSorts -1}
{Sort.Go}
{SelectBlock G2..G273}
{Sort.Block "G2..G273"}
{Sort.Type Top to bottom}
{Sort.Heading 0}
{Sort.Key_1 "G2"}
{Sort.Key_2 ""}
{Sort.Key_3 ""}
{Sort.Key_4 ""}
{Sort.Key_5 ""}
{Sort.BlankCellsFirst 0}
{Sort.Data Numbers First}
{Sort.PreviousSorts -1}
{Sort.Go}
{Selproperty Numeric_Format,"Fixed;2;South Africa"}
{SelectBlock A1..C1}
{EditCopy}
{SelectBlock E1}
{EditPaste}
{SelectBlock I1}
{DESCR "E1..E273";I1;C;"1";"1";"0";"0";"95%"}
{SelectBlock K1}
{DESCR "F1..F273";K1;C;"1";"1";"0";"0";"95%"}
{SelectBlock M1}
{DESCR "G1..G273";M1;C;"1";"1";"0";"0";"95%"}
{SelectBlock I19}
{PutCell2 "SIN"}
{SelectBlock J19}
{PutCell2 "FREQUENCY"}
{SelectBlock I19..J19}
{EditCopy}
{SelectBlock (K19..L19,M19..N19),M19}
{EditPaste}
{SelectBlock I20}
{PutCell2 "10"}
{SelectBlock I21}
{PutCell2 "20"}
{SelectBlock I20..I39}
{SpeedFill}
{EditCopy}
{SelectBlock M20}
{EditPaste}
{SelectBlock K20}
{PutCell2 "0.05"}
{SelectBlock K21}
{PutCell2 "0.1"}
{SelectBlock K20..K39}
{SpeedFill}
{SelectBlock J20}
{PutCell2 "@FREQDIST(E2..E273,I20..I39)"}
{SelectBlock L20}
{PutCell2 "@FREQDIST(F2..F273,K20..K39)"}
{SelectBlock N20}
{PutCell2 "@FREQDIST(G2..G273,M20..M39)"}
{SelectBlock J20..J40}
```

Sample 8b.

DCIRCLE	FCIRCLE	DNEW
14.54	0.51	28.5098
17.17	0.48	35.77083
16.46	0.81	20.32099
5.72	0.29	19.72414
24.4	0.86	28.37209
23.34	0.99	23.57576
34.76	0.83	41.87952
34.2	0.75	45.6
22.5	0.78	28.84615
64.3	0.7	91.85714
27.87	0.64	43.54688
18.34	0.71	25.83099
24.58	0.84	29.2619
32.74	0.76	43.07895
20.99	0.81	25.91358
60.56	0.59	102.678
65.7	0.49	134.0816
30.28	0.8	37.85
18.74	0.77	24.33766
85.68	0.51	168
39.27	0.84	46.75
68.93	0.56	123.0893
20.19	0.85	23.75294
28.19	0.83	33.96386
31.86	0.67	47.55224
25.47	0.89	28.61798
19.37	0.7	27.67143
23.72	0.81	29.28395
42.79	0.71	60.26761
17.85	0.38	46.97368
30.91	0.84	36.77262
23.91	0.57	41.94737
16.55	0.77	21.48351
26.34	0.89	29.59551
33.59	0.72	46.65278
26.95	0.8	33.6875
50.33	0.73	68.94521
90.89	0.39	233.0513
82.28	0.38	216.5263
22.1	0.7	31.57143
30.08	0.47	64
38.43	0.7	54.9
58.94	0.68	86.67647
26.73	0.71	37.64789
24.88	0.63	39.49206
33.1	0.65	50.92308
27.23	0.81	33.61728
28.3	0.49	57.7551
21.69	0.84	25.82143
23.66	0.78	30.33333
27.17	0.84	32.34524
34.46	0.76	45.34211
156.84	0.37	423.8919
20.19	0.62	32.56452
23.53	0.91	25.85714
25.71	0.86	29.21591
67.53	0.4	168.825
19.14	0.61	31.37705
143.82	0.27	532.6667
37.84	0.91	41.58242
30.52	0.58	52.62069
40.32	0.8	50.4
27.12	0.72	37.66667
45.97	0.61	75.36066
133.05	0.24	554.375
4.23	0.9	4.7
93.2	0.49	190.2041
60.02	0.78	76.94872
22.89	0.92	24.88043
38.11	0.7	54.44286
20.56	0.36	57.11111
31.95	0.8	39.9375
21.2	0.69	30.72464
11.95	0.54	22.12963
26.51	0.35	75.74286
21.96	0.71	30.92958
33.9	0.77	44.02597
34.07	0.84	40.55952
21.96	0.6	36.6
24.7	0.82	30.12195
21.96	0.71	30.92958
24.46	0.85	28.77647
19.67	0.86	22.87209
54.97	0.61	90.11475
26.78	0.89	30.08989
20.78	0.7	29.68571
30.03	0.47	63.89362
28.72	0.66	43.51515
32.78	0.81	40.46914
15.04	0.44	34.18182
89.12	0.55	162.0364
21.96	0.52	42.23077
44.22	0.78	56.69231
33.63	0.8	42.0375
31.2	0.85	36.70588
31.25	0.78	40.0641
39	0.76	51.31579
73.95	0.53	139.5283
23.34	0.81	28.81481
26.73	0.57	46.89474
14.74	0.74	19.91892
16.9	0.65	26
23.66	0.85	27.83529
21.41	0.6	35.68333
44.69	0.76	58.80263
32.32	0.58	55.72414
40.68	0.79	51.48367
21.89	0.7	31.27143
48.37	0.69	70.10145
31.01	0.75	41.34667
96.19	0.53	181.4906
44.99	0.74	60.7973
22.16	0.62	35.74194
24.34	0.74	32.89189
19.06	0.4	47.65
40.24	0.82	49.07317
55.85	0.55	101.5455
19.29	0.78	24.73077
13.69	0.67	20.43284
25.3	0.81	31.23457
18.34	0.65	28.21538
37.21	0.69	53.92754
21.89	0.92	23.79348
22.63	0.91	24.86813
50.6	0.71	71.26761
35.27	0.8	44.0875
29.93	0.75	39.90667
75.09	0.71	105.7606
23.84	0.64	37.25
52.59	0.57	92.26316
26.95	0.53	50.84906
22.36	0.81	27.60494
24.34	0.63	38.63492
23.21	0.47	49.38298
19.67	0.49	40.14286
21.96	0.8	27.45
120.22	0.3	400.7333
30.08	0.9	33.42222
26.95	0.89	30.2809
30.28	0.78	38.82051
41.62	0.76	53.35987
11.7	0.59	19.83051
47.44	0.7	67.77143
37.92	0.79	48
6.46	0.61	10.59016
35.15	0.66	53.25758
88.95	0.67	132.7612
45.71	0.7	65.3
25.42	0.83	30.62651
28.77	0.79	36.41772
24.88	0.75	33.17333
28.87	0.88	32.80682
16.55	0.67	24.70149
28.35	0.75	37.8
28.19	0.85	33.16471
21.62	0.53	40.79245
17.17	0.74	23.2027
16.9	0.7	24.14286
25.88	0.59	43.86441

DCIRCLE	FCIRCLE	DNEW
3.45	0.23	3.86
3.45	0.24	4.70
3.86	0.24	6.22
4.23	0.27	8.87
4.23	0.29	10.59
4.88	0.3	13.67
5.72	0.31	19.72
5.72	0.33	19.83
6.46	0.34	19.92
7.52	0.35	20.32
7.72	0.36	20.43
11.7	0.36	21.49
11.7	0.37	22.13
11.95	0.38	22.87
12.91	0.38	23.20
13.69	0.38	23.58
13.91	0.39	23.75
14.54	0.39	23.79
14.74	0.39	24.14
15.04	0.4	24.34
15.24	0.4	24.70
16.46	0.41	24.73
16.55	0.42	24.83
16.55	0.42	24.87
16.55	0.43	24.88
16.82	0.43	25.82
16.9	0.44	25.83
16.9	0.44	25.86
17.17	0.45	25.91
17.17	0.46	26.00
17.76	0.46	26.70
17.85	0.46	27.14
18.01	0.47	27.45
18.34	0.47	27.60
18.34	0.47	27.67
18.34	0.48	27.84
18.5	0.49	28.22
18.5	0.49	28.37
18.56	0.49	28.51
18.74	0.49	28.62
18.98	0.49	28.78
19.06	0.49	28.81
19.14	0.51	28.85
19.29	0.51	29.06
19.37	0.51	29.22
19.44	0.51	29.26
19.67	0.51	29.28
19.67	0.51	29.60
19.82	0.52	29.69
20.12	0.52	30.09
20.19	0.52	30.12
20.19	0.53	30.28
20.34	0.53	30.33
20.56	0.53	30.63
20.78	0.53	30.72
20.85	0.53	30.79
20.99	0.53	30.93
20.99	0.54	30.93
20.99	0.54	31.23
21.2	0.54	31.27
21.27	0.55	31.38
21.34	0.55	31.57
21.41	0.55	31.71
21.62	0.55	32.35
21.62	0.55	32.56
21.62	0.56	32.75
21.62	0.56	32.81
21.69	0.56	32.89
21.69	0.57	33.06
21.89	0.57	33.16
21.89	0.57	33.17
21.89	0.57	33.42
21.96	0.58	33.62
21.96	0.58	33.69
21.96	0.58	33.87
21.96	0.59	33.96
21.96	0.59	34.18
21.96	0.59	34.73
22.03	0.6	35.48
22.1	0.6	35.68
22.18	0.6	35.74
22.18	0.6	35.76
22.36	0.6	35.77
22.5	0.61	36.42
22.56	0.61	36.48
22.63	0.61	36.60
22.89	0.61	36.64
22.89	0.61	36.71
23.08	0.61	36.80
23.21	0.62	37.07
23.28	0.62	37.22
23.34	0.62	37.25
23.34	0.62	37.65
23.34	0.63	37.67
23.34	0.63	37.80
23.47	0.63	37.85
23.53	0.63	38.63
23.66	0.63	38.82
23.66	0.64	38.90
23.72	0.64	39.49
23.78	0.64	39.77
23.84	0.65	39.91
23.91	0.65	39.94
24.09	0.65	40.06
24.34	0.65	40.14
24.34	0.65	40.47
24.4	0.66	40.56
24.46	0.66	40.79
24.58	0.66	41.35
24.64	0.67	41.47
24.7	0.67	41.58
24.7	0.67	41.77
24.82	0.67	41.88
24.82	0.67	41.95
24.88	0.68	42.04
24.88	0.68	42.21
24.88	0.68	42.23
25.3	0.68	42.52
25.42	0.69	42.53
25.47	0.69	42.64
25.59	0.69	42.78
25.71	0.69	42.81
25.88	0.69	43.08
25.94	0.7	43.52
26.17	0.7	43.55
26.34	0.7	43.64
26.34	0.7	43.79
26.51	0.7	43.86
26.62	0.7	44.03
26.73	0.7	44.09
26.73	0.7	44.14
26.78	0.7	44.28
26.95	0.7	44.84
26.95	0.7	45.34
26.95	0.7	45.60
26.95	0.7	46.65
27.12	0.71	46.75
27.17	0.71	46.89
27.23	0.71	46.97
27.39	0.71	47.03
27.44	0.71	47.22
27.71	0.71	47.55
27.77	0.71	47.65
27.87	0.71	48.00
28.03	0.71	49.07
28.03	0.71	49.38
28.19	0.72	50.40
28.19	0.72	50.40
28.25	0.72	50.65
28.25	0.73	50.85
28.3	0.73	50.92
28.35	0.73	51.29
28.72	0.73	51.32
28.77	0.73	51.49
28.77	0.73	52.10
28.87	0.73	52.62
28.92	0.73	53.26
29.13	0.73	53.36
29.13	0.73	53.93

DCIRCLE/micron		FCIRCLE		DNEW	
Mean	35.86348	Mean	0.685117	Mean	63.64627
Standard Error	1.473183	Standard Error	0.009021	Standard Error	5.287971
Median	28.25	Median	0.73	Median	40.46914
Mode	21.96	Mode	0.78	Mode	30.92958
Standard Deviation	25.47371	Standard Deviation	0.155991	Standard Deviation	91.43756
Variance	648.9098	Variance	0.024333	Variance	8360.828
Kurtosis	9.274372	Kurtosis	-0.01793	Kurtosis	35.58135
Skewness	2.619871	Skewness	-0.75123	Skewness	5.37763
Range	194.65	Range	0.77	Range	857.4443
Minimum	3.45	Minimum	0.23	Minimum	3.86
Maximum	198.1	Maximum	1	Maximum	861.3043
Sum	10723.18	Sum	204.85	Sum	13429.36
Count	299	Count	299	Count	211
Confidence Level(0	2.887385	Confidence Level(0	0.017681	Confidence Level(0	12.33762

BIN	FREQUE	BIN	FREQUE	BIN	FREQUENCY
10	11	0.05	0	10	4
20	38	0.1	0	20	5
30	116	0.15	0	30	40
40	62	0.2	0	40	54
50	21	0.25	3	50	43
60	17	0.3	3	60	21
70	9	0.35	4	70	8
80	3	0.4	11	80	7
90	8	0.45	8	90	3
100	5	0.5	13	100	3
110	1	0.55	23	110	3
120	1	0.6	18	120	0
130	3	0.65	23	130	1
140	1	0.7	30	140	3
150	1	0.75	45	150	1
160	1	0.8	48	160	0
170	0	0.85	42	170	3
180	0	0.9	20	180	0
190	0	0.95	6	190	1
200	1	1	2	200	2
	0		0		9

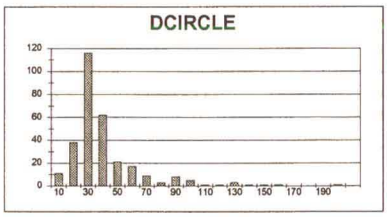

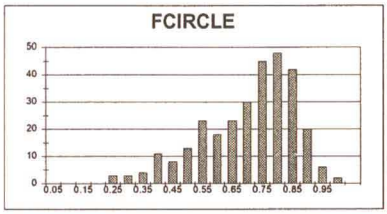

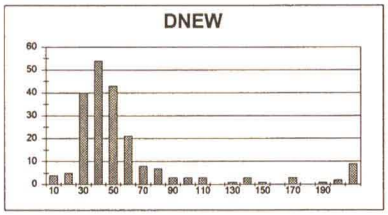


```
(SelectBlock C1)
(PutCell2 "DNEW")
(SelectBlock C2)
(PutCell2 "=A2..A300/B2..B300")
(SelectBlock A2..B300)
(EditCopy)
(SelectBlock E2)
(EditPaste)
(SelectBlock C2)
(BlockValues C2;G2)
(SelectBlock C3..C212)
(EditCopy)
(SelectBlock G3)
(EditPaste)
(SelectBlock E2..E300)
(Sort.Block "E2..E300")
(Sort.Type Top to bottom)
(Sort.Heading 0)
(Sort.Key_1 "E2")
(Sort.Key_2 "")
(Sort.Key_3 "")
(Sort.Key_4 "")
(Sort.Key_5 "")
(Sort.BlankCellsFirst 0)
(Sort.Data Numbers First)
(Sort.PreviousSorts -1)
(Sort.Go)
(SelectBlock F2..F300)
(Sort.Block "F2..F300")
(Sort.Type Top to bottom)
(Sort.Heading 0)
(Sort.Key_1 "F2")
(Sort.Key_2 "")
(Sort.Key_3 "")
(Sort.Key_4 "")
(Sort.Key_5 "")
(Sort.BlankCellsFirst 0)
(Sort.Data Numbers First)
(Sort.PreviousSorts -1)
(Sort.Go)
(SelectBlock G2..G300)
(Sort.Block "G2..G300")
(Sort.Type Top to bottom)
(Sort.Heading 0)
(Sort.Key_1 "G2")
(Sort.Key_2 "")
(Sort.Key_3 "")
(Sort.Key_4 "")
(Sort.Key_5 "")
(Sort.BlankCellsFirst 0)
(Sort.Data Numbers First)
(Sort.PreviousSorts -1)
(Sort.Go)
(Setproperty Numeric_Format,"Fixed;2;South Africa")
(SelectBlock A1..C1)
(EditCopy)
(SelectBlock E1)
(EditPaste)
(SelectBlock I1)
(DESCR "E1..E300";I1;C;"1";"1";"0";"0";"95%")
(SelectBlock K1)
(DESCR "F1..F300";K1;C;"1";"1";"0";"0";"95%")
(SelectBlock M1)
(DESCR "G1..G300";M1;C;"1";"1";"0";"0";"95%")
(SelectBlock I19)
(PutCell2 "BIN")
(SelectBlock J19)
(PutCell2 "FREQUENCY")
(SelectBlock I19..J19)
(EditCopy)
(SelectBlock (K19..L19;M19..N19);M19)
(EditPaste)
(SelectBlock I20)
(PutCell2 "10")
(SelectBlock I21)
(PutCell2 "20")
(SelectBlock I20..I39)
(SpeedFill)
(EditCopy)
(SelectBlock M20)
(EditPaste)
(SelectBlock K20)
(PutCell2 "0.05")
(SelectBlock K21)
(PutCell2 "0.1")
(SelectBlock K20..K39)
(SpeedFill)
(SelectBlock J20)
(PutCell2 "@FREQDIST(E2..E300,I20..I39)")
(SelectBlock L20)
(PutCell2 "@FREQDIST(F2..F300,K20..K39)")
(SelectBlock N20)
(PutCell2 "@FREQDIST(G2..G300,M20..M39)")
```

Sample 9a.

DCIRCLE	FCIRCLE	DNEW
25.47	0.93	27.3871
4.23	0.62	6.822581
24.7	0.93	26.55914
23.28	0.74	31.45946
5.18	0.35	14.8
23.4	0.43	54.4186
46.74	0.67	69.78119
37.17	0.72	51.625
59.64	0.76	78.47368
44.96	0.67	67.10448
33.59	0.86	39.05814
8.27	0.81	10.20988
48.55	0.71	65.58338
52.02	0.69	75.3913
13.14	0.54	24.33333
5.98	0.36	16.61111
76.54	0.55	139.1636
31.29	0.87	35.96552
19.67	0.8	24.5875
57.28	0.87	65.83908
41.98	0.75	55.97333
40.2	0.82	49.02439
20.34	0.83	24.50602
102.99	0.73	141.0822
25.42	0.86	29.55814
105.98	0.56	189.25
24.46	0.77	31.76623
25.06	0.9	27.84444
28.19	0.89	31.67416
30.38	0.82	37.04878
18.5	0.86	21.51163
30.67	0.84	36.5119
24.88	0.79	31.49367
89.82	0.47	191.1064
36.5	0.74	52.02703
23.84	0.84	28.38095
47.97	0.9	53.3
18.6	0.77	25.45455
120.97	0.57	212.2281
86.04	0.8	107.55
24.76	0.85	29.12941
4.56	0.72	6.333333
28.82	0.82	35.14634
50.27	0.81	62.06173
31.44	0.86	36.55814
24.52	0.92	26.65217
50.71	0.7	72.44286
31.44	0.84	37.42857
134.93	0.28	481.8929
20.05	0.92	21.79348
47.06	0.74	63.59459
27.61	0.81	34.08642
51.3	0.9	57
155.58	0.33	471.4545
31.29	0.89	35.1573
89.82	0.53	169.4717
45.84	0.77	59.53247
29.18	0.86	33.93023
51.07	0.83	61.53012
36.27	0.85	42.67059
43.99	0.84	52.36905
79.78	0.49	162.8163
18.74	0.83	22.57831
111.07	0.41	270.9024
22.69	0.85	26.69412
30.77	0.85	36.2
23.86	0.86	27.51163
22.43	0.97	23.12371
22.36	0.74	30.21622
37.32	0.84	44.42857
21.27	0.86	24.73256
46.2	0.88	52.5
58.18	0.72	80.80556
67.69	0.57	118.7544
25.06	0.77	32.54545
57.89	0.82	70.35366
41.44	0.85	48.75294
22.03	0.83	26.54217
26.17	0.91	28.75824
57.28	0.65	88.12308
17.68	0.85	20.8
140.39	0.32	438.7187
36.11	0.81	44.58025
19.06	0.75	25.41333
35.23	0.85	41.44706
49.23	0.85	57.91765
24.22	0.93	26.04301
28.56	0.81	35.25926
38.31	0.88	43.53409
20.41	0.9	22.67778
25.76	0.9	28.62222
42.05	0.77	54.61039
42.79	0.86	49.75581
251.3	0.19	1322.632
108.22	0.67	161.5224
20.63	0.85	24.27059
120.09	0.46	261.0652
31.34	0.79	39.67089
38.35	0.94	40.79787
68.62	0.49	140.0408
22.43	0.89	25.20225
19.21	0.81	23.71605
27.87	0.92	30.29348
26.39	0.71	37.16901
36.11	0.83	43.50602
31.15	0.93	33.49462
49.98	0.85	58.8
175.39	0.34	515.8529
4.23	0.56	7.553571
26.34	0.68	38.73529
108.45	0.5	216.9
41.44	0.79	52.4557
88.9	0.87	102.1839
132.83	0.31	428.4839
28.09	0.87	32.28736
43.27	0.9	48.07778
66.06	0.63	104.8571
17.25	0.51	33.82353
22.03	0.9	24.47778
46.42	0.73	63.58904
22.16	0.87	25.47126
183.77	0.35	525.0571
17.76	0.77	23.06494
17.6	0.83	21.20482
39.42	0.77	51.19481
23.78	0.88	27.02273
49.38	0.88	56.11364
23.15	0.76	30.46053
38.19	0.94	40.62766
64.19	0.87	73.78161
24.34	0.77	31.61039
19.37	0.87	28.91045
25.82	0.77	33.53247
40.76	0.81	50.32099
48.59	0.81	59.98765
27.01	0.86	31.40698
26.73	0.84	31.82143
109.88	0.47	233.7872
82.49	0.72	114.5694
18.5	0.4	46.25
47.19	0.71	66.46479
46.07	0.83	55.50602
19.37	0.93	20.82796
4.88	0.65	7.507692
23.47	0.9	26.07778
76.85	0.93	82.63441
29.58	0.64	46.21875
23.72	0.76	31.21053
22.3	0.95	23.47368
184.02	0.21	876.2857
30.33	0.87	34.86207
34.96	0.77	45.42857
32.26	0.74	43.62162
22.89	0.87	26.31034
24.34	0.79	30.81013
24.7	0.95	26
203.97	0.21	971.2857
14.94	0.67	22.29851
46.49	0.78	59.60256
4.23	0.19	6.33
4.23	0.21	6.82
4.56	0.21	7.51
4.88	0.28	7.55
5.18	0.31	10.21
5.98	0.32	14.80
8.27	0.33	16.61
13.14	0.34	20.80
14.94	0.35	20.83
17.25	0.35	21.20
17.6	0.36	21.51
17.68	0.4	21.79
17.76	0.41	22.30
18.5	0.43	22.58
18.5	0.46	22.68
18.74	0.47	23.06
19.06	0.47	23.12
19.21	0.49	23.47
19.37	0.49	23.72
19.37	0.5	24.27
19.6	0.51	24.33
19.67	0.53	24.48
20.05	0.54	24.51
20.34	0.55	24.59
20.41	0.56	24.73
20.63	0.56	25.20
21.27	0.57	25.41
22.03	0.57	25.45
22.03	0.62	25.47
22.16	0.63	26.00
22.3	0.64	26.04
22.36	0.65	26.08
22.43	0.65	26.31
22.43	0.67	26.54
22.69	0.67	26.56
22.89	0.67	26.65
23.15	0.67	26.69
23.28	0.67	27.02
23.4	0.68	27.39
23.47	0.69	27.51
23.66	0.7	27.84
23.72	0.71	28.38
23.78	0.71	28.62
23.84	0.71	28.78
24.22	0.72	28.91
24.34	0.72	29.13
24.34	0.72	29.56
24.46	0.72	30.22
24.52	0.73	30.29
24.7	0.73	30.46
24.7	0.74	30.81
24.76	0.74	31.21
24.88	0.74	31.41
25.06	0.74	31.46
25.06	0.74	31.49
25.42	0.75	31.61
25.47	0.75	31.67
25.76	0.76	31.77
25.82	0.76	31.82
26.17	0.76	32.29
26.34	0.77	32.55
26.39	0.77	33.49
26.73	0.77	33.53
27.01	0.77	33.82
27.61	0.77	33.93
27.87	0.77	34.09
28.09	0.77	34.86
28.19	0.77	35.15
28.56	0.77	35.16
28.82	0.77	35.26
29.18	0.78	35.97
29.58	0.79	36.20
30.33	0.79	36.51
30.38	0.79	36.56
30.67	0.79	37.05
30.77	0.8	37.17
31.15	0.8	37.43
31.29	0.81	38.74
31.29	0.81	39.06
31.34	0.81	39.67
31.44	0.81	40.63
31.44	0.81	40.80
32.28	0.81	41.45
33.59	0.81	42.67
34.96	0.81	43.51
35.23	0.82	43.53
36.11	0.82	43.62
36.11	0.82	44.43
36.27	0.82	44.58
37.17	0.83	45.43
37.32	0.83	46.22
38.19	0.83	46.25
38.31	0.83	48.08
38.35	0.83	48.75
38.5	0.83	49.02
39.42	0.83	49.76
40.2	0.84	50.32
40.76	0.84	51.19
41.44	0.84	51.63
41.44	0.84	52.03
41.98	0.84	52.37
42.05	0.84	52.46
42.79	0.85	52.50
43.27	0.85	53.30
43.99	0.85	54.42
44.96	0.85	54.61
45.84	0.85	55.51
46.07	0.85	55.97
46.2	0.85	56.11
46.42	0.85	57.00
46.49	0.85	57.92
46.55	0.85	58.80
46.74	0.86	59.53
47.06	0.86	59.60
47.19	0.86	59.99
47.97	0.86	61.53
48.59	0.86	62.06
49.23	0.86	63.59
49.38	0.86	63.59
49.98	0.86	65.56
50.27	0.86	65.84
50.71	0.87	66.46
51.07	0.87	67.10
51.3	0.87	69.76
52.02	0.87	70.35
57.28	0.87	72.44
57.28	0.87	73.78
57.69	0.87	75.39
58.18	0.87	78.47
59.64	0.88	80.81
64.19	0.88	82.63
66.06	0.88	88.12
67.69	0.88	102.18
68.62	0.89	104.86
76.54	0.89	107.55
76.85	0.89	114.57
79.78	0.9	118.75
82.49	0.9	139.16
86.04	0.9	140.04
88.9	0.9	141.08
89.82	0.9	161.52
89.82	0.9	162.82
102.99	0.9	169.47
105.98	0.9	189.25
106.22	0.91	191.11
108.45	0.92	212.23
109.88	0.92	216.90
111.07	0.92	233.79
120.09	0.93	261.07
120.97	0.93	270.90
132.83	0.93	428.48
134.93	0.93	438.72
140.39	0.93	471.45
155.58	0.93	481.89
175.39	0.94	515.85
183.77	0.94	525.06
184.02	0.95	876.29
203.97	0.95	971.29
251.3	0.97	1322.63

DCIRCLE/micron		FCIRCLE		DNEW	
Mean	46.38164	Mean	0.746918	Mean	89.57524
Standard Error	3.195096	Standard Error	0.013866	Standard Error	13.17404
Median	31.34	Median	0.81	Median	39.67089
Mode	4.23	Mode	0.77	Mode	NA
Standard Deviation	40.32648	Standard Deviation	0.174838	Standard Deviation	166.1183
Variance	1626.225	Variance	0.030568	Variance	27595.29
Kurtosis	6.680664	Kurtosis	1.325166	Kurtosis	26.6892
Skewness	2.40553	Skewness	-1.40439	Skewness	4.759751
Range	247.07	Range	0.78	Range	1316.296
Minimum	4.23	Minimum	0.19	Minimum	6.333333
Maximum	251.3	Maximum	0.97	Maximum	1322.632
Sum	7374.68	Sum	118.76	Sum	14242.46
Count	159	Count	159	Count	159
Confidence Level(0	6.268157	Confidence Level(0	0.027176	Confidence Level(0	25.82064

BIN	FREQUE	BIN	FREQUE	BIN	FREQUENCY
10	7	0.05	0	10	4
20	15	0.1	0	20	3
30	50	0.15	0	30	40
40	24	0.2	1	40	33
50	24	0.25	2	50	16
60	10	0.3	1	60	19
70	4	0.35	6	70	9
80	3	0.4	2	80	5
90	5	0.45	2	90	3
100	0	0.5	6	100	0
110	5	0.55	4	110	3
120	1	0.6	4	120	2
130	2	0.65	5	130	0
140	2	0.7	8	140	1
150	1	0.75	16	150	2
160	1	0.8	20	160	0
170	0	0.85	35	170	3
180	1	0.9	32	180	0
190	2	0.95	14	190	1
200	0	1	1	200	1
	2		0		14

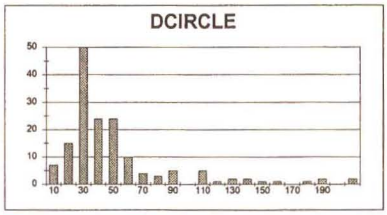

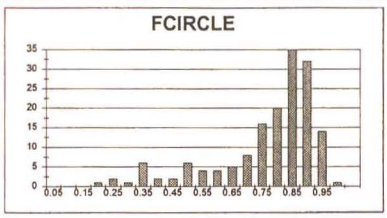

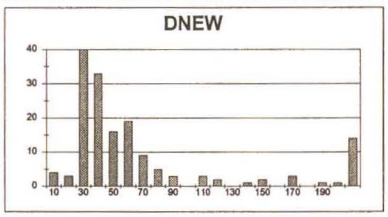


```
{SelectBlock C1}
{PutCell2 "DNEW"}
{SelectBlock C2}
{PutCell2 "=A2..A160/B2..B160"}
{SelectBlock A2..B160}
{EditCopy}
{SelectBlock E2}
{EditPaste}
{SelectBlock C2}
{BlockValues C2;O2}
{SelectBlock C3..C273}
{EditCopy}
{SelectBlock G3}
{EditPaste}
{SelectBlock E2..E160}
{Sort..Block "E2..E160"}
{Sort.Type Top to bottom}
{Sort.Heading 0}
{Sort.Key_1 "E2"}
{Sort.Key_2 ""}
{Sort.Key_3 ""}
{Sort.Key_4 ""}
{Sort.Key_5 ""}
{Sort.BlankCelleFirst 0}
{Sort.Data Numbers First}
{Sort.PreviousSorts -1}
{Sort.Go}
{SelectBlock F2..F160}
{Sort..Block "F2..F160"}
{Sort.Type Top to bottom}
{Sort.Heading 0}
{Sort.Key_1 "F2"}
{Sort.Key_2 ""}
{Sort.Key_3 ""}
{Sort.Key_4 ""}
{Sort.Key_5 ""}
{Sort.BlankCelleFirst 0}
{Sort.Data Numbers First}
{Sort.PreviousSorts -1}
{Sort.Go}
{SelectBlock G2..G160}
{Sort..Block "G2..G160"}
{Sort.Type Top to bottom}
{Sort.Heading 0}
{Sort.Key_1 "G2"}
{Sort.Key_2 ""}
{Sort.Key_3 ""}
{Sort.Key_4 ""}
{Sort.Key_5 ""}
{Sort.BlankCelleFirst 0}
{Sort.Data Numbers First}
{Sort.PreviousSorts -1}
{Sort.Go}
{Setproperty Numeric_Format,"Fixed;2;South Africa"}
{SelectBlock A1..C1}
{EditCopy}
{SelectBlock E1}
{EditPaste}
{SelectBlock I1}
{DESCR "E1..E160";I1;C;"1";"1";"0";"0";"95%"}
{SelectBlock K1}
{DESCR "F1..F160";K1;C;"1";"1";"0";"0";"95%"}
{SelectBlock M1}
{DESCR "G1..G160";M1;C;"1";"1";"0";"0";"95%"}
{SelectBlock I19}
{PutCell2 "BIN"}
{SelectBlock J19}
{PutCell2 "FREQUENCY"}
{SelectBlock I19..J19}
{EditCopy}
{SelectBlock (K19..L19;M19..N19);M19}
{EditPaste}
{SelectBlock I20}
{PutCell2 "10"}
{SelectBlock I21}
{PutCell2 "20"}
{SelectBlock I20..I39}
{SpeedFill}
{EditCopy}
{SelectBlock M20}
{EditPaste}
{SelectBlock K20}
{PutCell2 "0.05"}
{SelectBlock K21}
{PutCell2 "0.1"}
{SelectBlock K20..K39}
{SpeedFill}
{SelectBlock J20}
{PutCell2 "@FREQDIST(E2..E160,I20..I39)"}
{SelectBlock L20}
{PutCell2 "@FREQDIST(F2..F160,K20..K39)"}
{SelectBlock N20}
{PutCell2 "@FREQDIST(G2..G160,M20..M39)"}
{SelectBlock J20..J40}
```

Sample 9b.

DCIRCLE	FCIRCLE	DNEW
17.25	0.72	23.95833
23.91	0.62	29.15654
42.37	0.72	58.84722
43.31	0.81	53.46914
31.34	0.84	37.30952
19.44	0.86	22.60465
29.68	0.56	53
34.76	0.77	45.14286
3.45	0.72	4.791667
104.39	0.58	179.9828
47.41	0.66	71.83333
41.66	0.81	51.4321
63.35	0.47	134.7872
60.66	0.63	96.28571
37.52	0.71	52.84507
26.51	0.87	30.47126
33.63	0.76	44.25
22.95	0.61	37.62295
28.82	0.81	35.58025
32.37	0.91	35.57143
37.52	0.72	52.11111
19.97	0.9	22.18889
63.88	0.66	96.78788
18.82	0.78	24.12821
45.88	0.89	51.55056
49.26	0.8	61.575
19.21	0.89	21.58427
19.6	0.84	23.33333
19.37	0.73	26.53425
48.4	0.74	65.40541
82.53	0.6	137.55
25.3	0.61	41.47541
11.57	0.68	17.01471
46.49	0.66	70.43939
21.89	0.76	28.80263
30.67	0.4	76.675
26.34	0.88	29.93182
23.72	0.72	32.94444
56.04	0.77	72.77922
43.17	0.77	56.06494
44.26	0.74	59.81081
128.41	0.43	298.6279
19.44	0.58	33.51724
174.01	0.39	446.1795
58.05	0.71	81.76056
32	0.86	37.2093
20.85	0.69	30.21739
92.59	0.49	188.9592
51.53	0.68	75.77941
24.52	0.5	49.04
21.62	0.9	24.02222
144.97	0.41	353.5854
42.47	0.86	49.38372
48.19	0.59	81.67797
24.46	0.65	37.63077
30.13	0.92	32.75
25.42	0.84	30.2619
28.77	0.85	33.84706
116.02	0.37	313.5676
22.95	0.89	25.78652
26.22	0.88	29.79545
27.71	0.95	29.16842
53.26	0.88	60.52273
20.34	0.83	24.50602
109.26	0.45	242.8
22.69	0.76	29.85526
104.44	0.39	267.7949
42.12	0.73	57.69863
24.22	0.85	28.49412
34.68	0.88	39.40909
52.98	0.71	74.61972
30.18	0.85	35.50588
37.52	0.81	46.32099
17.76	0.96	18.5
32.83	0.75	43.77333
22.89	0.72	31.79167
13.25	0.79	16.77215
71.56	0.7	102.2286
38.43	0.76	50.56579
28.03	0.89	31.49438
38.43	0.48	80.0625
28.46	0.79	36.02532
31.48	0.86	36.60465
28.87	0.87	33.18391
19.44	0.54	36
140.23	0.44	318.7045
70.38	0.65	108.2769
28.92	0.92	31.43478
25.06	0.79	31.72152
17.93	0.88	20.375
26.78	0.94	28.48936
37.88	0.72	52.61111
65.4	0.81	80.74074
34.38	0.85	40.44706
19.9	0.74	26.89189
97.45	0.39	249.8718
27.17	0.58	46.84483
65.95	0.82	80.42683
59.94	0.75	79.92
25.06	0.94	26.65957
31.91	0.8	39.8875
4.23	0.51	8.294118
18.66	0.88	21.20455
34.16	0.75	45.54667
17.25	0.8	21.5625
50.01	0.79	63.3038
54.37	0.87	62.49425
34.46	0.83	41.51807
9.91	0.71	13.95775
4.56	0.52	8.769231
20.85	0.69	30.21739
17.34	0.82	21.14634
121.27	0.49	247.4898
24.76	0.93	26.62366
37.17	0.71	52.35211
31.29	0.73	42.86301
24.34	0.7	34.77143
26.56	0.86	30.88372
16.9	0.81	20.8642
50.09	0.85	58.92941
22.36	0.65	34.4
19.14	0.83	23.06024
25	0.83	30.12048
17.06	0.78	21.89744
24.4	0.63	38.73016
29.33	0.63	46.55556
26.51	0.86	30.82558
106.88	0.31	344.129
100.81	0.46	219.1522
22.63	0.92	24.59783
22.56	0.7	32.22857
31.34	0.87	36.02299
65.08	0.51	127.6078
69.83	0.52	134.2885
19.82	0.57	34.77193
31.2	0.59	52.88136
145.99	0.26	561.5
77.2	0.63	122.5397
30.23	0.87	34.74713
40.2	0.77	52.20779
38.46	0.79	48.68354
119.7	0.43	278.3721
34.76	0.8	43.45
40.87	0.81	50.45679
114.3	0.41	278.7805
22.63	0.6	37.71667
28.56	0.89	32.08989
31.2	0.9	34.66667
3.45	0.72	4.791667
77.01	0.66	116.6818
13.91	0.89	15.62921
4.56	0.47	9.702128
15.04	0.71	21.1831
4.23	0.4	10.575
42.61	0.8	53.2625
31.1	0.81	38.39506
21.89	0.81	27.02469
321.33	0.12	2677.75
32.46	0.81	40.07407

DCIRCLE	FCIRCLE	DNEW
3.45	0.12	4.79
3.45	0.26	4.79
4.23	0.26	8.29
4.23	0.31	8.77
4.56	0.37	9.70
4.56	0.39	10.58
8.27	0.39	13.34
9.91	0.39	13.96
11.57	0.4	15.63
13.25	0.4	16.77
13.91	0.41	17.01
15.04	0.41	18.50
16.9	0.43	20.38
17.08	0.43	20.86
17.25	0.44	21.15
17.25	0.45	21.18
17.34	0.46	21.20
17.76	0.47	21.56
17.93	0.47	21.58
18.66	0.48	21.90
18.82	0.49	22.19
19.14	0.49	22.60
19.21	0.5	23.06
19.37	0.51	23.33
19.44	0.51	23.96
19.44	0.52	24.02
19.44	0.52	24.13
19.6	0.54	24.51
19.82	0.56	24.60
19.9	0.57	25.67
19.97	0.58	25.79
20.34	0.58	26.53
20.85	0.58	26.62
20.85	0.59	26.66
21.62	0.59	26.89
21.89	0.6	27.02
21.89	0.6	28.49
22.36	0.61	28.49
22.56	0.61	28.90
22.63	0.62	29.16
22.63	0.63	29.17
22.69	0.63	29.80
22.89	0.63	29.86
22.95	0.63	29.93
22.95	0.65	30.12
23.72	0.65	30.22
23.91	0.65	30.22
24.22	0.66	30.26
24.34	0.66	30.47
24.4	0.66	30.83
24.46	0.66	30.88
24.52	0.68	31.43
24.64	0.68	31.49
24.76	0.69	31.72
25	0.69	31.79
25.06	0.7	32.09
25.06	0.7	32.23
25.3	0.7	32.75
25.42	0.71	32.94
26.22	0.71	33.18
26.34	0.71	33.52
26.51	0.71	33.85
26.51	0.71	34.40
26.56	0.71	34.67
26.78	0.72	34.75
27.17	0.72	34.77
27.71	0.72	34.77
28.03	0.72	35.22
28.46	0.72	35.51
28.56	0.72	35.57
28.77	0.72	35.58
28.82	0.72	36.00
28.87	0.73	36.02
28.92	0.73	36.03
29.06	0.73	36.90
29.23	0.74	36.81
29.33	0.74	37.21
29.68	0.74	37.31
30.13	0.75	37.62
30.18	0.75	37.63
30.23	0.75	37.72
30.67	0.76	38.40
31.1	0.76	38.73
31.2	0.76	39.41
31.2	0.76	39.89
31.29	0.77	40.07
31.34	0.77	40.45
31.34	0.77	41.48
31.48	0.77	41.52
31.91	0.78	42.85
32	0.78	42.86
32.37	0.79	43.45
32.46	0.79	43.77
32.83	0.79	44.25
33.63	0.79	45.14
33.85	0.79	45.55
34.16	0.79	46.32
34.38	0.79	46.56
34.46	0.8	46.84
34.68	0.8	48.68
34.76	0.8	49.04
34.76	0.8	49.38
37.17	0.8	50.46
37.52	0.81	50.57
37.52	0.81	51.43
37.52	0.81	51.55
37.88	0.81	52.11
38.43	0.81	52.21
38.43	0.81	52.35
38.46	0.81	52.61
40.2	0.81	52.85
40.87	0.81	52.86
41.66	0.81	53.00
42.12	0.82	53.26
42.37	0.82	53.47
42.47	0.82	56.06
42.61	0.83	57.70
43.17	0.83	58.85
43.31	0.83	58.93
44.26	0.83	59.81
45.88	0.83	60.52
46.49	0.84	61.58
47.41	0.84	62.49
48.19	0.84	63.30
48.4	0.85	65.41
49.26	0.85	70.44
50.01	0.85	70.51
50.09	0.85	71.83
51.53	0.85	72.78
52.98	0.86	74.62
53.26	0.86	75.78
54.37	0.86	76.68
56.04	0.86	79.92
58.05	0.86	80.06
59.94	0.86	80.43
60.66	0.87	80.74
63.35	0.87	81.68
63.46	0.87	81.76
63.88	0.87	96.29
65.08	0.87	96.79
65.4	0.88	102.23
65.95	0.88	108.28
69.83	0.88	116.68
70.38	0.88	122.54
71.56	0.88	127.61
77.01	0.88	134.29
77.2	0.89	134.79
82.53	0.89	137.55
92.59	0.89	179.98
97.45	0.89	185.96
100.81	0.89	219.15
104.39	0.89	242.80
104.44	0.9	247.49
106.88	0.9	249.87
109.26	0.9	267.79
114.3	0.9	278.37
116.02	0.91	278.78
119.7	0.92	296.63
121.27	0.92	313.57

DCIRCLE/micron		FCIRCLE		DNEW	
Mean	43.46789	Mean	0.718735	Mean	88.43028
Standard Error	3.020435	Standard Error	0.012873	Standard Error	17.35768
Median	31.15	Median	0.76	Median	39.06962
Mode	19.44	Mode	0.81	Mode	4.791667
Standard Deviation	38.91558	Standard Deviation	0.165856	Standard Deviation	223.6381
Variance	1514.423	Variance	0.027508	Variance	50013.98
Kurtosis	16.38432	Kurtosis	0.594294	Kurtosis	110.3541
Skewness	3.267929	Skewness	-1.00506	Skewness	9.742626
Range	317.85	Range	0.84	Range	2672.958
Minimum	3.45	Minimum	0.12	Minimum	4.791667
Maximum	321.33	Maximum	0.96	Maximum	2677.75
Sum	7215.67	Sum	119.31	Sum	14679.43
Count	166	Count	166	Count	166
Confidence Level(0	5.919944	Confidence Level(0	0.02523	Confidence Level(0	34.02043

BIN	FREQUE	BIN	FREQUE	BIN	FREQUENCY
10	8	0.05	0	10	5
20	23	0.1	0	20	7
30	47	0.15	1	30	32
40	32	0.2	0	40	41
50	16	0.25	0	50	17
60	9	0.3	2	60	18
70	8	0.35	1	70	5
80	4	0.4	6	80	8
90	1	0.45	6	90	5
100	2	0.5	7	100	2
110	5	0.55	5	110	2
120	3	0.6	9	120	1
130	2	0.65	10	130	2
140	0	0.7	11	140	3
150	3	0.75	23	150	0
160	0	0.8	22	160	0
170	1	0.85	26	170	0
180	1	0.9	27	180	1
190	0	0.95	8	190	1
200	0	1	2	200	0
	1		0		16

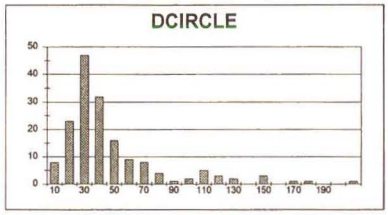

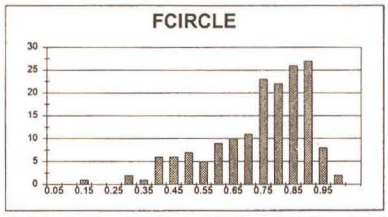

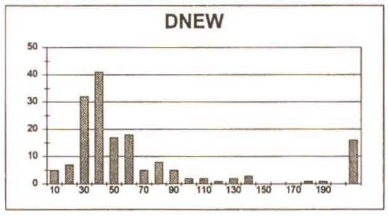


```
(SelectBlock C1)
(PutCell2 "DNEW")
(SelectBlock C2)
(PutCell2 "=A2..A167/B2..B167")
(SelectBlock A2..B167)
(EditCopy)
(SelectBlock E2)
(EditPaste)
(SelectBlock C2)
(BlockValues C2:G2)
(SelectBlock C3..C167)
(EditCopy)
(SelectBlock G3)
(EditPaste)
(SelectBlock E2..E167)
(Sort.Block "E2..E167")
(Sort.Type Top to bottom)
(Sort.Heading 0)
(Sort.Key_1 "E2")
(Sort.Key_2 "")
(Sort.Key_3 "")
(Sort.Key_4 "")
(Sort.Key_5 "")
(Sort.BlankCellsFirst 0)
(Sort.Data Numbers First)
(Sort.PreviousSorts -1)
(Sort.Go)
(SelectBlock F2..F167)
(Sort.Block "F2..F167")
(Sort.Type Top to bottom)
(Sort.Heading 0)
(Sort.Key_1 "F2")
(Sort.Key_2 "")
(Sort.Key_3 "")
(Sort.Key_4 "")
(Sort.Key_5 "")
(Sort.BlankCellsFirst 0)
(Sort.Data Numbers First)
(Sort.PreviousSorts -1)
(Sort.Go)
(SelectBlock G2..G167)
(Sort.Block "G2..G167")
(Sort.Type Top to bottom)
(Sort.Heading 0)
(Sort.Key_1 "G2")
(Sort.Key_2 "")
(Sort.Key_3 "")
(Sort.Key_4 "")
(Sort.Key_5 "")
(Sort.BlankCellsFirst 0)
(Sort.Data Numbers First)
(Sort.PreviousSorts -1)
(Sort.Go)
(Selproperty Numeric_Format,"Fixed,2,South Africa")
(SelectBlock A1..C1)
(EditCopy)
(SelectBlock E1)
(EditPaste)
(SelectBlock I1)
(DESCR "E1..E167";I1;C;"1";"1";"0";"0";"95%")
(SelectBlock K1)
(DESCR "F1..F167";K1;C;"1";"1";"0";"0";"95%")
(SelectBlock M1)
(DESCR "G1..G167";M1;C;"1";"1";"0";"0";"95%")
(SelectBlock I19)
(PutCell2 "BIN")
(SelectBlock J19)
(PutCell2 "FREQUENCY")
(SelectBlock I19..J19)
(EditCopy)
(SelectBlock (K19..L19,M19..N19),M19)
(EditPaste)
(SelectBlock I20)
(PutCell2 "10")
(SelectBlock I21)
(PutCell2 "20")
(SelectBlock I20..I39)
(SpeedFill)
(EditCopy)
(SelectBlock M20)
(EditPaste)
(SelectBlock K20)
(PutCell2 "0.05")
(SelectBlock K21)
(PutCell2 "0.1")
(SelectBlock K20..K39)
(SpeedFill)
(SelectBlock J20)
(PutCell2 "@FREQDIST(E2..E167,I20..I39)")
(SelectBlock L20)
(PutCell2 "@FREQDIST(F2..F167,K20..K39)")
(SelectBlock N20)
(PutCell2 "@FREQDIST(G2..G167,M20..M39)")
```

Sample Optimum 1.

DCIRCLE	FCIRCLE	DNEW
23.25	0.68	34.19118
39.25	0.83	47.28916
50.82	0.66	77
24.8	0.84	29.52381
16.66	0.84	19.83333
6.23	0.8	7.7875
57.02	0.56	101.8214
36.53	0.73	50.0411
46.5	0.74	62.83784
50.26	0.67	75.01493
26.32	0.82	32.09756
22.82	0.91	25.18681
19.16	0.85	22.54118
27.05	0.85	31.82353
55.65	0.63	88.33333
67.68	0.54	125.3333
33.95	0.81	41.91358
23.31	0.88	26.48864
25.45	0.87	29.25287
58.45	0.64	91.32813
23.05	0.87	26.49425
21.09	0.82	25.71951
29.22	0.92	31.76087
33.6	0.92	36.52174
29.48	0.9	32.77556
32.56	0.78	41.74359
44.59	0.68	65.57353
25.63	0.81	31.64198
24.13	0.77	31.33766
51.98	0.82	63.39024
90.81	0.37	245.4324
19.78	0.88	22.47727
40.6	0.72	56.38889
33.28	0.8	41.6
19.63	0.95	20.66316
35.24	0.77	45.76623
32.19	0.85	37.87059
63.3	0.49	129.1837
34.17	0.86	39.73256
56.47	0.71	79.53521
4.89	0.32	15.28125
66.36	0.5	132.72
53.4	0.54	98.88889
20.81	0.72	28.90278
26.38	0.91	28.98901
45.32	0.88	51.5
19.7	1	19.7
17.28	0.73	23.67123
39.25	0.7	56.07143
22.13	0.97	22.81443
55.16	0.7	78.8
3.86	1	3.86
62.33	0.5	124.66
52.7	0.62	85
36.82	0.85	43.31765
23.05	0.87	26.49425
3.46	0.6	5.766667
28.08	0.81	34.66667
9.31	0.5	18.62
20.74	0.76	27.28947
23.44	0.74	31.67568
28.81	0.74	38.93243
34.9	0.84	41.54762
44.33	0.69	64.24638
26.55	0.94	28.24468
23.88	0.89	26.83146
16.21	0.29	55.89655
4.23	1	4.23
26.88	0.87	30.89655
34.6	0.74	46.75676
36.04	0.82	43.95122
26.77	0.77	34.76623
28.24	0.94	30.04255
28.76	0.87	33.05747
85.09	0.42	202.5952
68.34	0.48	142.375
42.61	0.7	60.87143
45.91	0.78	58.85897
76.07	0.58	131.1552
86.74	0.56	154.8929
47.26	0.83	56.93976
4.23	0.51	8.294118
58.5	0.47	124.4681
37.5	0.8	46.875
13.82	0.65	21.26154
68.14	0.51	133.6078
54.18	0.6	90.3
32.28	0.79	40.89076
16.66	0.98	17
28.45	0.93	30.5914
44.89	0.83	53.84337
115.71	0.33	350.6364
20.66	0.81	25.50617
30.77	0.72	42.73611
59.36	0.55	126.1455
27.32	0.88	31.04545
59.36	0.52	114.1538
34.89	0.8	43.7375
31.66	0.75	42.48
52.01	0.61	85.2623
27.76	0.87	31.90805
26.09	0.79	33.02532
20.45	0.77	26.55844
58.14	0.55	105.7091
30.28	0.88	34.40909
41.65	0.71	58.66197
44.39	0.64	69.35938
18.53	0.74	25.04054
37.18	0.88	42.25
23.68	0.83	28.77108
48.51	0.83	58.44578
41.11	0.69	59.57971
53.18	0.72	73.86111
34.04	0.81	42.02469
21.86	0.7	31.22857
70.17	0.46	152.5435
29.27	0.84	34.84524
60.01	0.59	101.7119
21.51	0.72	29.875
61.26	0.7	87.51429
24.38	0.86	28.34884
23.88	0.81	29.48148
40.67	0.73	55.71233
18.04	0.79	22.83544
50.65	0.69	73.4058
42.43	0.79	53.70886
79.11	0.47	168.3191
21.09	0.9	23.43333
40.38	0.59	68.44068
22.46	0.89	25.23596
29.93	0.89	33.62921
48.64	0.87	56.13793
39.86	0.76	52.44737
26.26	0.87	30.18391
66.97	0.68	98.48529
30.91	0.84	36.79762
27.21	0.88	30.92045
21.93	0.9	24.36667
36.53	0.82	44.54878
38.02	0.51	74.54902
26.83	0.92	29.16304
56.95	0.75	75.93333
22.6	0.87	25.97701
20.23	0.88	22.98864
48.38	0.71	68.14085
84.64	0.51	165.9608
29.22	0.92	31.76087
40.12	0.62	64.70968
29.73	0.82	36.2561
30.86	0.9	34.28889
53.65	0.84	63.86905
22.53	0.81	27.81481
65.46	0.69	94.86957
54.59	0.7	77.98571
32.24	0.85	37.92941
52.67	0.64	82.29688
21.3	0.93	22.90323
22.26	0.86	25.88372
6.47	0.22	29.40909
3.46	0.22	3.86
3.46	0.26	4.23
3.46	0.29	4.81
3.86	0.31	5.37
3.86	0.32	5.77
4.23	0.33	5.77
4.23	0.37	6.03
4.89	0.39	6.66
4.89	0.4	7.00
5.18	0.42	7.79
5.46	0.44	8.29
6.23	0.44	11.45
6.47	0.46	15.28
9.31	0.46	17.00
9.62	0.46	17.29
13.82	0.47	18.62
14.25	0.47	19.34
14.35	0.47	19.70
15.65	0.47	19.83
16.21	0.48	20.66
16.39	0.49	21.26
16.66	0.49	22.15
16.66	0.5	22.23
17.02	0.5	22.31
17.28	0.5	22.36
18.04	0.5	22.48
18.53	0.51	22.54
18.69	0.51	22.81
19.16	0.51	22.84
19.63	0.51	22.90
19.63	0.52	22.99
19.7	0.53	23.25
19.78	0.54	23.36
19.78	0.54	23.40
20.23	0.54	23.43
20.23	0.55	23.67
20.45	0.55	24.10
20.59	0.55	24.37
20.66	0.56	25.04
20.74	0.56	25.04
20.81	0.58	25.19
21.09	0.58	25.23
21.09	0.59	25.24
21.16	0.59	25.51
21.16	0.59	25.53
21.3	0.6	25.72
21.3	0.6	25.87
21.44	0.6	25.88
21.51	0.61	25.98
21.51	0.61	26.30
21.58	0.61	26.32
21.65	0.62	26.49
21.86	0.62	26.49
21.93	0.62	26.49
21.93	0.62	26.56
21.99	0.63	26.83
21.99	0.63	26.85
22.13	0.63	27.04
22.2	0.64	27.13
22.26	0.64	27.29
22.46	0.64	27.29
22.53	0.64	27.41
22.6	0.64	27.81
22.73	0.65	27.84
22.78	0.65	28.00
22.92	0.66	28.06
22.92	0.67	28.11
22.99	0.67	28.19
23.05	0.67	28.24
23.05	0.67	28.35
23.12	0.67	28.47
23.25	0.67	28.59
23.31	0.68	28.73
23.31	0.68	28.77
23.44	0.68	28.90
23.5	0.68	28.90
23.88	0.68	28.99
23.88	0.68	29.16
23.88	0.69	29.20
24.07	0.69	29.25
24.07	0.69	29.41
24.13	0.69	29.48
24.19	0.69	29.52
24.25	0.69	29.52
24.38	0.7	29.88
24.8	0.7	30.04
24.92	0.7	30.07
25.16	0.7	30.18
25.22	0.7	30.59
25.4	0.7	30.71
25.45	0.7	30.72
25.51	0.71	30.90
25.51	0.71	30.92
25.63	0.71	30.98
25.63	0.71	31.05
25.8	0.72	31.22
25.86	0.72	31.23
25.86	0.72	31.34
26.09	0.72	31.64
26.15	0.72	31.68
26.26	0.72	31.73
26.32	0.72	31.76
26.38	0.73	31.76
26.43	0.73	31.82
26.55	0.73	31.85
26.55	0.73	31.89
26.77	0.73	31.91
26.83	0.73	32.10
26.88	0.73	32.33
27.05	0.74	32.36
27.05	0.74	32.36
27.16	0.74	32.69
27.16	0.74	32.76
27.21	0.74	32.86
27.27	0.74	33.03
27.32	0.74	33.05
27.7	0.74	33.06
27.76	0.74	33.26
27.76	0.74	33.37
27.76	0.75	33.46
27.92	0.75	33.63
27.97	0.75	33.81
28.08	0.75	33.83
28.08	0.76	33.92
28.24	0.76	34.19
28.34	0.76	34.29
28.45	0.76	34.41
28.76	0.76	34.57
28.81	0.76	34.67
29.02	0.77	34.70
29.07	0.77	34.77
29.12	0.77	34.85
29.17	0.77	35.02
29.22	0.77	35.26
29.22	0.77	36.26
29.27	0.78	36.32
29.48	0.78	36.51
29.73	0.78	36.52
29.93	0.78	36.80
30.28	0.78	36.89
30.42	0.78	37.84
30.42	0.79	37.87
30.67	0.79	37.93
30.77	0.79	37.99
30.77	0.79	38.07
30.86	0.79	38.83
30.91	0.79	38.93
31.06	0.79	39.05
31.2	0.79	39.49
31.63	0.8	39.66
31.86	0.8	39.73
31.96	0.8	39.85
32.19	0.8	40.31
32.24	0.8	40.52
32.28	0.8	40.73
32.28	0.8	40.80
32.56	0.8	40.86
32.83	0.8	40.96
33.28	0.8	41.15

DCIRCLE/micron		*FCIRCLE*		*DNEW*	
Mean	36.30298	Mean	0.752241	Mean	55.3075
Standard Error	1.106105	Standard Error	0.008595	Standard Error	2.961845
Median	31.63	Median	0.8	Median	39.65574
Mode	3.46	Mode	0.88	Mode	5.766667
Standard Deviation	19.16093	Standard Deviation	0.148816	Standard Deviation	51.21508
Variance	367.1414	Variance	0.022057	Variance	2622.985
Kurtosis	2.536484	Kurtosis	0.851156	Kurtosis	19.89938
Skewness	1.287891	Skewness	-1.05635	Skewness	3.734537
Range	113.89	Range	0.78	Range	447.4562
Minimum	3.46	Minimum	0.22	Minimum	3.86
Maximum	117.35	Maximum	1	Maximum	451.3462
Sum	10854.59	Sum	224.92	Sum	16536.94
Count	299	Count	299	Count	299
Confidence Level(0	2.171847	Confidence Level(0	0.016845	Confidence Level(0	5.805109

BIN	FREQUE	BIN	FREQUE	BIN	FREQUENCY
10	15	0.05	0	10	11
20	19	0.1	0	20	8
30	105	0.15	0	30	66
40	64	0.2	0	40	67
50	35	0.25	1	50	40
60	29	0.3	2	60	30
70	17	0.35	3	70	13
80	4	0.4	3	80	13
90	5	0.45	3	90	10
100	3	0.5	14	100	10
110	0	0.55	12	110	3
120	3	0.6	10	120	3
130	0	0.65	17	130	6
140	0	0.7	26	140	3
150	0	0.75	32	150	1
160	0	0.8	36	160	4
170	0	0.85	62	170	2
180	0	0.9	46	180	1
190	0	0.95	26	190	1
200	0	1	6	200	0
	0		0		7

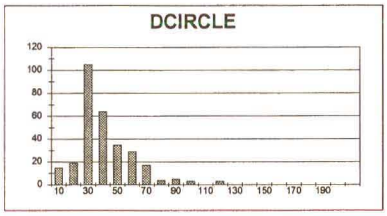

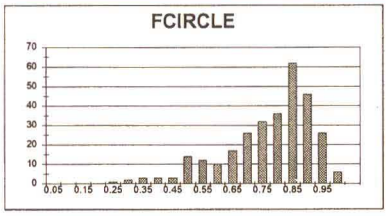

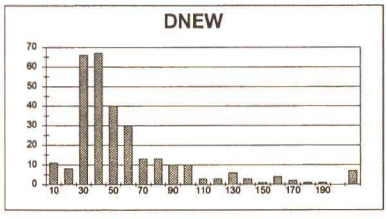


```
{SelectBlock C1}
{PutCell2 "DNEW"}
{SelectBlock C2}
{PutCell2 "=A2..A300/B2..B300"}
{SelectBlock A2..B300}
{EditCopy}
{SelectBlock E2}
{EditPaste}
{SelectBlock C2}
{BlockValues C2;G2}
{SelectBlock C3..C300}
{EditCopy}
{SelectBlock G3}
{EditPaste}
{SelectBlock E2..E300}
{Sort,Block "E2..E300"}
{Sort,Type Top to bottom}
{Sort,Heading 0}
{Sort,Key_1 "E2"}
{Sort,Key_2 ""}
{Sort,Key_3 ""}
{Sort,Key_4 ""}
{Sort,Key_5 ""}
{Sort,BlankCellsFirst 0}
{Sort,Data Numbers First}
{Sort,PreviousSorts -1}
{Sort,Go}
{SelectBlock F2..F300}
{Sort,Block "F2..F300"}
{Sort,Type Top to bottom}
{Sort,Heading 0}
{Sort,Key_1 "F2"}
{Sort,Key_2 ""}
{Sort,Key_3 ""}
{Sort,Key_4 ""}
{Sort,Key_5 ""}
{Sort,BlankCellsFirst 0}
{Sort,Data Numbers First}
{Sort,PreviousSorts -1}
{Sort,Go}
{SelectBlock G2..G300}
{Sort,Block "G2..G300"}
{Sort,Type Top to bottom}
{Sort,Heading 0}
{Sort,Key_1 "G2"}
{Sort,Key_2 ""}
{Sort,Key_3 ""}
{Sort,Key_4 ""}
{Sort,Key_5 ""}
{Sort,BlankCellsFirst 0}
{Sort,Data Numbers First}
{Sort,PreviousSorts -1}
{Sort,Go}
{Selproperty Numeric_Format,"Fixed,2,South Africa"}
{SelectBlock A1..C1}
{EditCopy}
{SelectBlock E1}
{EditPaste}
{SelectBlock I1}
{DESCR "E1..E300";I1;C;"1";"1";"0";"0";"95%"}
{SelectBlock K1}
{DESCR "F1..F300";K1;C;"1";"1";"0";"0";"95%"}
{SelectBlock M1}
{DESCR "G1..G300";M1;C;"1";"1";"0";"0";"95%"}
{SelectBlock I19}
{PutCell2 "BIN"}
{SelectBlock J19}
{PutCell2 "FREQUENCY"}
{SelectBlock I19..J19}
{EditCopy}
{SelectBlock (K19..L19;M19..N19);M19}
{EditPaste}
{SelectBlock I20}
{PutCell2 "10"}
{SelectBlock I21}
{PutCell2 "20"}
{SelectBlock I20..I39}
{SpeedFill}
{EditCopy}
{SelectBlock M20}
{EditPaste}
{SelectBlock K20}
{PutCell2 "0.05"}
{SelectBlock K21}
{PutCell2 "0.1"}
{SelectBlock K20..K39}
{SpeedFill}
{SelectBlock J20}
{PutCell2 "@FREQDIST(E2..E300,I20..I39)"}
{SelectBlock L20}
{PutCell2 "@FREQDIST(F2..F300,K20..K39)"}
{SelectBlock N20}
{PutCell2 "@FREQDIST(G2..G300,M20..M39)"}
```

Sample Optimum 2.

DCIRCLE	FCIRCLE	DNEW	DCIRCLE	FCIRCLE	DNEW
3.86	0.6	6.433333	3.46	0.25	4.81
4.23	0.45	9.4	3.46	0.29	4.81
18.37	0.61	30.11475	3.46	0.29	4.81
33.1	0.84	39.40476	3.46	0.29	5.77
27.32	0.85	32.14118	3.46	0.32	6.43
22.99	0.87	26.42529	3.86	0.4	6.43
28.5	0.79	36.07595	3.86	0.41	6.66
16.93	0.83	20.39759	4.23	0.41	7.73
32.65	0.83	39.33735	4.23	0.41	7.86
40.86	0.79	51.72152	4.23	0.41	8.29
20.74	0.83	24.98795	4.57	0.42	9.00
30.47	0.81	37.61728	5.18	0.42	9.40
31.58	0.82	38.5122	5.46	0.43	10.05
26.03	0.84	30.9881	5.73	0.44	10.16
26.77	0.86	31.12791	5.73	0.44	13.96
67.46	0.5	134.92	7.73	0.45	16.45
57.08	0.85	67.15294	14.66	0.45	16.47
21.37	0.9	23.74444	15.46	0.45	20.40
33.24	0.73	45.53425	16.93	0.45	20.91
82.46	0.54	152.7037	17.87	0.46	21.83
52.16	0.76	68.63158	18.12	0.46	22.90
23.57	0.82	28.7439	18.37	0.47	22.99
20.23	0.67	30.19403	18.61	0.47	23.08
35.46	0.82	43.2439	18.77	0.48	23.46
34.21	0.86	39.77907	19.09	0.49	23.53
3.46	0.72	4.805556	19.24	0.49	23.57
78.85	0.4	197.125	19.63	0.5	23.74
25.92	0.78	33.23077	19.85	0.51	23.84
32.42	0.88	36.84091	19.85	0.51	24.99
53.68	0.81	66.2716	20	0.51	25.01
25.04	0.82	30.53659	20.15	0.52	25.07
32.7	0.83	39.39759	20.23	0.52	25.24
43.58	0.93	46.86022	20.23	0.52	25.29
24.98	0.84	29.7381	20.23	0.54	25.46
3.46	0.6	5.766667	20.66	0.54	25.80
60.82	0.52	116.9615	20.74	0.54	26.13
40.04	0.88	45.5	20.74	0.54	26.23
22.46	0.7	32.08571	20.95	0.55	26.43
66.97	0.54	124.0185	21.16	0.55	26.49
36.41	0.79	46.08861	21.3	0.55	26.76
4.23	0.51	8.294118	21.37	0.56	26.99
46.14	0.72	64.08333	21.93	0.57	27.26
26.88	0.88	30.54545	22.33	0.57	27.35
27.16	0.87	31.21839	22.46	0.57	27.38
24.5	0.73	33.56164	22.46	0.59	27.42
27.27	0.86	31.7093	22.53	0.59	27.52
39.63	0.73	54.28767	22.66	0.6	27.55
45.03	0.78	57.73077	22.99	0.6	27.60
3.86	0.6	6.433333	23.05	0.6	27.65
26.13	0.93	30.24731	23.12	0.6	27.69
24.13	0.92	26.22826	23.25	0.6	27.69
24.68	0.9	27.42222	23.5	0.61	27.84
34.34	0.76	45.18421	23.57	0.61	27.86
30.57	0.95	32.17895	23.69	0.61	28.09
83.2	0.41	202.9268	23.76	0.61	28.11
35.41	0.75	47.21333	23.76	0.61	28.22
22.46	0.51	44.03922	23.82	0.61	28.39
35.54	0.81	43.87654	23.82	0.62	28.63
39.18	0.78	50.23077	23.82	0.62	28.67
37.58	0.65	57.81538	23.82	0.62	28.74
35.5	0.75	47.33333	23.88	0.62	28.89
44.22	0.88	50.25	23.94	0.63	29.26
32.1	0.88	36.47727	24.07	0.63	29.35
93.58	0.32	292.4375	24.07	0.64	29.37
26.66	0.82	32.5122	24.13	0.64	29.74
28.6	0.86	33.25581	24.13	0.64	29.75
26.21	0.94	27.88298	24.13	0.64	29.76
35.07	0.85	41.25882	24.25	0.65	29.93
20	0.87	22.98851	24.31	0.65	29.94
20.23	0.68	29.75	24.38	0.66	29.94
23.25	0.74	31.41892	24.38	0.66	30.11
44.26	0.84	52.69048	24.5	0.66	30.19
25.86	0.92	28.1087	24.5	0.66	30.25
46.37	0.71	65.30986	24.56	0.66	30.25
27.16	0.94	28.89362	24.56	0.66	30.54
24.38	0.69	35.33333	24.68	0.67	30.54
5.73	0.41	13.97561	24.74	0.67	30.55
21.3	0.93	22.90323	24.92	0.67	30.57
33.42	0.82	40.7561	24.98	0.67	30.67
4.57	0.45	10.15556	25.04	0.67	30.86
25.75	0.93	27.68817	25.1	0.68	30.88
45.03	0.73	61.68493	25.26	0.68	30.99
27.81	0.75	37.08	25.4	0.68	31.03
47.83	0.65	73.58462	25.45	0.68	31.08
49.96	0.68	73.47059	25.63	0.69	31.13
22.53	0.77	29.25974	25.63	0.69	31.22
37.26	0.81	46	25.75	0.69	31.40
30.18	0.81	37.25926	25.75	0.69	31.42
30.18	0.89	33.91011	25.8	0.69	31.46
18.12	0.77	23.53247	25.8	0.7	31.49
28.02	0.88	31.84091	25.86	0.7	31.67
59.31	0.54	109.8333	25.86	0.7	31.71
72.2	0.51	141.5686	25.92	0.7	31.84
50.79	0.55	92.34545	26.03	0.7	31.93
19.85	0.55	36.09091	26.15	0.7	31.95
63.14	0.44	143.5	26.15	0.7	31.99
29.73	0.88	33.78409	26.21	0.7	32.00
48.75	0.73	66.78082	26.32	0.71	32.09
37.98	0.69	55.04348	26.38	0.71	32.14
50.2	0.68	73.82353	26.43	0.71	32.17
22.33	0.78	28.62821	26.66	0.71	32.18
33.51	0.89	37.65169	26.66	0.72	32.20
50.82	0.61	83.31148	26.71	0.72	32.33
31.96	0.86	37.16279	26.71	0.72	32.51
3.46	0.72	4.805556	26.77	0.72	32.57
18.77	0.86	21.82558	26.83	0.72	32.59
26.38	0.82	32.17073	26.88	0.72	32.72
39.02	0.8	48.775	26.88	0.72	32.85
30.67	0.92	33.33696	26.88	0.72	32.90
55.51	0.75	74.01333	26.99	0.73	33.00
49.27	0.61	80.77049	27.05	0.73	33.03
32.83	0.8	41.0375	27.16	0.73	33.12
5.18	0.67	7.731343	27.16	0.73	33.19
28.5	0.9	31.66667	27.16	0.73	33.23
36.49	0.8	45.6125	27.16	0.73	33.26
45.72	0.86	53.16279	27.21	0.73	33.33
38.99	0.78	49.98718	27.27	0.73	33.34
32.97	0.9	36.63333	27.32	0.73	33.36
25.6	0.9	28.66667	27.32	0.73	33.56
33.99	0.83	40.95181	27.36	0.73	33.61
27.38	0.92	29.76087	27.49	0.73	33.78
47.73	0.66	72.31818	27.54	0.74	33.91
48.81	0.62	78.72581	27.7	0.74	33.91
39.63	0.83	47.74699	27.7	0.74	33.97
41.72	0.75	55.62667	27.81	0.74	34.02
59.23	0.85	69.68235	27.97	0.74	34.20
30.23	0.87	34.74713	28.02	0.75	34.33
38.72	0.72	53.77778	28.02	0.75	34.33
19.85	0.86	23.0814	28.02	0.75	34.37
15.46	0.46	33.6087	28.13	0.75	34.59
51.06	0.61	83.70492	28.24	0.75	34.61
64.05	0.61	105	28.24	0.75	34.75
100.06	0.29	345.0345	28.5	0.75	34.91
44.53	0.92	48.40217	28.5	0.75	35.11
40.12	0.78	51.4359	28.6	0.75	35.33
30.18	0.89	33.91011	28.91	0.75	35.34
37.74	0.92	41.02174	29.48	0.75	36.06
24.38	0.83	29.37349	29.73	0.76	36.09
24.92	0.9	27.68889	29.73	0.76	36.09
24.31	0.76	31.98684	29.73	0.76	36.48
38.64	0.83	46.55422	29.93	0.76	36.63
44.86	0.66	67.9697	30.18	0.76	36.76
70.78	0.42	168.5238	30.18	0.76	36.84
46.01	0.9	51.12222	30.18	0.76	36.84
83.62	0.41	203.9512	30.23	0.77	37.05
40.52	0.7	57.88571	30.47	0.77	37.08
23.82	0.95	25.07368	30.57	0.77	37.16
40.89	0.91	44.93407	30.62	0.77	37.26
31.96	0.93	34.36559	30.67	0.77	37.41
24.74	0.64	38.65625	30.72	0.77	37.62
36.04	0.81	44.48383	30.77	0.78	37.65
3.46	0.44	7.863636	31.25	0.78	38.16
45.16	0.68	66.41176	31.25	0.78	38.51
28.02	0.84	33.35714	31.58	0.78	38.66
41.76	0.92	45.3913	31.86	0.78	38.84
26.71	0.91	29.35165	31.96	0.78	38.92
18.61	0.89	20.91011	31.96	0.78	39.34
26.15	0.62	42.17742	32	0.78	39.40
38.25	0.75	51	32	0.78	39.40

DCIRCLE/micron		FCIRCLE		DNEW	
Mean	36.15128	Mean	0.751189	Mean	54.73298
Standard Error	0.99925	Standard Error	0.007978	Standard Error	2.978347
Median	32.375	Median	0.79	Median	40.66618
Mode	3.46	Mode	0.81	Mode	4.805556
Standard Deviation	18.09718	Standard Deviation	0.144496	Standard Deviation	53.94016
Variance	327.5081	Variance	0.020879	Variance	2909.541
Kurtosis	6.876085	Kurtosis	0.746847	Kurtosis	30.95333
Skewness	1.72614	Skewness	-1.08519	Skewness	4.798999
Range	151.94	Range	0.7	Range	531.0565
Minimum	3.46	Minimum	0.25	Minimum	4.805556
Maximum	155.4	Maximum	0.95	Maximum	535.8621
Sum	11857.62	Sum	246.39	Sum	17952.42
Count	328	Count	328	Count	328
Confidence Level(0	1.958494	Confidence Level(0	0.015637	Confidence Level(0	5.837453

BIN	FREQUE	BIN	FREQUE	BIN	FREQUENCY
10	16	0.05	0	10	12
20	14	0.1	0	20	5
30	111	0.15	0	30	53
40	80	0.2	0	40	92
50	56	0.25	1	50	53
60	22	0.3	3	60	37
70	12	0.35	1	70	24
80	9	0.4	1	80	11
90	3	0.45	13	90	5
100	1	0.5	8	100	3
110	3	0.55	13	110	9
120	0	0.6	11	120	4
130	0	0.65	18	130	2
140	0	0.7	28	140	3
150	0	0.75	40	150	2
160	1	0.8	38	160	1
170	0	0.85	69	170	2
180	0	0.9	55	180	1
190	0	0.95	29	190	1
200	0	1	0	200	1
	0		0		7

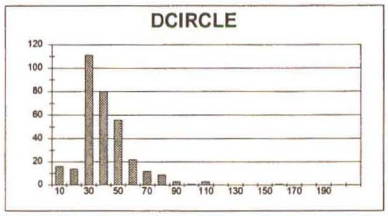

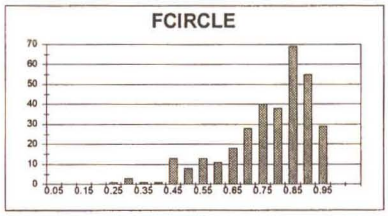

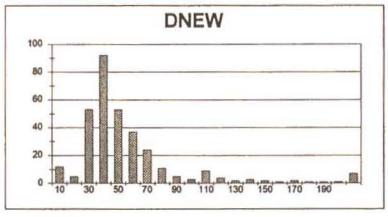


```
{SelectBlock C1}
{PutCell2 "DNEW"}
{SelectBlock C2}
{PutCell2 "=A2..A329/B2..B329"}
{SelectBlock A2..B329}
{EditCopy}
{SelectBlock E2}
{EditPaste}
{SelectBlock C2}
{BlockValues C2;G2}
{SelectBlock C3..C329}
{EditCopy}
{SelectBlock G3}
{EditPaste}
{SelectBlock E2..E329}
{Sort.Block "E2..E329"}
{Sort.Type Top to bottom}
{Sort.Heading 0}
{Sort.Key_1 "E2"}
{Sort.Key_2 ""}
{Sort.Key_3 ""}
{Sort.Key_4 ""}
{Sort.Key_5 ""}
{Sort.BlankCellsFirst 0}
{Sort.Data Numbers First}
{Sort.PreviousSorts -1}
{Sort.Go}
{SelectBlock F2..F329}
{Sort.Block "F2..F329"}
{Sort.Type Top to bottom}
{Sort.Heading 0}
{Sort.Key_1 "F2"}
{Sort.Key_2 ""}
{Sort.Key_3 ""}
{Sort.Key_4 ""}
{Sort.Key_5 ""}
{Sort.BlankCellsFirst 0}
{Sort.Data Numbers First}
{Sort.PreviousSorts -1}
{Sort.Go}
{SelectBlock G2..G329}
{Sort.Block "G2..G329"}
{Sort.Type Top to bottom}
{Sort.Heading 0}
{Sort.Key_1 "G2"}
{Sort.Key_2 ""}
{Sort.Key_3 ""}
{Sort.Key_4 ""}
{Sort.Key_5 ""}
{Sort.BlankCellsFirst 0}
{Sort.Data Numbers First}
{Sort.PreviousSorts -1}
{Sort.Go}
{SetProperly Numeric_Format,"Fixed;2;South Africa"
{SelectBlock A1..C1}
{EditCopy}
{SelectBlock E1}
{EditPaste}
{SelectBlock I1}
{DESCR "E1..E329";I1;C;"1";"1";"0";"0";"95%"}
{SelectBlock K1}
{DESCR "F1..F329";K1;C;"1";"1";"0";"0";"95%"}
{SelectBlock M1}
{DESCR "G1..G329";M1;C;"1";"1";"0";"0";"95%"}
{SelectBlock I19}
{PutCell2 "BIN"}
{SelectBlock J19}
{PutCell2 "FREQUENCY"}
{SelectBlock I19..J19}
{EditCopy}
{SelectBlock (K19..L19;M19..N19),M19}
{EditPaste}
{SelectBlock I20}
{PutCell2 "10"}
{SelectBlock I21}
{PutCell2 "20"}
{SelectBlock I20..I39}
{SpeedFill}
{EditCopy}
{SelectBlock M20}
{EditPaste}
{SelectBlock K20}
{PutCell2 "0.05"}
{SelectBlock K21}
{PutCell2 "0.1"}
{SelectBlock K20..K39}
{SpeedFill}
{SelectBlock J20}
{PutCell2 "@FREQDIST(E2..E329,I20..I39)"}
{SelectBlock L20}
{PutCell2 "@FREQDIST(F2..F329,K20..K39)"}
{SelectBlock N20}
{PutCell2 "@FREQDIST(G2..G329,M20..M39)"}
```

A4 Analysis of Variance (ANOVA)

A4.1 Statistical Calculation

ANOVA[26] establishes the relative significance of the individual factors. The steps are as follows:

Step 1: Total of all the results:

$$T = \sum_{i=1}^{9} y_i \quad \text{... (6.1)}$$

$$= 59.25 + 78.03 + 133.74 + 74.61 + 98.39 + 55.33 + 124.42 + 65.54 + 89.00$$
$$= 778.313$$

Step 2: Correction Factor:

$$C.F. = \frac{T^2}{n} \quad \text{... (6.2)}$$

$$= \frac{7778.313^2}{9} = 67307.93$$

Note: n = total number of experiments.

Step 3: Total Sum of Squares:

$$S_T = \sum_{i=1}^{9} y_i^2 - C.F. \quad \text{... (6.3)}$$

$$= 59.25^2 + 78.03^2 + 133.74^2 + 74.61^2 + 98.39^2 + 55.33^2 + 124.42^2 + 65.54^2 + 89.00^2$$
$$= 6184.05$$

Step 4: Factor Sum Of Squares:

$$S_A = \frac{A_1^2}{N_{A1}} + \frac{A_2^2}{N_{A2}} + \frac{A_3^2}{N_{A3}} - C.F. \quad \ldots \textbf{(6.4)}$$

$$= \frac{271.02^2}{3} + \frac{228.33^2}{3} + \frac{278.96^2}{3} - 67307.93$$

$$= 494.31$$

where:

N_{A1} = Total number of experiments in which factor A_1 is present; similarly for N_{A2} and N_{A3}.

A_1 = Sum of results where factor A_1 is present in experiment; similarly for A_2 and A_3.

$$S_B = \frac{B_1^2}{N_{B1}} + \frac{B_2^2}{N_{B2}} + \frac{B_3^2}{N_{B3}} - C.F. \quad \ldots \textbf{(6.5)}$$

$$= \frac{258.28^2}{3} + \frac{241.95^2}{3} + \frac{278.07^2}{3} - 67307.93$$

$$= 218.20$$

where:

N_{B1} = Total number of experiments in which factor B_1 is present; similarly for N_{B2} and N_{B3}.

B_1 = Sum of results where factor B_1 is present in experiment; similarly for B_2 and B_3.

$$S_C = \frac{C_1^2}{N_{C1}} + \frac{C_2^2}{N_{C2}} + \frac{C_3^2}{N_{C3}} - C.F. \quad \ldots \textbf{(6.6)}$$

$$= \frac{258.28^2}{3} + \frac{241.95^2}{3} + \frac{278.07^2}{3} - 67307.93$$

$$= 5346.49$$

where:

N_{C1} = Total number of experiments in which factor C_1 is present; similarly for N_{C2} and N_{C3}.

C_1 = Sum of results where factor C_1 is present in experiment; similarly for C_2 and C_3.

$$S_e = S_T - \left(S_A + S_B + S_C\right) \quad \text{... (6.7)}$$

$$= 6184.05 - (494.31 + 218.20 + 5346.49)$$

$$= 125.05$$

where:

S_e = Error Sum of Squares.

Step 5: Total and Factor Degrees of Freedom (DOF):

DOF total = Number of test runs - 1

$f_T = n - 1 = 9 - 1 = 8$

DOF factor = Number of levels - 1

f_A = (Number of levels of factor A) - 1 = 3 - 1 = 2

f_B = (Number of levels of factor B) - 1 = 3 - 1 = 2

f_C = (Number of levels of factor C) - 1 = 3 - 1 = 2

DOF error = $f_e = f_T - (f_A + f_B + f_C)$

$= 8 - (2 + 2 + 2) = 2$

Step 6: Mean Square (Variance):

$$V_i = \frac{S_i}{f_i} \quad \text{... (6.8)} \qquad \text{where } i = \text{A, B, C}$$

therefore:

$$V_A = \frac{S_A}{f_A} = \frac{494.31}{2} = 247.15$$

$$V_B = \frac{S_B}{f_B} = \frac{218.20}{2} = 109.10$$

$$V_C = \frac{S_C}{f_C} = \frac{5346.49}{2} = 2673.25$$

$$V_e = \frac{S_e}{f_e} = \frac{125.05}{2} = 62.52$$

Step 7: Percentage Contribution:

$$P_i = \frac{S_i}{S_T} \quad \text{where } i = \text{A, B, C} \quad \ldots \textbf{(6.9)}$$

therefore:

$$P_A = \frac{S_A}{S_T} = \frac{494.31}{6184.05} = 0.080 \equiv 8.0\ \%$$

$$P_B = \frac{S_B}{S_T} = \frac{218.20}{6184.05} = 0.035 \equiv 3.5\ \%$$

$$P_C = \frac{S_C}{S_T} = \frac{5346.49}{6184.05} = 0.865 \equiv 86.5\ \%$$

$$P_e = \frac{S_e}{S_T} = \frac{125.05}{6184.05} = 0.020 \equiv 2.0\ \%$$

A4.2 Average Effects

The average performance of a factor level is the average of the results for experimental trials including that factor's level. (i.e. the average performance of factor A at level 1 is the mean of the results whose trial runs include factor A_1).

Computation of average performance[26]:

$$\overline{A_1} = \frac{(y_1 + y_2 + y_3)}{3} = \frac{59.25 + 78.03 + 133.74}{3} = 90.34$$

$$\overline{A_2} = \frac{(y_4 + y_5 + y_6)}{3} = \frac{74.61 + 98.39 + 55.33}{3} = 76.11$$

$$\overline{A_3} = \frac{(y_7 + y_8 + y_9)}{3} = \frac{124.42 + 65.54 + 89.00}{3} = 92.99$$

$$\overline{B_1} = \frac{(y_1 + y_4 + y_7)}{3} = \frac{59.25 + 74.61 + 124.42}{3} = 86.09$$

$$\overline{B_2} = \frac{(y_2 + y_5 + y_8)}{3} = \frac{78.03 + 98.39 + 65.54}{3} = 80.65$$

$$\overline{B_3} = \frac{(y_3 + y_6 + y_9)}{3} = \frac{133.74 + 55.33 + 89.00}{3} = 92.69$$

$$\overline{C_1} = \frac{(y_1 + y_6 + y_8)}{3} = \frac{59.25 + 55.33 + 65.54}{3} = 60.04$$

$$\overline{C_2} = \frac{(y_2 + y_4 + y_9)}{3} = \frac{78.03 + 74.61 + 89.00}{3} = 80.55$$

$$\overline{C_3} = \frac{(y_3 + y_5 + y_7)}{3} = \frac{133.74 + 98.39 + 124.42}{3} = 118.85$$

The average effects are the differences between the average performances of a factor at the various levels. A plot of the average effects, as shown in figure 1, gives a visual confirmation of the influence of each factor as well as the optimum condition of all the factors' settings. The influence of the factors is represented by the range of the average effects plots. The optimum condition is determined by selecting the extrema of each average effects plot depending of the quality characteristic required.

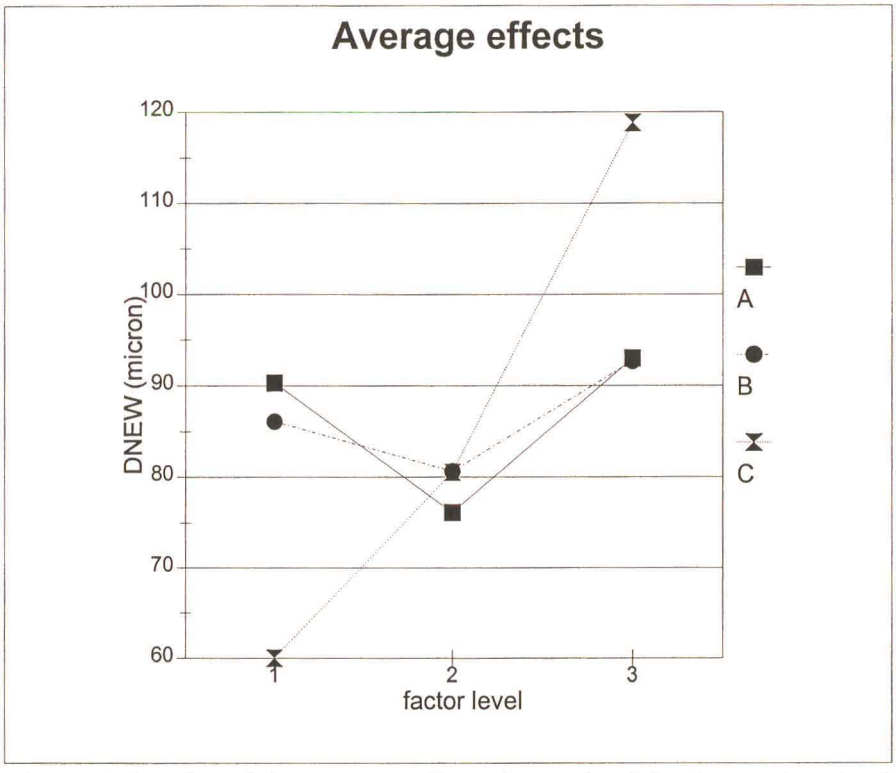

Figure A4.1 Plot of the average effects for each of the factors involved in the L_9 experiment.

The quality characteristics, required of the results, can be described as:

- the bigger the better
- the smaller the better
- the nominal the best

Thus, if "the bigger the better" quality characteristic of the result is required, all the maximum average performances are selected. Likewise for the "smaller the better" characteristic, all the minima values are selected; and for "the nominal is best" characteristic, the values nearest the nominal value is selected. The factor level of each of

the average performances selected represents the optimum level of each factor to deliver the optimum result. E.g. for the research project, a "smaller the better" quality characteristic of D_{NEW} was required therefore A_2, B_2 and C_1 factor levels were selected as the optimum condition.

References

[1] C. Pluchon, W. Loué, P. Menet, M. Garat, "Development of Semi-solid Metal Forming Feedstock and Finished Parts", *the Minerals, Metals, & Materials Society, edited by J. Evans, 1995: Light Metals,* 1995.

[2] M.C, Flemings, "Behaviour of Metal Alloys in the Semi Solid State", *Metallurgical Transactions*, Vol. 22A, May 1991, pp 957 - 981.

[3] M. P. Kenney, J. A. Courtois, R. D. Evans, G. M. Farrior, C.P. Kyonka, A. A. Koch, K. P. Young, "Semi Solid Metal Casting and Forging", *ASM Handbook, Molding and Casting Processes*, pp. 327 - 338.

[4] C. Vives, "Elaboration of Semisolid Alloys by Means of New Electromagnetic Rheocasting Processes", *Metallurgical Transactions*, Vol. 23B, April 1992, pp. 189 - 206.

[5] R. W. Heine, C. R. Loper, P. C. Rosenthal, *Principles of Metal Casting*, 2nd edition, "Ch. 12 - Aluminium and Magnesium casting alloys", pp.292-311, New Delhi, Tata McGraw-Hill Publishing Company, ISBN 0-07-099348-3.

[6] A. Kearney, E. L. Rooy, "Aluminium Foundry Products", *Properties and Selection: Nonferrous Alloys and Special - Purpose Materials, ASM Int. Metals Handbook*, Vol. 2, 10th edition, pp. 123 - 151.

[7] I. J. Polmear, *Light Alloys - Metallurgy of the Light Metals*, 3rd edition, London, Arnold - A member of the Hodder Headline Group, ISBN 0-340-63207-0.

[8] R. W. Heine, C. R. Loper, P. C. Rosenthal, *Principles of Metal Casting*, 2nd edition, "Chapter 9 - Pouring and Feeding Castings", pp. 211-253, New Delhi, Tata McGraw-Hill Publishing Company, ISBN 0-07-099348-3.

[9] R. W. Heine, C. R. Loper, P. C. Rosenthal, *Principles of Metal Casting*, 2nd edition, "Chapter 8 - Solidification of Metals", pp.178-209, New Delhi, Tata McGraw-Hill Publishing Company, ISBN 0-07-099348-3.

[10] Mikell P. Groover, *Fundamental of Modern Manufacturing - Materials, Processes and Systems*, Chapter 12, New Jersey, Prentice Hall.

[11] D.R. Askeland, *The Science and Engineering of Materials*, 3rd S.I. edition, London, Chapman & Hall, ISBN 0-412-53910-1.

[12] J. Datsko, *Cooling and Solidification*, Material Properties & Manufacturing Processes, pp. 150-174.

[13] H. Müller-Späth, M. Achten, P. R. Sahm, "SSP Process - A New Technology for Homogeneous Billet Production", *4th International Conference on Semi Solid Processing of Alloys and Composites*, June 1996, University of Sheffield, England, pp. 174-179.

[14] M. Zillgen, G. Hirt. Sahm, "Microstructural Effects of Electromagnetic Stirring in Continuous Casting of Various Aluminium Alloys", *4th International Conference on Semi Solid Processing of Alloys and Composites*, June 1996, University of Sheffield, England pp. 180-186.

[15] K. P. Young, "Process for Preparing A Slurry Structured Metal Composition", *United States Patent*, No. 4 565 241, January 1986.

[16] D. S. Shin, J. I. Lee, J. C. Lee, H. I. Lee. Sahm, "Microstructural Evolution of Primary Crystals in Rheocast Al-si Alloys", *Proceedings of the 4th International Conference on Semi Solid Processing of Alloys and Composites*, June 1996, University of Sheffield, England, pp. 92-96.

[17] A. Hellawell, S. Liu, S. Z. Lu, "Dendrite Fragmentation and the Effects of Fluid Flow in Castings", *Journal of Materials*, March 1997. pp.18 - 20.

[18] Y.S. Yang & C.Y.A. Tsao, "Thixotropic Behavior and Structure Evolution of A356 Alloy in the Semi-solid State", *Scripta metallurgica et Materialia*, Vol. 30, No.12, 1994, pp. 1541-1546.

[19] J.A. Dantzig, "Process and Apparatus Having Improved Efficiency for Producing A Semi Solid Slurry", *United States Patent,* No. 4 465 118, August 1984.

[20] J. Winter, "Process and Apparatus Making Thixotropic Metal Slurries", United States Patent , No. 4 434 837, March 1984.

[21] J. A. Dantzig, D. E. Tyler, "Mold for Use in Metal of Metal Alloy Casting Systems", *United States Patent* , No. 4 457 354, July 1984.

[22] K. P. Young, D. E. Tyler, H. P. Cheskis, W. G. Watson, "Process and Apparatus for Continuous Slurry Casting", *United States Patent*, No. 4 482 012, November 1984.

[23] J. P. Gabathuler, D. Barras, Y. Krahenbuhl, J. C. Weber, "Evaluation of Various Processes for the Production of Billets with Thixotropic Properties", *Proceedings of the 2nd International Conference on the Semi Solid Processing of Alloys and Composites*, June 1992, MIT, Cambridge, Massachussetts, pp. 33 - 46.

[24] O. J. Ilegbusi, J. Szekely, "Mathematical Modelling of the Electromagnetic Stirring of Molten Metal-solid Suspensions", *Transactions ISIJ*, Vol. 28, 1988, pp 97 - 103.

[25] C. Vives, "Elaboration of Metal Matrix Composites from Thixotropic Alloy Slurries using a New Magnetohydrodynamic Caster", *Metallurgical Transactions B*, Vol. 24B, June 1993, pp 493 - 509.

[26] R. Roy, *A Primer on the Taguchi Method*, Society of Manufacturing Engineers, Jan 1990, ISBN 0-87263-468-X

[27] ASTM Standard E 794, "Standard Test Method for Melting and Crystallization Temperatures by Thermal Analysis"

[28] S. Sircar, "Method of Forming Product Having Globular Microstructure", *United States Patent*, No. 5 730 198, March 1998.

[29] K. W. Andrews, *Physical Metallurgy, Techniques and Applications*, Volume 1, London, George Allen & Unwin Ltd, 1973, ISBN 0 04 669 005 0.

[30] C. Vivès, "New Electromagnetic Rheocaster for the Production of Thixotropic Aluminium Alloy Slurries", *the Minerals, Metals, & Materials Society, 1991: Light Metals, edited by E. R. Cutshall*, 1992.

[31] *AC Tech Variable Speed AC Motor Drives - MC 1000 Series Installation and Operation Manual,* "Chapter 6 - Theory", Uxbridge, Massachussetts, AC Technology Corporation.

[32] *Kontron Elektronik Imaging System KS300 Manual,* Vol.1.

[33] C.J. Thwaites, "The Tri Vertical Casting Method", *Metal and Materials - the Philosophy and Practice of Materials Engineering*, Vol.6, No. 2, February 1972, pp. 84 - 88.